THE UNIVERSITY OF CALGARY

1,5-Diphosphadithiatetrazocines : Synthesis, Isomers, Metal Complexes and Anions

by

Mark Edwards

A THESIS
SUBMITTED TO THE FACULTY OF GRADUATE STUDIES
IN PARTIAL FULFILLMENT OF THE REQUIREMENTS FOR THE
DEGREE OF DOCTOR OF PHILOSOPHY

DEPARTMENT OF CHEMISTRY

CALGARY, ALBERTA

APRIL, 1992

ISBN 0-315-75293-9

THE UNIVERSITY OF CALGARY
FACULTY OF GRADUATE STUDIES

The undersigned certify that they have read, and recommend to the Faculty of Graduate Studies for acceptance, a thesis entitled "1,5-Diphosphadithiatetrazocines : Synthesis, Isomers, Metal Complexes, and Anions." submitted by Mark Edwards in partial fulfillment of the requirements for the degree of Doctor of Philosophy.

T. Chivers
Chairman, Dr. T. Chivers
Department of Chemistry

P.M. Boorman
Dr. P.M. Boorman
Department of Chemistry

Ted Sorensen
Dr. T.S. Sorensen
Department of Chemistry

D. W. Pattison
Dr. D. Pattison
Department of Geology and Geophysics

Robert H. Neilson
Dr. R.H. Neilson (External Examiner) Texas Christian University

April 2, 1992

ABSTRACT

The 1,5-diphosphadithiatetrazocines, 1,5-$R_4P_2N_4S_2$, are a class of unsaturated PNS heterocycles which have the unique feature of a cross-ring sulfur-sulfur interaction. This thesis describes several new aspects of the chemical and physical properties of these rings with an emphasis on the novel features imposed by the presence of this transannular S-S bond. These include an improved synthesis, the preparation of structural isomers, transition metal complexes, and PNS anions, as well as a ^{31}P solid state NMR study.

An improved method of preparing 1,5-diphosphadithiatetrazocines has been developed. The cyclocondensation of $RR'PN_2(SiMe_3)_3$ with $SOCl_2$ instead of SCl_2 gives rise to a better yield of 1,5-$Ph_4P_2N_4S_2$ (56%) and allows for the preparation of 1,5-$Et_4P_2N_4S_2$, which is not available from SCl_2. Furthermore, elemental sulfur is not produced and thus the product is more easily purified. The X-ray structure of 1,5-$Et_4P_2N_4S_2$ (R_w= 0.057) shows a bicyclic system in which two five-membered PS_2N_2 rings share a common S-S bond. Isomeric mixtures of 1,5-diphosphadithiatetrazocines were obtained from the reaction of $Me(Ph)PN_2(SiMe_3)_3$ with $SOCl_2$ or $Cl_3C(Cl)PN_2(SiMe_3)_3$ with SCl_2. The mixtures were partially separated using TLC or fractional recrystallization respectively. The structure of a pure sample of 1,5-[(*endo*-Cl)(*exo*-CCl_3)P]$_2N_4S_2$ was confirmed by X-ray analysis (R_w= 0.064) in which the less bulky Cl substituents occupy the *endo* positions.

The reaction of $Pt(PPh_3)_2(C_2H_4)$ with 1,5-$R_4P_2N_4S_2$ (R=Ph, Et, Me) produces the monomeric complexes $Pt(PPh_3)_2$(1,5-$R_4P_2N_4S_2$) as air-stable yellow solids, which were characterized by ^{31}P NMR. Similarly, reaction between $Pd(PPh_3)_4$ and 1,5-$Ph_4P_2N_4S_2$ or $Pd(PPh_2Me)_4$ and 1,5-$R_4P_2N_4S_2$ (R=Ph, Et) produces $Pd(PPh_3)_2$(1,5-$Ph_4P_2N_4S_2$) or $Pd(PPh_2Me)_2$(1,5-$R_4P_2N_4S_2$), respectively, which were also characterized by ^{31}P NMR spectroscopy. The X-ray structure of $Pt(PPh_3)_2$(1,5-$Ph_4P_2N_4S_2$) (R_w= 0.049) shows that the heterocycle is bonded to Pt in an η^2-S,S′ fashion. Mild heating of the monomeric Pt or Pd complexes, either in solution or in the solid state, results in the reversible dissociation of one of the phosphine ligands to give the dimers [$M(PPh_2R)$(1,5-$R'_4P_2N_4S_2$)]$_2$. The

$P_2N_4S_2$ rings in $[Pt(PPh_3)(1,5\text{-}Ph_4P_2N_4S_2)]_2$ act as chelating (N,S) ligands toward one Pt and form a bridge to the other Pt via the second sulfur atom to give a centrosymmetric dimeric structure. Variable temperature ^{31}P NMR investigations of some of these bimetallic complexes reveal a fluxional process, which is proposed to involve a [1,3]-metallotropic rearrangement.

The treatment of $1,5\text{-}Ph_4P_2N_4S_2$ with nucleophilic reagents gives rise to the first anions of PNS rings. The reaction of $1,5\text{-}Ph_4P_2N_4S_2$ with $Li[BEt_3H]$ (1:2 molar ratio) in THF produces the corresponding dianion as its insoluble dilithium salt, $Li_2[1,5\text{-}Ph_4P_2N_4S_2]$, which reacts with CH_2I_2, MeI, $PtCl_2(PR_3)_2$ (R=Ph, Et), or $NiCl_2$(diphos) to produce $Ph_4P_2N_4S_2CH_2$, $1,5\text{-}Ph_4P_2N_4S_2Me_2$, $Pt(PR_3)_2(1,5\text{-}Ph_4P_2N_4S_2)$, or Ni(diphos)$(1,5\text{-}Ph_4P_2N_4S_2)$, respectively. An X-ray structure of $Ph_4P_2N_4S_2CH_2$ (R_w= 0.060) shows that a methylene group bridges the two sulfur atoms of the $P_2N_4S_2$ ring. Alkylated monoanions, $1,5\text{-}Ph_4P_2N_4S_2R^-$ (R=Me, t-butyl), are prepared by reaction of $1,5\text{-}Ph_4P_2N_4S_2$ with alkyl lithium reagents. Such anions have been shown by variable temperature ^{31}P NMR to be fluxional, likely involving both [1,3]-N,N′ and [1,2]-N,S alkyl migrations.

Solid-state CP/MAS ^{31}P NMR spectra were measured for $1,5\text{-}R_4P_2N_4S_2$ (R=Ph, Et, Me), $1,5\text{-}Ph_4P_2N_4S_2Ph_2$, and $Ph_2PN_3S_2$. The isotropic chemical shift for each compound correlates well with the corresponding shift in solution, indicating that there are no phase-dependent structural features. Analysis of the principal elements of the chemical shift tensor by the spinning-sideband method showed that the element σ_{33} is primarily responsible for the anomalously low field isotropic chemical shifts of the 1,5-diphosphadithiatetrazocines, but no correlation was found between this individual tensor component and any of the structural parameters of these folded eight-membered rings. Two isotropic shifts were observed for the crystallographically inequivalent phosphorus atoms of $1,5\text{-}Et_4P_2N_4S_2$, but the individual ^{31}P isotropic shifts of $1,5\text{-}Me_4P_2N_4S_2$ were not resolved.

ACKNOWLEDGEMENTS

There are many people who must be acknowledged for their various contributions to this work. First of all, special thanks go to my supervisor Dr. T. Chivers, whose guidance, patience, and enthusiasm have been outstanding. It has been a privilege working with him.

I must also acknowledge the invaluable assistance of the following people; Dr. M. Parvez, Dr. M. Cowie, Dr. R.W. Hilts, Dr. J.C. van de Grampel, and A. Meetsma who performed the X-ray analyses; Dr. R. Yamdagni and D. Fox for their assistance in obtaining NMR spectra; Dr. C. Fyfe and Dr. L. Randall for obtaining the solid state NMR data; and Dr. A.S. Hinman and D. Jones for acquiring the electrochemical data.

The contributions of all members of the "Chivers group" (past and present) are very much appreciated, especially those of my laboratory partners and good friends D.D. Doxsee and Dr. R.W. Hilts. Thanks also go to the other graduate students, faculty members, and support staff, particularly G. Prihodko , who have made the past 9 years at the University of Calgary so enjoyable.

Funding from the University of Calgary and the Natural Sciences and Engineering Research Council of Canada is greatly appreciated.

And finally, for the support, patience, and love I have received from my family members, especially my wife, Katarina, I will always be grateful.

To my Father,

who taught me that science can be fun

and to my Mother,

who taught me that science isn't everything.

TABLE OF CONTENTS

PAGE

Table of Contents (cont'd) **PAGE**

Table of Contents (cont'd) **PAGE**

Table of Contents (cont'd) **PAGE**

LIST OF TABLES

List of Tables (cont'd)

LIST OF FIGURES

List of Figures (cont'd)

List of Figures (cont'd)

List of Figures (cont'd)

FORMULA INDEX

1. $(NPCl_2)_3$
2. S_4N_4
3. $B_3N_3H_6$
4. $R_{12}P_6N_7$
5. $[(R_2PN)_2(RPN)]_2$
6. $R_9P_5N_6$
7. $N_3P_3F_5BEt_3^-Li^+$
8. S_2N_2
9. $S_5N_5^+$
10. $1,5\text{-}X_2N_4S_4$
11. S_5N_6
12. $S_3N_3^-$
13. $S_3N_3O^-$
14. $S_3N_3O_2^-$
15. $R_2PN_3S_2$
16. $1,5\text{-}R_4P_2N_4S_2$
    - **a.** R=Ph
    - **b.** R=Me
    - **c.** R=Et
    - **d.** R=Cl
17. $1,3\text{-}R_4P_2N_4S_2$
    - **a.** R=Ph
    - **b.** R=Me
    - **c.** R=Et
18. $(NPMe_2)_4HCuCl_3$

CHAPTER 1

Unsaturated P-N and S-N Heterocycles

1.1 General Introduction

Although the first examples of unsaturated inorganic heterocycles, $(NPCl_2)_3$ **1** [1], S_4N_4 **2** [2], and borazine $(B_3N_3H_6)$ **3** [3], were discovered in the 19th and early 20th century, progress in this area of chemistry was surprisingly slow. When compared to the extremely well developed area of cyclic hydrocarbon chemistry, the study of inorganic heterocycles is at a much earlier stage of development. This is due, in large part, to the initial lack of sophisticated physical techniques such as X-ray crystallography and high-resolution, multinuclear NMR spectroscopy for structural elucidation. However, rapid advances in such techniques in the latter half of this century have sparked interest in this and many other areas of inorganic chemistry. The concomitant development of the siloxane and phosphazene polymer industries, as well as the discovery of the unusual properties of the conducting polymer $(SN)_x$ [4] have also fueled progress in this area. Advances in computational theoretical chemistry have also emerged to the point where MO calculations agree very well with spectroscopic measurements of inorganic heterocycles.

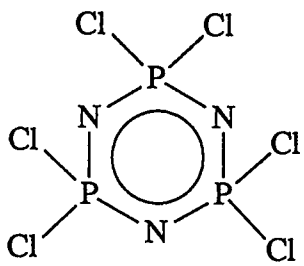

1

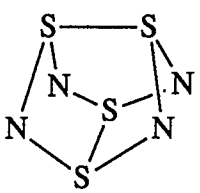

2

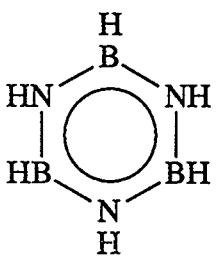

3

The concept of unsaturation often implies aromaticity and, although many cyclic inorganic compounds are believed to have electronic structures analogous to those of benzene or other aromatic hydrocarbons, direct comparisons are often impossible or entirely inaccurate. For example, unsaturated inorganic heterocycles are generally far more reactive than aromatic organic compounds as a result of the polarization of π-electron density, which arises from electronegativity differences in the constituent atoms of the ring, thus making the prediction of chemical or physical properties very difficult.

The most extensively studied unsaturated inorganic heterocycles are the cyclophosphazenes and the cyclothiazenes. Cyclophosphazenes are heterocycles made up of R_2PN units with phosphorus in a pentavalent (V) oxidation state (R is an exocyclic ligand). An extensive homologous series, $(NPR_2)_n$ (n=3-17), of these π-electron precise rings (i.e. the number of π-electrons is equal to the number of atoms in the ring) has been developed [5]. More complex structural types such as fused rings, **4**, coupled rings, **5**, and spirocycles, **6**, are also known. Simple anionic cyclophosphazenes such as **7** have been recently reported [6], but cations are, as yet, unknown.

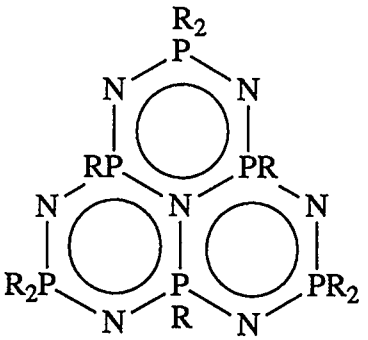

4

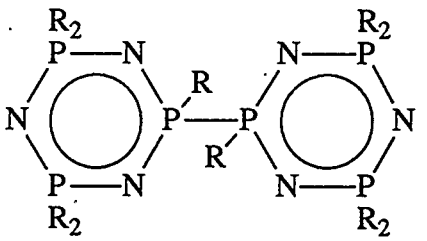

5

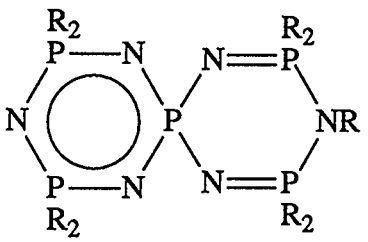

6

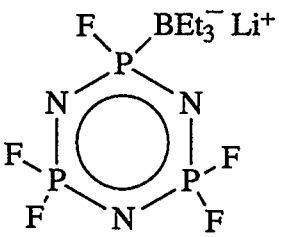

7

The cyclothiazenes are binary S-N systems for which known rings range in size from four (S_2N_2, **8** [7]) to ten ($S_5N_5^+$, **9**) atoms. The formation of long transannular S-S bonds among larger S-N rings gives rise to more complex bicyclic (folded) (**10** [8]) or cage structures such as S_4N_4 (**2**) or S_5N_6 (**11** [9,10]). The occurrence of bicyclic and cage compounds and a series of compounds such as **12** [11,12, 13], **13** [14,15], and **14** [14,15], is a result of the wide range of oxidation states (+2, +3, +4, or +6) available for sulfur.

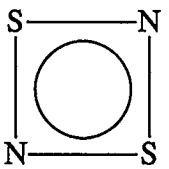

8

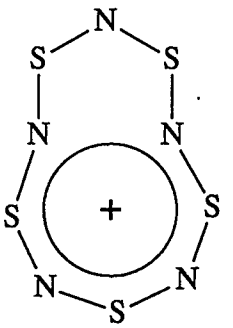

9

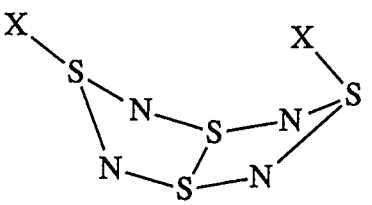

10

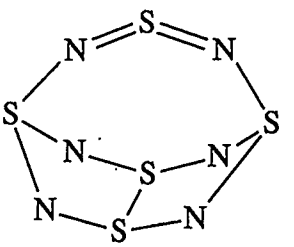

11

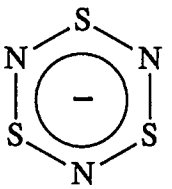

12

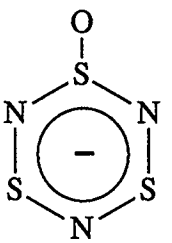

13

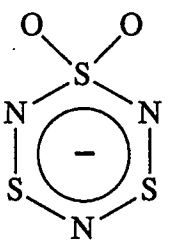

14

It is a natural outcome of cyclophosphazene and cyclothiazene research that a hybrid class of heterocycles, composed of a combination of R_2PN and SN units, would be developed. Such rings, termed cyclophosphathiazenes, are the subject of this thesis. The first example of a mixed P-N-S heterocycle containing sulfur in a low oxidation state was the six-membered ring **15** (R=Me_3SiNH [16]). More recently the two isomeric eight-membered rings of $R_4P_2N_4S_2$ (**16** and **17**) have been characterized and studied [17,18]. This work will focus on the chemistry of the 1,5 isomers, **16**, which possess the interesting feature of a weak cross-ring S-S bond similar to that found in S_4N_4.

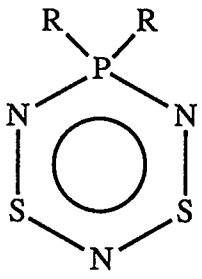

15

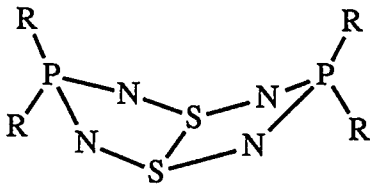

16

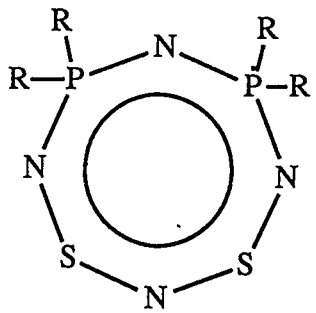

17

As relatively little is known about cyclophosphathiazenes it is often useful to describe their properties in relation to the known behavior of the related parent P-N and S-N systems. Thus, a brief overview of the chemistry, structure and bonding of the cyclophosphazenes and cyclothiazenes will be presented first. A more detailed analysis of cyclophosphathiazenes will follow and, finally, the objectives and an outline of this thesis will be given.

1.2 Cyclophosphazenes

1.2.1 Introduction

Since the initial discovery of $(NPCl_2)_3$, **1**, in 1834 [1], literally thousands of cyclophosphazenes have been prepared and characterized. These systems range from rings containing 6 to 34 atoms, to more complex multicyclic (**4** and **5**) and spirocyclic (**6**) molecules. Partial or complete replacement of the halogen atoms of halocyclophosphazenes by other atoms or functional groups is possible and increases the number of derivatives enormously. In many of the compounds the phosphorus-nitrogen linkages are equivalent, and in the cyclic derivatives there is a formal resemblance to the Kekulé-type resonance which occurs in benzene. There are, however, essential differences which will be discussed in the next section (Section 1.2.2).

Most cyclophosphazenes have been prepared for use as polyphosphazene monomers. The thermal polymerization of hexachlorotriphosphazene, **1**, was first described by Stokes in 1897 [19] and has since spawned a large polyphosphazene industry.

1.2.2 Synthesis, Structure, and Bonding

(a) Synthesis

Hexachlorocyclotriphosphazene, **1**, was first synthesized by the action of gaseous ammonia on phosphorus pentachloride [1] (Equation 1.1), and this route (aminolysis of a phosphorus (V) halide) is still the most widely used in preparing a wide variety of cyclophosphazenes.

$$NH_3 \quad + \quad PCl_5 \longrightarrow (NPCl_2)_n \quad + \quad NH_4Cl \qquad (1.1)$$

An improved synthetic technique involves the use of ammonium chloride in place of ammonia (Equation 1.2). The reaction proceeds in two distinct steps; isolation of a high

yield of $Cl_3PNPCl_3^+Cl^-$ followed by chain growth by condensation of linear phosphazenes with NH_4Cl and finally cyclization [20]. This process has been studied in great detail by ^{31}P NMR spectroscopy and other techniques, which is likely a result of the commercial applications of the product.

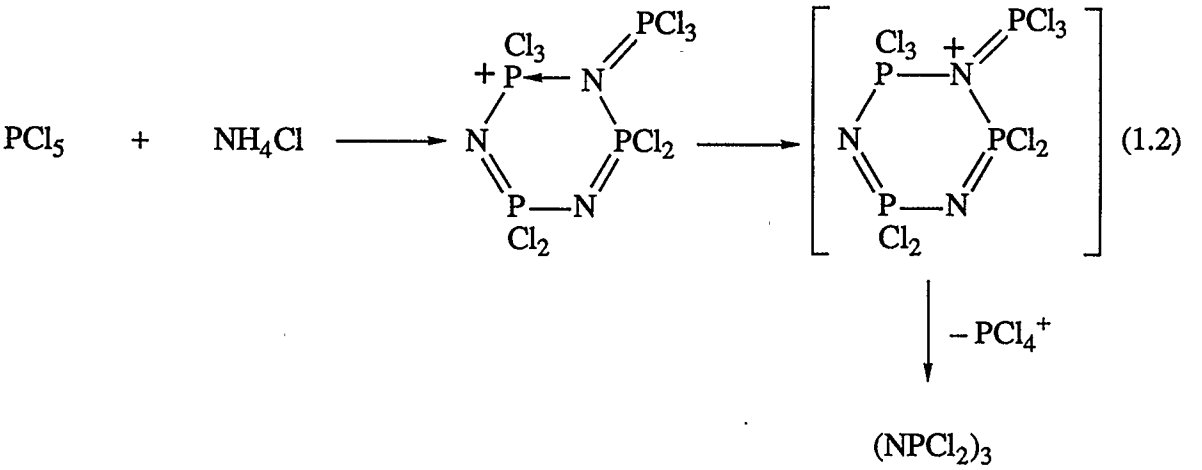

(1.2)

Alternatively, reactions between ammonium chloride and tri- or tetrahalophosphoranes yield cyclic products which have exocyclic substituents other than halogen atoms. Examples are illustrated in Equations 1.3 and 1.4.

$$MePCl_4 + NH_4Cl \longrightarrow (NPMeCl)_n \qquad (1.3)$$

(Ref [21])

$$(C_3F_7)_2PCl_3 + NH_4Cl \longrightarrow [NP(C_3F_7)_2]_n \qquad (1.4)$$

(Ref [22])

Cyclophosphazenes can also be prepared via the pyrolysis of cyclic aminophosphoranes. Pyrolyses of $(MeNPPhCl_2)_2$ and $(MeNPF_3)_2$ give $(NPPhCl)_n$ and $(NPF_2)_n$ respectively [23] (Equation 1.5).

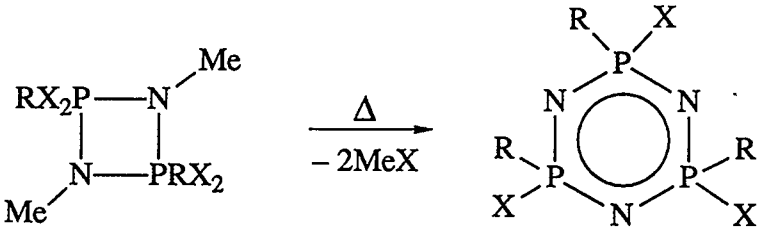

(1.5)

R=Ph, X=Cl
R=X=F

A related preparative route involves the thermal elimination of trimethylsilyl halide or trimethylsilyl trifluoroethoxide from N-silylphosphinimines [24,25] (Equation 1.6). This technique has also been used successfully for the preparation of polyphosphazenes [26] (Equation 1.7).

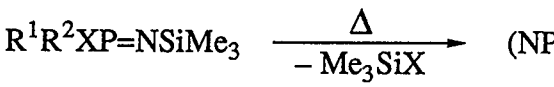

(1.6)

R^1=F, R^2=Ph, NMe_2, Me, X=F
R^1=Ph, R^2=Ph, X=F or Br
R^1=Me, R^2=Me, X=F or Br
R^1=R^2=Ph, Me, X=OCH_2CF_3
n=3-6

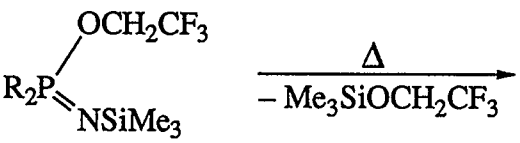

(1.7)

R=Me
MW ≈50 000

Three other methods employed in the synthesis of cyclophosphazenes include : (1) the elimination of nitrogen from azides derived from P(III) compounds [27,28] (Equations 1.8 and 1.9); (2) the cyclization of linear P-N compounds such as 1-amino-3-imino-

1,1,3,3-tetraorganodiphosphazenes [29,30,31,32] (Equations 1.10 and 1.11); and (3) the condensation of amidophosphines with phosphines in the presence of carbon tetrachloride [33] (Equation 1.12).

$$P(CF_3)MeN_3 \xrightarrow{-N_2} [NP(CF_3)Me]_n \qquad (1.8)$$

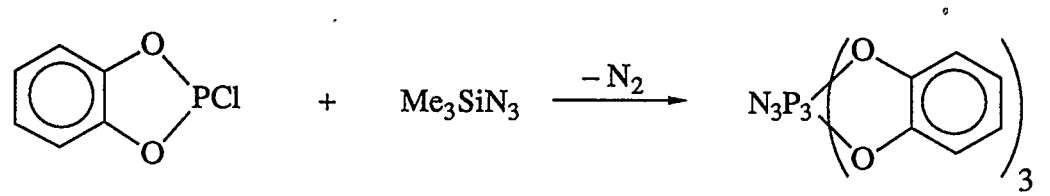

(1.9)

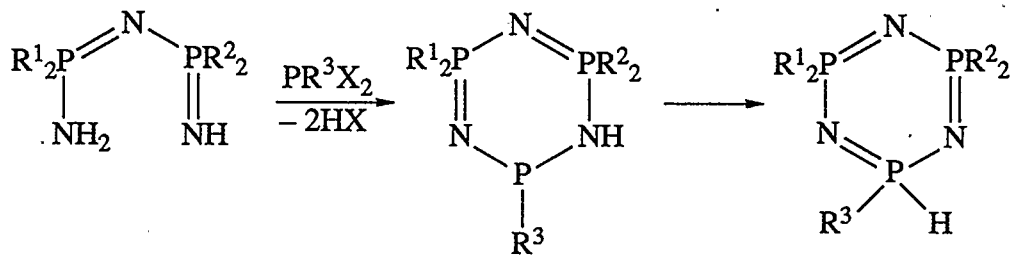

(1.10)

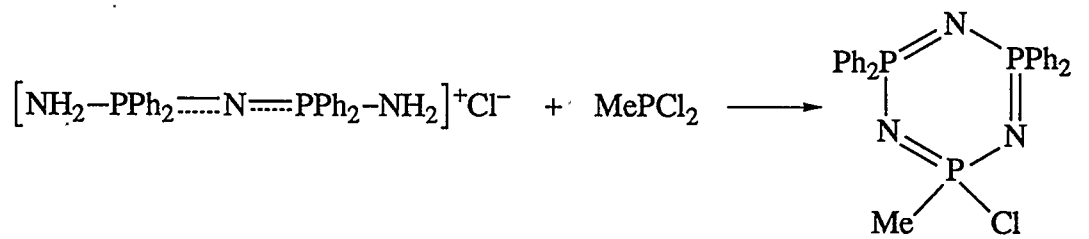

(1.11)

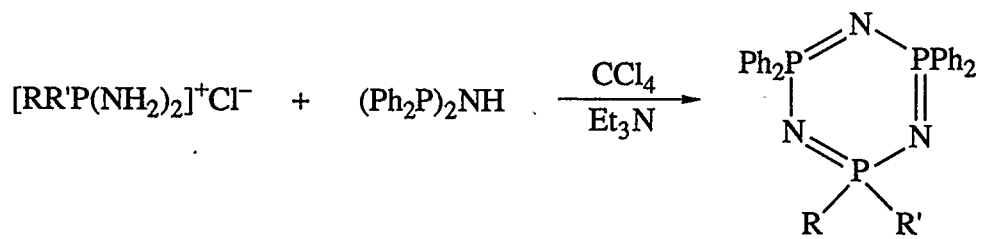

(1.12)

Other miscellaneous syntheses are covered in more detail in reference [34]. As mentioned earlier, the largest number of cyclophosphazenes has been prepared by the nucleophilic substitution of halogen atoms in halocyclophosphazenes by organic substituents.

(b) Structure and Bonding

The structures of many cyclic and polymeric phosphazenes have been determined. Three detailed surveys of structural work are available covering pre-1970 [35,36] and pre-1983 [34] data, respectively.

In general the trimeric halides all have planar ring structures with D_{3h} symmetry, and with halogens disposed symmetrically above and below the plane of the ring. Most symmetrically substituted cyclotriphosphazenes, $(NPR_2)_3$ or $(NPRR')_3$, are also planar. Tetrameric and larger rings adopt a wide variety of conformations although almost all are puckered (non-planar).

The P-N bond lengths of symmetrically substituted cyclophosphazenes, $(NPR_2)_n$ or $(NPRR')_n$, are generally equal and typically fall in the range of 1.50-1.60 Å. No separation occurs into alternating short (π) and long (σ) bonds, even when ring-puckering exists. A P-N single bond, typically quoted as 1.77 Å, is derived from X-ray studies of α sodium phosphoramidate ($NaNH_3PO_3$) [37]. Thus the bond lengths of cyclophosphazenes represent an average contraction of 0.22 Å when compared to the single bond distance. This bond shortness and equality can be compared to the similar situation with the C-C bonds in benzene, where single-double bond resonance occurs. However, such an analogy is of limited value. For example, p_π-p_π bonding in aromatic carbon systems requires coplanarity for resonance to occur. When ring folding or puckering does occur, as in cyclooctatetraene for example, a breakdown to alternating single and double bonds takes place. This is in contrast to cyclophosphazenes, which often adopt puckered conformations, yet still possess

short, equal P-N bonds.

The most widely accepted model of bonding in cyclophosphazenes, involves the participation of the phosphorus d orbitals [38,39,40]. In the d_{π}-p_{π} model the σ-bonding framework is built up from sp^3 orbitals of phosphorus and sp^2 orbitals at nitrogen. The remaining two sp^3 lobes of phosphorus form σ bonds to the exocyclic moieties, while the remaining sp^2 lobe of nitrogen contains a lone pair of electrons (in the plane of the ring). The lone electron occupying the p_z orbital of nitrogen can interact with an electron in a d_{xz} or d_{yz} orbital of phosphorus (Figure 1.1a and 1.1b). A second bonding interaction can be formed by donation of the lone pair of electrons at nitrogen into the unoccupied $d_{x^2-y^2}$ or d_{xy} orbitals of phosphorus (Figure 1.1c and 1.1d).

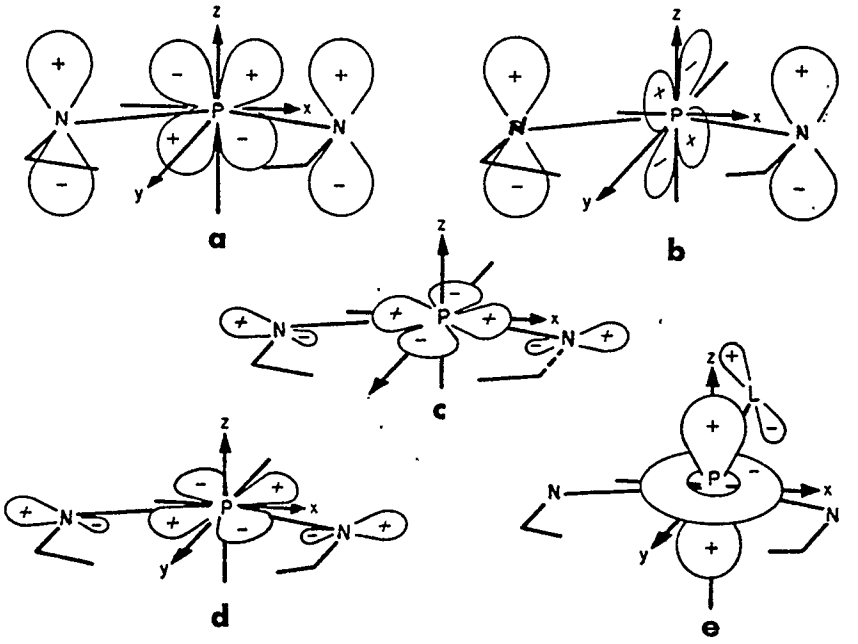

Figure 1.1 - Overlap schemes for π bonding of (a) d_{xz} and (b) d_{yz} orbitals with p_z orbitals; (c) π′ bonding of $d_{x^2-y^2}$ and (d) d_{xy} orbitals with an s-p_y hybrid, and (e) π bonding of a d_{z^2} orbital with a ligand p orbital. From Ref.. [40].

Alternatively, a linear combination of the d_{xz} and d_{yz} orbitals of phosphorus generates two new d_{π} orbitals, each oriented along a P-N bond. Overlap with the $2p_z$ orbital of N would generate a π-system that extends over a P-N-P fragment but has a nodal point at each P atom (Figure 1.2). This *island* bonding model is considered to be the most accurate description of π-bonding in cyclophosphazenes based on agreement with results from : (1) MO calculations at the CNDO/2 level [41], (2) NMR spectroscopy (lack of ring current effects) [36], (3) Magnetic susceptibility measurements [42], and (4) MS fragmentation experiments [39]. More recent calculations (Hartree-Fock method, STO-3G* level) by Haddon also strongly suggest that the phosphorus d orbitals are significant participants in the phosphazene bond [43].

Although two models have been developed it will likely be some time before a theory is developed that will satisfactorily explain all of the experimental facts. At present, however, the discontinuous island type π-orbital arrangement is perhaps the most compatible with the experimental data.

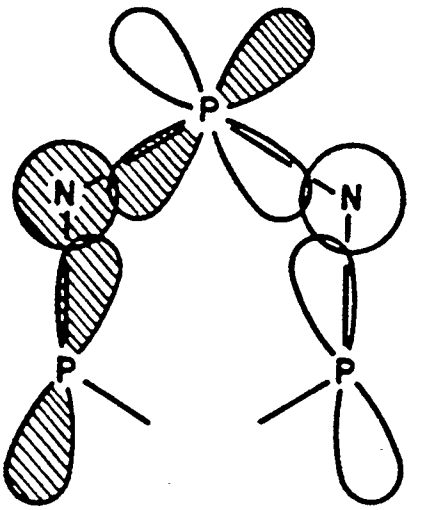

Figure 1.2 - Projection of atomic orbitals to be combined as molecular orbitals for three-center *island* delocalization (From Ref. [44]).

1.2.3 Isomerism in Cyclophosphazenes

In general, three types of isomerism may be encountered amongst cyclophosphazenes : (1) Positional isomerism, (2) Geometrical isomerism, and (3) Conformational isomerism. Each is described in detail below.

(1) Positional Isomerism .

Positional isomers arise when a given exocyclic substituent (or ligand) has a choice of phosphorus atoms to which it may be attached. In the simplest example, $N_3P_3Cl_2Br_4$, which is synthesized from PCl_3, Br_2 and NH_4Br, two positional isomers are possible [45]. One of these has both Cl atoms on the same phosphorus atom (Figure 1.3a). This isomer is said to be geminally substituted. The second isomer has each Cl atom on a different P atom (Figure 1.3b). Such an isomer is said to be non-geminally substituted.

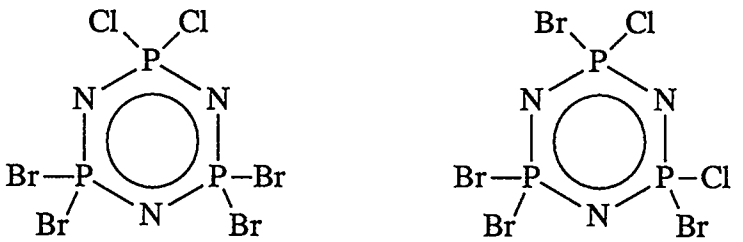

Figure 1.3 - (a) The geminal isomer of $N_3P_3Cl_2Br_4$ (b) The non-geminal isomer of $N_3P_3Cl_2Br_4$. Note : No assignment has been made as to which side of the N_3P_3 plane each halogen atom resides.

As positional isomers (geminal and non-geminal) involve phosphorus and nitrogen atoms in different environments, variations in their ^{31}P and ^{15}N NMR spectra are expected and usually observed [5,36,46]. Similarly, if the environments of the various exocyclic substituents are dissimilar, other nuclei such as ^{1}H, ^{13}C, and ^{19}F can be used to differentiate

between such isomers.

Geminal and non-geminal isomers can also be distinguished using mass spectrometry. For example, a MS study of the bromofluorocyclotriphosphazenes $N_3P_3Br_nF_{6-n}$ (n=3-5), has shown that the loss of a bromine atom from a $\equiv PBr_2$ occurs more easily than for a $\equiv PBrF$ center [47]. The use of infrared spectroscopy to differentiate between positional isomers has been reported for $N_3P_3F_4Ph_2$ based on the number of bands observed in the PF_2 region [48]. Separation of isomeric mixtures has been reported by using either gas-liquid chromatography (GLC) [49] or thin-layer chromatography (TLC) [50].

(2) Geometrical Isomerism

Geometrical isomerism arises for non-geminally substituted rings since geometrically different forms can be obtained by placing a substituent alternatively above or below the plane of the ring when attached to the same phosphorus atom. Returning to the non-geminal isomer of $N_3P_3Br_4Cl_2$ [45], the Cl atoms may be on the same side of the N_3P_3 plane (cis, non-geminal isomer; Figure 1.4a) or on opposite sides (trans, non-geminal isomer; Figure 1.4b).

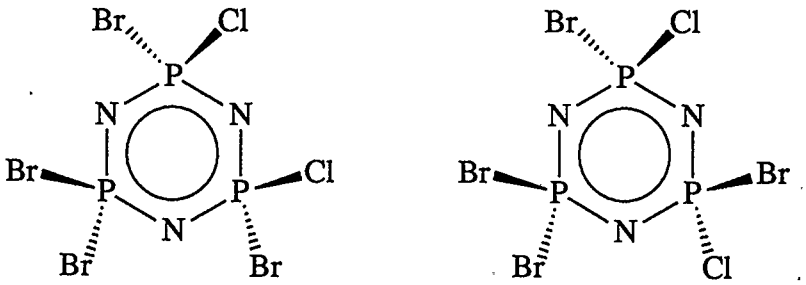

Figure 1.4 - (a) cis, non-geminal isomer of $N_3P_3Br_4Cl_2$
(b) trans, non-geminal isomer of $N_3P_3Br_4Cl_2$

Conversions between cis and trans isomers can take place under a variety of conditions. Uncatalyzed isomerizations in boiling solvents have been reported [51] while isomerizations

catalyzed by hydrogen halides, ammonium halides [52,53], or aluminum chloride [54] also occur.

The different positional and geometrical isomers are obtained either in the preparation of an unsymmetrically substituted cyclophosphazene or from the derivatization of simpler cyclophosphazenes via substitution reactions. In general, substitution reactions of the halogenocyclophosphazenes result from nucleophilic attack on phosphorus. In the case of geminal substitution, replacement of the first halogen atom by a new group promotes further reaction at the same phosphorus atom, while for non-geminal reactions, further reaction is directed towards an unsubstituted phosphorus atom. In general, the substitution path is often unpredictable and not fully understood. However, in some cases, criteria such as group electronegativity, may decide the pattern of substitution. The strong electron-withdrawing effect of fluorine may promote a geminal product (Figure 1.5a) [55] while an electron-donating group, such as NMe_2, may favour a non-geminal path (Figure 1.5b) [56].

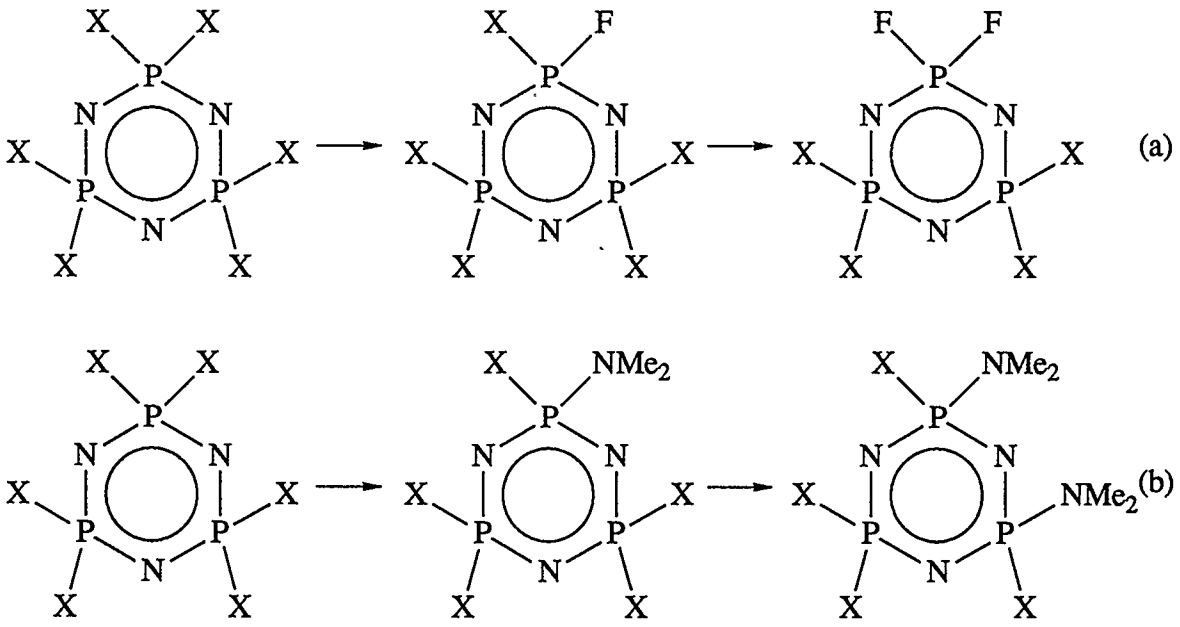

Figure 1.5 - (a) Geminal substitution pathway
(b) Non-geminal substitution pathway

The combination of positional and geometrical isomerism results in a very large number of possible isomers for large rings. For example, a tetrameric ring with two types of ligands, $N_4P_4A_{8-n}B_n$ (n=1-7), has a total of 29 possible isomers (excluding conformational isomers).

As was the case for positional isomers, geometrical isomers can be distinguished by using a variety of experimental techniques. Again, the P and N atoms, as well as the respective exocyclic groups, are inequivalent so the various NMR active nuclei (^{31}P, ^{15}N, ^{1}H, ^{13}C, ^{19}F ...) can be used for differentiation [45,46]. Dipole moment studies have also been used effectively for the assignment of cis and trans isomers [36]. As with positional isomers, the separation of geometrical isomers is accomplished by using GLC or TLC techniques [49,50].

(3) Conformational Isomerism

The third, and final type of isomerism is conformational isomerism. The best example of conformational isomerism is illustrated by the existence of two solid-state structures, chair and boat, for the cyclotetraphosphazene $N_4P_4Cl_8$ [57,58].

1.2.4 Coordination Chemistry

Cyclophosphazenes form a wide range of coordination complexes with either metal halides or metal carbonyls [34,36,59]. This behavior can be largely attributed to the donation of electron density from the lone-pair electrons of the skeletal nitrogen atoms to electron poor metal centers.

Although many of the smaller rings such as $N_3P_3Cl_6$ [60] and $N_3P_3(NMe_2)_6$ [61] do not undergo complex formation with transition-metal salts, larger rings readily form σ complexes. Octamethylcyclotetraphosphazene reacts with anhydrous copper (II) chloride to form a σ complex in which $CuCl_3^-$ is coordinated to one nitrogen atom and a proton is attached to the distant nitrogen, **18** [62].

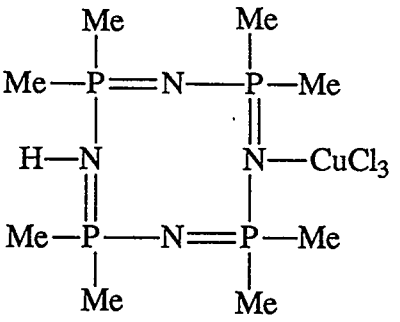

18

Coordination complexes of this type have been proposed as intermediates in copper-catalyzed Grignard reactions of $N_3P_3Cl_6$ (Section 4.2) [63]. This is in contrast to the reactions of various metal halides with hydridophosphazenes, which give materials in which the metal atom is coordinated to the ring through a phosphorus atom (Equation 1.13) [64].

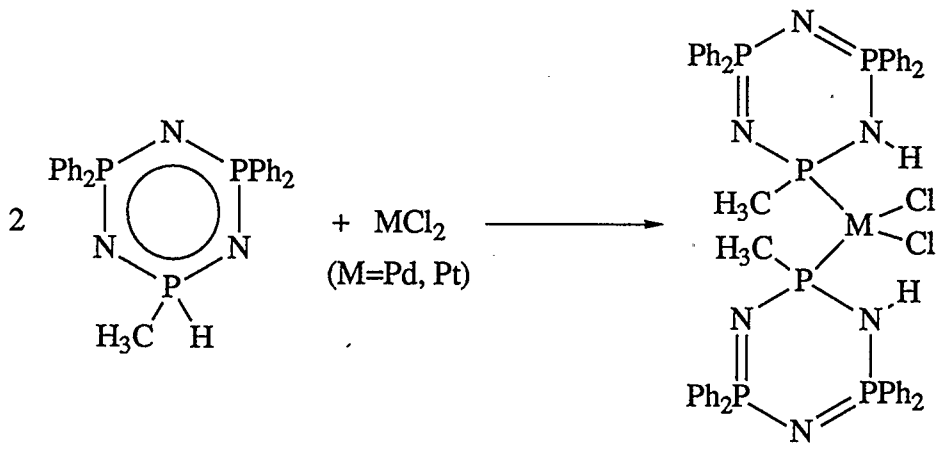

(1.13)

Complexes in which the cyclophosphazene acts as a chelating ligand through two or more nitrogen atoms are also known. The platinum complex $[NP(NHMe)_2]_4PtCl_2$,**19**, exhibits bidentate coordination of the cyclotetraphosphazene ring [65], while for $(NPMe_2)_8Co(NO_3)^+NO_3^-$, **20**, tetradentate coordination is observed [66].

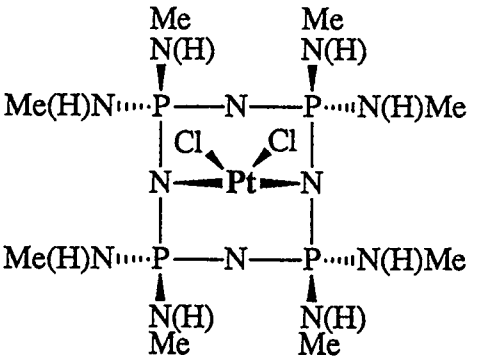

19

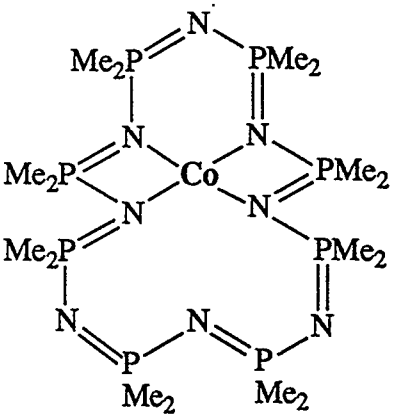

20

A similar chelated product is formed in the reaction between $[NP(NMe_2)_2]_6$ and copper (II) chloride, in which a copper atom is coordinated to four of the six skeletal nitrogen atoms (Figure 1.6) [67].

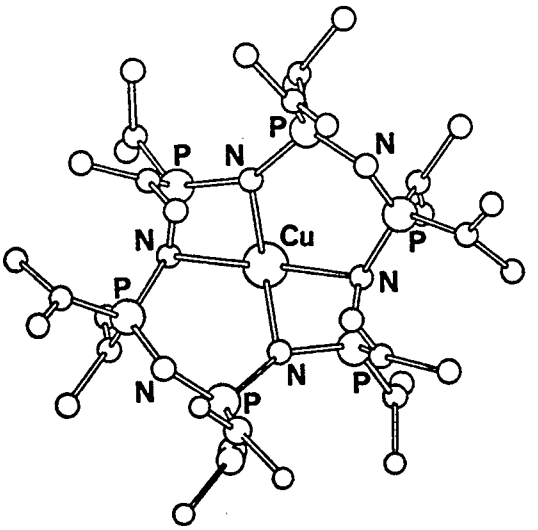

Figure 1.6 - X-ray structure of $[N_6P_6(NMe_2)_{12}CuCl]^+[CuCl_2]^-$. From Ref. [67].

The alkylphosphazenes $(NPMe_2)_{4,5}$ react with metal hexacarbonyls $M(CO)_6$ (M=Mo, W) to give products of the type $(NPMe_2)_{4,5}\bullet M(CO)_3$ [68,69] while for $N_4P_4(NMe_2)_8\bullet W(CO)_4$ bidentate coordination is observed [70,71].

Even though all of the previous examples involve simple σ coordination by skeletal

nitrogen atoms, for at least one complex a π-type interaction has been proposed. The reaction of $N_3P_3Cl_6$ with $Cr(CO)_3(CH_3CN)_3$ gives $N_3P_3Cl_6 \cdot Cr(CO)_3$, for which a π-complex structure has been proposed [72], but not confirmed.

An alternative coordination mode for cyclophosphazenes involves bonding to exocyclic donor sites such as amine nitrogen atoms. However, such complexes are of little interest to this work. A detailed review is provided in reference [34].

1.3 Cyclothiazenes

1.3.1 Introduction

As mentioned in Section 1.1, S_4N_4, the first example of S-N heterocycles, was synthesized over one and a half centuries ago [2]. However, the chemistry of such compounds has only attracted substantial attention in the last two decades due, in large part, to the discovery of the unusual properties of the conducting polymer $(SN)_x$ [4]. Numerous reviews, published in the 1970's [73,74,75,76,77] and 1980's [78,79,80,81,82,83], are a reflection of the high degree of interest in the area of thiazene chemistry. Such detailed reviews preclude the need for a complete description of S-N heterocycles and, as such, the material presented in the following sections will focus on those areas which are most pertinent to this thesis. A general overview of the synthesis, structure and bonding of unsaturated binary S-N rings, especially S_4N_4, will be presented first. This will be followed by an account of the interactions of such rings with both transition-metal centers and nucleophiles as such areas are of primary interest to this work.

1.3.2 Synthesis, Structure, and Bonding

(a) Synthesis

The most widely used route to cyclothiazenes employs the cyclocondensation of ammonia with sulfur halides (Figure 1.7).

The tetrasulfur tetranitride molecule **2**, exhibits a very versatile chemical behavior [73-

83] and has proven to be a particularly useful source of many S-N heterocycles. Some of the extensive chemistry of S_4N_4 is illustrated in Figure 1.8.

The easily obtained cyclothiazyl halides, $S_3N_2Cl^-Cl^+$ (**21**) and $(NSCl)_3$ (**23**), have also proven to be useful for preparing S-N ring systems. The five-membered ring **21**, undergoes various cyclocondensation reactions (Figure 1.9) while the six-membered ring **23**, reacts with nucleophilic or reducing reagents resulting in ring expansion to give S-N cages (Figure 1.10).

Several other preparative techniques are available and, although not described here, are discussed in detail in the review articles referenced in the introduction to this section. However, the examples illustrated in the following figures should provide a good indication of the diversity of preparative methods for cyclothiazenes.

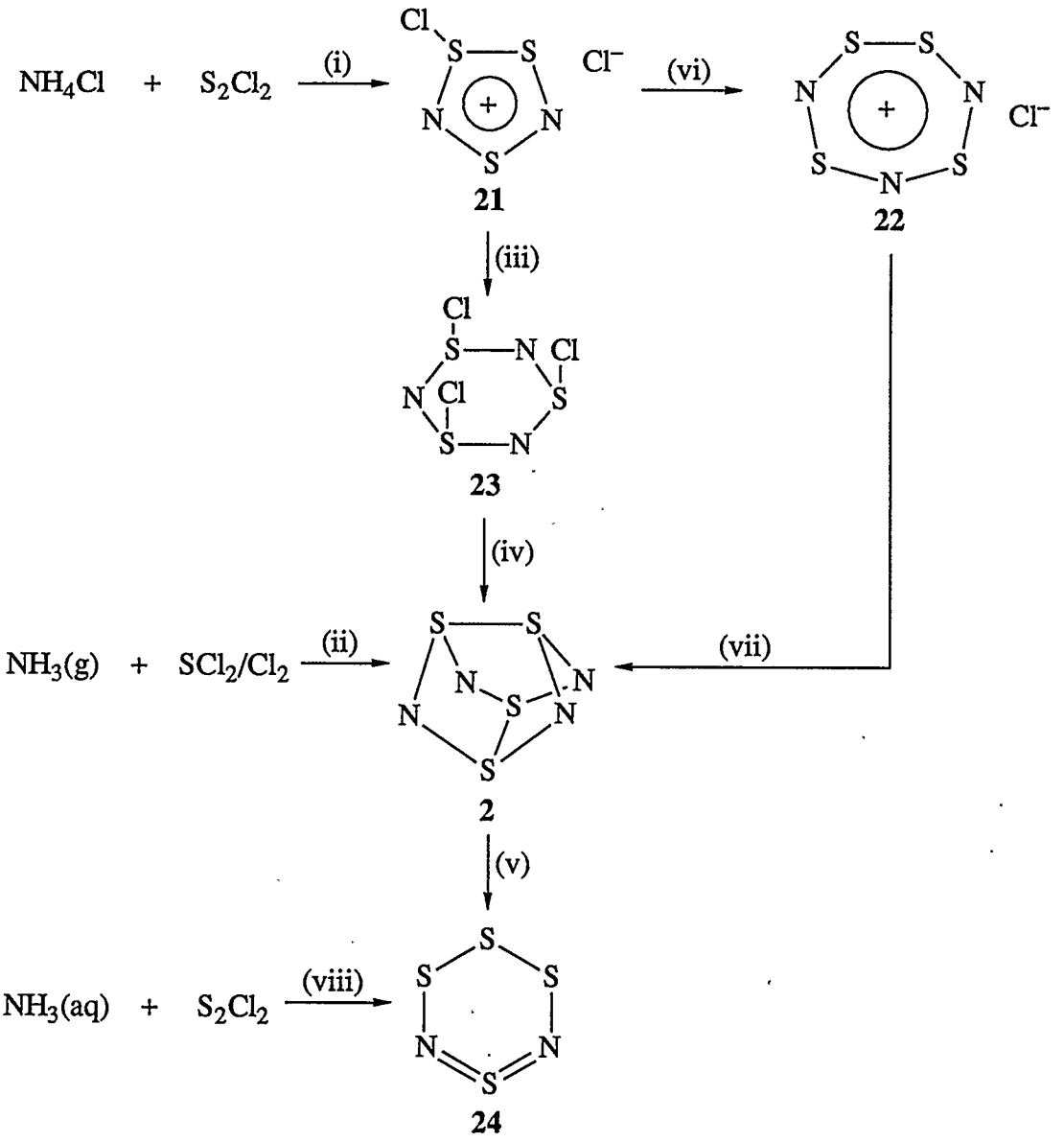

Figure 1.7 - Preparation of various S-N heterocycles from ammonia and ammonium salts and sulfur halides : (i) reflux [84] (ii) CCl_4 or CH_2Cl_2 [85] (iii) Cl_2 or SO_2Cl_2 [86] (iv) Fe, Hg, or Ph_3Sb [87,88,89] (v) S_8/CS_2 [90] (vi) S_2Cl_2 [84] (vii) KI [88,91,92] (viii) 0-5°C [93,94].

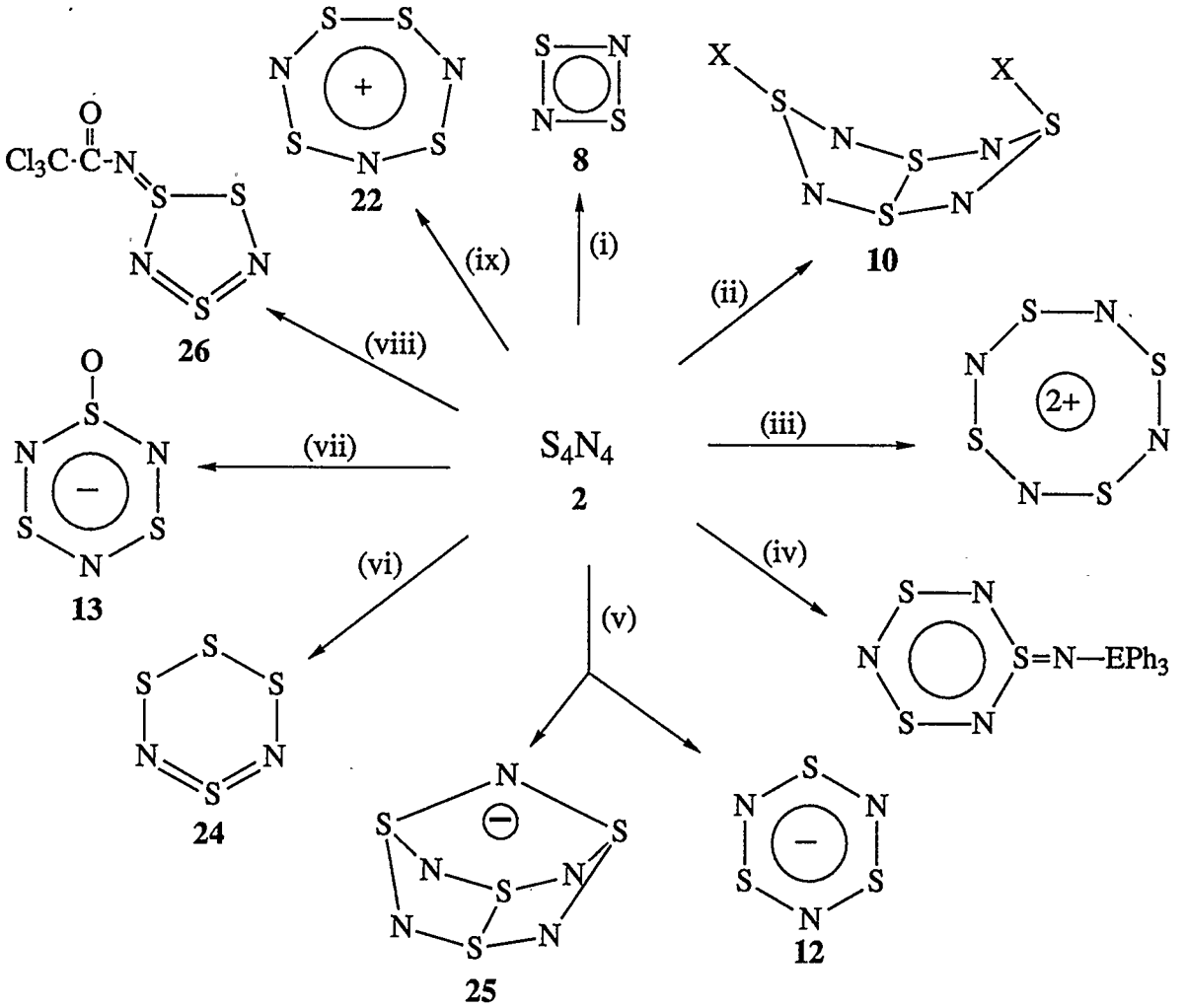

Figure 1.8 - Preparation of S-N heterocycles from S_4N_4

(i) Δ/Ag [7]
(ii) Cl_2, -60°C [95,96,97]
(iii) SbF_5, $SbCl_5$, AsF_5, or HSO_3F [98,99]
(iv) Ph_3P [100,101] or $Ph_3PNSiMe_3$ [102] or Ph_3As [103,104]
(v) N_3^- or S^{2-} or CN^- or e^- [12,13,105]
(vi) $CS_2 + S_8$ [90]
(vii) $(Me_2N)_3S^+NSO^-$ [106]
(viii) $(Cl_3CCO)_2O$ [107,108]
(ix) $Br_{2(l)}$ [109]

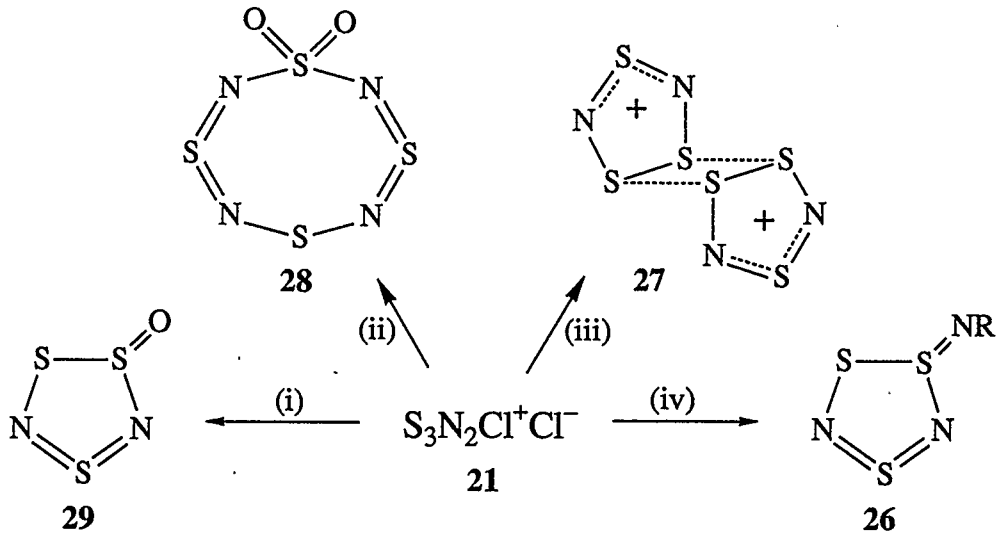

Figure 1.9 - Preparation of S-N heterocycles from $S_3N_2Cl_2$

(i) Formic acid [108]
(ii) $SO_2(NH_2)_2$ [108]
(iii) Δ in vacuo [110]
(iv) $RN(SiMe_3)_2$ [108,111,112]

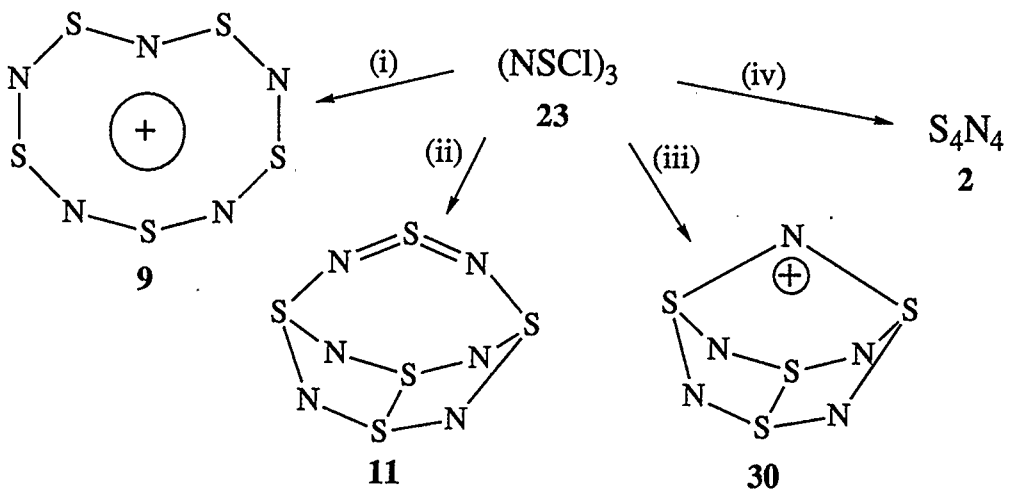

Figure 1.10 - Preparation of S-N heterocycles from $(NSCl)_3$

(i) $S_4N_4/FeCl_3$ in $SOCl_2$ [113,114,115,116]
(ii) $(Me_3Sn)_3N$ [117,118]
(iii) $(Me_3SiN)_2S$ [119,120]
(iv) Fe, Hg, or Ph_3Sb [87-89]

(b) Structure and Bonding

Current bonding models for S-N heterocycles are much more successful than those for cyclophosphazenes in the description of observed structures and chemical reactivities. The first systematic investigation of the bonding of cyclic S-N compounds was made by Banister in 1972. He proposed that planar S-N compounds belong to a class of "electron-rich aromatics" which conform to the Hückel (4n + 2)-π-electron rule [121]. In his description of a binary S-N monocyclic compound, each sulfur atom contributes two and each nitrogen one electron to the π system. Most known monocyclic S-N rings do in-fact conform to such a rule [S_2N_2 (**8**, 6 πe^-), $S_3N_3^-$ (**12**, 10 πe^-), $S_4N_3^+$ (**22**, 10 πe^-), and $S_5N_5^+$ (**9**, 14 πe^-)].

More accurate representations of planar S-N systems have been discussed at the simple Hückel level [122], at the extended Hückel level [78], and at the *ab initio* level [120]. In all cases, antibonding π*-levels (or nπ levels) are occupied to some extent. The accommodation of surplus π-electrons in π* (or nπ) orbitals is likely responsible for lower π bond orders when compared to aromatic hydrocarbons. For example, the HMO π-orbital pattern of $S_3N_3^-$ is similar to that of benzene, except that the degenerate pair of π* orbitals is fully occupied. Consequently the π-bond order in $S_3N_3^-$ is considerably lower than in benzene [122,123] and as a result the skeletal framework is readily broken upon heating. The stability of electron-rich S-N rings relative to the hypothetical carbon analogs is likely due to two factors; (1) the higher electronegativity of nitrogen compared to sulfur lowers the energy of the antibonding π* and the bonding π levels and (2) the larger S-N bond length reduces the repulsion between electron pairs, thus lowering the total energy of the π system [78].

One particularly unusual feature exhibited by many of the larger S-N rings (eight atoms or more) is the strong tendency for the formation of long transannular S-S bonds (2.4-2.7 Å). The formation of such bonds gives rise to bicyclic (folded), tricyclic, or cage structures as depicted in Figure 1.11.

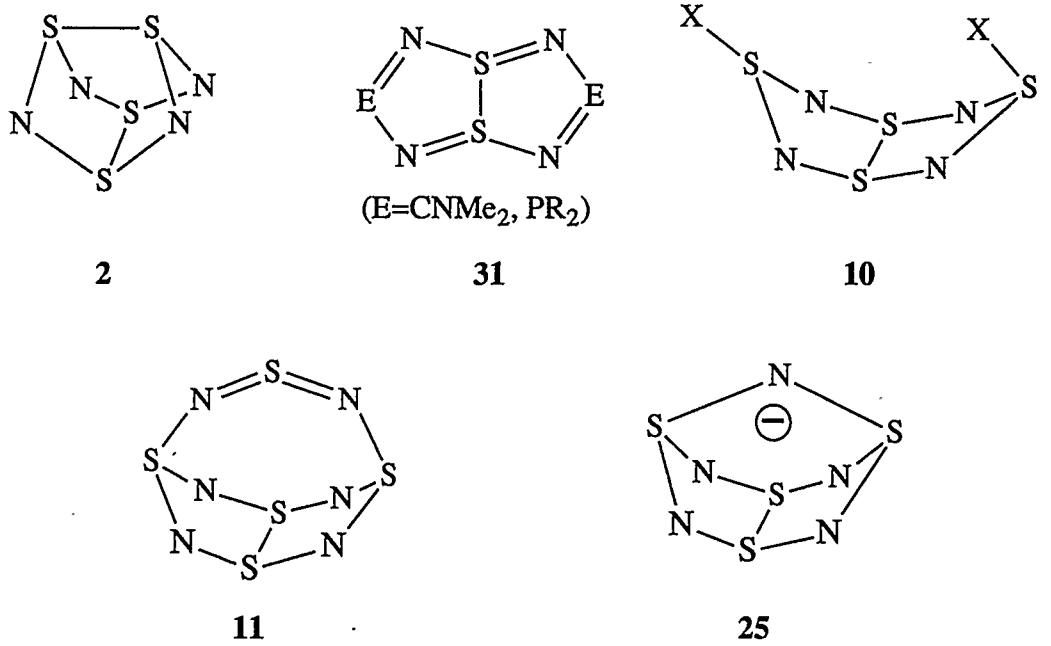

2 **31** **10**

11 **25**

Figure 1.11 - Examples of bicyclic, tricyclic, and cage S-N molecules with transannular S-S interactions

Of the S-N compounds with transannular S-S bonds S_4N_4, **2**, has been the subject of the largest number of theoretical discussions. The solid-state structure of **2**, first established in 1963 [124], and more recently in 1978 [125], shows two cross-ring S-S interactions of 2.601 and 2.597 Å. Extended Hückel MO (EHMO) calculations for S_4N_4 by Gleiter provide an appealing explanation for the cage structure [78,126]. A planar S_4N_4 molecule of D_{4h} symmetry would be a 12 π-electron ring with an open-shell configuration (Figure 1.12a). Such a structure predicts a triplet ground state, which would be unstable with respect to Jahn-Teller distortion. Distortions from perfect D_{4h} symmetry show no or little significant splitting of the orbitals. However, the formation of two transannular S-S bonds does yield a singlet ground state (Figure 1.12b). As a result, the four electrons, previously in degenerate π^* orbitals, are now accommodated in two S-S bonds.

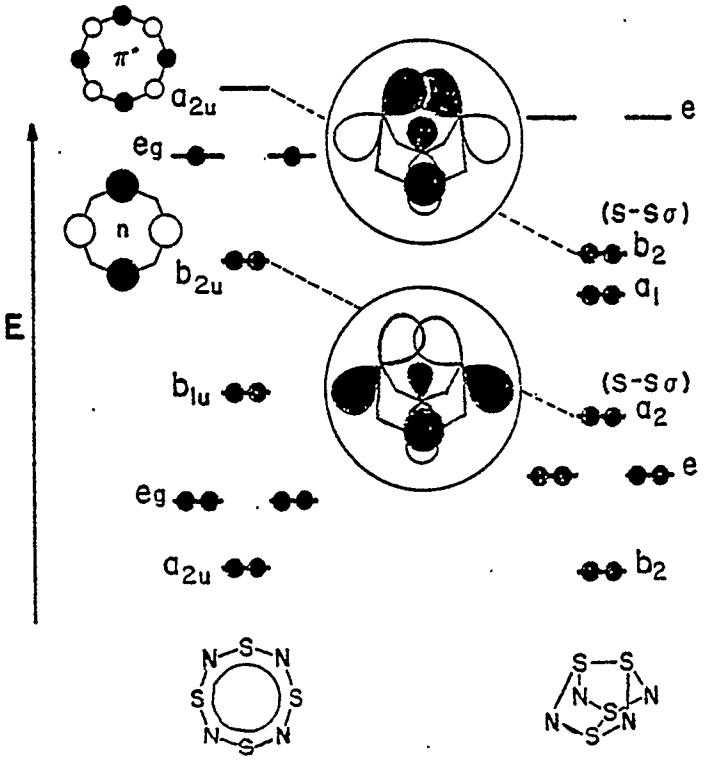

Figure 1.12 - Orbital correlation diagram for the π-orbitals of (a) the hypothetical, planar S_4N_4 molecule and of (b) the observed cage structure (From Ref. [127]).

According to *ab initio* calculations, however, the HOMO of S_4N_4 is a nitrogen based lone pair orbital and not the cross-ring S-S bond, while the LUMO is an S-S (σ*) orbital (Figure 1.13) [120,128,129]. The X-ray fluorescence spectra of **2** support this MO model [130].

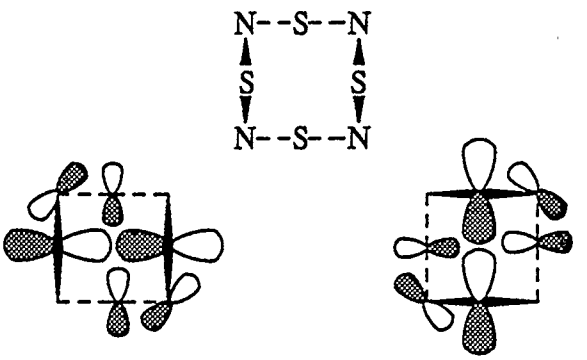

Figure 1.13 - The LUMOs of S_4N_4. From Ref. [81].

Transannular S-S contacts are also observed for the 1,5-disubstituted derivatives of S_4N_4 , **10**. The X-ray crystal structures of three compounds of the type 1,5-$X_2S_4N_4$ (X=Cl [8], NMe_2 [131,132], and Ph_3PN [133,134]) have been determined. For each compound a folded, bicyclic structure, i.e. **10**, is observed and the S-S bond is strengthened compared with S_4N_4, as a result of substitution [d(S-S) = 2.45 Å (X=Ph_3PN, Me_2N) and 2.48 Å (X=Cl), cf. 2.60 Å in S_4N_4]. In each case the X groups adopt *exo*, *endo* positions.

MNDO (Modified Neglect of Diatomic Overlap) molecular orbital calculations of the heats of formation of planar (no S-S bond) and puckered [d(S-S)=2.6 Å] forms of **10** (X=Cl, F, NH_2) predict a higher stability for the latter conformation [135]. The planar form of **10** is calculated to have an antibonding orbital localized over the NSN linkages. Puckering of the molecule alleviates the weakness of these bonds by redistributing the orbital into a transannular S-S interaction.

In extended Hückel MO calculations for 1,5-$X_2S_4N_4$ and the related molecules **11** and **25**, the NSN units involving the unsubstituted (or unbridged) sulfur atoms are considered as two pseudo-allylic five-π-electron fragments [136]. If the substituents X in **10**, or the bridging groups (**11** and **25**) are are able to withdraw π^*-electron density from the S_4N_4 cage, e.g. N^+, the S-S σ-interaction will be weakened and a large S-S separation is expected, and is found for $S_4N_5^+$ [120]. However, if the high lying orbitals of the substituents or bridge atoms are filled (electron rich), eg. N^-, –N=S=N–, or a halogen, then stable cage structures with short S-S distances are predicted, consistent with the observed structures **10**, **11**, and **25**.

A related class of eight-membered S-N rings are the heterocyclothiazenes of the type 1,5-$(RC)_2N_4S_2$ (R=Ph, NMe_2) [137]. The structure of the ring exhibits a remarkable dependence upon the nature of the exocyclic group bound to carbon. A planar 10-π-electron structure is observed for R=Ph (**32**) and a folded structure, with a weak S-S bond (2.50 Å) is observed for R=NMe_2 (**33**).

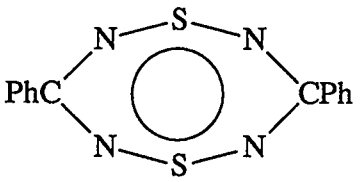

32

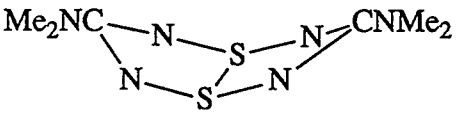

33

Extended Hückel MO calculations show that the structure of the ring depends on the electronegativity of the exocyclic R group, whereby more electronegative groups, e.g. R=Ph, favour a planar structure [138]. Similar results are predicted on the basis of *ab initio* and MNDO calculations which show that electron-rich 10π systems prefer a planar monocyclic structure, while π-donor substituents can induce a pseudo-Jahn-Teller distortion leading to a bicyclic 8-π system with a S-S bond [136,138,139]. Figure 1.20 shows the resulting transformation of the π^* orbital (HOMO) of a planar ring into an S-S bonding interaction of a folded bicyclic ring, i.e. intramolecular π^*-π^* interaction. (See Section 1.4.2).

By contrast, intermolecular S-S bonding is observed for the dimer $S_6N_4^{2+}$, **27** [d(S-S) = 2.99-3.12 Å] [98,140,141]. Experimetal and computational evidence indicates that the five-membered ring radical $S_3N_2^+$ has a $^2A_2$ ground state with the odd electron based primarily in an orbital that is antibonding with respect to the S-S bond (i.e. the dimer exhibits an intermolecular π^*-π^* interaction) [142]. On the basis of a model involving two interacting $H_2S_2^+$ species, MO arguments suggest that $S_6N_4^{2+}$ can be pictured as two monomer units loosely held together by a six-electron four-center bond [142].

Many of the mixed P-N-S rings (cyclophosphathiazenes) also exhibit cross-ring S-S interactions. These will be discussed in section 1.4.2.

1.3.3 Coordination Chemistry (Transition-Metal Complexes)

Cyclothiazenes form a wide variety of transition-metal complexes. A review of early work on such complexes was published by Weiss in 1966 [143]. There has since been a dramatic increase in interest in this area, which is likely a result of advances in X-ray

crystallography as a physical characterization technique, rather than NMR spectroscopy, as neither sulfur nor nitrogen are readily amenable NMR nuclei. Consequently, more complete reviews by Chivers and Edelmann [144] and by Kelly and Woollins [145] were published in 1986 . For this work only two classes of S-N complexes will be covered; σ-(N) bonded complexes of S_2N_2 and S_4N_4, and cyclometallathiazenes, MS_xN_y.

(a) σ-(N) bonded Complexes

Metal complexes of binary sulfur nitrides such as S_2N_2 and S_4N_4 can be considered typical Lewis acid-Lewis base adducts in which the ligand is bonded to the metal via a nitrogen atom. While S_4N_4 complexes of this type, such as $MoCl_5 \cdot S_4N_4$ [146] and $TiCl_4 \cdot S_4N_4$ [147], were first described early this century, the first complex of S_2N_2 was not reported until 1980 [148]. The delayed development of the coordination chemistry of S_2N_2 is probably due to the difficulties involved in handling this explosively labile compound.

Complexes of S_2N_2 have been prepared by reactions of transition-metal halides with a variety of S-N precursors. Examples of the three most widely used preparative routes are outlined below :

(i) Cleavage of S_4N_4 complexes

This thermolytic technique has been reported for AlX_3 (X=Cl [149] and Br [150]), $CuCl_2$ [148], VCl_4 [151], and $TiCl_4$ [152] (Eq. 1.14).

$$2\ TiCl_4 \cdot S_4N_4 \xrightarrow{125°C} 2\ TiCl_4 \cdot S_2N_2 + S_4N_4 \qquad (1.14)$$

(ii) Reduction of $(NSCl)_3$ (**23**) or $S_3N_2Cl_2$ (**21**).

In some cases chlorides of transition metals react with **23** or **21** to give S_2N_2 complexes [153,154] (Eq. 1.15).

$$[Ph_4As][VCl_5] + (NSCl)_3 \xrightarrow{CH_2Cl_2} [Ph_4As][(\mu\text{-}S_2N_2)(VCl_5)_2] \quad (1.15)$$

$$\downarrow (NSCl)_3$$

$$[Ph_4As][(S_2N_2)VCl_4]$$

(iii) Thermolysis of thiazyl chloride complexes

Thermolysis of the complexes $MCl_5(NSCl)$ (M=Nb or Ta) results in the reductive elimination of Cl_2 to give S_2N_2-bridged complexes [155] (Eq. 1.16).

$$2\,MCl_5(NSCl) \xrightarrow{\Delta} (\mu\text{-}S_2N_2)(MCl_5)_2 + Cl_2 \quad (1.16)$$

The preparation of metal complexes by direct reaction with S_2N_2 has only been reported for $TiCl_4 \cdot S_2N_2$ [152].

Both mono- and bidentate coordination modes are observed for disulfur dinitride, although monodentate coordination has only been proven for $[(Ph_3P)_2(CO)_2(S_2N_2)RuCl][AlCl_4]$ [152] (Figure 1.14a). In all other structurally characterized compounds S_2N_2 acts as a bidentate, bridging ligand with nitrogen atoms as the donor sites (Figure 1.14b). The geometry of coordinated S_2N_2 is not substantially different than that of free S_2N_2 [d(SN) = 1.60-1.68 Å, <(NSN) = 84-86°, <(SNS) = 94-96°] [7]. Bonding of all four ring atoms of S_2N_2 can also be envisioned, and, although no such complexes have been reported, EHMO calculations predict that π-type sandwich complexes such as $M(\eta^4\text{-}S_2N_2)_2$ and $(\eta^4\text{-}S_2N_2)M(C_5H_5)$ (M=Cr, Mo, or W) may be possible [156].

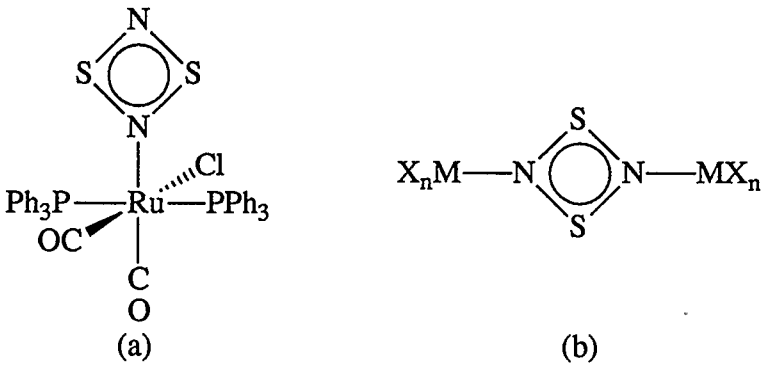

Figure 1.14 - Coordination modes of S_2N_2.
(a) Monodentate N-coordination
(b) Bidentate, bridging coordination

Numerous claims have been made with regard to the preparation of transition-metal complexes of S_4N_4. Such complexes were the subject of a review by Alange and Banister in 1978 [157]. However, reactions between S_4N_4 and transition-metal halides often result in fragmentation of the S_4N_4 ring to give S_2N_2 complexes or cyclometallathiazenes. This, combined with a lack of an adequate NMR probe, makes structural assignment somewhat tentative unless it is supported by X-ray crystallographic data.

The structures of five 1:1 adducts of S_4N_4 with transition-metal halides have been determined by X-ray crystallography, $TaCl_5 \cdot S_4N_4$ [158], $FeCl_3 \cdot S_4N_4$ [159], $CuCl \cdot S_4N_4$ [160], $CuBr \cdot S_4N_4$ [161], and $CuCl_2 \cdot S_4N_4$ [162]. For the Ta and Fe complexes the S_4N_4 ligand is coordinated via one of the nitrogen atoms. The cage structure of S_4N_4 is not retained however. Instead a boat-shaped eight-membered ring with approximately coplanar sulfur atoms results (Figure 1.15a).

A different coordination mode is exhibited by S_4N_4 in the three copper complexes. For the two CuX (X=Cl, Br) compounds, polymeric structures are formed in which the metal centers are bridged by two 1,3-N,N′-bidentate S_4N_4 ligands (Figure 1.15b). The $CuCl_2$ adduct also has a polymeric structure, with the metal centers bridged both by chlorine and 1,3-N,N′-bidentate S_4N_4 ligands (Figure 1.15c). The conformation and structural

parameters for these bidentate ligands are not significantly different from those of free S_4N_4.

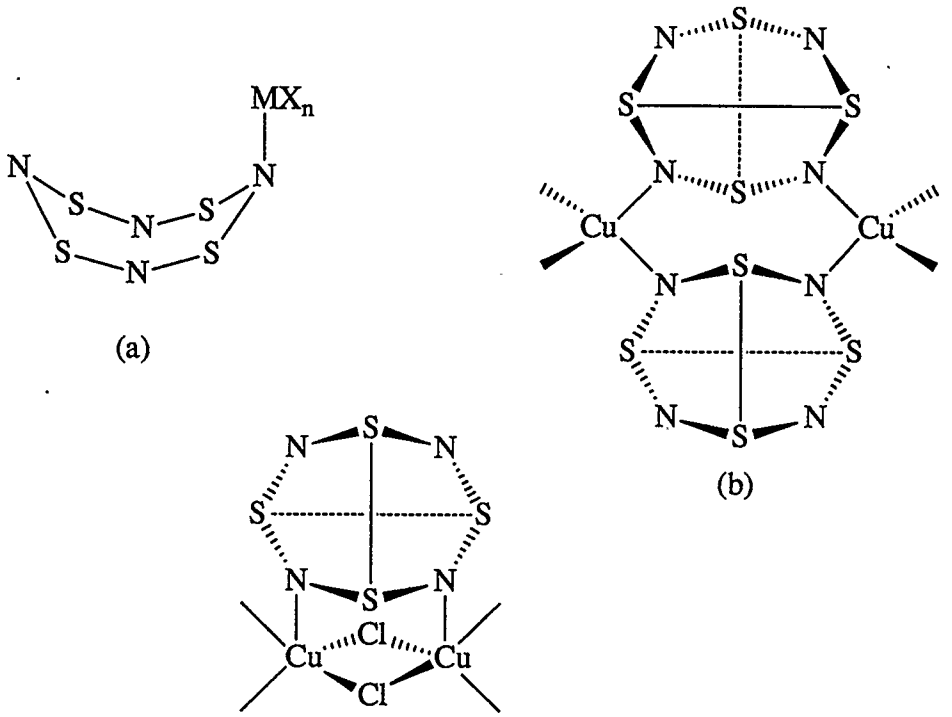

Figure 1.15 - Structures of 1:1 adducts of S_4N_4
(a) $MX_n \cdot S_4N_4$ (MX_n=$TaCl_5$, $FeCl_3$)
(b) $CuX \cdot S_4N_4$ (X=Cl, Br)
(c) $CuCl_2 \cdot S_4N_4$

(b) Cyclometallathiazenes

Cyclometallathiazenes, represented by the general formula MS_xN_y, are an important class of compounds in which the metal atom is a constituent of the S-N ring. They can be considered as complexes of cationic metal fragments and binary S-N anions.

The five-membered metallacycles MS_2N_2 (M=Co, Ir, Ni, Pd, Pt, and Pb), and the related protonated rings MS_2N_2H (M=Co, Ni, Pd, and Pt), represent the best characterized group of S-N ring systems containing a transition-metal center. The compounds of greatest

interest to this work are those metallacycles which contain a platinum group metal center (Ni, Pd, Pt). With few exceptions compounds of this type have been synthesized by the reaction of S_4N_4 with various metal complexes. Although represented as mononuclear five-membered rings, **34**, the S_2N_2 unit can also be part of a dimeric structure, **35**.

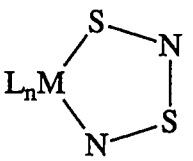

34

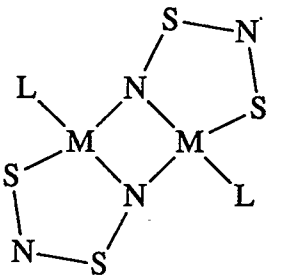

35

The mononuclear platinum complex $(Ph_3P)_2PtS_2N_2$, is obtained on treatment of the Pt(0) reagents $(Ph_3P)_2Pt(C_2H_4)$ [163] or $(Ph_3P)_4Pt$ [164] with S_4N_4 in a 2:1 molar ratio in CH_2Cl_2-ether (Eq. 1.17). The related anionic nickel complex containing two $S_2N_2^{2-}$ chelate ligands has been prepared by a different approach. In this case $Ni(S_2N_2H)_2$ is deprotonated by KOH in methanol to give red $K_2[Ni(S_2N_2)_2]$ [165] (Eq. 1.18).

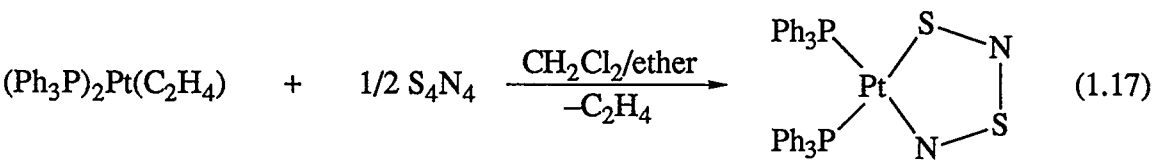

(1.17)

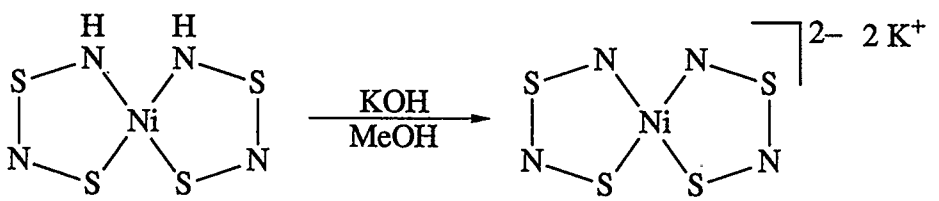

(1.18)

Neutral dinuclear MS_2N_2 complexes of the structural type **35** have also been described for Ni, Pd, and Pt. For example, reaction between $[(Ph_3P)_2Ni(C_3Ph_3)][ClO_4]$ and S_4N_4 in CH_2Cl_2 gives $[(Ph_3P)NiS_2N_2]_2$ in low yield [165,166]. The analogous palladium complex is obtained from S_4N_4 and $(Ph_3P)_2Pd(C_2H_4)$ [166] or $(Ph_3P)_4Pd$ [167]. As indicated above the mononuclear platinum complex $(Ph_3P)_2PtS_2N_2$, is formed from $(Ph_3P)_2Pt(C_2H_4)$ and S_4N_4 in CH_2Cl_2-ether. However, if THF or benzene is employed as the reaction solvent, the dinuclear complex $[(Ph_3P)PtS_2N_2]_2$, **35** (M=Pt, L=PPh_3), is formed [166]. The same product is also produced by using $(Ph_3P)_4Pt$ in a 1:1 molar ratio with S_4N_4 [167].

The most notable feature of the transition-metal complexes of the $S_2N_2^{2-}$ ion, as determined by X-ray crystallography, is that there are two short and one long S-N bonds indicating a localization of π-bonding within the thiazene unit. The longer S-N bond (1.66-1.69 Å) approximates a single bond whereas the latter two (1.51-1.58 Å) are close to double bond values. Such localized bonding is consistent with the valence bond description illustrated by structure **36**.

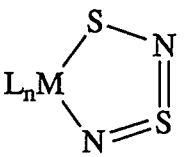

36

Several platinum group metal complexes of other S-N anions are also known. Syntheses of a platinum complex of S_3N^- have been reported recently. Reaction of S_4N_4 with *cis*-$PtCl_2(PMe_2Ph)_2$ at ≈140°C in xylene [168] or at 0°C by use of photolysis [169] gives $Pt(S_3N)Cl(PMe_2Ph)$, although no structural information is available. Another S_3N^- complex, $Ni(S_3N)_2$, has been known for many years. It is best prepared via metathetical reactions of salts of the free S_3N^- ion [170,171]. The related complex ion $[(NiS_3N)_3S_2]^-$,

37, is obtained in the reaction of S_7NH with KOH in the presence of $NiCl_2 \cdot 6\ H_2O$ in methanol [172]. Each of the three Ni atoms is chelated to an S_3N^- ion and the central cluster is an Ni_3S_2 unit.

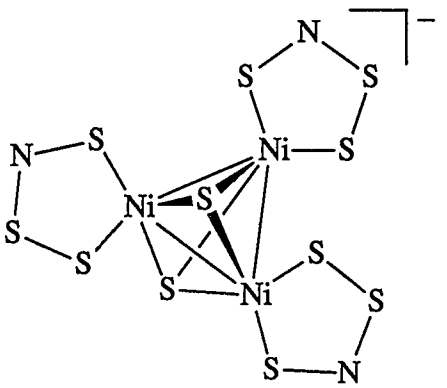

37

There has been one brief report of the preparation of a tridentate (N,S,S′) S_4N_3-platinum complex, **38**, whose structure was determined by X-ray crystallography [173]. It is obtained by heating *cis*-$PtCl_2(NCC_6H_5)_2$ with S_4N_4 in toluene under reflux.

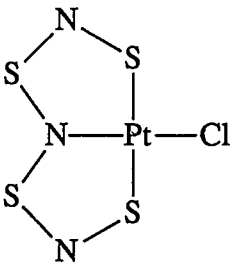

38

As illustrated by the previous examples, reaction of S_4N_4 with transition-metal reagents often results in disruption of the S_4N_4 cage to give products that are formally complexes of smaller, binary S-N anions. Until just recently the only complexes in which S_4N_4 remained intact were those which involved coordination of the metal atom to a nitrogen atom via a lone pair of electrons. However, in 1986 Roesky reported the first example of a tridentate

$S_4N_4^{2-}$ complex, $IrCl(CO)(Ph_3P)(S_4N_4)$, **39** [174]. The distinguishing feature of the structure of this compound is that the metal fragment has inserted into an S-N bond of S_4N_4 and is also coordinated to a second sulfur atom, thus resulting in the formation of a bicyclometallathiazene (facial geometry).

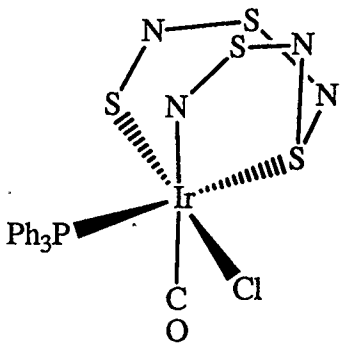

39

The preparation of $Pt(S_4N_4)Cl_2(PMe_2Ph)$, **40**, from the reaction of S_4N_4 with $PtCl_2(PMe_2Ph)$ represents only the second example of a complex of $S_4N_4^{2-}$ [175]. The $S_4N_4^{2-}$ ligand is again tridentate (N,S,S′), but its geometry differs substantially from **39**, displaying meridional rather than facial coordination. It is proposed that **40** undergoes meridional to facial isomerization upon heating in $CHCl_3$, on the basis of ^{15}N-labelling studies [176] (Equation 1.19).

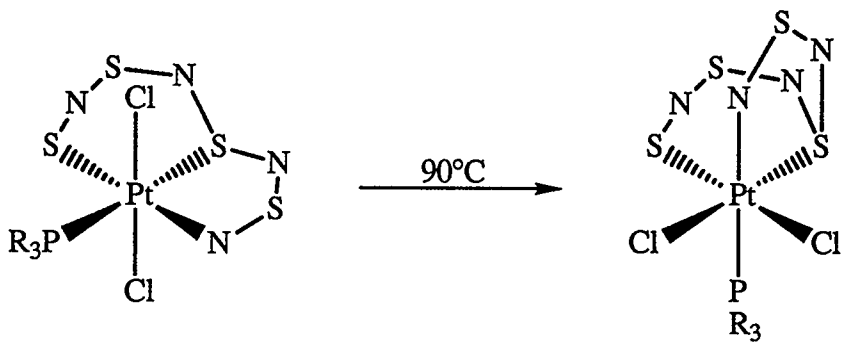

(1.19)

40
(meridional isomer)

41
(facial isomer)

1.4 Cyclophosphathiazenes

1.4.1 Introduction

As mentioned in the introduction to this chapter, the combination of monomer R_2PN and SN units provides many possibilities for the class of inorganic heterocycles called cyclophosphathiazenes. Although at a much earlier stage of development than cyclophosphazene or cyclothiazene chemistry enough work has been published to warrant a review of cyclophosphathiazene chemistry. Early reviews of such rings containing two- or three-coordinate sulfur [177] and four-coordinate sulfur [178], as well as a recent account of the chemistry of the diphosphadithiatetrazocines and their related S,S′-dialkyl(aryl) derivatives [179] have been published (Note: The suffix *ocine* refers to an unsaturated eight-membered ring containing nitrogen).

With the combination of phosphazene and thiazene units one can create a homologous series of two-coordinate cyclophosphathiazenes, $(R_2PN)_x(SN)_y$ (Figure 1.16). Similarly, the combination of R_2PN and NSX units affords heterocyles containing phosphorus, nitrogen, and three-coordinate sulfur (Figure 1.16) which may be considered hybrids of the cyclophosphazenes and $(NSCl)_3$.

All of the P-N-S rings illustrated in Figure 1.16, apart from 1,3-$(R_2PN)_2(NSX)_2$, **45**, which readily converts to the six-membered ring **44** (X=Cl), or to the salts $[Ph_8P_4N_6S_2]^{2+}[X_3^-]_2$ (X=Br, I), have been isolated and characterized. This section describes the preparation, molecular and electronic structures, and reactions of these various cyclophosphathiazenes with emphasis on the 1,5-diphosphadithiatetrazocines, **16**.

Cyclophosphathiazenes of the general formula $(R_2PN)_x(SN)_y$:

(y must be even for neutral, non-radical rings)

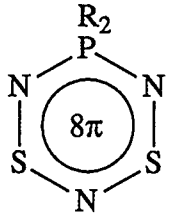

15

x=1, y=2

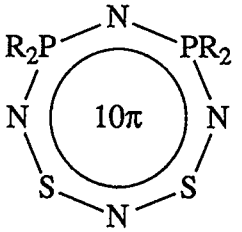

17

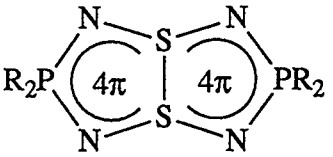

16

x=2, y=2

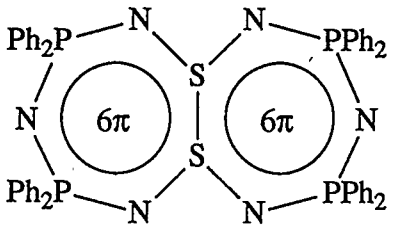

42

x=4, y=2

Cyclophosphathiazenes of the general formula $(R_2PN)_x(NSX)_y$:

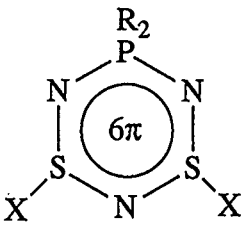

43

x=1, y=2

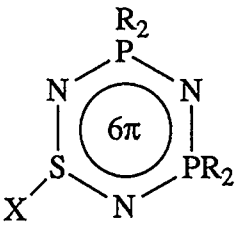

44

x=2, y=1

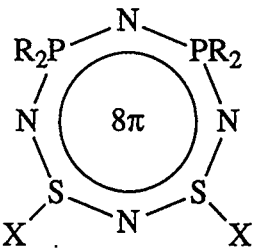

45

x=2, y=2

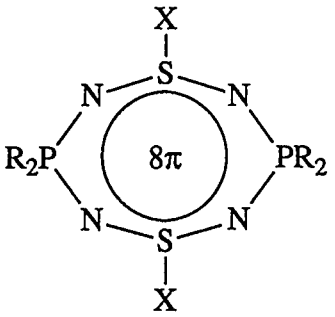

46

x=2, y=2

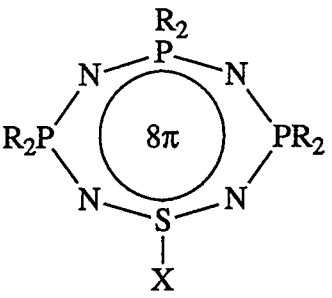

x=3, y=1

Figure 1.16 - Cyclophosphathiazenes with 2 or 3 coordinate sulfur.

1.4.2 Synthesis, Structure, and Bonding

(a) Synthesis

The first reported example of a cyclophosphathiazene containing a two- or three coordinated sulfur atom was the six-membered ring $(Cl_2PN)_2NSCl$, (**44**, R=X=Cl), which was isolated as a colorless oil from the reaction of PCl_5 with $Me_3SiN{=}S{=}NSiMe_3$ [180]. This six-membered ring has been recently shown to undergo thermally induced ring-opening to yield the first example of a new class of inorganic polymers, the poly(thiophosphazenes), i.e. repeating P(V)-N and S(IV)-N units [181]. Heterocycles of type **44** are also produced in reactions between S_4N_4 and trivalent phosphorus compounds containing P-Cl bonds. For example, moisture-sensitive, pale-yellow crystals of $(Ph_2PN)_2NSCl$ (**44**, R=Ph, X=Cl) are obtained in the reaction of Ph_2PCl with S_4N_4 in a 3:1 molar ratio [182] (Equation 1.20).

$$3\ Ph_2PCl + S_4N_4 \xrightarrow[3\ hr.]{CH_3CN\ reflux} \text{(1.20)}$$

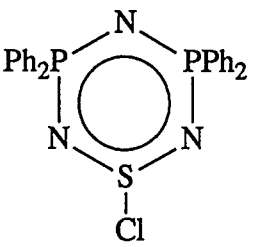

44 : R=Ph, X=Cl

The other known members of the cyclophosphathiazene series with three-coordinate sulfur **43**, **45**, and **46**, are synthesized by the oxidation of the corresponding two-coordinate sulfur heterocyles **15**, **17**, and **16**, respectively. As such, these compounds will be discussed in the next section which describes the chemical properties of the cyclophosphathiazenes.

Just as the first reported cyclophosphathiazene containing a three-coordinate sulfur was a six-membered ring, so too was the first two-coordinate sulfur ring. The heterocycle $(Me_3SiNH)_2PN_3S_2$ (**15**, R=Me_3SiNH), is produced by the reaction of S_4N_4 with the phosphorus (V) reagent, $(Me_3Si)_2NP(NSiMe_3)_2$ [16]. A more general route to six-

membered rings of this type is the reaction of R_2PPR_2 (R=Ph, Me) [183,184] or, preferably, Ph_2PH [185] with S_4N_4 in toluene under reflux. A high-yield synthesis (86%) of $Ph_2PN_3S_2$ (**15**, R=Ph), from S_4N_4 and the phosphorus (V) reagent $Ph_2P(NHSiMe_3)(NSiMe_3)$, has recently been reported [186].

The nucleophilic degradation of S_4N_4 by Ph_2PH or R_2PPR_2 (R=Ph, Me) also yields minor amounts of both the 1,3 and 1,5 isomers of the eight-membered rings $R_4P_2N_4S_2$ (**16** and **17**) [183-185,187]. Other preparative techniques, which are discussed in more detail in Chapter 2, include the reaction between $S_3N_3^-$ and Ph_2PCl [188] and the cyclocondensation of the silylamino(phosphinimines), $R_2PN_2(SiMe_3)_3$, with SCl_2 [186]. The latter preparative route is the preferred one as it gives good yields (>50%) from readily available starting materials.

(b) Structure and Bonding

X-ray crystallographic studies have confirmed the existence of a six-membered heterocyclic ring for two derivatives of $R_2PN_3S_2$, R=Ph [183,184] and R=Me_3SiNH [189]. The structure of $Ph_2PN_3S_2$ shows an essentially planar NSNSN unit with the phosphorus atom tilted out of the plane by 0.28 Å (Figure 1.17).

Ab initio HFS calculations on $H_2PN_3S_2$ have verified the conclusions of a simple Hückel MO analysis that the heterocyclic ring is an eight π-electron system in which the HOMO is a π^* orbital [184].

The structure of the eight-membered ring 1,3-$Ph_4P_2N_4S_2$ resembles that of the six-membered ring $Ph_2PN_3S_2$, in that the NSNSN unit is again essentially planar while the phosphorus atoms lie out of and on opposite sides of this plane [185]. An ORTEP plot of 1,3-$Ph_4P_2N_4S_2$ is shown in Figure 1.18.

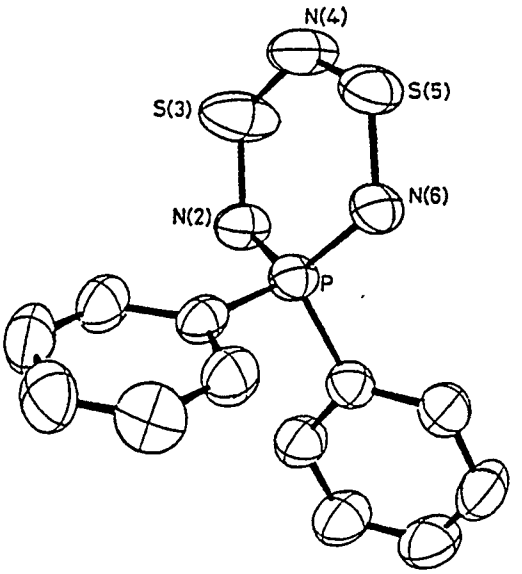

Figure 1.17 - ORTEP drawing of $Ph_2PN_3S_2$. From Ref. [183].

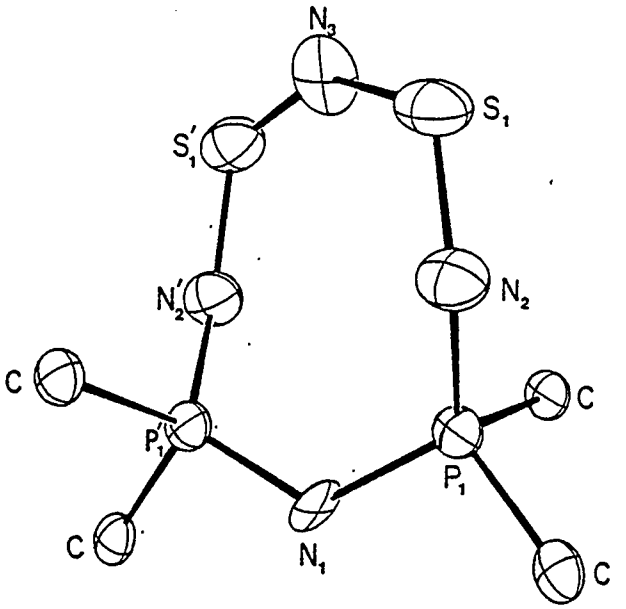

Figure 1.18 - ORTEP drawing of 1,3-$Ph_4P_2N_4S_2$ (**17**, R=Ph). Only the α-carbons of each Ph ring are shown. From Ref. [185].

The structures of two derivatives of the 1,5-isomer **16** (R=Ph [185], Me [187]) have been determined by X-ray crystallography. For both derivatives a folded eight-membered ring with a transannular S-S bond is observed [d(S-S) = 2.55 Å (R=Me), 2.53 Å (R=Ph)]. An ORTEP plot of 1,5-$Ph_4P_2N_4S_2$, including some of the pertinent bond lengths and angles, is shown in Figure 1.19.

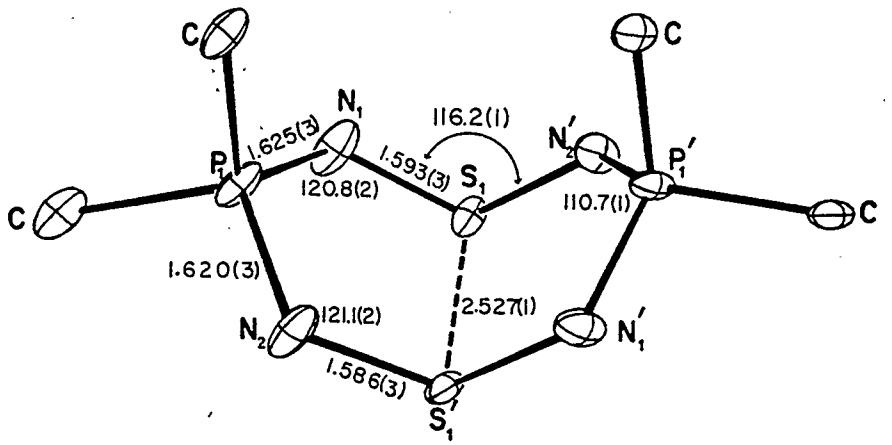

Figure 1.19 - ORTEP drawing of 1,5-$Ph_4P_2N_4S_2$ (**16**, R=Ph) showing pertinent bond lengths (Å) and angles (°). From Ref. [185].

For each derivative the two sulfur and four nitrogen atoms form two four-membered S_2N_2 planes which intersect at angles of ca. 115° (R=Me) and ca. 117° (R=Ph). The phosphorus atoms of the phenyl compound lie 0.214 Å below the respective S_2N_2 planes while for the methyl derivative the phosphorus atoms lie above and below the planes by ca. +0.19 and –0.48 Å, respectively. This difference is apparently due to a solid-state effect [187]. However, in solution the phosphorus atoms are equivalent based on ^{31}P NMR data.

Because of the S-S interactions and the consequent angle strain associated with the PS_2N_2 rings, the geometry of each R_2PN_2 unit differs significantly from that found in methyl- or phenylcyclophosphazene structures; the mean endocyclic bond angles at

phosphorus [110.7° (R=Ph), 108.6° (R=Me)] and nitrogen [121.0° (R=Ph), 120.7° (R=Me)] are smaller than in $(Ph_2PN)_4$ [190] ($<P_{endo}$=119.9°, <N=127.9°) and $(Me_2PN)_4$ [191] ($<P_{endo}$=119.8°, <N=132.0°). The mean P-N distances for 1,5-$R_4P_2N_4S_2$ [1.623 Å (R=Ph), 1.636 Å (R=Me)] are also significantly longer than in $(Ph_2PN)_4$ (d(P-N)=1.590 Å) and $(Me_2PN)_4$ (d(P-N)=1.596 Å). This lengthening of the P-N bond has been attributed to the relative weakness of the π bonds of the four-electron three-center subunits of 1,5-$R_4P_2N_4S_2$ as opposed to the π bonds found for the cyclophosphazenes [185,187].

The existence of the short transannular S-S interaction is the most interesting feature of the 1,5-diphosphadithiatetrazocines. As was discussed earlier in this chapter (Section 1.3.2(b)), such an interaction is not uncommon for the larger cyclothiazenes. The theoretical arguments for the cyclothiazenes have been extended to include the 1,5-diphosphadithiatetrazocines, based on the electronegativity of the heteroatoms in the 1,5-positions rather than their exocyclic ligands [187]. Simple HMO calculations for the two limiting structures, the 10-π planar ring **47**, and the folded, bicyclic **31**, show that changing the electronegativity of the heteroatom, E, has predictable effects on each system.

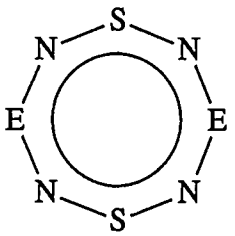

47

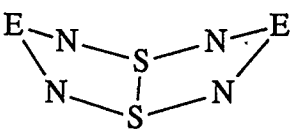

31

The planar model **47** is stabilized by more electronegative elements such as S^+, while the folded structures are favoured for heterocycles containing less electronegative elements such as phosphorus (Figure 1.20 shows a correlation diagram for the two limiting structures). However, it is conceivable that through modification of the ligands on phosphorus, e.g., by replacement of the alkyl/aryl groups by fluorine, the electronegative perturbation might be

sufficient to induce planarity. As the electronegativity of carbon falls between that of phosphorus and sulfur, the structures of the carbon-containing rings are highly sensitive to the electronegativity of the exocyclic groups.

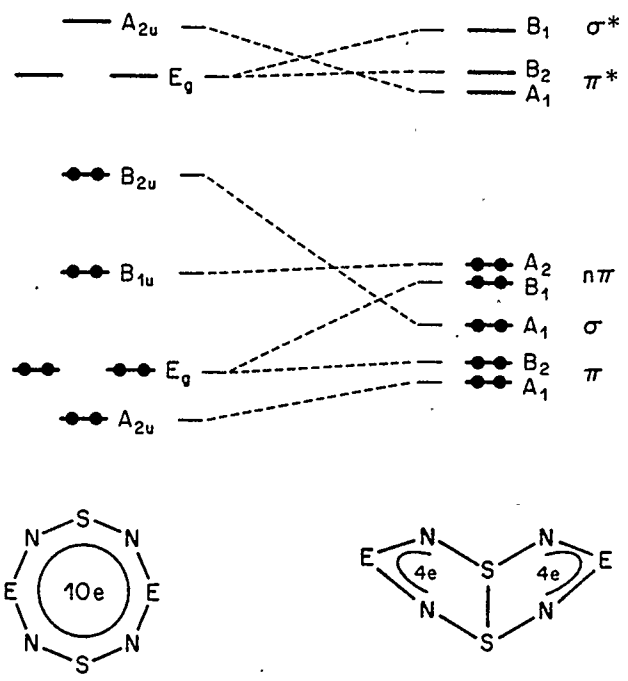

Figure 1.20 - Orbital symmetry correlation diagram for the planar (left) and folded (right) structures of 1,5-$E_4N_4S_2$ (From Ref. [187]).

The HOMO of the folded structure **16** (Figure 1.21) can be viewed as an intramolecular π^*–π^* interaction and it is the main contributor to the transannular interaction [192].

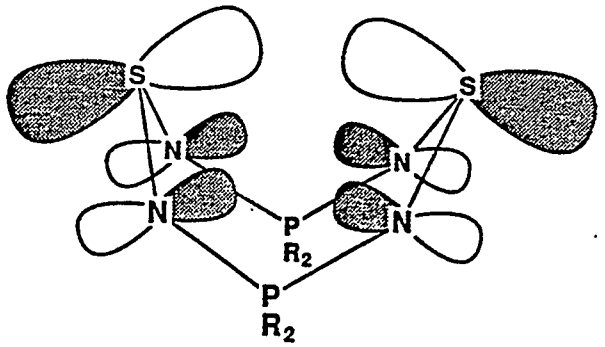

Figure 1.21 - The HOMO of 1,5-diphosphadithiatetrazocines.

The tendency of π-electron-rich cyclophosphathiazenes to form intra-ring S-S bonds is also exhibited by the twelve-membered ring $Ph_8P_4N_6S_2$ (**42**) [193] , and the fifteen-membered spirocycle $Ph_8P_4N_8S_3$ (**48**) [194].

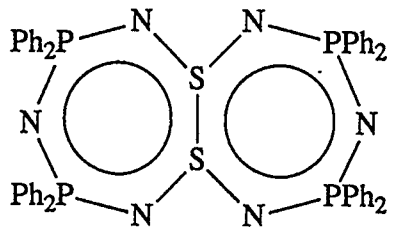

42

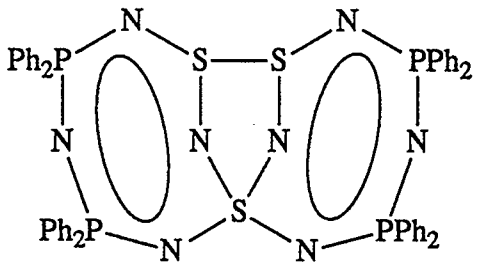

48

1.4.3 Chemical Properties

(a) Oxidative-addition reactions

It is not surprising that the electron-rich P-N-S heterocycles are easily oxidized. The smooth oxidative-addition of Cl_2 to $R_2PN_3S_2$ (**15**, R=Ph, Me), using SO_2Cl_2 or, preferably, $PhICl_2$ yields the dichlorinated rings $R_2PN_3S_2Cl_2$ (**43**, R=Ph, Me) [195,196]. Subsequent reaction with $Me_3SiNSNSiMe_3$ gives the bicyclic compounds $R_2PN_5S_3$ (**49**, R=Ph, Me), which, upon thermolysis, regenerate the six-membered rings, $R_2PN_3S_2$, via reductive elimination of NSN [196] (Equation 1.21).

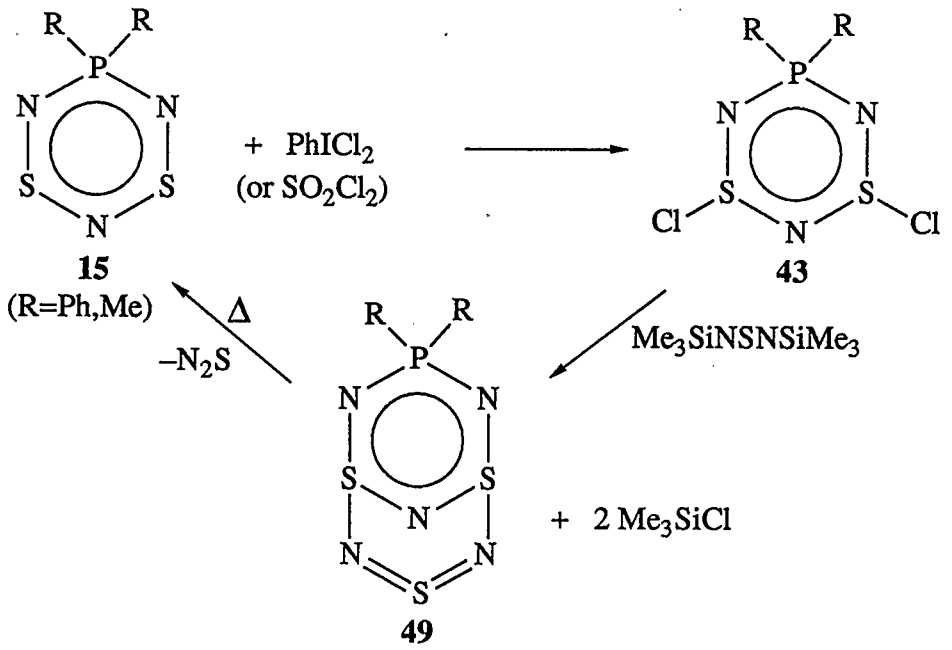

(1.21)

The 1,5-diphosphadithiatetrazocine 1,5-$Ph_4P_2N_4S_2$ (**16**, R=Ph), is also easily oxidized by either Br_2 or Cl_2 (as SO_2Cl_2) at room temperature in CH_2Cl_2 to give the bifunctional heterocycles 1,5-$Ph_4P_2N_4S_2X_2$ (**46**, R=Ph, X=Br, Cl) [197] (Equation 1.22).

1,5-$Ph_4P_2N_4S_2$ + Br_2 or SO_2Cl_2 ⟶ 1,5-$Ph_4P_2N_4S_2X_2$ (1.22)

16 (R=Ph) **46** (R=Ph, X=Br, Cl)

The structure of the brominated derivative consists of an eight-membered ring in which the two phosphorus atoms and four nitrogen atoms are planar and the two sulfur atoms are displaced on either side of the plane by 0.54 and 0.58 Å respectively, to give a chair conformation (Figure 1.22). The exocyclic bromine substituents adopt a *trans* configuration.

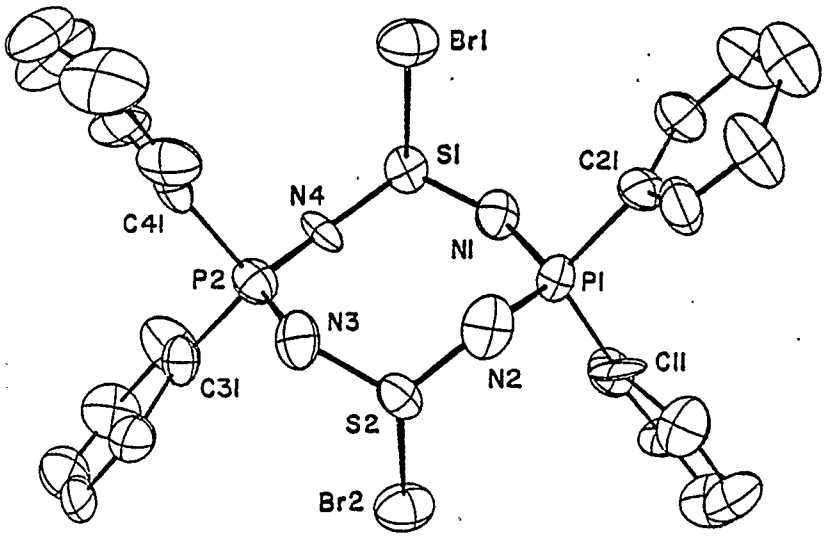

Figure 1.22 - ORTEP drawing of 1,5-$Ph_4P_2N_4S_2Br_2$ (**46**, R=Ph, X=Br). From Ref [197].

The observed *trans*-stereochemistry for this polar oxidation is similar to that observed for the halogenation of alkenes, suggesting an isolobal correspondence between the σ and σ^* orbitals of the S-S bond, and the π and π^* orbitals of an alkene (Figure 1.23) [198]. The halogenation of 1,5-$Ph_4P_2N_4S_2$ can thus be viewed as involving attack of X^+ on the S-S bonding orbital (HOMO) (Figure 1.21) followed by uptake of X^- in a position *trans* to that of X^+ (Figure 1.24).

Oxidation of 1,3-$Ph_4P_2N_4S_2$ (**17**, R=Ph) by halogens occurs even more readily than for the 1,5-isomer, however, the expected bifunctional products, 1,3-$Ph_4P_2N_4S_2X_2$ (**45**, R=Ph, X=halogen), are not isolated. Instead, reaction with Br_2 or I_2 produces the twelve-membered dication ring $[Ph_8P_4N_6S_2]^{2+}[X_3^-]_2$, while oxidation by SO_2Cl_2 results in ring contraction to give the six-membered ring $Ph_4P_2N_3SCl$ (**44**,R=Ph, X=Cl) (Figure 1.25). The different behaviors are attributed to the stabilities of the Br_3^- and I_3^- anions compared to Cl_3^- [199].

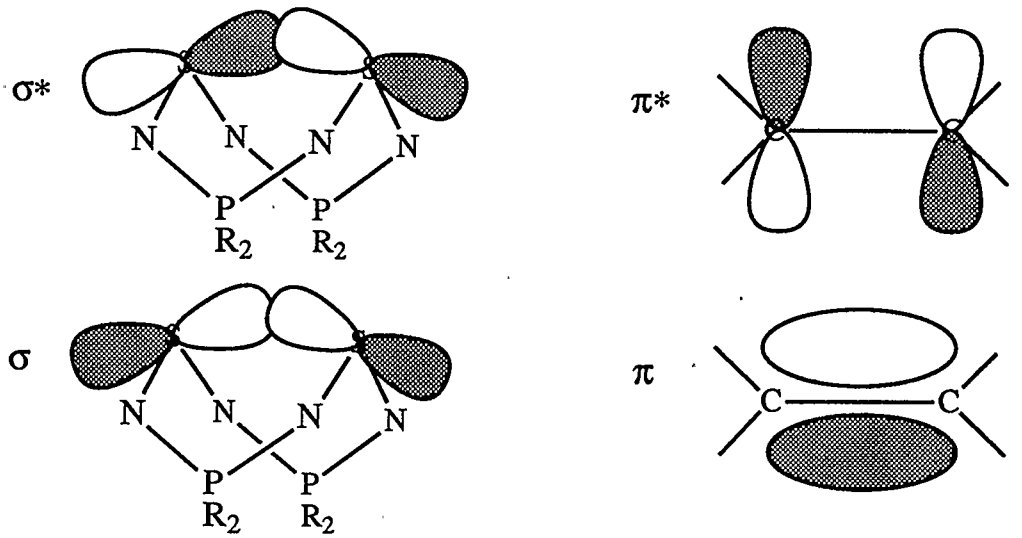

Figure 1.23 - Isolobal correspondence between 1,5-$R_4P_2N_4S_2$ and an alkene (for clarity contributions from nitrogen atomic orbitals to the σ (HOMO) and σ*(LUMO) orbitals of 1,5-$R_4P_2N_4S_2$ are omitted) (See Figure 1.21).

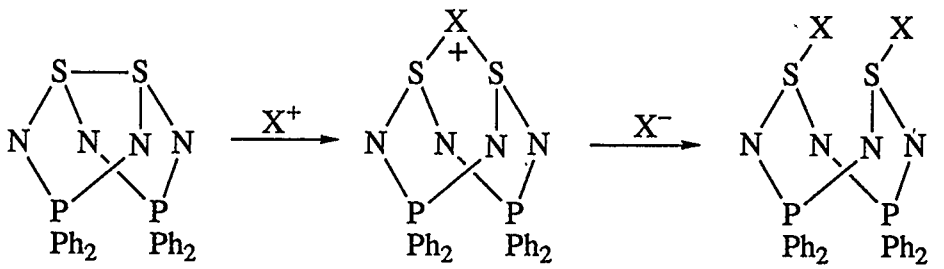

Figure 1.24 - *Trans* oxidative-addition of halogens to 1,5-$Ph_4P_2N_4S_2$

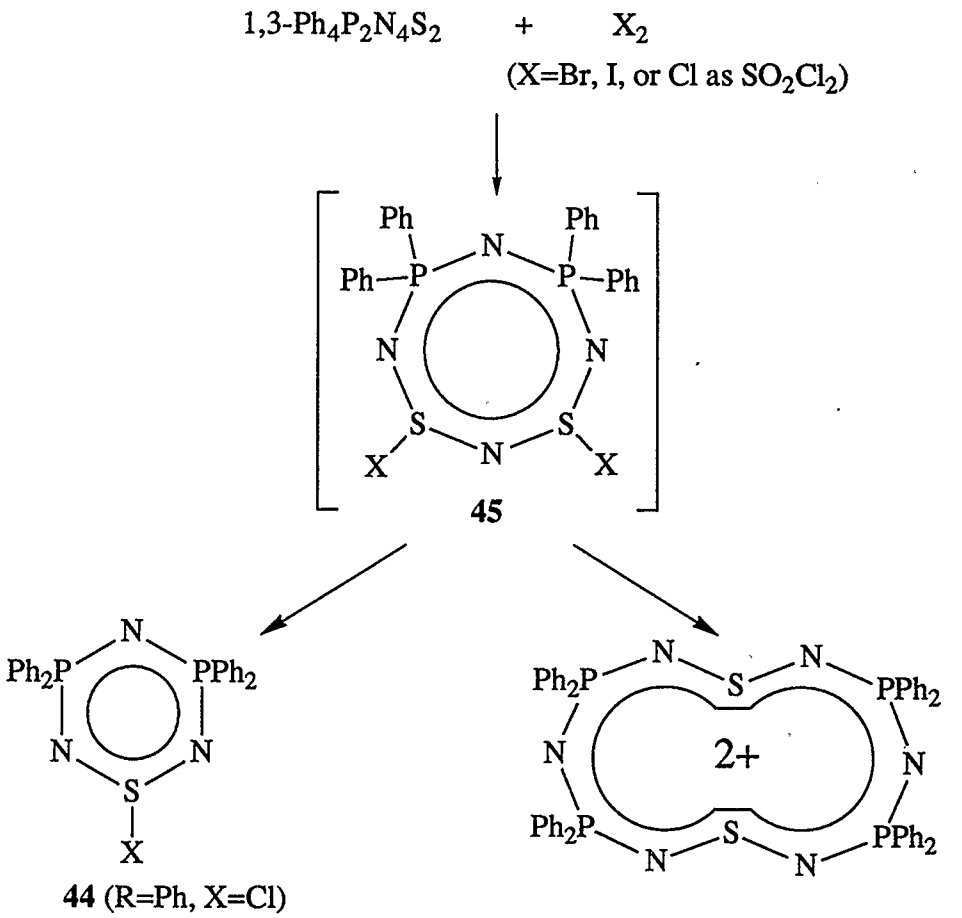

Figure 1.25 - Oxidative addition of halogens to 1,3-$Ph_4P_2N_4S_2$.

(b) Cycloaddition reactions

The six-membered ring $Ph_2PN_3S_2$ (**15**, R=Ph) readily undergoes a cycloaddition reaction with norbornadiene to give an adduct in which the olefin is symmetrically bound to the two sulfur atoms of the heterocyclic ring **50** [184] (Eq. 1.23). As the HOMO and LUMO of the six-membered ring are primarily sulfur based this mode of addition is expected. Since the characteristics of the HOMO and LUMO of 1,3-$R_4P_2N_4S_2$ are almost identical with those of the $R_2PN_3S_2$, a similar cycloaddition mode is predicted. The addition of norbornadiene to 1,3-$Ph_4P_2N_4S_2$ (**17**, R=Ph) produces a yellow crystalline product, which, on the basis of ^1H and ^{13}C NMR data, is also a symmetrical S,S′ addition product **51** [197] (Eq. 1.24). By contrast, the 1,5-isomer does not form an adduct with norbornadiene.

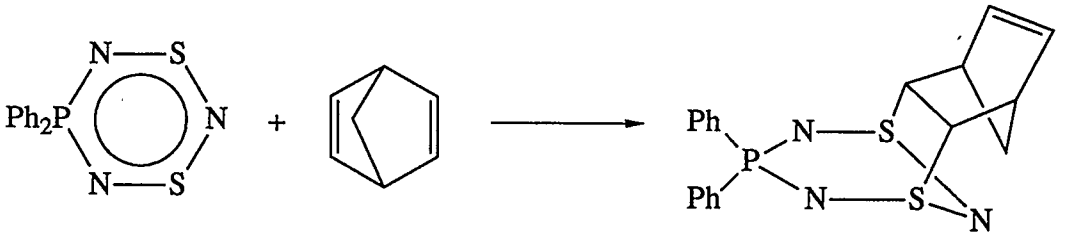

15 **50** (1.23)

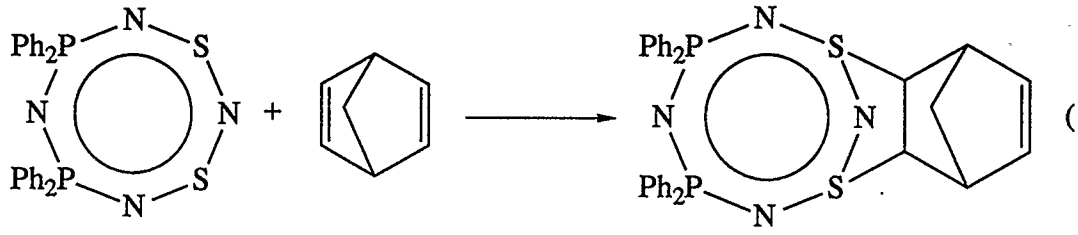

17 (R=Ph) **51** (1.24)

(c) Lewis/Brønsted acid adducts

The Lewis base behavior of several of the cyclophosphathiazenes has been investigated in terms of their ability to form adducts with Lewis or Brønsted acids. In all cases coordination occurs via an endocyclic nitrogen atom. The interaction of the phosphadithiatriazine $Ph_2PN_3S_2$ (**15**, R=Ph), with Lewis/Brønsted acids such as H^+, Me^+, BCl_3, and $SnCl_4$ occurs at the nitrogen atom adjacent to the phosphorus atom of the PN_3S_2 ring [201]. Lewis acid adducts of 1,3-$Ph_4P_2N_4S_2$ (**17**, R=Ph) with H^+, Me^+, BF_3, BCl_3 or $SnCl_4$ are obtained by the addition of an excess of the appropriate reagent to a stirred solution of the heterocycle [200,201]. Only the methylated and protonated derivatives can be recrystallized without dissociation. In all cases coordination occurs at the nitrogen atom between phosphorus and sulfur and, on the basis of an X-ray structural determination of the methylated derivative, results in lengthening of the bonds associated with the coordinated nitrogen, with retention of the eight-membered ring.

The behavior of 1,5-$Ph_4P_2N_4S_2$ (**16**, R=Ph) towards Lewis and Brønsted acids has also

been investigated [201,202]. The Me^+, H^+, and BCl_3 monoadducts were obtained in high yields by using the same procedure described for the preparation of the adducts of the 1,3-isomer. However, only the methylated derivative can be recrystallized without dissociation. The ^{31}P NMR spectra for the monoadducts show two doublets with chemical shifts in the range 83-95 and 125-129 ppm, on either side of the singlet observed for the free ligand. Four bond ^{31}P-^{31}P coupling between the inequivalent phosphorus atoms ranges from 16 to 23 Hz.

The crystal structure for 1,5-$Ph_4P_2N_4S_2Me^+CF_3SO_3^-$ (Figure 1.26) shows that the folded structure of the free ligand is maintained and the transannular S-S interaction is strengthened (d(S-S)=2.437 Å compared to 2.528 Å in the free ligand). Also, as was observed for the methylated 1,3-isomer, the P-N and S-N bonds associated with the coordinated nitrogen are longer than in the uncoordinated ring, while the other S-N bonds show a slight contraction. These structural changes have been attributed to polarization of π^*-electron density of the π-electron rich ring into the skeletal bonds of the coordinated nitrogen.

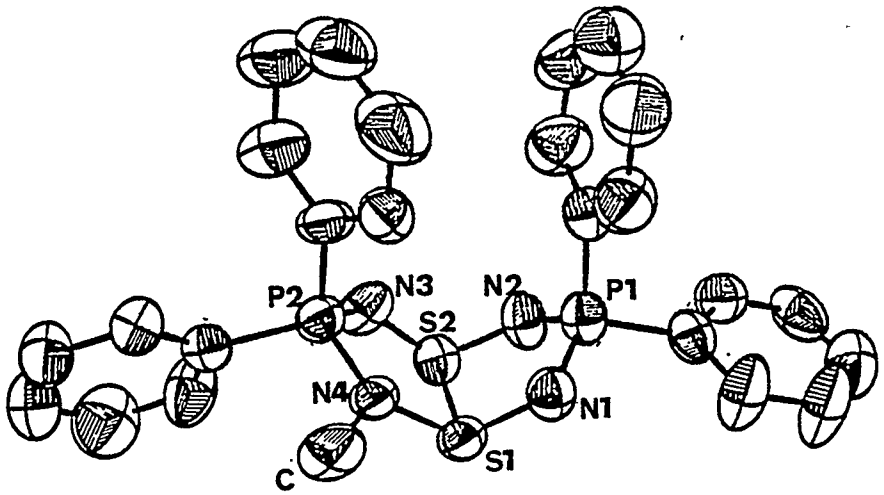

Figure 1.26 - ORTEP drawing of 1,5-$Ph_4P_2N_4S_2Me^+CF_3SO_3^-$. From Ref. [202].

The nonregiospecific formation of adducts of 1,5-$Ph_4P_2N_4S_2$ with stoichiometries other than 1:1 has also been reported [201,202]. The diprotonated adduct [1,5-$Ph_4P_2N_4S_2H_2^{2+}$] [$CF_3SO_3^-$]$_2$ is obtained as a mixture of isomers although none have been structurally characterized by X-ray crystallography, while the 4:3 adduct [1,5-$Ph_4P_2N_4S_2$]$_4$•3$SnCl_4$ is assigned the structure illustrated in Figure 1.27, on the basis of ^{119}Sn Mössbauer spectroscopy data.

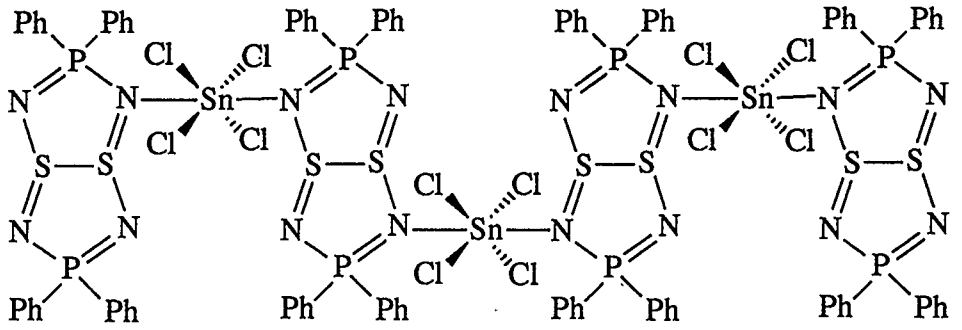

Figure 1.27 - Proposed structure of [1,5-$Ph_4P_2N_4S_2$]$_4$•3$SnCl_4$. From Ref. [202].

(d) Transition-metal complexes

N-bonded transition metal complexes, analogous in structure to the Lewis acid adducts described above, have only been recently reported [203]. The reaction of 1,5-$R_4P_2N_4S_2$ (R=Ph, Et) with the chloro-bridged platinum (II) complex, [$PtCl_2(PEt_3)$]$_2$, in a polar solvent gives the N-bonded monadducts **52a** and **52b** (Equation 1.25).

$$2\ \text{1,5-}R_4P_2N_4S_2\ (\text{R=Ph, Et}) + [PtCl_2(PEt_3)]_2 \longrightarrow 2\ \underline{\text{trans}}\text{-}PtCl_2(PEt_3)(\text{1,5-}R_4P_2N_4S_2) \quad (1.25)$$

52a, R=Ph; **52b**, R=Et

The X-ray structure of **52a** (Figure 1.28) reveals η^1-nitrogen coordination and the structural perturbations observed for the heterocycle upon attachment to platinum (II) are similar to those described previously for the N-methylated adduct of 1,5-$Ph_4P_2N_4S_2$, i.e.

contraction of the S-S bond and a lengthening of the bonds associated with the coordinated nitrogen atom [203].

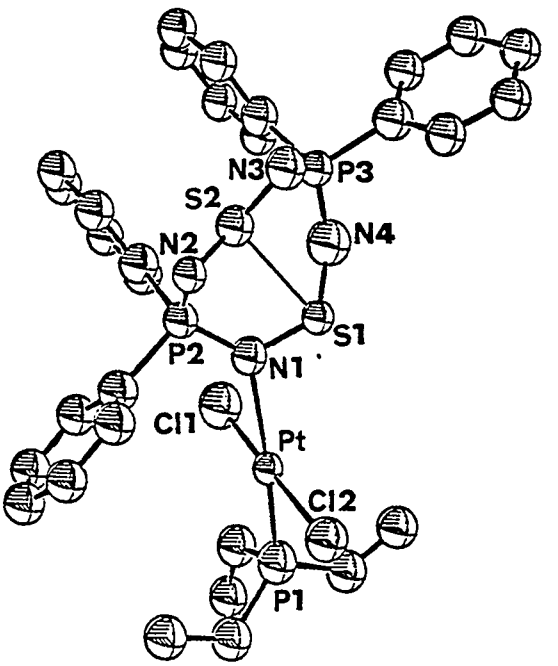

Figure 1.28 - ORTEP plot for *trans*-[$PtCl_2(PEt_3)(1,5\text{-}Ph_4P_2N_4S_2)$], **52a**. From Ref. [203].

The reaction of $Pt(C_2H_4)(PPh_3)_2$ with the dithiatetrazocines, $1,5\text{-}E_2N_4S_2$ (**31**, E=Ph_2P, Me_2NC), in acetonitrile produces high yields of 1:1 complexes in which ethylene has been displaced by the heterocyclic ligand [204]. Preliminary X-ray crystallographic data for the complex of $1,5\text{-}(Me_2NC)_2N_4S_2$ suggests that these complexes likely exhibit a novel bonding mode involving an η^2-S,S′ interaction between platinum and the heterocyclic ligand. Density functional calculations show this interaction to be analogous to that found in η^2-alkene complexes. The formation of such complexes provides support for the isolobal analogy between 1,5-diphosphadithiatetrazocines and alkenes developed to explain the stereochemistry of oxidation of the 1,5-diphosphadithiatetrazocines (See Section 1.3.3(a)) [197,198]. These complexes are discussed in much greater detail in Chapter 3.

(e) ^{31}P NMR Spectra

Solution ^{31}P NMR spectroscopy has proved to be an important tool in cyclophosphathiazene chemistry both for monitoring reactions and for the structural identification of products [179]. The two 1,5-diphosphadithiatetrazocines characterized to date, 1,5-$R_4P_2N_4S_2$ (**16**, R=Ph, Me), exhibit anomalously low field isotropic solution ^{31}P NMR chemical shifts (114 and 120 ppm, respectively) compared to those of other unsaturated P-N-S rings, which typically fall in the region +30 to -20 ppm [184,205]. As described in the previous section these low field shifts persist in the N-bonded Lewis acid adducts of **16** in which the S-S interaction is maintained [202]. Consequently, it has been suggested that these anomalous shifts are determined in some way by the structural constraints imposed by the cross-ring S-S interaction [202]. In particular, relatively narrow endocyclic bond angles at phosphorus for strained ring compounds have been proposed to result in low field ^{31}P NMR shifts [206,207]. Thus, the unusual chemical shifts for the 1,5-diphosphadithiatetrazocines may be due to the narrow angles at P of 110-111° [185,187] imposed by the S-S bonds.

1.5 Objectives and Outline of the Thesis

The cyclophosphazenes and cyclothiazenes have been thoroughly investigated and their chemistry is at an advanced level of development. The hybrid cyclophosphathiazenes, however, are a relatively new class of inorganic heterocycles whose chemical properties have only recently been studied. Early research has been concerned with the synthesis and structural characterization of various cyclophosphathiazenes while more recent work has dealt with some of their chemical properties, e.g., oxidative-addition of halogens, cycloaddition of olefins, and the formation of Lewis acid adducts. However, compared to the parent P-N and S-N systems the study of cyclophosphathiazenes is still at an early stage of development. The main objective of this thesis is, therefore, to extend our understanding of the chemical and physical properties of these unsaturated heterocycles - specifically the

family of 1,5-diphosphadithiatetrazocines.

This thesis presents research conducted on the 1,5-diphosphadithiatetrazocines with an emphasis on novel features of their behavior imposed by the presence of a S-S cross-ring interaction. Chapter 2 describes the synthesis and characterization of the first structural isomers of 1,5-diphosphadithiatetrazocines, as well as an improved synthesis of these ring systems. Chapter 3 focusses on the preparation and structures of η^2-S,S′ metal complexes of 1,5-diphosphadithiatetrazocines and their thermal decomposition products. The reactions of 1,5-diphosphadithiatetrazocines with nucleophiles, e.g. organolithium reagents or the hydride ion, which occur at the sulfur centers to give the first anions of unsaturated P-N-S rings, are the subject of Chapter 4. In order to gain some insight into the anomalous nature of the ^{31}P chemical shifts of these compounds, a ^{31}P solid-state NMR study of cyclophosphathiazenes was conducted and the results are presented in Chapter 5. Final conclusions and possibilities for future research are discussed in Chapter 6.

CHAPTER 2

Preparation of 1,5-Diphosphadithiatetrazocines

2.1 Introduction

As discussed in Chapter 1, the diphosphadithiatetrazocines can be prepared using one of four possible methods. The first involves the nucleophilic degradation of S_4N_4 with Ph_2PH or R_2PPR_2 (R=Me, Ph) and results in a complex mixture of products, as illustrated in Equation 2.1, whose subsequent separation and purification require tedious and time-consuming procedures such as gel permeation chromatography and selective recrystallizations [183,184,185].

$$S_4N_4 + Ph_2PH \xrightarrow{\text{Toluene}} Ph_2PN_3S_2\ (12\%) + 1,3\text{-}Ph_4P_2N_4S_2\ (29\%) + 1,5\text{-}Ph_4P_2N_4S_2\ (<1\%) + (Ph_2PN)_{3,4} + Ph_2P(S)H + \text{other, unidentified products} \quad (2.1)$$

(or Ph_2PPPh_2)

A second, related method relies on the thermal decomposition of the six-membered cyclophosphadithiatriazine, $Me_2PN_3S_2$, which is itself difficult to prepare from S_4N_4 and Me_2PPMe_2 (Equation 2.2) [187].

$$S_4N_4 + Me_2PPMe_2 \xrightarrow{\text{Toluene}} Me_2PN_3S_2 \xrightarrow[\text{1 Week}]{\text{Toluene, 23°C}} 1,5\text{-}Me_4P_2N_4S_2\ (40\%) + S_4N_4 + (Me_2PN)_{3,4} \quad (2.2)$$

The reaction between $S_3N_3^-$ and Ph_2PCl also leads to the formation of 1,5-diphosphadithiatetrazocines but, like the first method, a complex mixture of products requiring tedious purification is produced (Equation 2.3) [188].

$$CsS_3N_3 + Ph_2PCl \xrightarrow{CH_2Cl_2} Ph_2PN_3S_2 + 1,5\text{-}Ph_4P_2N_4S_2 + S_8 + S_4N_4 + Ph_2P(S)Cl + CsCl \quad (2.3)$$

Recently a more directed synthetic approach, termed the "building block" method, has been developed and found to have fewer drawbacks than do the previous procedures. This technique is based on the one utilized for the synthesis of the organic analogues of the 1,5-diphosphadithiatetrazocines, namely the 1,5-dithia-2,4,6,8,-tetrazocines, in which the R_2P groups are replaced by RC groups [137]. These related compounds can be prepared via cyclocondensation reactions of $RC(NH)NH_2$ with SCl_2 (Equation 2.4), suggesting that a similar approach might be successful for the preparation of the 1,5-diphosphadithiatetrazocines.

$$2RC(NH)NH_2 + 3\,SCl_2 + 6\,DBU \xrightarrow{CH_2Cl_2} 1,5\text{-}R_4C_2N_4S_2 + 1/8\,S_8 + 6\,DBU{\bullet}HCl \quad (2.4)$$

(R=Ph, NMe_2)

(DBU=diazabicycloundecene)

Application of this methodology to the phosphorus-containing rings involves the cyclo-condensation of the bis(trimethylsilyl)aminophosphinimines, $R_2PN_2(SiMe_3)_3$, with SCl_2 (Equation 2.5) [186].

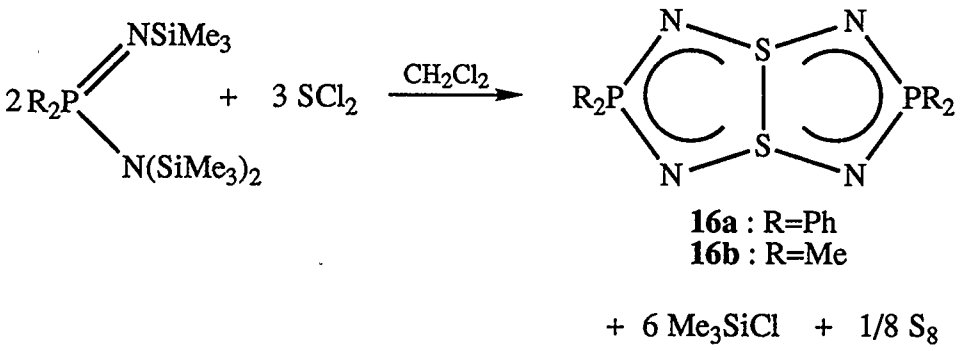

(2.5)

16a : R=Ph
16b : R=Me

+ 6 Me_3SiCl + 1/8 S_8

Yields of the 1,5-diphosphadithiatetrazocines obtained with this method are vastly improved (>50%) and purification is much easier.

In this chapter an improved synthesis of known 1,5-diphosphadithiatetrazocines from bis(trimethylsilyl)aminophosphinimines using thionyl chloride in place of sulfur dichloride will be presented. Also, the synthesis of several new 1,5-diphosphadithiatetrazocines using either $SOCl_2$ or SCl_2 will be described, as will attempts to prepare structural isomers in the reactions between those phosphorus (V) reagents with two different substituents on phosphorus, i.e. $RR'PN_2(SiMe_3)_2$, and $SOCl_2$ or SCl_2. All experimental details of the work described in this chapter are presented at the end of this chapter.

2.2 Synthesis of 1,5-Diphosphadithiatetrazocines Using Thionyl Chloride

The reaction of $Ph_2PN_2(SiMe_3)_3$, **53**, with $SOCl_2$, in CH_2Cl_2, in a 1:1 molar ratio produces 1,5-$Ph_4P_2N_4S_2$ (**16a**, R=Ph) in a 57% yield. This is a small improvement over the 50% yield obtained when SCl_2 is employed, but, more important, the use of $SOCl_2$ eliminates the presence of sulfur as a by-product in the reaction [186]. Also, the purity of $SOCl_2$ is much more reliable than that of SCl_2, as SCl_2 readily begins to decompose to S_2Cl_2 and Cl_2 in the presence of even trace impurities such as moisture.

Similarly, the reaction of $Et_2PN_2(SiMe_3)_3$, **54**, with $SOCl_2$, under the same conditions as above, produces 1,5-$Et_4P_2N_4S_2$ (**16c**, R=Et) a new derivative of the 1,5-diphospha-dithiatetrazocines, in 67% yield. This result is especially important as previous attempts to prepare **16c** using SCl_2 have resulted in the production of the corresponding 1,3 isomer **17c**, exclusively [208]. Compound **16c** is shown by ^1H NMR and ^{13}C NMR to have inequivalent pairs (*exo* and *endo*) of ethyl groups, as is true for the tetramethyl derivative, **16b**. An X-ray structural determination of **16c** has been carried out and is described in section 2.2.1.

In contrast to these results, the reaction between $Me_2PN_2(SiMe_3)_3$, **55**, and $SOCl_2$ results in the formation of both the 1,5 and 1,3 isomers, **16b** and **17b**, respectively. This, however, has provided an unexpected route to the synthesis of significant quantities of the 1,3 isomer. Previous preparative methods for this isomer have suffered due to very low yields and purification problems [185]. The separation of these two isomers using selective recrystallization was unsuccessful; gel permeation chromatography may provide a complete separation. Also, no cycloaddition-adduct is formed between the 1,3-isomer and norbornadiene in contrast to the behavior of the tetraphenyl derivative, **17a** [127]. Overall then the best route to 1,5-$Me_4P_2N_4S_2$ still involves the use of SCl_2 rather than $SOCl_2$, as the product acquired in this manner contains no significant quantity of the 1,3 isomer as a contaminant.

2.2.1 X-ray Analysis of 1,5-$Et_4P_2N_4S_2$, **16c**

The structure of **16c** was determined by X-ray crystallography by Dr. M. Parvez of this department. An ORTEP drawing of **16c** with its atomic numbering scheme is shown in Figure 2.1 and the crystallographic data are given in Table 2.1. The pertinent bond lengths and angles are given in Table 2.2. A comparison of the structural parameters for the series of 1,5-diphosphadithiatetrazocines **16a-c** and **56b** is provided in Table 2.4 and the data are discussed in Section 2.3.4. Complete structure analysis details as well as a listing of atomic coordinates and isotropic thermal parameters are given in reference [209].

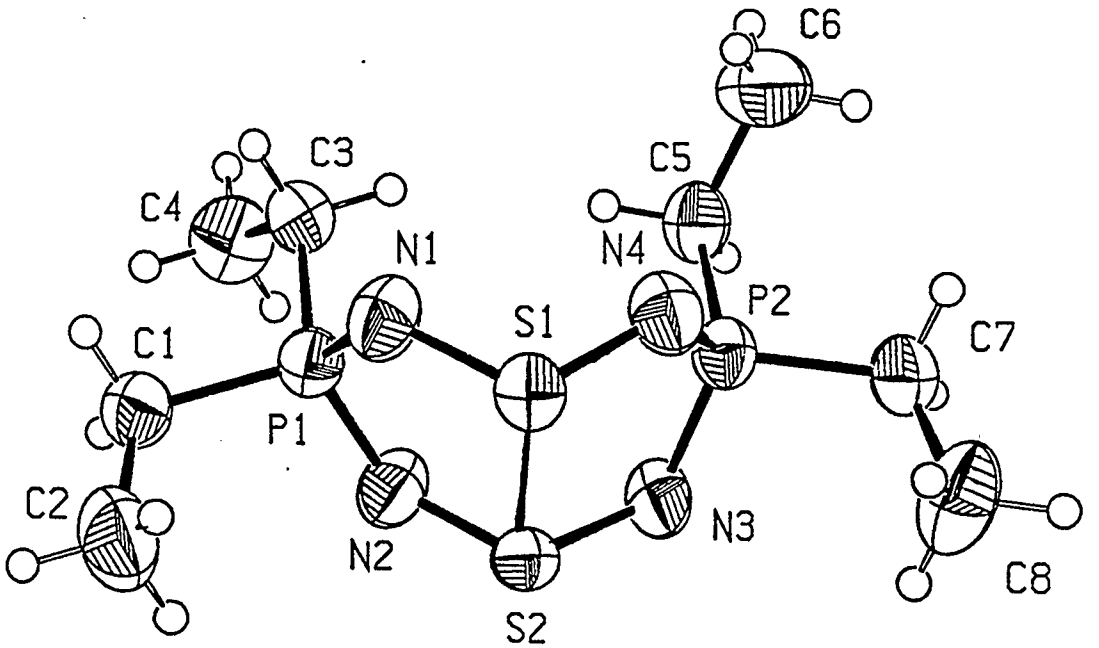

Figure 2.1 : ORTEP Plot (50% Probability Ellipsoids) of 1,5-$Et_4P_2N_4S_2$, **16c**, Showing the Atomic Numbering Scheme.

Table 2.1 : Crystallographic Data for **16c** and **56b**

Compound	**16c**	**56b**
formula	$C_8H_{20}N_4P_2S_2$	$C_2Cl_8N_4P_2S_2$
formula wt.	298.35	489.75
space group	$P2_1/a$	$P2_1/n$
a (Å)	15.244(3)	10.944(3)
b (Å)	9.494(3)	5.859(2)
c (Å)	10.210(2)	23.831(4)
β (deg.)	102.51(1)	100.13(2)
V (Å^3)	1442.6	1504.2
Z	4	4
T (K)	295	165
λ (Å)	0.71069	0.71069
ρ_{calcd} (g cm^{-1})	1.374	2.163
μ (mm^{-1})	0.512	1.834
R[a]	0.055	0.060
R_w[b]	0.057	0.064

a. $R = \Sigma||F_o|- |F_c||/|F_o|$

b. $R_w = [\Sigma w\Delta^2/\Sigma F_o^2]^{1/2}$

Table 2.2 : Selected Bond Lengths (Å) and Bond Angles (°) for **16c**

Bond Lengths (Å)		Bond Angles (°)	
S(1)-N(1)	1.591(7)	N(4)-S(1)-N(1)	115.1(3)
S(1)-N(4)	1.584(6)	N(3)-S(2)-N(2)	115.3(3)
S(2)-N(2)	1.598(7)	N(2)-P(1)-N(1)	110.6(4)
S(2)-N(3)	1.571(6)	N(2)-P(1)-C(1)	109.2(4)
P(1)-N(1)	1.623(6)	N(2)-P(1)-C(3)	113.7(4)
P(1)-N(2)	1.606(8)	N(1)-P(1)-C(1)	109.6(3)
P(1)-C(1)	1.769(8)	N(1)-P(1)-C(3)	109.6(4)
P(1)-C(3)	1.778(8)	C(1)-P(1)-C(3)	103.9(4)
P(2)-N(3)	1.620(7)	N(4)-P(2)-N(3)	109.0(3)
P(2)-N(4)	1.613(7)	N(4)-P(2)-C(7)	109.2(3)
P(2)-C(5)	1.796(8)	N(4)-P(2)-C(5)	113.1(4)
P(2)-C(7)	1.787(8)	N(3)-P(2)-C(7)	108.3(4)
C(1)-C(2)	1.52(1)	N(3)-P(2)-C(5)	111.8(4)
C(3)-C(4)	1.52(1)	C(7)-P(2)-C(5)	105.2(4)
C(5)-C(6)	1.50(1)	S(1)-N(1)-P(1)	120.9(4)
C(7)-C(8)	1.52(1)	S(2)-N(2)-P(1)	122.5(4)
S(1)-S(2)	2.495(3)	S(2)-N(3)-P(2)	121.3(4)
		S(1)-N(4)-P(2)	122.2(4)
		C(2)-C(1)-P(1)	112.2(6)
		C(4)-C(3)-P(1)	116.3(6)
		C(6)-C(5)-P(2)	117.0(6)
		C(8)-C(7)-P(2)	113.9(6)

2.3 Structural Isomers of the 1,5-Diphosphadithiatetrazocines

2.3.1 Introduction

As was discussed in Chapter 1 all 1,5-diphosphadithiatetrazocines characterized to date have the unique feature of a cross-ring sulfur-sulfur bond, which results in the ring adopting a folded or butterfly-like configuration. In fact, it is possible to distinguish between the resulting inequivalent sets of alkyl groups of **16b** and **16c** (*exo* and *endo*) by ^{1}H or ^{13}C NMR. Also, these groups remain inequivalent at temperatures up to 130°C as determined by VT ^{1}H and ^{13}C NMR studies, indicating that the folded structure of the eight-membered ring is non-fluxional, or rigid, with respect to inversion at the sulfur centers (Figure 2.2) [210]. Consequently, the possibility of preparing isomers in which two

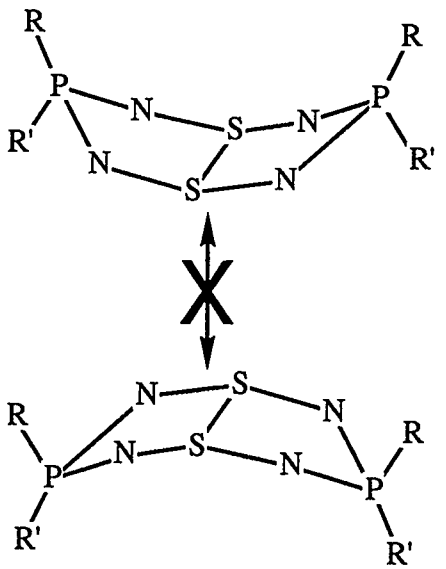

(R=R'=Me or R=R'=Et)

Figure 2.2 : Rigid, Folded Structure of the 1,5-Diphosphadithiatetrazocines.

different groups are attached to the same phosphorus atom arises. A total of three configurational isomers is possible, viz. *exo/exo*, *endo/endo*, and *exo/endo* isomers (see Figure 2.3).

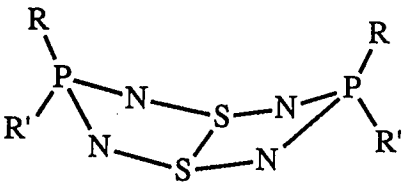

exo/exo isomer
56a : R=Me, R'=Ph
56b : R=Cl, R'=CCl_3
56c : R=I, R'=Et

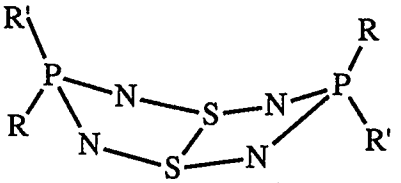

exo/endo isomer
57a : R=Me, R'=Ph
57b : R=Cl, R'=CCl_3
57c : R=I, R'=Et

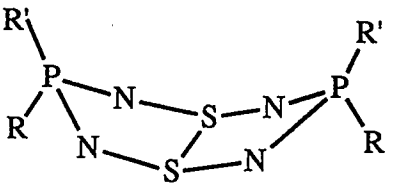

endo/endo isomer
58a : R=Me, R'=Ph
58b : R=Cl, R'=CCl_3
58c : R=I, R'=Et

Figure 2.3 : Isomers of the 1,5-Diphosphadithiatetrazocines

The terms *exo* and *endo* have been used to describe the outward or inward directionality with respect to the $P_2N_4S_2$ ring, of the most sterically bulky substituent, i.e. Ph in **56-58a**, CCl_3 in **56-58b**, and Et in **56-58c**.

2.3.2 Preparation and ^{31}P NMR Spectra of Isomer Mixtures

Since $SOCl_2$ was found to be preferable to SCl_2 in the synthesis of 1,5-$R_4P_2N_4S_2$ (R=Ph, Et) this reagent was employed in the initial attempts to prepare the isomers **56-58**. The reaction between $Me(Ph)PN_2(SiMe_3)_3$ and $SOCl_2$ (1:1 molar ratio) in dichloromethane yields a mixture of products whose ^{31}P NMR spectrum is consistent with the presence of all three possible isomers **56a**, **57a**, and **58a** (Figure 2.4). This spectrum is typical of those observed for the isomer mixtures of the other derivatives mentioned in the proceeding sections.

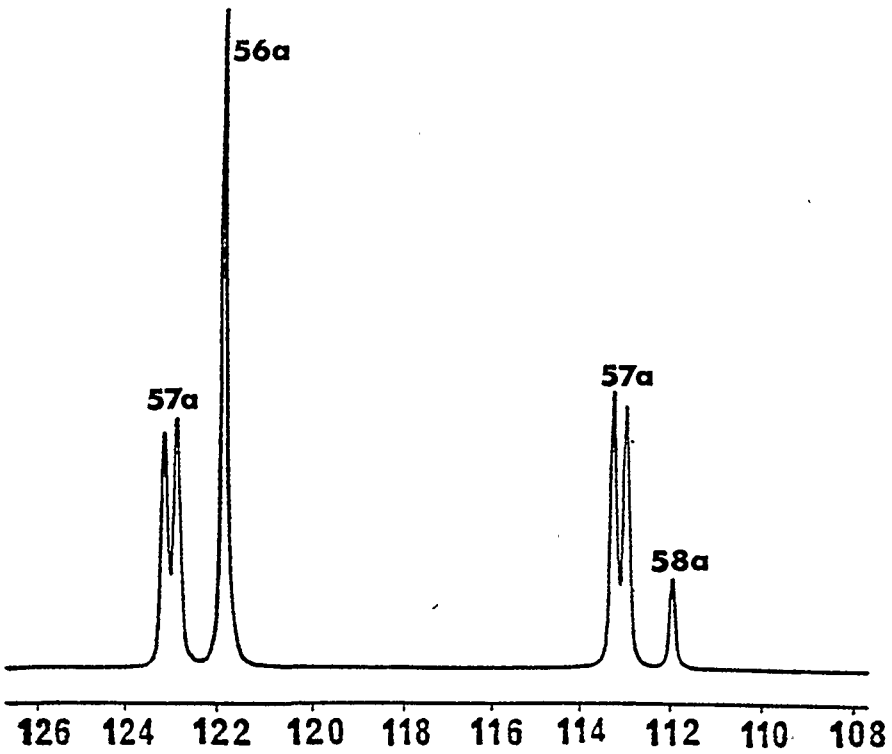

Figure 2.4 : ^{31}P NMR Spectrum and Assignments for a Mixture of 1,5-$[Me(Ph)P]_2N_4S_2$ Isomers **56-58a**.

The interpretation of this spectrum is fairly straightforward as two of the observed resonances are doublets with identical coupling constants. The coupled, and therefore related, resonances could only arise from the isomer whose phosphorus atoms are not related by symmetry, namely the *exo/endo* isomer, **57a**. Assignment of the remaining two singlets to the other two isomers, whose phosphorus atoms are related by symmetry, is based solely on steric grounds, i.e. the most abundant of the two isomers has the less bulky methyl substituents in the *endo* positions. Thus, the more intense of the two singlets is assigned to the *exo/exo* isomer, **56a**, and the remaining signal is assigned to the *endo/endo* isomer, **58a**. The composition of the isomeric mixture is approximately **56a**(34%), **57a**(62%), and **58a**(4%) based on the integrated areas of their ^{31}P NMR signals. Of

particular note is the large four bond coupling constant (45.3 Hz) between the inequivalent phosphorus atoms of isomer **57a**. This value is much larger than any reported in the literature for cyclophosphazenes [211,212]. For comparison, values in the range 16-23 Hz have previously been observed for the corresponding interaction in N-bonded Lewis or Brønsted acid adducts of **16a**, which also possess a cross-ring S--S interaction [202]. It is not clear whether this large coupling is a result of geometrical or electronic factors or a combination of both.

The reaction of $Cl_3C(Cl)PN_2(SiMe_3)_3$ with $SOCl_2$ was not successful for the preparation of the desired isomers **56b**, **57b**, and **58b**. However, the use of SCl_2, in a 2:3 molar ratio, did produce a mixture of these isomers (Figure 2.5). The integrated areas of the ^{31}P NMR signals revealed an isomer distribution similar to that found for **56-58b**.

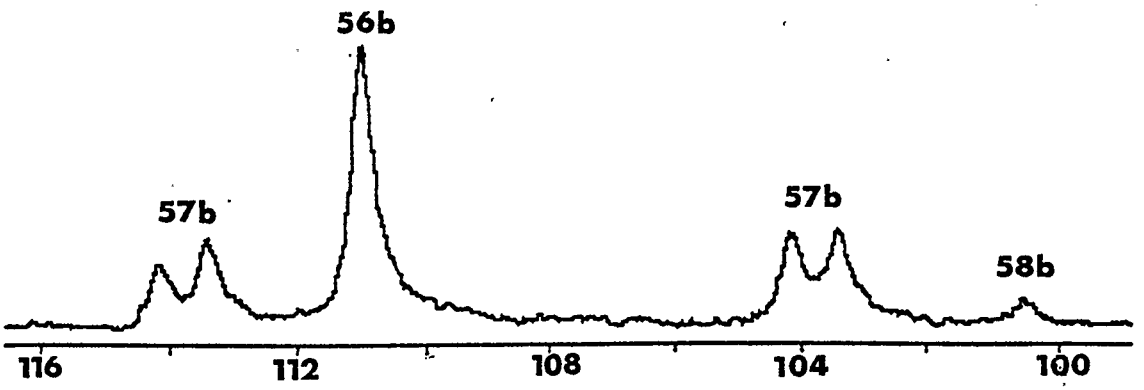

Figure 2.5 : ^{31}P NMR Spectrum and Assignments for a Mixture of 1,5-$[Cl_3C(Cl)P]_2N_4S_2$ Isomers **56-58b**.

Similarly, the reaction of $Et(I)PN_2(SiMe_3)_3$ with $SOCl_2$ was not successful for the preparation of **56c**, **57c**, and **58c**, but the use of SCl_2 (in a 2:3 molar ratio) did give rise to a mixture of the desired isomers. The ^{31}P NMR spectrum of this reaction mixture provides good evidence for the production of **57c** and either **58c** or, more likely, **56c** (Table 2.6). However, the major phosphorus-containing products from this reaction give rise to signals in the region -10 to +30 ppm and it was not feasible to isolate pure samples of this particular diphosphadithiatetrazocine. The low yield of eight-membered ring produced is likely due to side reactions of the relatively labile phosphorus-iodine bond.

As was the case for the *exo/endo*-Me, Ph isomer, **57a**, the halogenated derivatives **57b** and **57c** also show significant phosphorus-phosphorus coupling in the ^{31}P NMR spectrum ($^4J(P\text{-}P)$=61.0 and 61.5 Hz, respectively). These are by far the largest four bond, phosphorus(V)-phosphorus(V) coupling constants ever reported and again it is unclear what role geometrical or electronic factors play in these unusually high values.

2.3.3 Separation of Isomers

Two techniques were employed for the separation of isomeric mixtures. A pure sample of *exo/endo*-$[Me(Ph)P]_2N_4S_2$, **57a**, was successfully separated by preparative thin-layer chromatography (TLC) on silica-gel plates, using pure chloroform as an eluent. However, it was not possible to separate the *exo/exo*, **56a**, and *endo/endo*, **58a**, isomers by using this technique. This separation was attempted for several solvent systems, but none was found to work as well as pure chloroform.

A pure sample of the most abundant symmetrical isomer of the CCl_3, Cl derivative was obtained by fractional recrystallization from a mixture of toluene and pentane (2:1). This isomer was assumed to be **56b**, i.e. that isomer with the less bulky Cl substituents in the *endo* positions, on the basis of the steric arguments outlined earlier (Section 2.3.2). This assumption was confirmed by X-ray crystallography (Section 2.3.4).

2.3.4 X-ray Analysis of 1,5-[(*exo*-CCl_3, *endo*-Cl)$P]_2N_4S_2$, **56b**

The structure of **56b** was determined by X-ray crystallography by Dr. M.Parvez of this department. An ORTEP drawing of **56b** with its atomic numbering scheme is shown in Figure 2.5. The crystallographic data are given in Table 2.1 and the pertinent bond lengths and angles are given in Table 2.3. Complete structure analysis details as well as a listing of atomic coordinates and isotropic thermal parameters are given in reference [209]. The structural parameters of this heterocycle are compared with the corresponding data for **16a**, **16b**, and **16c** in Table 2.4.

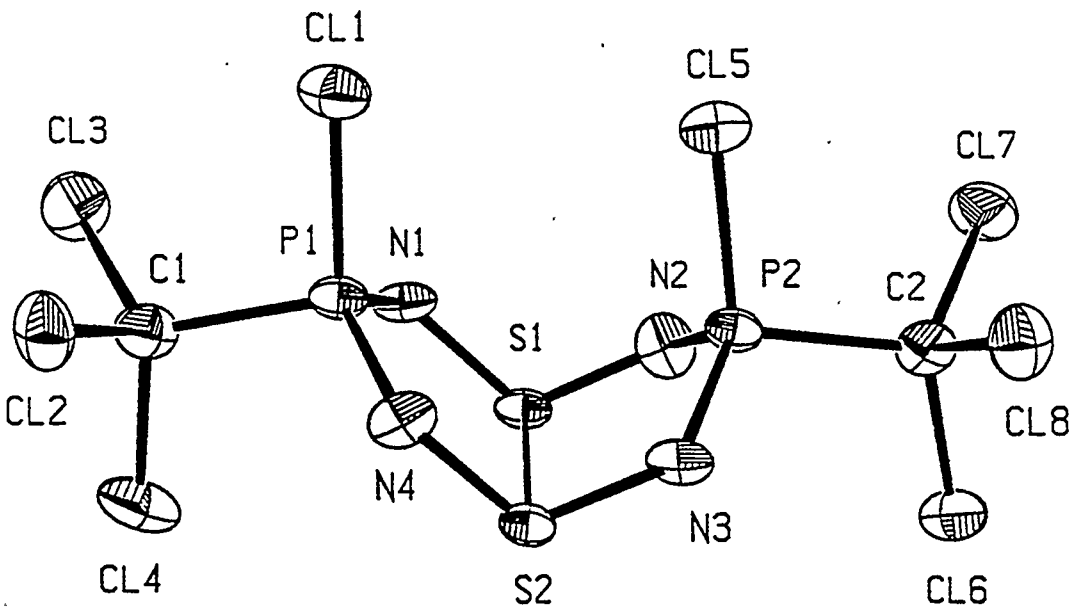

Figure 2.6 : ORTEP Plot (50% Probability Ellipsoids) of 1,5-[(*exo*-CCl_3,*endo*-Cl)$P]_2N_4S_2$, **56b**, Showing the Atomic Numbering Scheme.

Table 2.3 : Selected Bond Lengths (Å) and Bond Angles (°) for **56b**

Bond Lengths (Å)		Bond Angles (°)	
S(1)-S(1)	2.525(3)	N(1)-P(1)-N(4)	114.3(3)
P(1)-N(1)	1.595(6)	N(1)-P(1)-C(1)	107.2(4)
P(1)-N(4)	1.599(6)	N(1)-P(1)-Cl(1)	111.6(3)
P(1)-C(1)	1.854(8)	N(4)-P(1)-C(1)	108.4(4)
P(1)-Cl(1)	1.978(3)	N(4)-P(1)-Cl(1)	112.8(3)
P(2)-N(2)	1.607(7)	C(1)-P(1)-Cl(1)	101.6(3)
P(2)-N(3)	1.626(6)	N(2)-P(2)-N(3)	112.0(4)
P(2)-C(2)	1.854(8)	N(2)-P(2)-C(2)	107.7(4)
P(2)-Cl(5)	1.985(3)	N(2)-P(2)-Cl(5)	113.5(3)
S(1)-N(2)	1.599(7)	N(3)-P(2)-C(2)	108.8(3)
S(1)-N(1)	1.607(6)	N(3)-P(2)-Cl(5)	112.7(2)
S(2)-N(4)	1.577(6)	C(2)-P(2)-Cl(5)	102.2(3)
S(2)-N(3)	1.584(7)	N(2)-S(1)-N(1)	113.3(4)
Cl(2)-C(1)	1.766(8)	N(4)-S(2)-N(3)	112.7(4)
Cl(3)-C(1)	1.747(8)	P(1)-S(1)-N(1)	118.8(4)
Cl(4)-C(1)	1.764(8)	S(1)-N(2)-P(2)	117.0(4)
Cl(6)-C(2)	1.769(8)	S(2)-N(3)-P(2)	117.3(4)
Cl(7)-C(2)	1.746(8)	S(2)-N(4)-P(1)	121.1(4)
Cl(8)-C(2)	1.780(9)	Cl(3)-C(1)-Cl(4)	110.9(5)
		Cl(3)-C(1)-Cl(2)	110.2(4)
		Cl(3)-C(1)-P(1)	110.4(4)
		Cl(4)-C(1)-Cl(2)	109.3(4)
		Cl(4)-C(1)-P(1)	106.1(4)
		Cl(2)-C(1)-P(1)	109.8(5)
		Cl(7)-C(2)-Cl(6)	111.0(4)
		Cl(7)-C(2)-Cl(8)	110.8(5)
		Cl(7)-C(2)-P(2)	109.7(4)
		Cl(6)-C(2)-Cl(8)	110.0(4)
		Cl(6)-C(2)-P(2)	107.4(5)
		Cl(8)-C(2)-P(2)	107.9(4)

The structures of the heterocyclic rings **16c** and **56b** show the same general features as those of **16a** [185] and **16b** [187], namely a folded, bicyclic system in which two five-membered PN_2S_2 rings share a common S--S bond with d(S-S) ≅ 2.5 Å. The major difference between the structures of these four eight-membered rings involves the position of each phosphorus atom relative to its respective S_2N_2 plane. For **16a** both phosphorus atoms are situated below the S_2N_2 planes by 0.214 Å, while in **16b** the phosphorus atoms lie out of and on opposite sides of the S_2N_2 plane by +0.194 and -0.474 Å. By contrast, one of the phosphorus atoms in **16c** deviates only slightly (0.064 Å) while the other lies 0.238 Å above their respective S_2N_2 planes. This inequivalence was also observed in the solid-state CP MAS ^{31}P NMR spectrum of **16c** as two resonances could be resolved for the phosphorus atoms (Section 5.2.1). The phosphorus atoms in **56b** show a behavior similar to that of **16c** as one PN_2S_2 ring is essentially planar whereas the other is 0.413 Å below the S_2N_2 plane.

The endocyclic bond angles at phosphorus are larger for **56b** than for the other three alkyl/aryl derivatives, **16a-c**, (112.0° and 114.3° versus 107.3° to 110.8°) and those at nitrogen are somewhat smaller (118.6° versus 120.7° to 121.8°). The phosphorus-nitrogen and sulfur-nitrogen bond lengths for the series **16a-c** and **56b** show no significant deviations or trends (d(P-N) = 1.607 to 1.636 Å, d(S-N) = 1.590 to 1.595 Å).

Table 2.4 : Comparison of Structural Parameters for the 1,5-Diphosphadithiatetrazocines **16a**, **16b**, **16c**, and **56b**

Compound	**16a**[a]	**16b**[b]	**16c**[c]	**56b**[c]
d(P-N) (Å)[d]	1.621(3)	1.636(3)	1.616(8)	1.607(7)
d(S-N) (Å)[d]	1.590(3)	1.595(3)	1.586(7)	1.592(7)
d(S-S) (Å)	2.528(1)	2.551(2)	2.495(3)	2.525(3)
<(NPN) (deg)	110.8(1)	110.0(2)	110.6(4)	114.3(3)
	110.8(1)	107.3(2)	109.0(3)	112.0(4)
<(PNS) (deg)[d]	120.9(2)	120.7(2)	121.8(4)	118.6(4)
Angle between two S_2N_2 planes	117.3	114.9	115.5	113.2
Deviation of P atoms from S_2N_2 planes (Å)	-0.214	+0.194	+0.064	+0.030
	-0.214	-0.474	+0.238	-0.413

a. Data taken from ref. [185]. Compound **16a** has a twofold axis that passes through the center of the S-S bond and is perpendicular to it.
b. Data taken from ref. [187].
c. This work.
d. Mean values.

2.4 Preparation of 1,5-$Cl_4P_2N_4S_2$, **16d** : A Polymer Precursor ?

The reaction between $Cl_2PN_2(SiMe_3)_3$ and SCl_2 in CH_3CN produces what is likely 1,5-$Cl_4P_2N_4S_2$ as the product exhibits a singlet at +94 ppm in the ^{31}P NMR spectrum, i.e. in a region characteristic of the 1,5-diphosphadithiatetrazocines. However, this material has proven extremely difficult to fully characterize as it appears to decompose quite rapidly in solution to a material that is insoluble in most common organic solvents. Sulfur and

nitrogen analytical data have been obtained that are consistent with the formation of the empirical unit Cl_2PN_2S. It is quite possible that this material is polymeric and, as such, it would be the first example of P-N-S polymer with alternating PN and SN units in the backbone and two-coordinate sulfur (Equation 2.6). As mentioned in Section 1.4.2(a), thermolysis of the six-membered ring $(Cl_2PN)_2NSCl$ (**44**, R=X=Cl) has been shown to induce ring-opening, resulting in the formation of a polymer with sulfur in the +4 oxidation state and a P:S ratio of 2:1 (Equation 2.7) [181(a)]. Similarly, thermolysis of the related six-membered ring $(Cl_2PN)_2NS(O)Cl$ (sulfur in the +6 oxidation state) gives the analogous PNS polymer with 4-coordinate sulfur centers [181(b)].

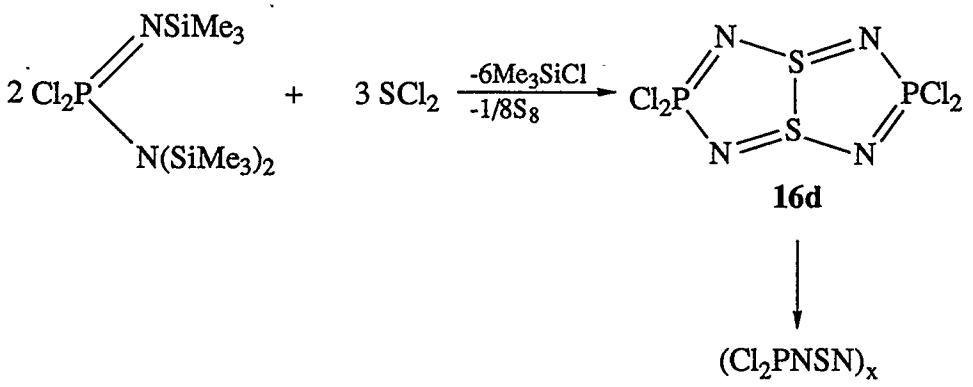

(2.6)

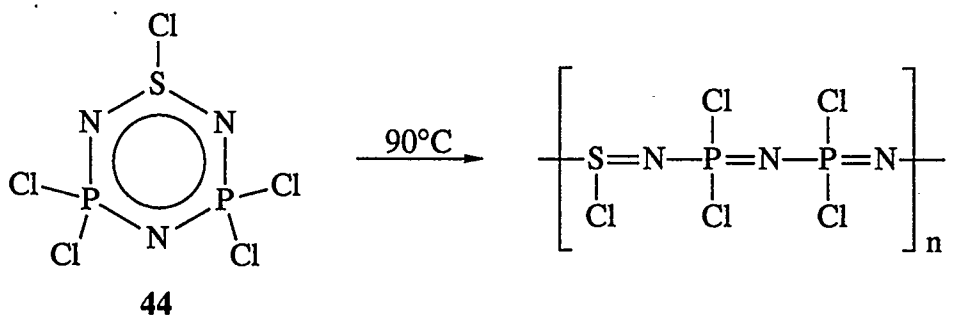

(2.7)

If this proposal is correct, the process shown in Equation 2.6 represents an unusually facile polymerization of a cyclophosphazene and, as such, the polymerization mechanism is probably different from that of **44** or $(NPCl_2)_3$, i.e. thermolysis. The polymerization of **16d** likely involves ring opening via cleavage of a labile S-N bond.

2.5 Conclusion

The cyclocondensation of the bis(trimethylsilyl)aminophosphinimines, $R(R')PN_2(SiMe_3)_3$, with thionyl chloride results in both improved yields and simplified purification of tetraalkyl or tetraaryl 1,5-diphosphadithiatetrazocines compared to the use of sulfur dichloride. In fact, the use of $SOCl_2$ has allowed for the preparation of 1,5-$Et_4P_2N_4S_2$, **16c**, while the use of SCl_2 appears to produce the 1,3 isomer exclusively. The synthesis of 1,5-$Me_4P_2N_4S_2$, **16b**, using $SOCl_2$ also results in the production of a considerable amount of the 1,3 isomer. The reasons for the preferential formation of one isomer, depending upon which sulfur halide reagent is used, are not understood. Further investigations are neccessary to determinine the reaction pathway for this very complex cyclocondensation reaction.

All three possible structural isomers of the 1,5-diphosphadithiatetrazocines are formed in reactions between those bis(trimethylsilyl)aminophosphinimines having two different substituents on phosphorus and either $SOCl_2$ or SCl_2. The major product in each case is the unsymmetrical *exo/endo* isomer, all of which exhibit a large four-bond coupling between the inequivalent phosphorus atoms (45 to 65 Hz). Of the remaining two symmetrical isomers, that having the least sterically demanding groups in the *endo* positions predominates.

Finally, it appears that the preparation of 1,5-diphosphadithiatetrazocines with at least one halogen atom on each phosphorus is only successful if one employs SCl_2 rather than $SOCl_2$ as the cyclocondensation reagent. The halogenated 1,5-diphosphadithiatetrazocines, **56-58b** and **16d** have been prepared in this manner and represent the first examples of this ring system with potentially reactive, exocyclic P-Cl linkages. As such they offer a unique opportunity to investigate reactions at phosphorus rather than at the sulfur or nitrogen centers or, in the case of the tetrachloro derivative, **16d**, they may provide a precursor to novel P-N-S polymers.

2.6 Experimental Section

2.6.1 Reagents and General Procedures

All solvents were dried and distilled before use, toluene (Na), dichloromethane (P_4O_{10}), hexanes and pentane (Na), acetonitrile (CaH_2 and P_4O_{10}), and carbon tetrachloride (P_4O_{10}). All reactions and the manipulation of air/moisture-sensitive materials were carried out under a atmosphere of nitrogen (99.99% purity) passed through silica gel and P_4O_{10}.

Sulfur dichloride and PCl_3 (Aldrich) were distilled before use. All other reagents were used as received ; $SnCl_4$, n-BuLi, EtMgBr, MeMgBr, $PhPCl_2$, Ph_2PCl, $(Me_3Si)_2NH$ (Aldrich), $SOCl_2$ and EtI (Fisher), Me_3SiN_3 (Petrarch). Preparative TLC plates were Macheney-Nagel, 20 x 20 cm, 2 mm silica gel.

Literature procedures were used for the preparation of $Me_2PN_2(SiMe_3)_3$ [213], $Me(Ph)PN_2(SiMe_3)_3$ [214], $Me(Cl)PN_2(SiMe_3)_3$ [215], $Et(I)PN_2(SiMe_3)_3$ [216], $CCl_3(Cl)PN_2(SiMe_3)_3$ [217], $Cl_2PN_2(SiMe_3)_3$ [217]. $Et_2PN_2(SiMe_3)_3$ and $Ph_2PN_2(SiMe_3)_3$ were prepared from Me_3SiN_3 and $Et_2PN(SiMe_3)_2$ [218] or $Ph_2PN(SiMe_3)_2$, respectively, using the procedure described for $Me(Ph)PN_2(SiMe_3)_3$[214]. The ^{31}P NMR chemical shifts for all reagents are given in Table 2.5.

2.6.2 Instrumentation

Infrared spectra (4000-400 cm^{-1}) were recorded as Nujol mulls (KBr windows) on a Nicolet 5DX-FTIR spectrophotometer. ^1H and ^{13}C NMR spectra were recorded on a Bruker ACE-200 spectrometer. ^{31}P NMR spectra were obtained on a Varian XL-200 or a Bruker AM-400 spectrometer with 85% H_3PO_4 as an external reference. Mass spectra were recorded on a Kratos MS80RFA operating at 70 eV. Chemical analyses were performed by the Analytical Services of the Department of Chemistry, The University of Calgary.

Table 2.5 : ^{31}P NMR Chemical Shifts for $RR'PN_2(SiMe_3)_3$ reagents.

Compound[a]	$\delta(^{31}P)$[b]
$Ph_2PN_2(SiMe_3)_3$, **53**	9.2 (7.3) [186]
$Et_2PN_2(SiMe_3)_3$, **54**	29.2
$Me_2PN_2(SiMe_3)_3$, **55**	15.2
$Me(Ph)PN_2(SiMe_3)_3$	12.8
$Cl_3C(Cl)PN_2(SiMe_3)_3$	2.8 (3.8) [217]
$Et(I)PN_2(SiMe_3)_3$	-10.9 (-10.7) [218]
$Cl_2PN_2(SiMe_3)_3$	-24.2 (-24.0) [217]
$Me(Cl)PN_2(SiMe_3)_3$	22.0 (20.3) [216]

a. In CH_2Cl_2 (D_2O insert).
b. Reference : 85% external H_3PO_4; literature values are given in parentheses (all in $CDCl_3$).

2.6.3 Preparation of 1,5-$Ph_4P_2N_4S_2$, **16a**, using $SOCl_2$

A solution of $SOCl_2$ (2.00 g, 16.7 mmol) in dichloromethane (30 ml) was added dropwise, via transfer needle (25 min), to a stirred solution of $Ph_2PN_2(SiMe_3)_3$ (7.23 g, 16.7 mmol) in dichloromethane (75 ml) at 23°C. The solution immediately turned an intense yellow color and gradually darkened during the addition to a clear orange-red. During the addition a clear liquid, presumably Me_3SiCl, was observed to condense on the sides of the flask. The resulting solution was stirred at room temperature for 3.5 h to give a clear red solution. The solvent and other volatiles were then removed under vacuum leaving 5.35 g of a light pink solid. Recrystallization from acetonitrile (0°C) afforded pale pink crystals of **16a** (2.31 g, 4.71 mmol, 57% yield) identified by comparison of the ^{31}P NMR and IR spectra with those of an authentic sample. The very pale pink color is due to the presence of minute quantities of $Ph_2PN_3S_2$. The ^{31}P NMR chemical shift of **16a** is reported in Table 2.6.

2.6.4 Preparation of 1,5-$Et_4P_2N_4S_2$, **16c**, using $SOCl_2$

A solution of $SOCl_2$ (1.09 g, 9.17 mmol) in dichloromethane (20 ml) was added dropwise, via transfer needle (20 min), to a stirred solution of $Et_2PN_2(SiMe_3)_3$ (2.73 g, 9.17 mmol) in dichloromethane (50 ml) at 0°C. The reaction proceeded exactly as it did in the preparation of **16a** to give a clear orange-red solution, which was stirred at room temperature for 15 h. Solvent and volatile products were removed under vacuum leaving a purple semi-solid residue which was recrystallized twice from hot toluene to yield light purple crystals of **16c** (0.91 g, 3.10 mmol, 67% yield).

Anal. Calcd. for $C_8H_{20}N_4S_2P_2$: C, 32.21 ; H, 6.76 ; N, 18.87. Found : C, 31.90 ; H, 6.79 ; N, 18.64. The infrared spectrum of 1,5-$Et_4P_2N_4S_2$ (1300-400 cm^{-1}) shows bands at 1260 w, 1096 s, 1061 vs, 1042 vs, 1028 s, 1005 s, 980 s, 873 w, 797 m, 780 s, 753 s, 722 m, 662 m, 648 w, 623 s, 565 w, 560 w, 451 s cm^{-1}.

The mass spectrum shows the following peaks : m/e, (ion, rel. int.) ; 298 (M^+, 57%), 269 (M^+-Et, 3.2%), 252 (M^+-SN, 40%), 223 (M^+-SN-Et, 52%), 194 (M^+-$SNEt_2$, 61%), 64 (S_2^+, 100%) and 46 (SN^+, 29%).

The ^1H NMR spectrum in $CDCl_3$ shows a complex pattern :

PCH_2Me (*endo* or *exo*)	δ = 0.84 ppm, doublet of triplets, $^3J(H\text{-}P)$ = 18.6 Hz, $^3J(H\text{-}H)$ = 7.6 Hz
PCH_2Me (*exo* or *endo*)	δ = 1.16 ppm, doublet of triplets $^3J(H\text{-}P)$ = 17.9 Hz, $^3J(H\text{-}H)$ = 7.5 Hz
PCH_2Me (*exo* and *endo*)	δ = 1.6 - 1.8 ppm, complex multiplet

The $\{^1H\}^{13}C$ NMR spectrum in $CDCl_3$ shows :

PCH_2Me (*endo* or *exo*)	δ = +24.2 ppm, doublet, $^1J(C\text{-}P)$ = 72.0 Hz
PCH_2Me (*exo* or *endo*)	δ = +21.2 ppm, doublet, $^1J(C\text{-}P)$ = 85.6 Hz
PCH_2Me (*endo* or *exo*)	δ = +7.2 ppm, singlet
PCH_2Me (*exo* or *endo*)	δ = +4.7 ppm, singlet

The ^{31}P NMR data are given in Table 2.6.

2.6.5 Preparation of 1,5-$Me_4P_2N_4S_2$, **16b**, and 1,3-$Me_4P_2N_4S_2$, **17b**, using $SOCl_2$

A solution of $SOCl_2$ (1.42 g, 12.0 mmol) in CH_2Cl_2 (50 ml) was added dropwise to a stirred solution of $Me_2PN_2(SiMe_3)_3$ (3.69 g, 12.0 mmol) in CH_2Cl_2 (100 ml) at 0°C, over a 40 min. period. The resulting solution was a clear orange-red color. After stirring for 24 h at room temperature solvent and volatiles were removed under vacuum. The resulting orange residue was recrystallized twice from CH_3CN (20 ml) at -20°C to yield pale orange crystals containing a mixture of **16b** and **17b** (0.485 g, 2.0 mmol). The ratio of **16b**:**17b** was 45:55 by integration of the ^{31}P NMR spectrum. The ^{31}P NMR chemical shift of each product is listed in Table 2.6.

Attempts at separating the mixture of isomers using fractional recrystallization were unsuccessful. Also, an attempt to isolate the 1,3 isomer as its norbornadiene adduct failed. The formation of this NBD adduct is either extremely slow or does not occur at all.

2.6.6 Preparation of 1,5-[Me(Ph)P]$_2N_4S_2$ Isomers **56-58a** Using $SOCl_2$

A solution of $SOCl_2$ (1.81 g, 15.2 mmol) in CH_2Cl_2 (70 ml) was added dropwise (45 min), by transfer needle, to a stirred solution of $Me(Ph)PN_2(SiMe_3)_3$ (5.63 g, 15.2 mmol) in CH_2Cl_2 (150 ml) at 0°C. After 12 h the ^{31}P NMR spectrum of the reaction mixture revealed the presence of all three isomers **56a**, **57a**, and **58a** (Figure 2.4). The orange-red solution was stirred at room temperature for a total of 18 h, then the solvent and volatile products were removed under vacuum to give a viscous purple oil. This oil was dissolved in a minimum of CH_2Cl_2 and transferred dropwise to rapidly stirred pentane (150 ml) at -78°C. Removal of the solvents under vacuum afforded a pale orange solid (3.00 g) which was extracted once with CH_2Cl_2 (50 ml). Pentane (40 ml) was added to the CH_2Cl_2 extract and, after 24 h at -25°C, a red, viscous oil separated out of solution. The solution was decanted from the oil and pumped to dryness. The residue was then redissolved in CH_2Cl_2 (10 ml) and pentane(40 ml) and after a further 24 h at -25°C the solution was again

decanted from the resulting oil. Solvent was removed under vacuum leaving 0.36 g of a gummy purple material which was shown by ^{31}P NMR to be a mixture of all three isomers (no other phosphorus-containing products were present). This residue was separated by TLC on silica gel (developed with $CHCl_3$) to give a pure sample of **57a** (0.15 g, 0.41 mmol) and a mixture of all three isomers almost completely depleted in **57a** (0.07 g, 0.19 mmol). Anal. Calcd. for $C_{14}H_{16}N_4P_2S_2$: C, 45.90 ; H, 4.40 ; N, 15.29. Found for pure sample of **57a** : C, 46.12 ; H, 4.36 ; N, 13.72. Found for mixture of isomers depleted in **57a** : C, 44.99 ; H, 4.09 ; N,14.21. For **57a** : ^1H NMR ($CDCl_3$) : 0.60 ppm (doublet, $^2J(H-P)$ = 13.9 Hz, 3 H, $\underline{CH_3}$), 1.80 ppm (doublet, $^2J(H-P)$ = 14.3 Hz, 3 H, $\underline{CH_3}$), 7.3-7.9 ppm (multiplet, 10 H, $\underline{C_6H_5}$). The ^1H NMR parameters for the methyl groups of **56a** and **58a** were obtained from the spectrum of the mixture of isomers by comparison with the relative abundance of these isomers as indicated by the ^{31}P NMR spectrum. For **56a** : 1.54 ppm (doublet, $^2J(H-P)$ = 14.2 Hz), 6.8-7.3 ppm (multiplet, $\underline{C_6H_5}$). For **58a** : 1.58 ppm (doublet, $^2J(H-P)$ = 15.9 Hz), 6.8-7.3 ppm (multiplet, $\underline{C_6H_5}$).

The ^{31}P NMR data for **56a**, **57a**, and **58a** are given in Table 2.6.

2.6.7 Preparation of 1,5-$[Cl_3C(Cl)P]_2N_4S_2$ Isomers, **56b**, **57b** and **58b** Using SCl_2

A solution of SCl_2 (2.38 g, 23.1 mmol) in CH_2Cl_2 (20 ml) was added dropwise (15 min), via transfer needle, to a stirred solution of $Cl_3C(Cl)PN_2(SiMe_3)_3$ (6.66 g, 15.4 mmol) in CH_2Cl_2 (150 ml) at 0°C. Observations made during the addition were the same as for all previous reactions. The resulting clear purple solution was allowed to warm to room temperature and was stirred for 24 h, after which a yellow solid (S_8) had settled out of solution. The solution was decanted with a filter needle and the filtrate was pumped to dryness leaving a mixture of yellow and light-purple solids, which were extracted once with 30 ml of CH_2Cl_2 and again pumped to dryness. The resulting solid was then recrystallized twice from toluene/pentane (25 ml: 25 ml) at -25°C to yield 100 mg of **56b**, the *exo/exo*

isomer of 1,5-$[Cl_3C(Cl)P]_2N_4S_2$. The combined toluene/pentane filtrates were found by ^{31}P NMR to be a mixture of all three isomers depleted in **56b** versus the composition of the crude reaction mixture.

Anal. Calcd. for $C_2Cl_8N_4P_2S_2$: C, 4.91 ; N, 11.44. Found : C, 5.08 ; N, 11.39. IR (Nujol, cm^{-1}) : 1116 s, 1100 s, 1067 s, 1033 m, 971 w, 777 m, 747 vs, 723 s, 591 s, 568 m, 546 m, 511 s, 499 s, 432 m. The MS shows the following significant peaks (ion, rel. int.) : 488 (M^+,13%), 453 (M^+-Cl,0.8%), 371 (M^+-CCl_3,58%), 323 ($Cl_5CP_2N_3S$, 8%), 288 ($Cl_4CP_2N_3S$, 25%), 252 ($Cl_2P_2N_4S$, 17%), 229 (Cl_4CPNS, 40%), 206 ($Cl_2P_2N_3S_2$,48%), 182 ($P_2N_4S_2$, 19%), 136 ($P_2N_3S_2$, 18%) ... 35 (^{35}Cl, 100%).

The ^{31}P NMR parameters for **56b**, **57b**, and **58b** are given in Table 2.6.

2.6.8 Preparation of 1,5-$[Et(I)P]_2N_4S_2$ Isomers **56c**, **57c**, and **58c** Using SCl_2

A solution of SCl_2 (0.87 g, 8.4 mmol) in CH_2Cl_2 (15 ml) was added dropwise to a stirred solution of $Et(I)PN_2(SiMe_3)_3$ (2.44 g, 5.62 mmol) in CH_2Cl_2 (50 ml) at 23°C. After 1 h the ^{31}P NMR spectrum revealed a complex mixture of products with chemical shifts in the range -10 to +30 ppm and only small amounts of **57c**, and **56c** or **58c**. It was not possible to isolate pure samples of these isomers. ^{31}P NMR parameters for the two isomers are given in Table 2.6.

2.6.9 Preparation of 1,5-$Cl_4P_2N_4S_2$, **16d**, Using SCl_2

A solution of SCl_2 (1.36 g, 3.89 mmol) in CH_3CN (30 ml) was added dropwise to a stirred solution of $Cl_2PN_2(SiMe_3)_3$ (0.60 g, 5.84 mmol) in CH_3CN (75 ml) at 0°C. The resulting solution is a brilliant purple color with a yellow precipitate. After stirring at 0°C for 2 h, the precipitate (0.52 g) was separated by use of a filter needle and washed with CH_3CN (3 x 20 ml). The washings were combined with the original filtrate. The ^{31}P NMR spectrum of the filtrate showed only one peak at +94 ppm, however, it was not possible to obtain an

adequate elemental analysis for this compound as it appeared to decompose both in solution and as a solid [219]. Elemental analysis obtained by Dr. Rao, on material produced in a similar manner, gave the following results :

Anal. Calcd. for Cl_2N_2PS : N, 17.30 ; S, 19.80. Found : N, 19.0-19.5 ; S, 19.4-20.9. The range of values quoted represents the results of four determinations on different samples of **16d.**

2.6.10 Attempted Preparation of 1,5-$[Me(Cl)P]_2N_4S_2$

Reaction of $Me(Cl)PN_2(SiMe_3)_3$ with either $SOCl_2$ or SCl_2, in CH_2Cl_2, failed to produce the desired mixture of 1,5-eight-membered ring isomers. The ^{31}P NMR spectra showed a variety of phosphorus-containing products, none of which exhibits signals in the region characteristic of 1,5-diphosphadithiatetrazocines (100-136 ppm).

Table 2.6 : ^{31}P NMR Chemical Shifts for 1,5-Diphosphadithiatetrazocines

Compound[a]	$\delta(^{31}P)$[b]
1,5-$Ph_4P_2N_4S_2$, **16a**	114.1 (113.8) [186]
1,5-$Me_4P_2N_4S_2$, **16b**	120.0[c] (119.7) [186]
1,5-$Et_4P_2N_4S_2$, **16c**	136.1
1,5-$[Me(Ph)P]_2N_4S_2$, **56a**	121.8
1,5-$[Me(Ph)P]_2N_4S_2$, **57a**	113.1, 123.0[d]
1,5-$[Me(Ph)P]_2N_4S_2$, **58a**	111.9
1,5-$[Cl_3C(Cl)P]_2N_4S_2$, **56b**	111.0
1,5-$[Cl_3C(Cl)P]_2N_4S_2$, **57b**	103.8, 113.8[e]
1,5-$[Cl_3C(Cl)P]_2N_4S_2$, **58b**	100.5
1,5-$[Et(I)P]_2N_4S_2$, **56c** or **58c**	125.2
1,5-$[Et(I)P]_2N_4S_2$, **57c**	120.2, 131.8[f]
1,5-$Cl_4P_2N_4S_2$, **16d**	94.0

a. In CH_2Cl_2 (D_2O insert).
b. Reference : external 85% H_3PO_4; literature values are given in parentheses (all in $CDCl_3$).
c. $\delta(^{31}P)$ for 1,3-$Me_4P_2N_4S_2$ = 28.3 [185].
d. Two doublets, ^4J(P-P) = 45.3 Hz.
e. Two doublets, ^4J(P-P) = 61.0 Hz.
f. Two doublets, ^4J(P-P) = 61.5 Hz.

CHAPTER 3

Transition-Metal Complexes of 1,5-Diphosphadithiatetrazocines

3.1 Introduction

As discussed in Chapter 1, a great deal of research in inorganic sulfur-nitrogen chemistry has been directed towards the coordination chemistry of S-N ligands. This is likely a result of the combination of hard (N) and soft (S) basic centers present in binary S-N compounds and is exemplified by the multifaceted behavior of S_4N_4 (**2**) [157,144,145]. Coordination to a metal usually results in disruption of the S-N framework to give products that are formally complexes of binary S-N anions. For example, the reaction of the platinum group metals and S_4N_4 produces both mono- and dinuclear complexes containing five-membered MSNSN rings (M = Pt, Pd, Ni) [166,167,164] via the proposed, unstable adduct $Pt(S_4N_4)(PPh_3)_2$ of unknown structure [220]. In fact, only two examples of complexes in which the S_4N_4 ring is not fragmented, $Ir(CO)Cl(S_4N_4)(PPh_3)$ **39** [174] and $Pt(S_4N_4)Cl_2(PMe_2Ph)$ **40** [175,176], have been reported. In both cases the $S_4N_4^{2-}$ ligand exhibits tridentate (N, S, S) coordination as illustrated in Figure 3.1 (See Section 1.3.3).

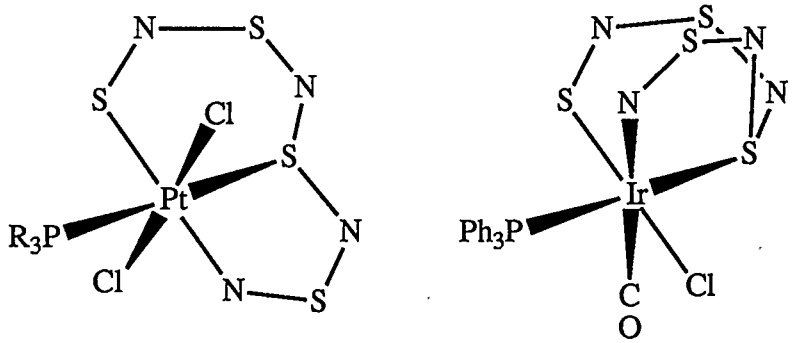

40 **39**

Figure 3.1 - Structures of $Pt(S_4N_4)Cl_2(PMe_2Ph)$ and $Ir(CO)Cl(S_4N_4)(PPh_3)$.

By contrast, it has been shown that the integrity of the related class of S-N compounds, the dithiatetrazocines, 1,5-$E_2N_4S_2$ (**31**, E = Me_2NC; E = Ph_2P), is retained upon coordination to platinum, in the formation of the 1:1 complexes, $Pt(PPh_3)_2(1,5\text{-}E_2P_2N_4S_2)$ (**59**, E = Me_2NC; **60a**, E = Ph_2P) (Equation 3.1) [204].

$$Pt(PPh_3)_2(C_2H_4) + \underset{\mathbf{31}}{1,5\text{-}E_2N_4S_2} \xrightarrow[-C_2H_4]{\text{toluene}} Pt(PPh_3)_2(1,5\text{-}E_2N_4S_2) \quad (3.1)$$

$$\mathbf{59} : E = CNMe_2$$
$$\mathbf{60a} : E = PPh_2$$

While the NMR data for **59** and **60a** do not distinguish between the two structural possibilities in Figure 3.2, preliminary X-ray structural data have established an η^2-S, S′ bonding mode for **59** and density functional calculations have shown the bonding between platinum and the heterocyclic ligand to be analogous to that found in η^2-alkene-platinum complexes [204].

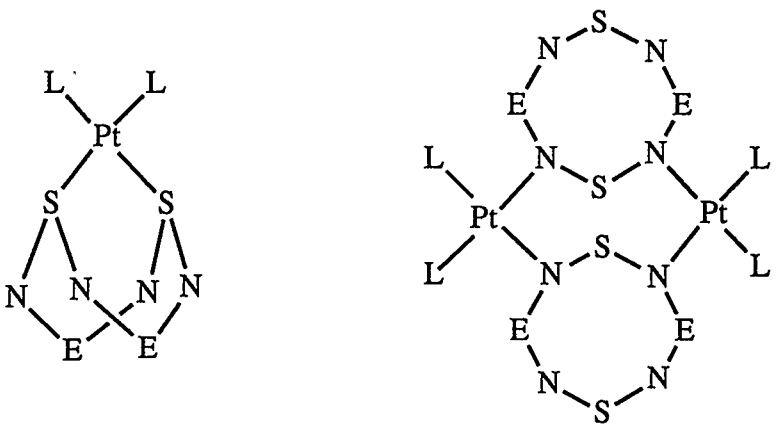

Figure 3.2 - Structural Possibilities for the Dithiatetrazocine Complexes

This unusual bonding mode provided good evidence for the isolobal correspondence, proposed by Oakley *et al.*, between the σ and σ* orbtials of the S-S bond present in the dithiatetrazocines, **31**, and the π and π* orbitals of an electron-deficient alkene (Section 1.4.3, Figure 1.24) [198].

The X-ray analysis of a crystal grown by Dr. Kapoor by diffusion of hexane into a C_6H_6-CH_2Cl_2 solution of **60a** provided some unexpected results. As indicated in Figure 3.3, the structure of the complex **62a** so obtained is dimeric [221]. Each $P_2N_4S_2$ ring acts as a chelating (N, S) ligand towards one platinum atom and as a bridging (S′) ligand to the second platinum.

In this chapter the synthesis and characterization of several new monomeric platinum complexes, and the first palladium complexes of the 1,5-diphosphadithiatetrazocines will be described. A complete X-ray analysis of one of these monomeric complexes, namely $Pt(PPh_3)_2(1,5\text{-}Ph_4P_2N_4S_2)$, will then be presented. The subsequent transformation of each monomeric complex to its corresponding bimetallic complex will also be reported, as will some reactions between such bimetallic complexes and various phosphines. The fluxional behavior of some of the bimetallic complexes will be demonstrated by VT ^{31}P NMR and a mechanism for the fluxional behavior will be proposed.

These results will demonstrate that (i) the incorporation of a ^{31}P NMR probe facilitates the spectroscopic study of the coordination chemistry of S-N ligands and that (ii) the incorporation of phosphorus into an S-N framework enhances the structural stability of their transition-metal complexes.

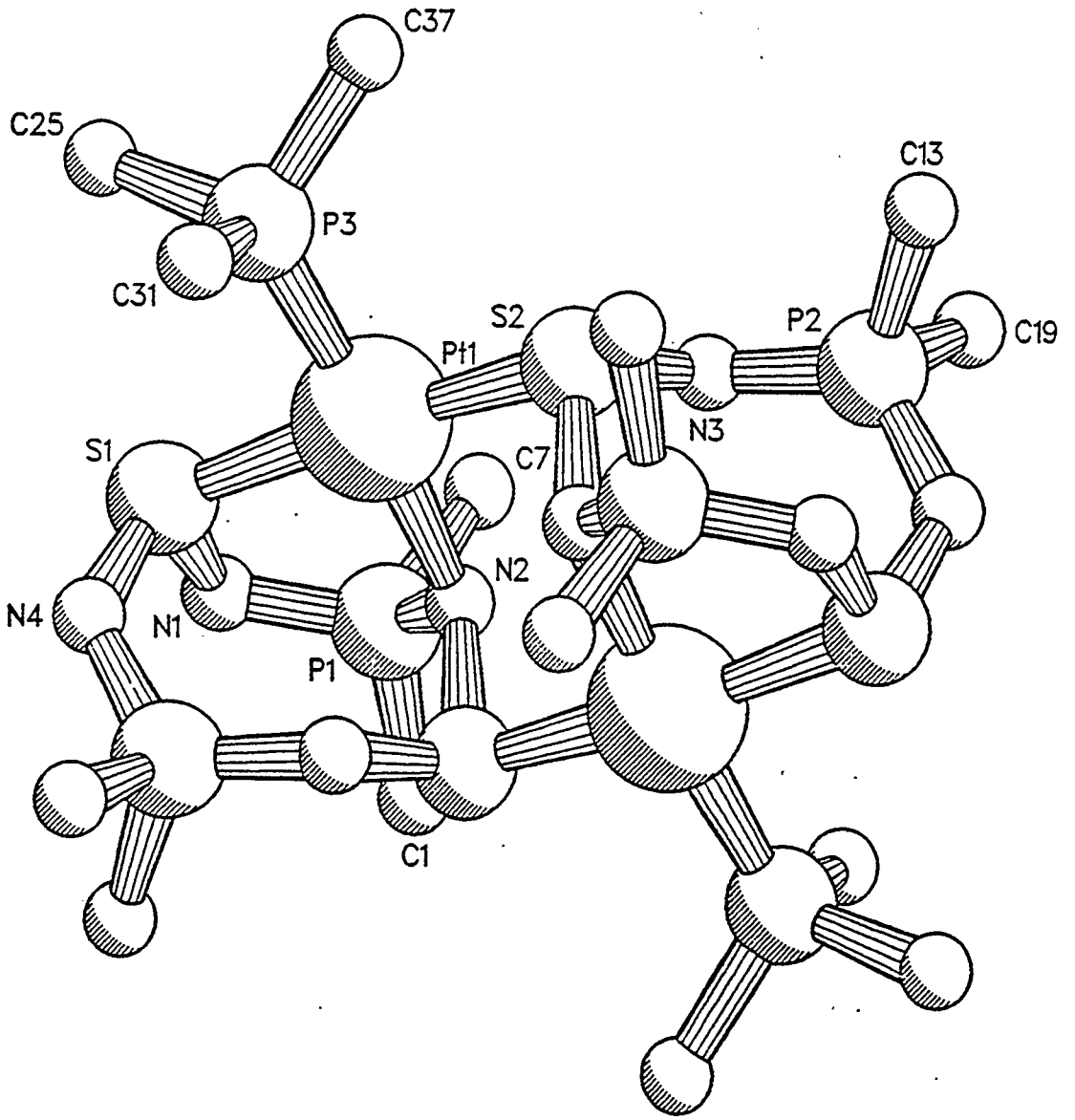

Figure 3.3 - PLUTO drawing of the Bimetallic Complex $[Pt(PPh_3)(1,5\text{-}Ph_4P_2N_4S_2)]_2$, **62a.**

3.2 Monomeric Platinum and Palladium Complexes

3.2.1 Preparation and Characterization

The reactions of $Pt(PPh_3)_2(C_2H_4)$ or $Pd(PPh_2R)_4$ (R = Me, Ph) with 1,5-diphospha-dithiatetrazocines proceed rapidly in toluene at room temperature according to Equations 3.3 and 3.4.

$$Pt(PPh_3)_2(C_2H_4) + 1,5\text{-}R_4P_2N_4S_2 \xrightarrow[-C_2H_4]{\text{toluene}} Pt(PPh_3)_2(1,5\text{-}R_4P_2N_4S_2) \quad (3.3)$$

60a : R = Ph
60b : R = Et
60c : R = Me

$$Pd(PPh_2R')_4 + 1,5\text{-}R_4P_2N_4S_2 \xrightarrow[-2PPh_2R']{\text{toluene}} Pd(PPh_2R')_2(1,5\text{-}R_4P_2N_4S_2) \quad (3.4)$$

61a : R = R′= Ph
61b : R = Ph, R′= Me
61c : R = Et, R′= Me

Compounds **60a**, **60b**, **61a**, and **61b** were isolated as air-stable yellow solids that could be purified by means of recrystallization, while **60c** and **61c** could only be characterized by ^{31}P NMR spectroscopy in solution. This is a consequence of **60c** spontaneously losing a phosphine ligand in solution, soon after synthesis, to give the corresponding dimer, **62c**, while **61c** undergoes a similar transformation to the dimer **63c** upon attempted recrystallization. A molecular weight determination of **60a**, performed by Galbraith Laboratories Ltd., provides good evidence that the compound is monomeric rather than dimeric.

Attempts to prepare monomeric nickel complexes by reacting either $Ni(PPh_3)_4$ or $Ni(diphos)(CO)_2$ with $1,5\text{-}Ph_4P_2N_4S_2$ in toluene proved unsuccessful. The only signals observed in the ^{31}P NMR spectra of the reaction solutions were those of the two reagents. However, one of the desired monomeric Ni complexes, $Ni(diphos)(1,5\text{-}Ph_4P_2N_4S_2)$, could be prepared from the metathetical reaction between "$Li_2(1,5\text{-}Ph_4P_2N_4S_2)$" and

Ni(diphos)Cl_2 (Section 4.6.3). One other Pt complex, Pt$(PEt_3)_2$(1,5-$Ph_4P_2N_4S_2$), has likely been prepared in this manner in the reaction between "Li_2(1,5-$Ph_4P_2N_4S_2$)" and cis-Pt$(PEt_3)_2Cl_2$ (Section 4.6.3). The ^{31}P NMR data for this monomeric Pt complex are presented in Table 3.1 for comparison.

3.2.2 ^{31}P NMR Spectra of Monomeric Complexes

The ^{31}P NMR spectra of the platinum complexes **60a** (Figure 3.4), **60b**, and **60c** consist of two equally intense signals at 18-19 ppm and 40-60 ppm, each with Pt satellites (Table 3.1), which can be assigned to the Ph_3P ligands and the R_2P groups of the coordinated heterocyclic ligand, respectively, on the basis of the magnitude of the ^{31}P-^{195}Pt coupling constants. For each Ph_3P signal this coupling constant falls in the range of 2820 to 2880 Hz, which is of the appropriate magnitude for a one bond P(III)-Pt(II) interaction [222,223]. The three bond R_2P-Pt interaction results in a remarkably large value for $^3J(^{31}P$-$^{195}Pt)$ (572 to 580 Hz), but appropriate literature data for comparison have not been found (For complexes of the type Pt$(S_3PPh)(PR_3)_2$, values for $^2J(^{31}P$-$^{195}Pt)$ are 210-245 Hz [224]). In each case the two observed signals could be resolved into 1:2:1 triplets that result from coupling between the inequivalent pairs of phosphorus atoms over four bonds [$^4J(^{31}P$-$^{31}P) = 4.4$ Hz].

The assignments for the ^{31}P NMR spectrum are confirmed by the ^{195}Pt NMR spectrum of **60a** (Figure 3.5, Obtained by Mr. K.J. Schmidt), which consists of a 1:2:1 triplet of 1:2:1 triplets, indicating that the Pt nucleus is coupled to two different pairs of equivalent phosphorus atoms with coupling constants of 2846 and 581 Hz, respectively.

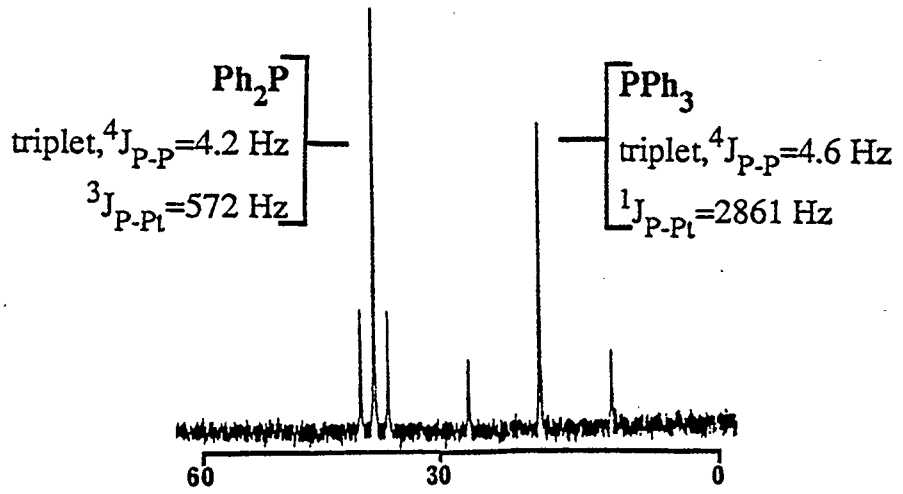

Figure 3.4 - ^{31}P NMR Spectrum of $Pt(PPh_3)_2(1,5\text{-}Ph_4P_2N_4S_2)$, **60a**

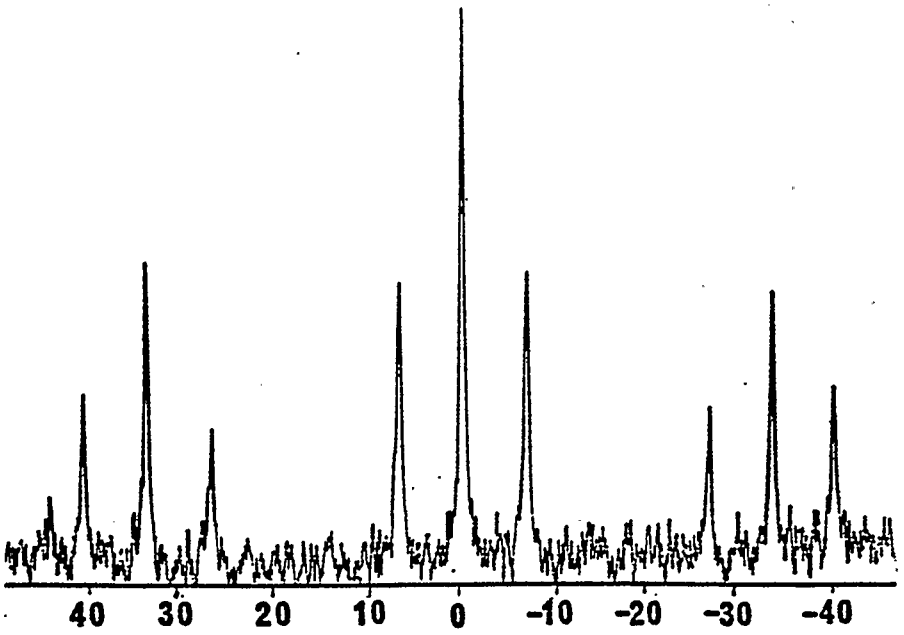

Figure 3.5 - ^{195}Pt NMR Spectrum of $Pt(PPh_3)_2(1,5\text{-}Ph_4P_2N_4S_2)$, **60a**

These NMR data clearly indicate that the heterocyclic ligand is symmetrically bound to platinum, and, in conjunction with the molecular weight determination which was discussed

in the previous section, provide strong evidence that the ligand is bonded in an η^2-S, S′ fashion. Also, as all three platinum complexes (**60a-c**) exhibit very similar coupling constants for the one-bond $Ph_3\underline{P}$-Pt interaction, the three-bond $R_2\underline{P}$-Pt interaction and the four-bond $R_2\underline{P}$-$\underline{P}Ph_3$ interaction, it is likely their structures are similar.

One other piece of ^{31}P NMR data which is nearly identical for each of the three platinum complexes is the change in chemical shift of the heterocyclic ligand upon coordination (Δ = -70 to -75 ppm). These large upfield shifts are observed as a result of the loss of the transannular S-S interaction, which is thought to be responsible for the characteristically low field ^{31}P NMR chemical shifts of the 1,5-diphospha-dithiatetrazocines [186,202].

The ^{31}P NMR spectra of the monomeric palladium complexes, **61a**, **61b**, and **61c** are very similar to those of the platinum complexes (Table 3.1). Again two signals of equal intensity are observed, each being a 1:2:1 triplet, which is consistent with two pairs of inequivalent phosphorus atoms (Figure 3.6).

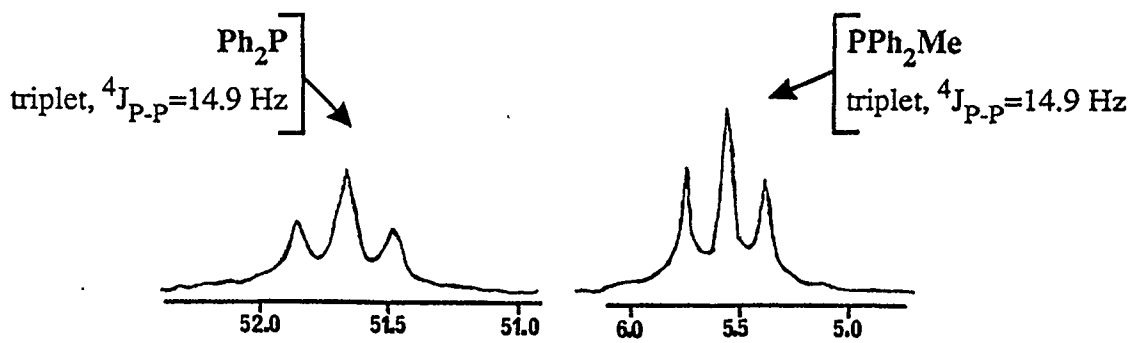

Figure 3.6 : ^{31}P NMR Spectrum of $Pd(PPh_3)_2(1,5\text{-}Ph_4P_2N_4S_2)$, **61a**

Table 3.1 : ^{31}P NMR Data for Monomeric Platinum and Palladium Complexes of 1,5-Diphosphadithiatetrazocines.

Compound	$\delta^{a,b}$	$^{1}J(P\text{-}Pt)^{c}$	$\delta^{a,d}$	$^{3}J(P\text{-}Pt)^{c}$	Δ^{e}
$Pt(PPh_3)_2(1,5\text{-}Ph_4P_2N_4S_2)$, **60a**[f,g]	18.3,t	2861	39.3,t	572	-74.9
$Pt(PPh_3)_2(1,5\text{-}Et_4P_2N_4S_2)$, **60c**[h,i,j]	18.7,t	2820	60.6,t	579	-75.5
$Pt(PPh_3)_2(1,5\text{-}Me_4P_2N_4S_2)$, **60b**[f]	18.7	2880	50.8	574	-69.2
$Pt(PEt_3)_2(1,5\text{-}Ph_4P_2N_4S_2)$, **73**[f,k,l]	4.5,t	2733	35.9,t	536	-78.0
	$\delta^{a,b}$		$\delta^{a,d}$	$^{4}J(P\text{-}P)^{c}$	Δ^{e}
$Pd(PPh_3)_2(1,5\text{-}Ph_4P_2N_4S_2)$, **61a**[f]	25.4,t	-	53.9,t	12.5	-60.2
$Pd(PPh_2Me)_2(1,5\text{-}Ph_4P_2N_4S_2)$, **61b**[f]	6.1,t	-	52.2,t	14.8	-61.9
$Pd(PPh_2Me)_2(1,5\text{-}Et_4P_2N_4S_2)$,**61c**[f,j]	5.9,t	-	73.7,t	13.5	-62.4

a. In ppm relative to external 85% H_3PO_4; t, triplet.
b. $\underline{P}Ph_3$, $\underline{P}Et_3$ or $\underline{P}Ph_2Me$.
c. In Hz.
d. $\underline{P}R_2$ of heterocyclic ligand.
e. $\Delta = \delta(^{31}P)$ coordinated 1,5-$R_4P_2N_4S_2$ - $\delta(^{31}P)$ free 1,5-$R_4P_2N_4S_2$.
f. In CH_2Cl_2.
g. $^{4}J(^{31}P\text{-}^{31}P) = 4.4$ Hz.
h. $^{4}J(^{31}P\text{-}^{31}P) = 4.5$ Hz.
i. In toluene.
j. Not isolated.
k. Prepared from "Li_2[1,5-$Ph_4P_2N_4S_2$]" and cis-$Pt(PEt_3)_2Cl_2$ (See Section 4.6.3)
l. $^{4}J(^{31}P\text{-}^{31}P) = 3.6$ Hz.

The triplet pattern is attributed to the four-bond $R_2\underline{P}$-$R'Ph_2\underline{P}$ coupling of ca. 13-15 Hz, which is significantly larger than the value of 4.4 Hz observed for the same interaction in the Pt complexes, **60a-c**. Although no literature data for such coupling could be uncovered two bond P-M-P coupling has been reported to follow the trend Ni<Pd>Pt [225]. Coordination to palladium causes a less pronounced (ca. 60 ppm) upfield coordination shift of the ^{31}P NMR resonance of the heterocyclic ligand compared to the Pt complexes (70-75 ppm), confirming the sequence of increasing shielding , i.e. 1st row < 2nd row < 3rd row, observed for the platinum group metals [225]. The ^{31}P NMR data in general however strongly suggest that the palladium complexes, **61a-c**, are analogous in structure to those of the platinum complexes, **60a-c**, i.e. all exhibit η^2-S, S′ coordination.

3.2.3 X-ray Analysis of $Pt(PPh_3)_2(1,5\text{-}Ph_4P_2N_4S_2)$, **60a**

The structure of one monomeric platinum complex, **60a**, was determined by X-ray crystallography by Dr. J.C. van de Grampel and co-workers of the Laboratory of Polymer Chemistry, University of Groningen. An ORTEP drawing of **60a** with its atomic numbering scheme is shown in Figure 3.7, and a PLUTO drawing is shown in Figure 3.8. The crystallographic data are given in Table 3.2. The pertinent bond lengths and angles are given in Table 3.3. Complete structure analysis details as well as a listing of atomic coordinates and isotropic thermal parameters are given in reference [226].

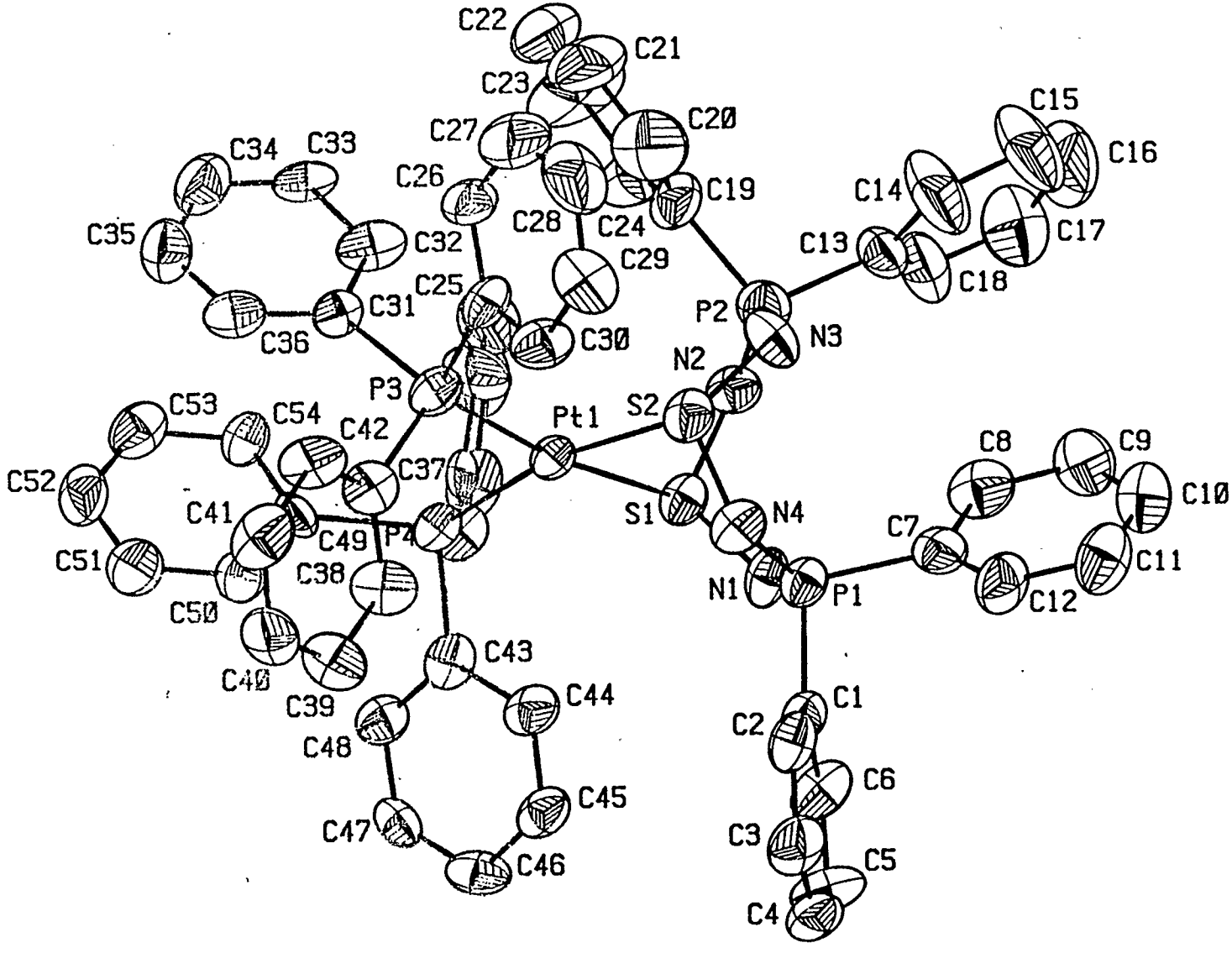

Figure 3.7 - ORTEP plot of $Pt(PPh_3)_2(1,5\text{-}Ph_4P_2N_4S_2)$, **60a**.

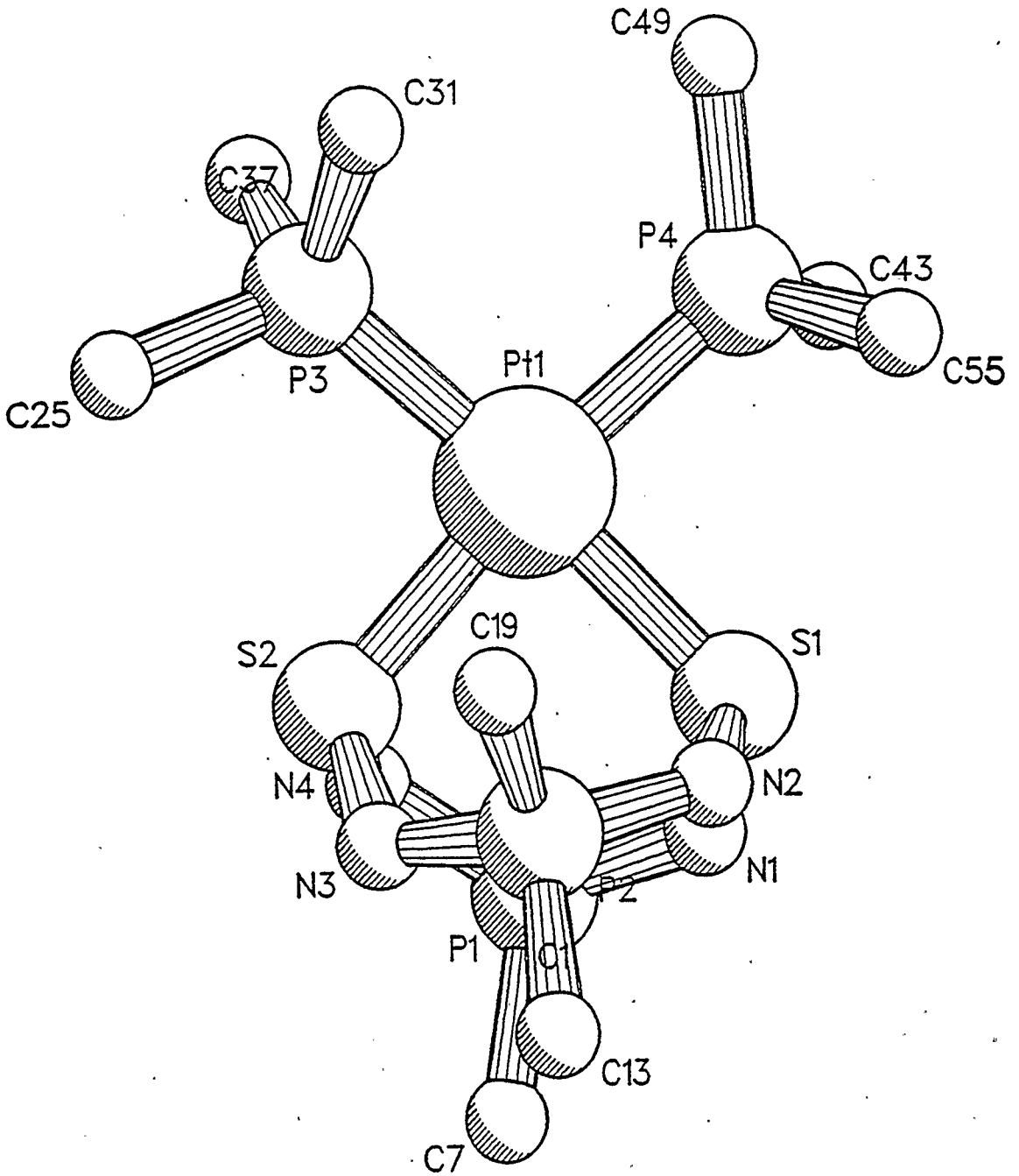

Figure 3.8 - PLUTO plot of $Pt(PPh_3)_2(1,5\text{-}Ph_4P_2N_4S_2)$, **60a.**

Table 3.2 : Crystallographic Data for $Pt(PPh_3)_2(1,5\text{-}Ph_4P_2N_4S_2)$, **60a**.

Chem formula $C_{60}H_{50}PtN_4P_4S_2 \cdot CH_2Cl_2$	fw = 1295.11
a = 22.295(2) Å	space group $P2_1/c$, No. 14
b = 10.500(1) Å	T = 25(2)°C
c = 24.268(3) Å	λ = 0.71073 Å
β = 101.10(1)°	ρ_{calcd} = 1.543 g cm^{-3}
V = 5575(1) Å^3	μ = 28.7 cm^{-1}
Z = 4	R^a = 0.062
	$R_w{}^b$ = 0.049

a. $R = \Sigma||F_o| - |F_c||/|F_o|$

b. $R_w = [\Sigma w\Delta^2/\Sigma F_o^2]^{1/2}$

Table 3.3 : Selected Bond Lengths (Å) and Bond Angles (°) for $Pt(PPh_3)_2(1,5\text{-}Ph_4P_2N_4S_2)$, **60a.**

Bond lengths (Å)

Pt(1)-S(1)	2.408(4)	S(2)-N(3)	1.628(13)
Pt(1)-S(2)	2.341(4)	S(2)-N(4)	1.635(12)
Pt(1)-P(3)	2.337(4)	P(1)-N(1)	1.598(12)
Pt(1)-P(4)	2.344(4)	P(1)-N(4)	1.627(13)
S(1)-N(1)	1.643(11)	P(2)-N(2)	1.594(14)
S(1)-N(2)	1.629(13)	P(2)-N(3)	1.602(14)

Bond angles (°)

S(1)-Pt(1)-S(2)	86.36(13)	Pt(1)-S(2)-N(4)	100.6(5)
S(1)-Pt(1)-P(4)	85.59(14)	N(3)-S(2)-N(4)	111.6(7)
S(2)-Pt(1)-P(3)	89.79(14)	N(1)-P(1)-N(4)	120.2(6)
P(3)-Pt(1)-P(4)	99.25(14)	N(2)-P(2)-N(3)	120.8(7)
Pt(1)-S(1)-N(1)	110.4(4)	S(1)-N(1)-P(1)	126.8(7)
Pt(1)-S(1)-N(2)	102.0(5)	S(1)-N(3)-P(2)	124.0(8)
N(1)-S(1)-N(2)	112.5(6)	S(2)-N(3)-P(2)	122.9(8)
Pt(1)-S(2)-N(3)	111.8(5)	S(2)-N(4)-P(1)	120.1(7)

The asymmetric unit consists of a molecule of **60a** and a molecule of CH_2Cl_2 solvent, which is highly disordered. The analysis clearly shows that the eight-membered heterocyclic ligand is attached to platinum by two Pt-S bonds with distances of 2.408(4) and 2.341(4) Å, and <(SPtS) = 86.36(13)°. The coordination sphere about Pt is approximately square planar and is completed by two PPh_3 ligands with d(P-Pt) = 2.337(4) and 2.344(4) Å, and <(PPtP) = 99.25(14)°. Except for a substantial opening of the transannular S-S separation, from 2.528(1) Å in the free ligand to 3.250 Å in **60a**, there is little change in the conformation of the eight-membered ring. The average S-N bond length increases slightly from 1.590(3) to 1.634(13) Å, while the average P-N bond lengths are essentially unchanged, 1.621(3) versus 1.605(14) Å. The NSN bond angles are reduced slightly from 116.1(1)° in the free ligand to 112.0(7)° in **60a** and the endocyclic bond angles at phosphorus increase from 110.8(1)° to 120.4(7)° upon coordination. The endocyclic bond angles at nitrogen for **60a** fall in the range 120.1-126.8(7)° versus 120.7(2)° and 121.2(2)° for free 1,5-$Ph_4P_2N_4S_2$ [185].

3.3 Bimetallic Platinum and Palladium Complexes

As mentioned in Setion 3.2, the recrystallization of the monomeric platinum complex **60a** results in the formation of the bimetallic complex **62a**. As this attempted recrystallization was performed by heating **60a** in benzene, it was concluded that dimer formation was probably the result of the thermolytic elimination of PPh_3 from the monomer. This process has been investigated in detail for all of the η^2-S,S′ metal complexes reported in this thesis.

3.3.1 Preparation and Characterization

The monomeric platinum and palladium complexes discussed in the previous sections form bimetallic metal complexes via the loss of one phosphine ligand (Equations 3.5 and 3.6).

$$2\ Pt(PPh_3)_2(1,5\text{-}R_4P_2N_4S_2) \xrightarrow{-2\ PPh_3} [Pt(PPh_3)(1,5\text{-}R_4P_2N_4S_2)]_2 \qquad (3.5)$$

60a : R = Ph
60b : R = Me
60c : R = Et

62a : R = Ph
62b : R = Me
62c : R = Et

$$2\ Pd(PPh_2R')_2(1,5\text{-}R_4P_2N_4S_2) \xrightarrow{-2\ PPh_2R'} [Pd(PPh_2R')(1,5\text{-}R_4P_2N_4S_2)]_2 \qquad (3.6)$$

61a : R = R′ = Ph
61b : R = Ph, R′ = Me
61c : R = Et, R′ = Me

63a : R = R′ = Ph
63b : R = Ph, R′ = Me
63c : R = Et, R′ = Me

This elimination occurs either spontaneously in solution during preparation (**60c** into **62c**) or recrystallization (**61c** into **63c**) of the monomer, or, with mild heating either in solution (**60a** into **62a**, toluene at reflux) or of the dry solid (**61a** into **63a**, **61b** into **63b**). The observation that the monomeric complexes of the tetraethyl eight-membered ring, 1,5-$Et_4P_2N_4S_2$, **60c** and **61c**, form bimetallic complexes more readily than monomers of the tetraphenyl ring is consistent with the recent finding that 1,5-$Et_4P_2N_4S_2$ binds more strongly than 1,5-$Ph_4P_2N_4S_2$ to platinum (II) in N-bonded complexes of the type trans-$PtCl_2(PEt_3)(\eta^1\text{-}Et_4P_2N_4S_2)$ [203]. That is, the nitrogen atoms of 1,5-$Et_4P_2N_4S_2$ are more strongly coordinating, or basic, than those of 1,5-$Ph_4P_2N_4S_2$.

The reversibility of phosphine elimination has been tested in two cases. The reaction between two molar equivalents of Ph_3P and a CH_2Cl_2 solution of **62a** resulted in the slow regeneration (several days) of the corresponding platinum monomer **60a**, at room temperature, as indicated by the ^{31}P NMR spectrum, while under the same conditions the palladium monomer **61a** was regenerated from **63a** within 2 hours.

3.3.2 ^{31}P NMR Spectra and Fluxional Behavior of Bimetallic Complexes

The ^{31}P NMR spectra of the bimetallic platinum and palladium complexes reveals equivalent environments (broad singlet (Pt) or doublet (Pd) resonance) for the two R_2P

groups of the heterocyclic ligand *at room temperature* indicative of a fluxional process (Table 3.4). The spectrum of **62a** at -58°C exhibits two equally intense singlets at +46.3 and +16.3 ppm for the inequivalent Ph_2P groups and one singlet for the two equivalent Ph_3P groups (Figure 3.9). This observation is consistent with the observed solid-state structure (Figure 3.3) for which the two phosphorus atoms of each eight-membered heterocycle are inequivalent.

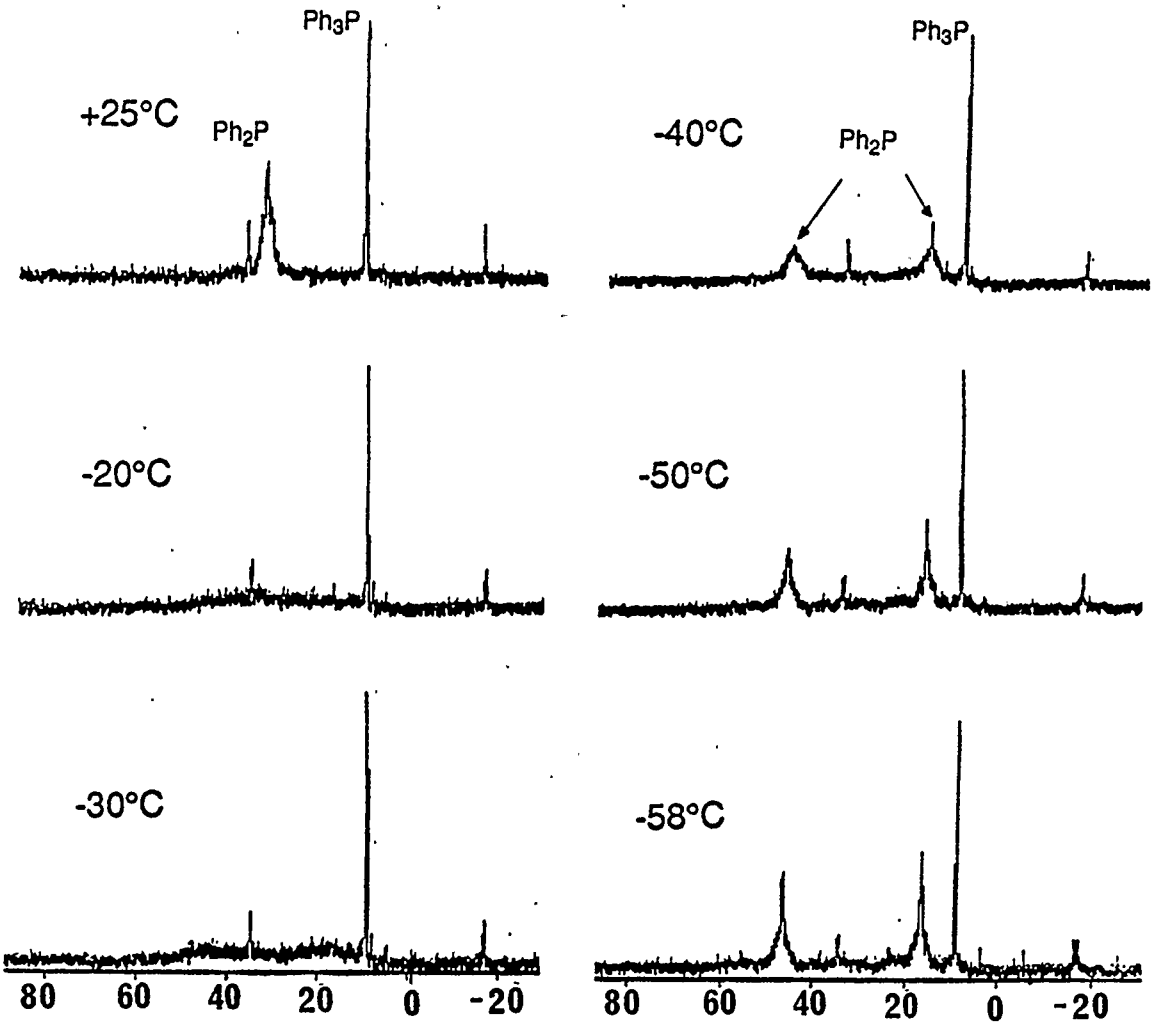

Figure 3.9 : VT ^{31}P NMR Spectra of $[Pt(PPh_3)(1,5\text{-}Ph_4P_2N_4S_2)]_2$, **62a.**

When the temperature of the solution is gradually raised the two Ph_2P singlets broaden and eventually collapse until at +25°C a new singlet is observed at +31.1 ppm (average of the two low temperature signals is +31.3 ppm). The reverse of these changes is observed when the solution is cooled again to -60°C. The coalescence temperature is ca. -30°C, which corresponds to an interconversion barrier of 10.2 ± 0.2 kcal mol^{-1} [227]. A [1,3]-metallotropic rearrangement involving a pendular movement of the Ph_3P-Pt groups between *vicinal* nitrogen atoms is proposed to account for these observations (Figure 3.10). No reports of similar fluxional behavior have been unearthed in the literature.

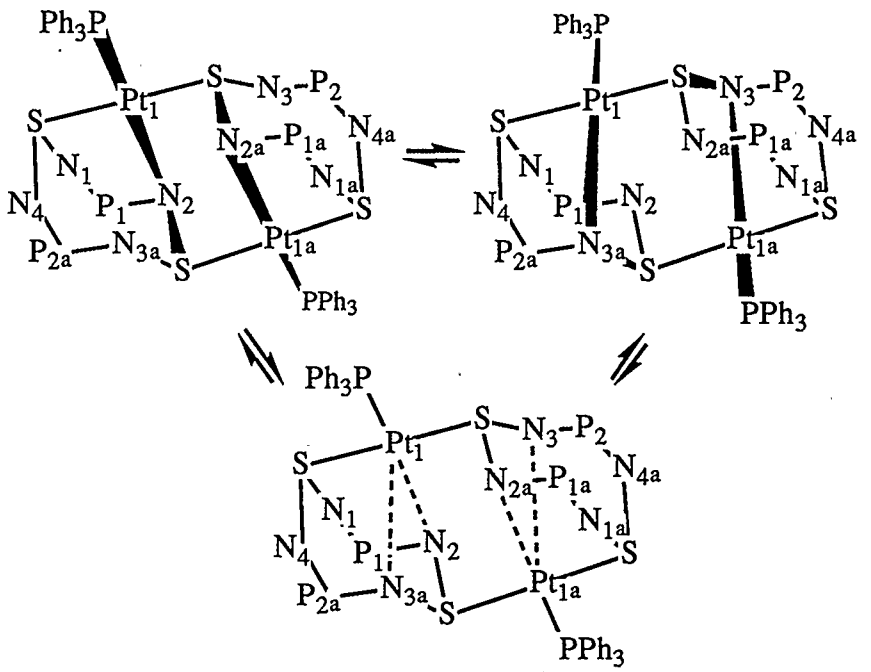

Figure 3.10 : Proposed Mechanism for the [1,3]-Metallotropic Rearrangement in $[Pt(PPh_3)(1,5\text{-}Ph_4P_2N_4S_2)]_2$, **62a**.

The platinum dimer, **62c**, was found to exhibit similar fluxional behavior. At -70°C its ^{31}P NMR spectrum exhibits two equally intense signals at +73.8 and +40.2 ppm (Figure 3.11) for the inequivalent Et_2P groups in addition to the signal for the two equivalent Ph_3P ligands at +12.9 ppm [$^1J(^{31}P\text{-}^{195}Pt) = 4140$ Hz].

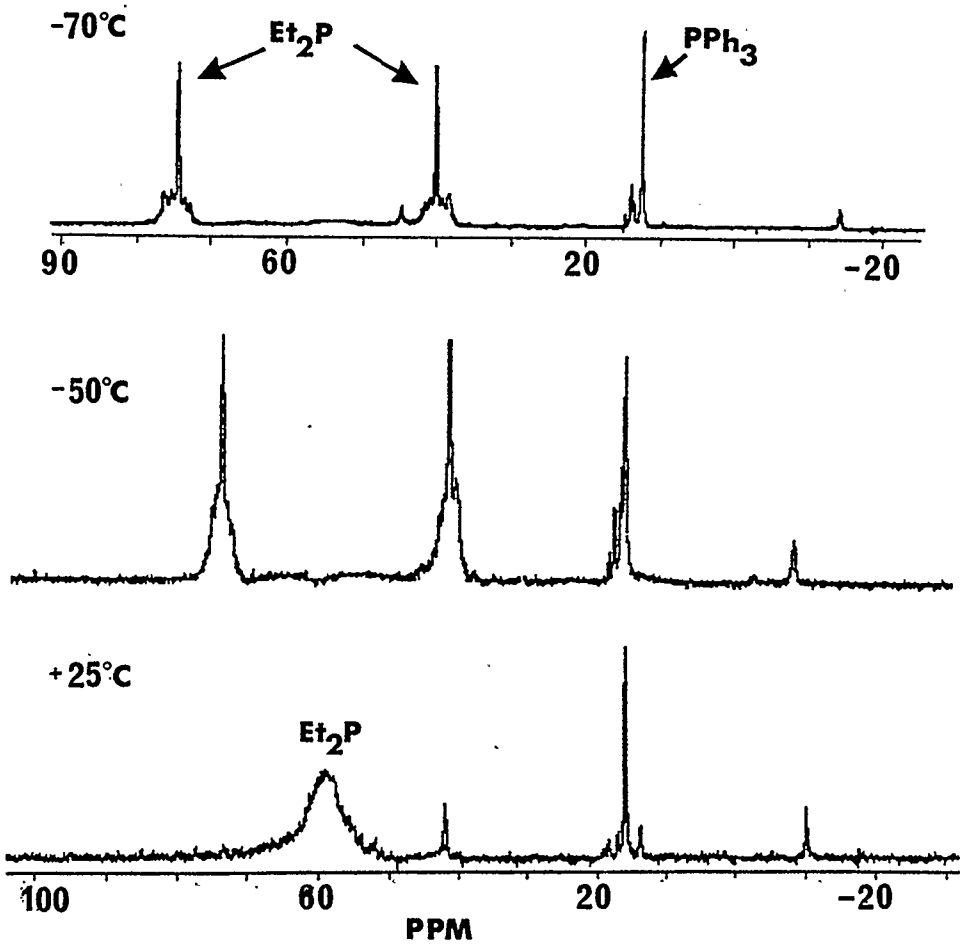

Figure 3.11 : VT^{31}P NMR Spectrum of $[Pt(PPh_3)(1,5\text{-}Et_4P_2N_4S_2)]_2$, **62c**.

As the temperature is raised the two Et_2P signals broaden and eventually collapse until at +25°C a singlet is observed at +58.0 ppm (average of the two low temperature signals is +57.0 ppm) while the signal for the two phosphine ligands shifts slightly to 15.3 ppm. However, because of impurities, the coalescence temperature, and hence the interconversion

barrier, could not be accurately determined, although it is estimated to be very similar to that of **62a**. The greater solubility of **62c** compared to **62a** in CH_2Cl_2 has enabled the acquisition of ^{31}P NMR spectra at lower temperatures with narrow lines. Consequently, extensive coupling patterns could be resolved (Figure 3.11 and Section 3.5.5). These coupling patterns are consistent with a solid-state structure analogous to that of **62a** (Figure 3.3).

The large value of $^1J(^{31}P\text{-}^{195}Pt)$ (ca. 4200 Hz) for the dimers **62a** and **62c** compared to the values of ca. 2850 Hz observed for the same interaction in the corresponding monomers **60a** and **60c** is presumably a reflection of the weak *trans* influence of nitrogen in the dimers compared to sulfur in the monomers [228,229,230].

The ^{31}P NMR spectra of the palladium dimers are slightly different than those for the platinum complexes. At room temperature the spectra for **63a**, **63b**, and **63c** consist of a doublet for the two R_2P groups and a 1:2:1 triplet for the PPh_2R ligands with relative intensities of 2:1 (Figure 3.12). The four bond $^{31}P\text{-}^{31}P$ couplings, which are not observed for the platinum dimers, are in the range 9-15 Hz. This coupling may be observable for the Pt dimers at elevated temperatures but at room temperature the signal for the R_2P groups is far too broad to resolve any coupling information. Also in contrast to the Pt dimers the resonances for the inequivalent PR_2 groups of the Pd dimers could not be resolved into the expected two signals, even at -90°C, although significant broadening of this resonance was observed at such a temperature. Thus it appears that the energy barrier for the [1,3]-metallotropic shift is of significantly lower energy when Pt is replaced by Pd in these dimers.

3.3.3 X-ray Structure of $[Pt(PPh_3)(1,5\text{-}Ph_4P_2N_4S_2)]_2$, **62a**

The structure of the bimetallic platinum complex, **62a**, was determined by X-ray crystallography by Dr. J.C. van de Grampel and co-workers of the Laboratory of Polymer Chemistry, University of Groningen. A PLUTO drawing of **62a** is shown in Figure 3.3.

The structure consists of a centrosymmetric dimer in which each $P_2N_4S_2$ ring acts as a chelating (N, S) ligand towards one platinum atom and as a bridging ligand (S′) towards the second platinum. Overall each heterocyclic ligand is involved in η^2-N,S-μ, η^1-S′ bonding mode. The geometry about platinum is approximately square planar. The sulfur atoms are both three coordinate and *trans* to each other, and the Pt-S bonds are equal. The central six-membered $Pt_2N_2S_2$ ring adopts a chair conformation, with the platinum atoms in the 1,4 positions.

Table 3.4 : ^{31}P NMR Data for Dimeric Platinum and Palladium Complexes of 1,5-Diphosphadithiatetrazocines.[a]

Compound	$\delta^{b,c}$	$^1J(P\text{-}Pt)^d$	$\delta^{b,e}$	$^3J(P\text{-}Pt)^d$	Δ^f
$[Pt(PPh_3)(1,5\text{-}Ph_4P_2N_4S_2)]_2$, **62a**[g]	9.0	4160	31.1	170	-83.0
$[Pt(PPh_3)(1,5\text{-}Et_4P_2N_4S_2)]_2$, **62c**[g]	15.3	4205	58.0	h	-78.1
$[Pt(PPh_3)(1,5\text{-}Me_4P_2N_4S_2)]_2$, **62b**					
	$\delta^{b,c}$		$\delta^{b,e}$	$^4J(P\text{-}P)^d$	Δ^f
$[Pd(PPh_3)(1,5\text{-}Ph_4P_2N_4S_2)]_2$, **63a**[g]	24.7,t	-	57.0,d	11.1	-57.1
$[Pd(PPh_2Me)(1,5\text{-}Ph_4P_2N_4S_2)]_2$, **63b**[i]	9.1,t	-	54.8,d	15.1	-59.3
$[Pd(PPh_2Me)(1,5\text{-}Et_4P_2N_4S_2)]_2$, **63c**[j]	9.2,t	-	76.9,d	8.6	-59.2

a. At 23°C.
b. In ppm relative to 85% H_3PO_4; d, doublet; t, triplet.
c. $\underline{P}Ph_3$ or $\underline{P}Ph_2Me$.
d. In Hz.
e. $\underline{P}R_2$ of heterocyclic ligand.
f. $\Delta = \delta(^{31}P)$ coordinated 1,5-$R_4P_2N_4S_2$ - $\delta(^{31}P)$ free 1,5-$R_4P_2N_4S_2$.
g. In CH_2Cl_2.
h. Not resolved.
i. In CH_2Cl_2/toluene.
j. In CH_2Cl_2/hexanes.

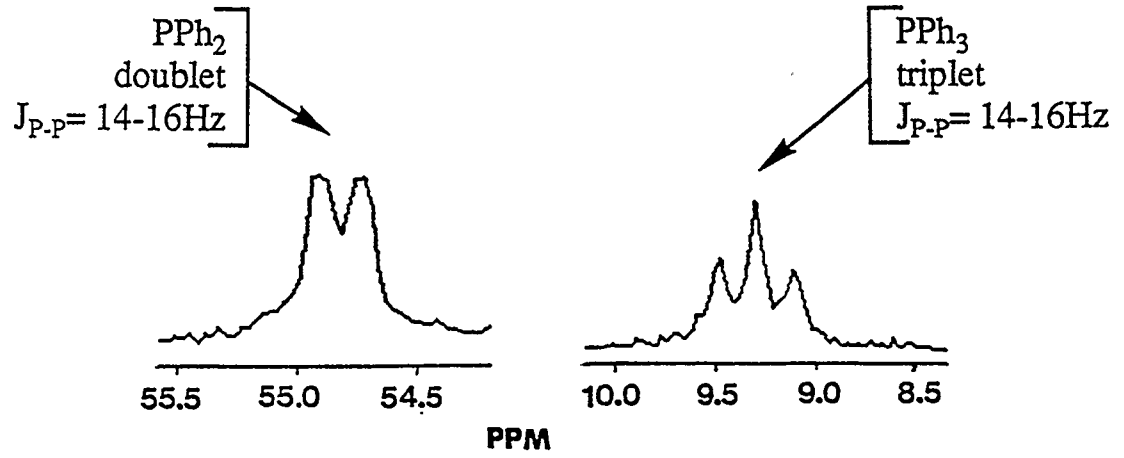

Figure 3.12 - ^{31}P NMR Spectrum of $[Pd(PPh_3)(1,5\text{-}Ph_4P_2N_4S_2)]_2$, **63a**

3.4 Conclusion

The 1,5-diphosphadithiatetrazocines react readily with zerovalent platinum or palladium complexes to give mononuclear complexes of the type $M(PPh_2R')_2(1,5\text{-}R_4P_2N_4S_2)$ (M = Pt, Pd; R = Ph, Et, Me; R′ = Ph, Me). The metal center has been shown to undergo insertion into the transannular S-S bond of the heterocyclic ring yielding products for which a η^2-S,S′ bonding mode has been established. Although no X-ray structure analysis has been performed on a palladium monomer, the ^{31}P NMR data strongly suggest that the palladium complexes are analogous in structure to those of the platinum complexes, i.e. all exhibit η^2-S, S′ coordination. Each monomer was found to readily lose one PR_3 molecule to give bimetallic complexes of the type $[M(PPh_2R')(1,5\text{-}R_4P_2N_4S_2)]_2$ (M = Pt, Pd; R = Ph, Et, Me; R′ = Ph, Me) in which the heterocyclic ligand exhibits an η^2-N,S-μ, η^1-S′ interaction with the metal centers. In two cases this phosphine elimination was found to be reversible, resulting in the reformation of the corresponding monomers and, although not tested for the

other dimers, it is likely that this reversibility holds true in all cases. Both the Pt and Pd dimers undergo a unique fluxional process that probably involves a [1,3]-metallotropic shift. The interconversion barrier for this process is approximately 10 kcal mol^{-1} for the Pt complexes and significantly lower for the Pd complexes.

As was shown in the introduction to this chapter reactions of S_4N_4 with electron-rich metal centers often result in fragmentation of the S-N ring and thus the identity of the initial product(s) can only be surmized. The related 1,5-diphosphadithiatetrazocines have the advantage of being more chemically robust than S_4N_4 and the initial reaction products can be isolated and structurally characterized. This characterization is greatly enhanced, relative to that of S_4N_4, by the incorporation of a ^{31}P NMR probe. This work illustrates that the 1,5-diphosphadithiatetrazocines can therefore be used as models for reactions of S_4N_4 and transition metal compounds, especially those involving attack at the S-S interactions.

3.5 Experimental Section

3.5.1 Reagents and General Procedures

All solvents were dried and distilled before use: tetrahydrofuran and toluene (Na), methylene chloride, chloroform, hexanes and pentane (P_4O_{10}). Drying agents employed for other solvents used in this section as well as details concerning the manipulation of moisture sensitive reagents and products are outlined in Chapter 2, Section 2.6.1. Commercial products were used as received : K_2PtCl_4 and PPh_2Me (Aldrich), $Pd(PPh_3)_4$, $Pd(PMePh_2)_4$, $Ni(diphos)(CO)_2$, $Ni(PPh_3)_4$ (all from Alfa), PPh_3 (Fisher), and ethylene (Linde).

Literature procedures were used for the preparation of 1,5-$R_4P_2N_4S_2$ (**16a**, R = Ph [209]; **16b**, Me [186]; **16c**, Et [209]; $Pt(PPh_3)_4$ [231] and $Pt(PPh_3)_2(C_2H_4)$ [232]. The ^{31}P NMR chemical shifts for these reagents are given in Table 3.5.

3.5.2 Instrumentation

Details concerning the instrumentation and methods employed for obtaining NMR (^{1}H, ^{13}C, and ^{31}P) spectra are outlined in Chapter 2, Section 2.5.2. Chemical analyses were performed by the Analytical Services of the Department of Chemistry, The University of Calgary, or by Canadian Microanalytical Service Ltd., Delta, B.C.. Molecular weight determinations were performed by Galbraith Laboratories Ltd., Knoxville, TN., by using the vapor pressure osmometry method.

3.5.3 Preparation of $Pt(PPh_3)_2(1,5\text{-}Ph_4P_2N_4S_2)$, **60a**

A solution of $Pt(PPh_3)_2(C_2H_4)$ (0.55 g, 0.74 mmol) in toluene (25 ml) was added dropwise (25 min), by transfer needle, to a stirred suspension of $1,5\text{-}Ph_4P_2N_4S_2$ (0.36 g, 0.73 mmol) in toluene (100 ml) at 23°C. The solution immediately became a transparent yellow color which darkened during the addition. After 17 h a yellow precipitate settled out of solution. Approximately half of the solvent was removed under vacuum and the remaining suspension was stored at -25°C for 24 h. The yellow solid was isolated by use of a filter needle and recrystallized from CH_2Cl_2/hexanes (1:10) to yield **60a** (0.66 g, 0.56 mmol). Anal. Calcd. for $C_{60}H_{50}N_4P_4PtS_2$: C, 59.55 ; H, 4.16 ; N, 4.63. Found : C, 58.55 ; H, 4.03 ; N, 4.99. Mol. wt. (3 point determination in $CHCl_3$, vapor pressure osmometry) : Calcd. 1210 g mol^{-1}. Found : 1149 g mol^{-1} (95%). FAB MS : m/e = 1210 (M^+), 948 (M^+-PPh_3). ^{31}P NMR data are given in Table 3.1. The structure of **60a**•CH_2Cl_2 was determined by X-ray crystallography (Section 3.2.3).

3.5.4 Preparation of $[Pt(PPh_3)(1,5\text{-}Ph_4P_2N_4S_2)]_2$, **62a**

A slurry of $Pt(PPh_3)_2(1,5\text{-}Ph_4P_2N_4S_2)$, **60a**, (0.30 g, 0.25 mmol) in toluene (30 ml) was heated at reflux. After 1 h the Pt complex had dissolved to give a yellow solution and after 6 h the reaction mixture was allowed to cool to 23°C and a bright yellow precipitate was separated by use of a filter needle, washed with toluene (5 ml) and dried under vacuum

to give the dimer **62a** (0.185 g, 0.098 mmol), which was recrystallized twice from CH_2Cl_2/pentane (5:2). Anal. Calcd. for $C_{42}H_{35}N_4P_3PtS_2$: C, 53.22 ; H, 3.72 ; N, 5.91. found : C, 52.92 ; H, 3.79 ; N, 5.59. The dimeric structure was established by X-ray crystallography (Section 3.3.3) [221]. ^{31}P NMR data are given in Table 3.4.

3.5.5 Preparation of $Pt(PPh_3)_2(1,5\text{-}Et_4P_2N_4S_2)$, **60c**, and $[Pt(PPh_3)(1,5\text{-}Et_4P_2N_4S_2)]_2$, **62c**

A solution of $Pt(PPh_3)_2(C_2H_4)$ (0.705 g, 0.943 mmol) in toluene (30 ml) was added dropwise (25 min) to a stirred solution of $1,5\text{-}Et_4P_2N_4S_2$ (0.281 g, 0.943 mmol) in toluene (40 ml) at 23°C. The ^{31}P NMR spectrum of the clear orange solution so formed was consistent with the formation of **60c**, but this monomeric species could not be isolated. After 5 days at -25°C this solution produced an orange solid, which was recrystallized from CH_2Cl_2/hexanes (1:1) to give orange crystals of the dimer **62c**. Anal. Calcd.. for $C_{26}H_{35}N_4P_3PtS_2$: C, 41.32 ; H, 4.67 ; N, 7.41. Found : C, 44.21 ; H, 4.62 ; N, 7.19. ^{31}P NMR data (23°C) are given in Table 3.4. The ^{31}P NMR data for **62c** at -71°C are as follows :

PEt_2	δ = 73.8 ppm, doublet with 2 sets of Pt satellites, $^3J(P\text{-}P)$ = 6.8 Hz, $^2J(P\text{-}Pt)$ = 266 Hz, $^3J(P\text{-}Pt)$ = 137 Hz.
PEt_2	δ = 40.2 ppm, singlet with 2 sets of Pt satellites, $^3J(P\text{-}Pt)$ = 240 Hz, $^3J(P\text{-}Pt)$ = 129 Hz.
PPh_3	δ = 12.9 ppm, doublet with one set of Pt satellites, $^3J(P\text{-}P)$ = 6.3 Hz, $^1J(P\text{-}Pt)$ = 4140 Hz.

3.5.6 Preparation of $Pt(PPh_3)_2(1,5\text{-}Me_4P_2N_4S_2)$, **60b**

A solution of $Pt(PPh_3)_2(C_2H_4)$ (0.36 g, 0.48 mmol) in toluene (25 ml) was added dropwise to a stirred suspension of $1,5\text{-}Me_4P_2N_4S_2$ (0.12 g, 0.50 mmol) in toluene (25 ml) at 23°C. The pale yellow solution became orange during the addition and after 15 h a yellow

precipitate was removed by filtration. The filtrate was dried under vacuum to give a sticky orange solid (0.37 g), which was recrystallized twice from CH_2Cl_2/pentane (1:2) at -25°C to give **60b** as a yellow powder (0.12 g, 0.12 mmol). Anal. Calcd. for $C_{40}H_{42}N_4P_4PtS_2 \cdot CH_2Cl_2$: C, 47.00 ; H, 4.24 ; N, 5.35 . Found : C, 47.85 ; H, 4.65 ; N, 5.42. ^{31}P NMR data for **60b** are given in Table 3.1. ^1H NMR (in $CDCl_3$) : 1.37 ppm (doublet, $^2J(H-P)$ = 6.73 Hz, 6 H, $\underline{CH_3}$), 1.44 ppm (doublet, $^2J(H-P)$ = 6.59 Hz, 6 H, $\underline{CH_3}$), 7.1 - 7.6 ppm (multiplet, 30 H, $\underline{C_6H_5}$) (cf. 1.46 ppm and 1.51 ppm for 1,5-$Me_4P_2N_4S_2$).

3.5.7 Preparation of $Pd(PPh_3)_2(1,5\text{-}Ph_4P_2N_4S_2)$, **61a** and $[Pd(PPh_3)(1,5\text{-}Ph_4P_2N_4S_2)]_2$, **63a**

A solution of 1,5-$Ph_4P_2N_4S_2$ (0.484 g, 0.99 mmol) in toluene (40 ml)/THF (2 ml) was added dropwise (30 min) to a stirred suspension of $Pd(PPh_3)_4$ (1.14 g, 0.99 mmol) in toluene (75 ml) to give a clear yellow solution. After 3 h a yellow-green precipitate had formed. The suspension was stored at -25°C for 18 h and then the yellow precipitate of **61a** (1.10 g, 0.98 mmol) was separated by use of a filter needle. Anal. Calcd. for $C_{60}H_{50}N_4P_4PdS_2$: C, 64.26 ; H, 4.49 ; N, 5.00. Found : C, 63.71 ; H, 4.47 ; N, 4.61. ^{31}P NMR data, given in Table 3.1, confirmed the purity of this product. Attempted recrystallization produced the dimer **63a**, which was characterized by ^{31}P NMR spectroscopy (Table 3.4).

3.5.8 Preparation of $Pd(PPh_2Me)_2(1,5\text{-}Ph_4P_2N_4S_2)$, **61b**

A solution of 1,5-$Ph_4P_2N_4S_2$ (0.114 g, 0.23 mmol) in toluene (25 ml) was added dropwise (15 min) to a stirred slurry of $Pd(PPh_3)_4$ (0.21 g, 0.23 mmol) in toluene (25 ml) to give a clear yellow solution. After 20 h the volume of the solution was reduced to 5 ml under vacuum and the resulting solution was stored at -25°C for 18 h to yield a yellow-green precipitate. This precipitate was separated by filter needle and recrystallized from CH_2Cl_2/hexanes (1:5) to give **61b** (0.12 g, 0.12 mmol) as a lime-green solid. Anal. Calcd.

for $C_{50}H_{46}N_4P_4PdS_2$: C, 60.21 ; H, 4.65 ; N, 5.62. Found : C, 60.30 ; H, 4.74 ; N, 5.43. ^{31}P NMR data are given in Table 3.1.

3.5.9 Preparation of $Pd(PPh_2Me)_2(1,5\text{-}Et_4P_2N_4S_2)$, **61c**, and $[Pd(PPh_2Me)(1,5\text{-}Et_4P_2N_4S_2)]_2$, **63c**

A solution of $1,5\text{-}Et_4P_2N_4S_2$ (0.145 g, 0.49 mmol) in toluene (40 ml) was added dropwise to an equimolar amount of $Pd(PPh_2Me)_4$ (0.440 g, 0.49 mmol) in toluene (40 ml) at 23°C. The resulting orange solution was stirred for 18 h and then filtered to remove a small amount of a black precipitate. The removal of solvent under vacuum followed by recrystallization from CH_2Cl_2/hexanes (5 ml:25 ml) at -20°C produced **61c** (0.28 g, 0.35 mmol). ^{31}P NMR data for **61c** are given in Table 3.1. An attempted second recrystallization resulted in the production of a mixture of **61c** and the corresponding dimer, **63c**. The ^{31}P NMR data for both **61c** and **63c** are given in Table 3.4.

3.5.10 Attempted Preparation of $Ni(PPh_3)_2(1,5\text{-}Ph_4P_2N_4S_2)$, $Ni(PPh_3)_2(1,5\text{-}Et_4P_2N_4S_2)$, and $Ni(diphos)(1,5\text{-}Ph_4P_2N_4S_2)$

A solution of $Ni(PPh_3)_4$ (0.075 g, 0.15 mmol) in toluene (15 ml) was added dropwise to a stirred solution of $1,5\text{-}Ph_4P_2N_4S_2$ (0.13 g, 0.15 mmol) in toluene(15 ml) at 23°C. Even after four months no reaction was apparent as the ^{31}P NMR spectrum showed signals only for the reagents. Similarly a solution of $1,5\text{-}Ph_4P_2N_4S_2$ (0.153 g, 0.312 mmol) in toluene (40 ml) was added to a stirred slurry of $Ni(diphos)(CO)_2$ (0.16 g, 0.312 mmol) in toluene (40 ml). Again , even after several days the only signals present in the ^{31}P NMR spectrum were those for the two reagents. The reaction was also attempted in benzene with the same results.

Also, no reaction was observed (^{31}P NMR) upon the addition of a toluene solution (10 ml) of $1,5\text{-}Et_4P_2N_4S_2$ (0.093 g, 0.31 mmol) to a slurry of $Ni(diphos)(CO)_2$ (0.16 g, 0.31 mmol) in toluene (20 ml), even after 1 month.

Table 3.5 : ^{31}P NMR Data for Selected 1,5-Diphosphadithiatetrazocines and Transition Metal Reagents

Compound	δ	Solvent
1,5-$Ph_4P_2N_4S_2$, **16a**	+120	CH_2Cl_2
1,5-$Et_4P_2N_4S_2$, **16c**	+136	CH_2Cl_2
1,5-$Me_4P_2N_4S_2$, **16b**	+114	CH_2Cl_2
$Pd(PPh_3)_4$	+24.9	toluene
$Pd(PPh_2Me)_4$	-2.9	toluene
$Pt(PPh_3)_2(C_2H_4)$	35.3	toluene
$Ni(diphos)(CO)_2$	47.2	toluene

CHAPTER 4

Reactions of 1,5-Diphosphadithiatetrazocines with Nucleophiles

4.1 Introduction

Although the formation of Lewis and Brønsted acid-adducts of the diphospha-dithiatetrazocines has been studied extensively (Chapter 1), very few data have been published regarding the reaction of such heterocycles with nucleophiles. In this chapter the results of such investigations as well as a study of the electrochemical reduction of the 1,5-diphosphadithiatetrazocines are presented.

A summary of reactions of the parent PN and SN heterocycles with nucleophiles will be presented first. Then the results of an electrochemical study of two 1,5-diphosphadithiatetrazocines will be briefly examined. Following this the results of investigations into the reactions of nucleophiles, in the form of alkyllithium (RLi) reagents or super hydride ($LiBEt_3H$), with 1,5-$Ph_4P_2N_4S_2$, and the subsequent reactions of the anions so formed will be described. Concluding remarks will follow and all experimental details are presented at the end of this chapter.

4.2 Reactions of Nucleophiles with Cyclophosphazenes

Reactions between cyclophosphazenes and nucleophiles have been studied in great detail. However, most research has been directed towards the study of substitution reactions

at the phosphorus centers of halophosphazenes. The reactions of such ring systems with nucleophiles such as amines (1° or 2°) [233,234], alkyl or aryloxides [235], thiolates [236], organolithium reagents or Grignard reagents [237] usually, although not always, results in simple substitution of one or more of the halogen atoms (Figure 4.1).

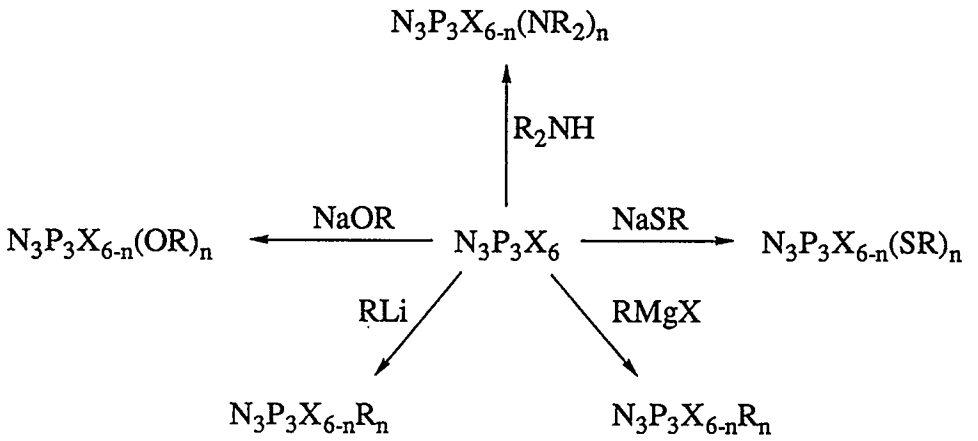

Figure 4.1 - Substitution Reactions of Halocyclophosphazenes

Reactions of cyclophosphazenes with organolithium reagents are of primary interest in relation to this work and have been studied in some detail. The low temperature deprotonation of a hydridophosphazene with n-BuLi gave the first reported phosphazene anion **64** (Equation 4.1) [63]. However, anion **64** is not stable above -50°C

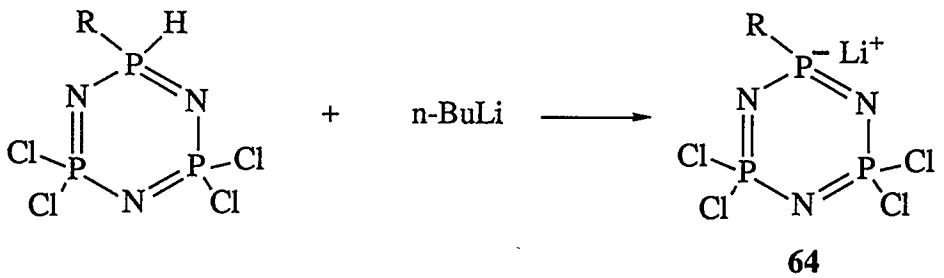

(4.1)

64

The reaction between alkyl Grignard reagents and chlorophosphazenes in the presence of an alkylcopper phosphine reagent generates another similar phosphazene anion, **65**, that,

although stable at room temperature, is of limited synthetic utility due to its low reactivity [238].

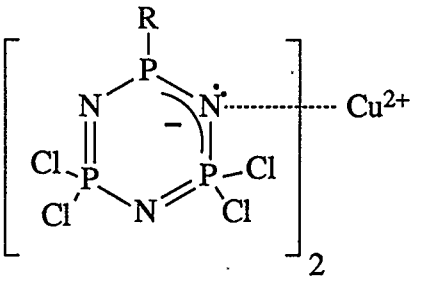

65

Phosphazene anions such as **64**, produced using organolithium reagents, have been found to be stabilized by coordination to triethylborane, **66**, resulting in enhanced thermal stability [239].

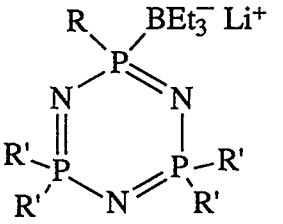

66, R'=Cl, OCH_2CF_3

Reactions between **66** and various electrophiles have been used to synthesize many new cyclophosphazene polymerization monomers and novel organometallic polyphosphazenes [240]. The reaction between hexafluorocyclotriphosphazene and super hydride has been recently reported [6]. The phosphazene anion produced, **7**, is again stabilized by BEt_3 and possess a synthetically useful nucleophilic P(V) center (Equation 4.2). The addition of excess $Li[BEt_3H]$ yields a variety of products including hydridophosphazene monoanions, dianions, and trianions, as well as ring-cleavage products.

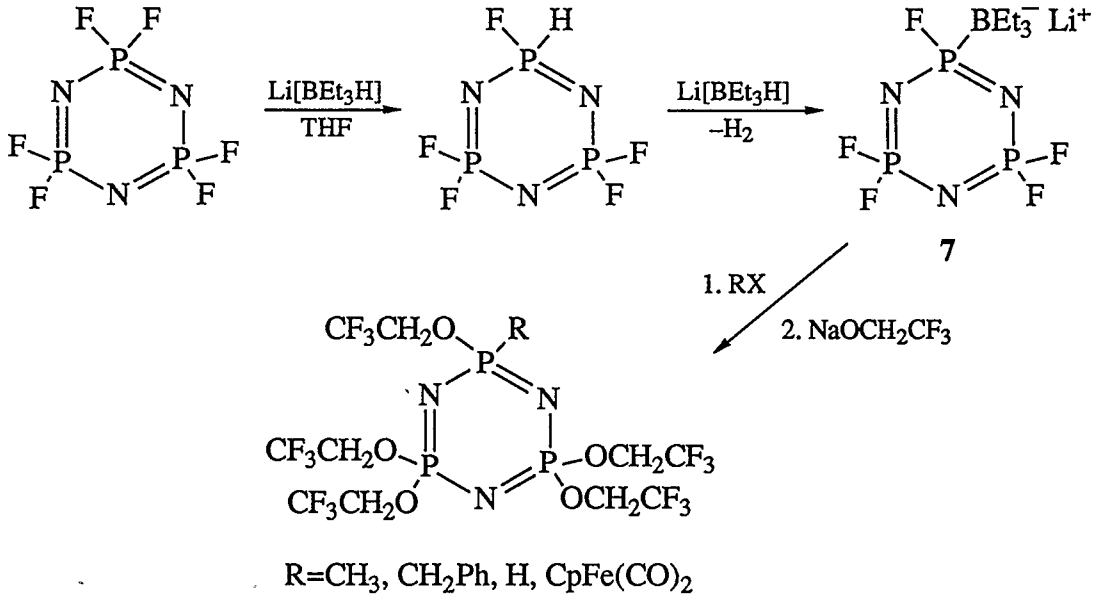

(4.2)

4.3 Reactions of Nucleophiles with Cyclothiazenes

It is perhaps surprising that nucleophiles or reducing agents react with such electron-rich heterocycles as cyclothiazenes. Fukui et al have pointed out, however, that the energetically low-lying LUMO of S_4N_4 implies electron-deficient properties [241] . This hypothesis is substantiated by the facile one electron reduction of S_4N_4 at -0.93 V (vs. Ag/0.1 M $AgClO_4$) in acetonitrile to give the anion radical $S_4N_4^-$ [242], which decomposes to $S_3N_3^-$ above 0°C [12,105] (Equation 4.3).

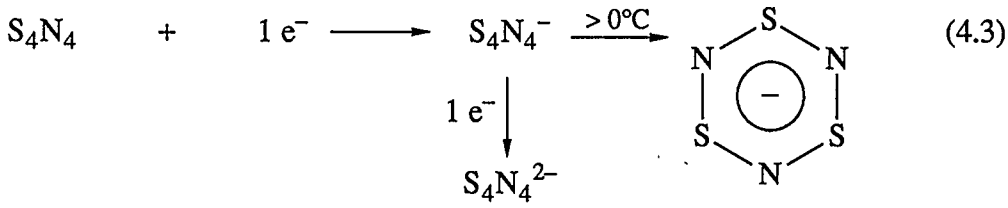

(4.3)

This unstable monoanion radical can be reduced further by an additional electron at low temperature to give the unstable dianion $S_4N_4^{2-}$ [243,244] (Equation 4.3). If such electrochemical reductions are carried out in the presence of a proton source the product is $S_4N_4H_4$ [242].

For the series of related six-membered rings, P_3N_3, $P_2SN_3^+$, PS_2N_3, and $S_3N_3^-$ the electrochemical reduction potentials correlate well with the energies of the LUMO's adjusted for the effect of charge (Figure 4.2) [245].

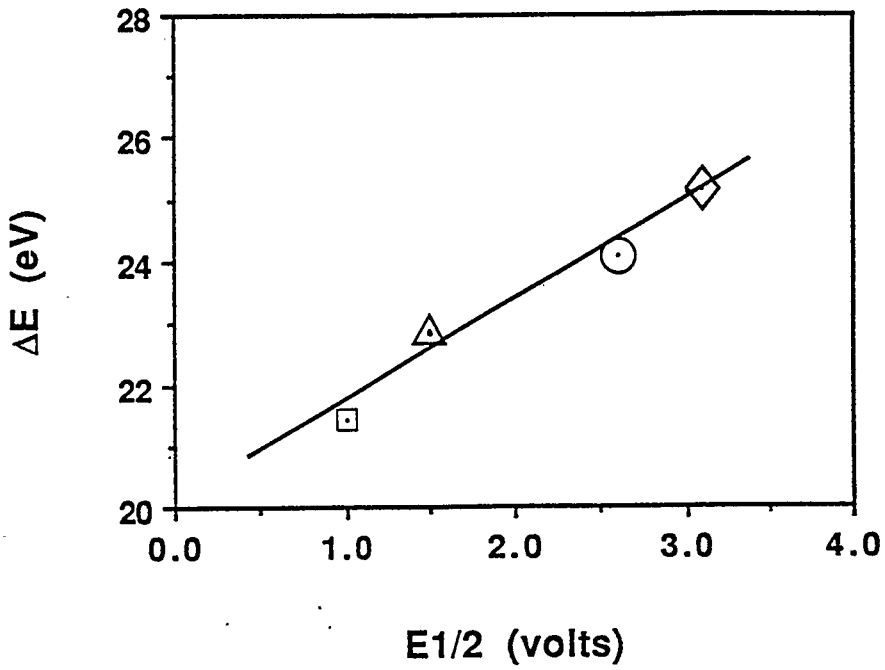

Figure 4.2 - Plot of $\Delta E = \Delta[\varepsilon(\pi\ LUMO) - \varepsilon(\pi\ LOMO)]$ versus $E_{1/2}$ for P_3N_3 (◊), $P_2SN_3^+$ ( ), PS_2N_3 (Δ), and $S_3N_3^-$ (O) where LUMO = Lowest Unoccupied Molecular Orbital and LOMO = Lowest Occupied π-Molecular Orbital. From Ref. [18].

This plot demonstrates that the six-membered rings, $P_2SN_3^+$, PS_2N_3, and $S_3N_3^-$ are better electron acceptors than the electron precise P_3N_3 ring as might be anticipated when one considers the relative LUMO energy levels (Figure 4.3) [80].

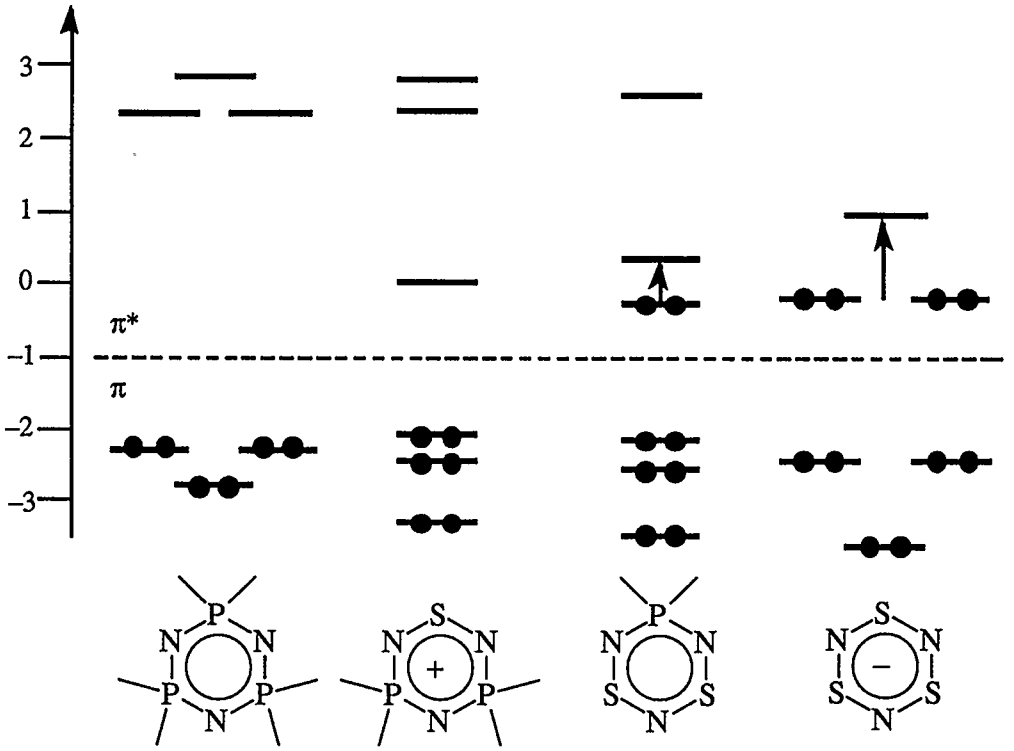

Figure 4.3 - Hückel MO energy levels for P_3N_3, $P_2SN_3^+$, PS_2N_3, and $S_3N_3^-$. The dotted line separates π and π* orbitals. From Ref. [80].

As was briefly mentioned in Chapter 1 (Section 1.3.1) the reaction of S-N heterocycles with nucleophiles usually results in either ring contraction, as is observed in the electrochemical reduction of S_4N_4, or chain formation. This behavior can be rationalized when one considers that both reduction and nucleophilic attack will populate the π* (S-N and S-S antibonding) LUMOs and thus foster ring-opening reactions (Figure 1.13 and Section 1.3.1). Examples of ring contraction for both electrochemical reduction and nucleophilic attack are illustrated in Equations 4.3, 4.4, and 4.5 [11,12,13,246].

$$S_4N_4 + \underset{\text{(or n-BuLi)}}{R_4N^+N_3^-} \longrightarrow \underset{\text{(or Li}^+\text{)}}{R_4N^+\ S_3N_3^-} \qquad (4.4)$$

$$S_4N_4O_2 + \underset{\text{(or Nuc}^-\text{)}}{1\ e^-} \longrightarrow S_3N_3O_2^- \qquad (4.5)$$

Based on the polarity of the SN bond, $S^{\partial+}$–$N^{\partial-}$, nucleophilic attack is expected at the sulfur atom (example - Equation 4.6) [247].

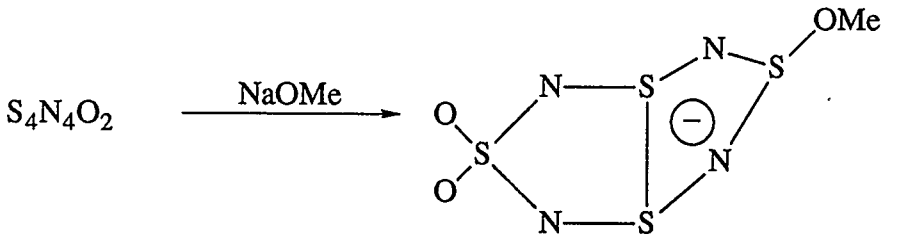

(4.6)

However, subsequent rearrangement often gives products in which the nucleophile is bonded to nitrogen (example - Equation 4.7) [248].

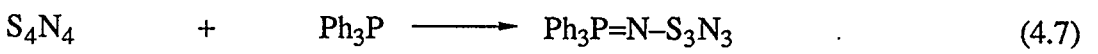

(4.7)

The reaction of S_4N_4 with some nucleophiles produces stable S-N chains. The cleavage of S_4N_4 by Si-N or Sn-N reagents is the most widely studied example of this behavior (Equations 4.8 and 4.9) [249,250,251].

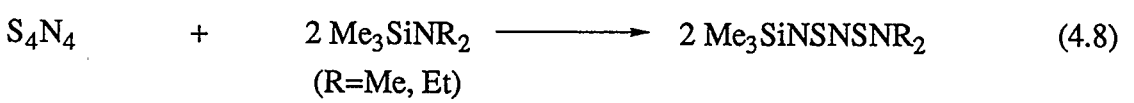

(4.8)

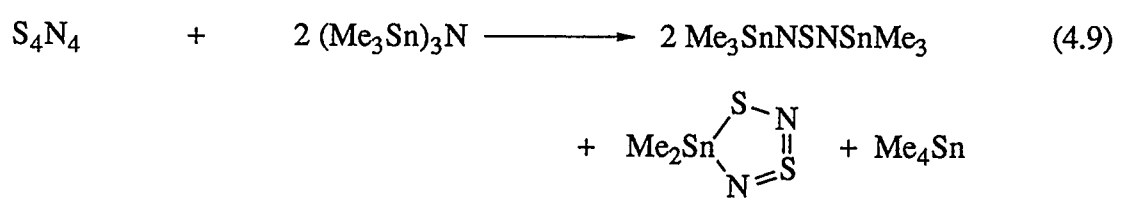

(4.9)

Treatment of S_4N_4 with aryl Grignard reagents yields small amounts of ArSNSNSAr, in addition to the major product, ArSSAr [252,253].

4.4 Electrochemical Reduction of 1,5-Diphosphadithiatetrazocines

An electrochemical study of the 1,5-diphosphadithiatetrazocines was conducted with the assistance of Dr. S. Hinman and D. Jones (University of Calgary). Two 1,5-diphosphadithiatetrazocines, 1,5-$Ph_4P_2N_4S_2$, **16a**, and 1,5-$Et_4P_2N_4S_2$, **16c**, were studied and each was found to undergo a one electron reduction in acetonitrile/0.1 M NEt_4ClO_4 at 23°C, presumably to give the corresponding monoanion radicals (Equation 4.10). A typical cyclic voltammogram (CV) is shown in Figure 4.4.

$$1,5\text{-}R_4P_2N_4S_2 \quad + \quad 1\,e^- \xrightarrow{CH_3CN} 1,5\text{-}R_4P_2N_4S_2^{\bullet -} \qquad (4.10)$$

R = Ph, E = -1.37 V vs. SCE
R = Et, E = -1.69 V vs. SCE

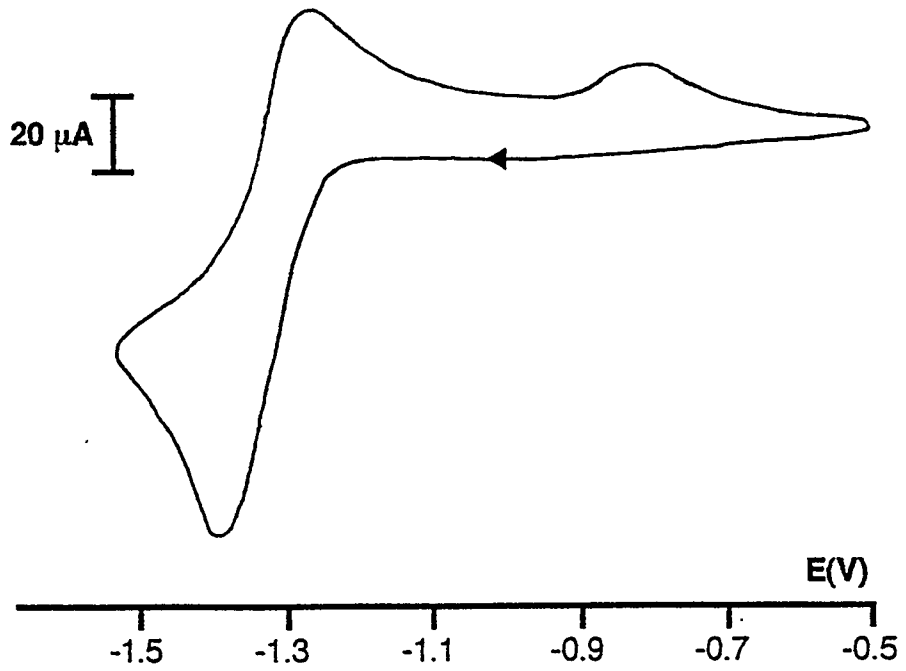

Figure 4.4 - Cyclic voltammogram for 1,5-$Ph_4P_2N_4S_2$ in CH_3CN/0.1 M NEt_4ClO_4. Scan rate = 400 mV/s.

The difference in reduction potentials (**16a**, E=-1.37 V; **16c**, E=-1.69 V) is consistent with the argument that the derivative with electron-releasing ethyl groups on phosphorus should be more difficult to reduce than the derivative with electron withdrawing phenyl groups, i.e. the $P_2N_4S_2$ ring of 1,5-$Et_4P_2N_4S_2$ is more electron-rich than that of 1,5-$Ph_4P_2N_4S_2$. Although the two systems studied could be reduced, the monoanion radicals formed were short-lived ($t_{1/2}\approx$ 2-3 seconds) as the CV plots distorted significantly at slow reduction rates.

4.5 Reaction of a 1,5-Diphosphadithiatetrazocine with Alkyl Lithium Reagents

4.5.1 Preparation and Reactions of 1,5-$Ph_4P_2N_4S_2Me^-$

The addition of one molar equivalent of a solution of MeLi in Et_2O to a solution of 1,5-$Ph_4P_2N_4S_2$ in THF at -78°C gives a soluble species whose derivative chemistry is consistent with the formation of the methyl monoanion 1,5-$Ph_4P_2N_4S_2Me^-$, **67**. The ^{31}P NMR spectrum of this species at room temperature consists of a very broad resonance at +20.6 ppm (Figure 4.5). This chemical shift differs substantially from that of the starting material, **16a** (114 ppm), indicating that the cross-ring S-S bond of **16a** has likely been cleaved as the ^{31}P chemical shifts of all 1,5-diphosphadithiatetrazocines appear at anomalously low fields (110-136 ppm). Also, the breadth of this resonance is indicative of a fluxional process. This aspect is covered in the next section.

Although no attempt was made to isolate the monoanion for elemental analysis or an X-ray structure it was found to be stable in THF, under an N_2 atmosphere, at room temperature, for at least 24 hours.

The addition of an excess of methyl iodide (MeI) to a solution of **67** in THF (Equation 4.11) yields the known heterocyclic compound 1,5-$Ph_4P_2N_4(SMe)_2$, **68** [254]. This ring was previously prepared from $(Ph_2PN)_2SMe_2$ and the explosive reagent $Me_2S(NBr)_2$ (Equation 4.12). The S,S′-dimethylated eight-membered ring **68** is also obtained on

treatment of a THF solution of 1,5-$Ph_4P_2N_4S_2Me^-Li^+$, **67**, with an excess of $Me^+CF_3SO_3^-$ [255].

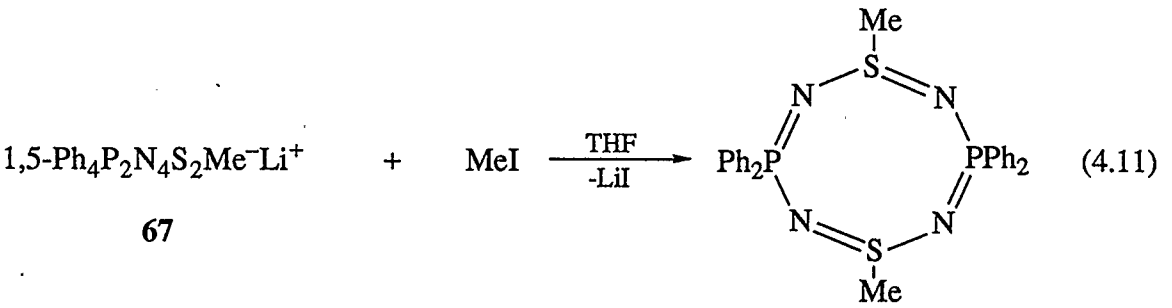

(4.11)

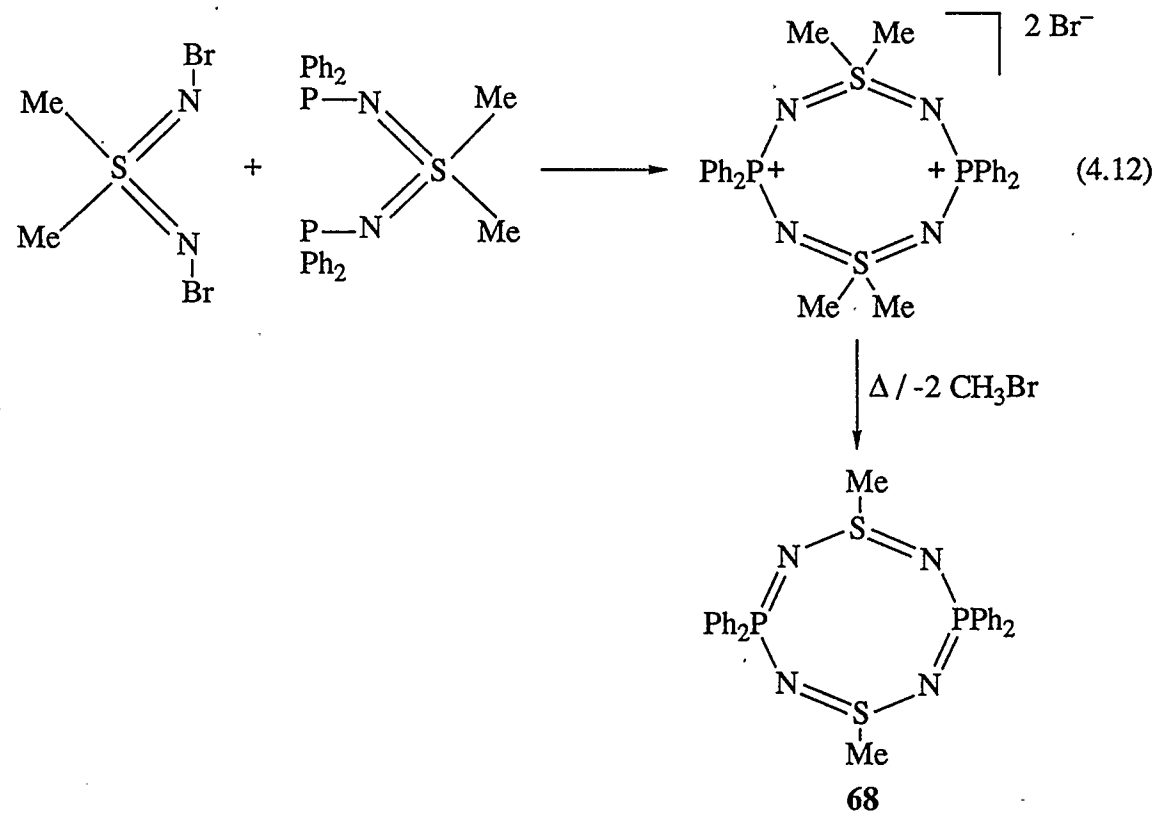

(4.12)

The ^1H and ^{13}C NMR as well as the MS data for the product obtained in this manner compare well with the literature data for 1,5-$Ph_4P_2N_4(SMe)_2$. Although no X-ray data for **68** have been published, the NMR data are consistent with the structure shown in Equations 4.11 and 4.12, i.e. each methyl group is bound to a sulfur atom rather than a nitrogen atom.

The ^{31}P NMR spectrum consists of a singlet at 27.0 ppm, indicating equivalent phosphorus atoms, while the ^{1}H and ^{13}C NMR spectra show that the two methyl groups are equivalent and coupled to two equivalent phosphorus centers. Consequently, the structure of the methyl monoanion is likely that in which the methyl group is bound to sulfur (Equation 4.13), although there is some evidence for the formation of the N-methylated isomer at low temperatures (Section 4.5.2). The mechanism for the formation of **67** undoubtedly involves nucleophilic attack by Me^- at sulfur resulting in rupture of the S-S bond. The negative charge of **67** is then likely to be delocalized over the N-S-N unit opposite the methyl group.

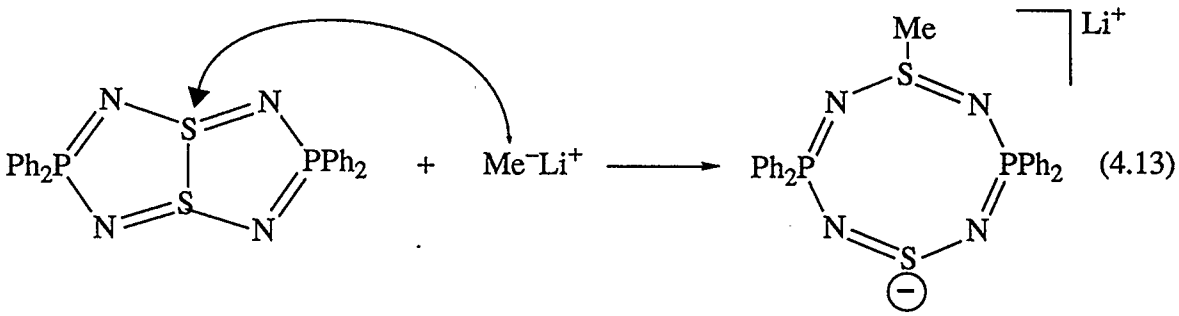

(4.13)

67

In order to determine if the alkylation of anion **67** occurs at nitrogen or sulfur the unsymmetrically substituted product 1,5-$Ph_4P_2N_4S(Me)S(Et)$, was prepared from the reaction of 1,5-$Ph_4P_2N_4S_2Me^-$ with an excess of ethyl iodide (EtI). The ^{31}P NMR chemical shift of the material obtained in this manner is not significantly different from that of the symmetrically substituted dimethyl derivative **68** (+25.7 and +27.0 ppm respectively). Such a result is expected as the substitution of an ethyl group for a methyl group should have little effect on $\delta(^{31}P)$. More importantly, if alkylation had occurred at nitrogen, the ^{31}P NMR spectrum of 1,5-$Ph_4P_2N_4S(Me)S(Et)$ would have been much more complex, as the two phosphorus atoms of an N-alkylated product would have been inequivalent.

The methyl-monoanion **67** represents the first example of a stable 1,5-diphospha-

dithiatetrazocine anion and is a potentially useful reagent in reactions with a variety of electrophiles. For example, the reactions between **67** and several platinum and palladium halides, which yield sulfur coordinated metal complexes, are currently under investigation [256].

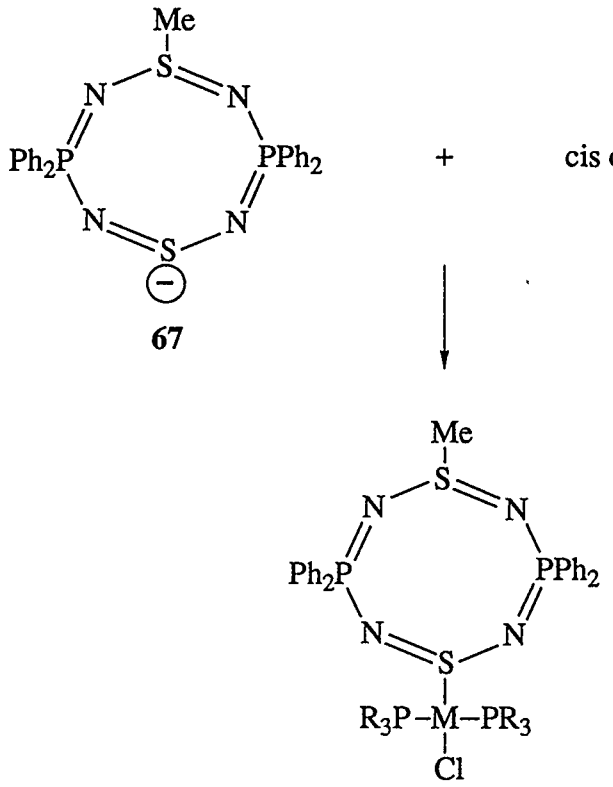

4.5.2 VT ^{31}P NMR and Fluxional Behavior of 1,5-$Ph_4P_2N_4S_2Me^-$

As noted in the previous section the ^{31}P NMR spectrum of the methyl-monoanion, **67**, at room temperature exhibited a very broad resonance indicative of fluxional behavior. A VT ^{31}P NMR study was therefore undertaken and the results are shown in Figure 4.5.

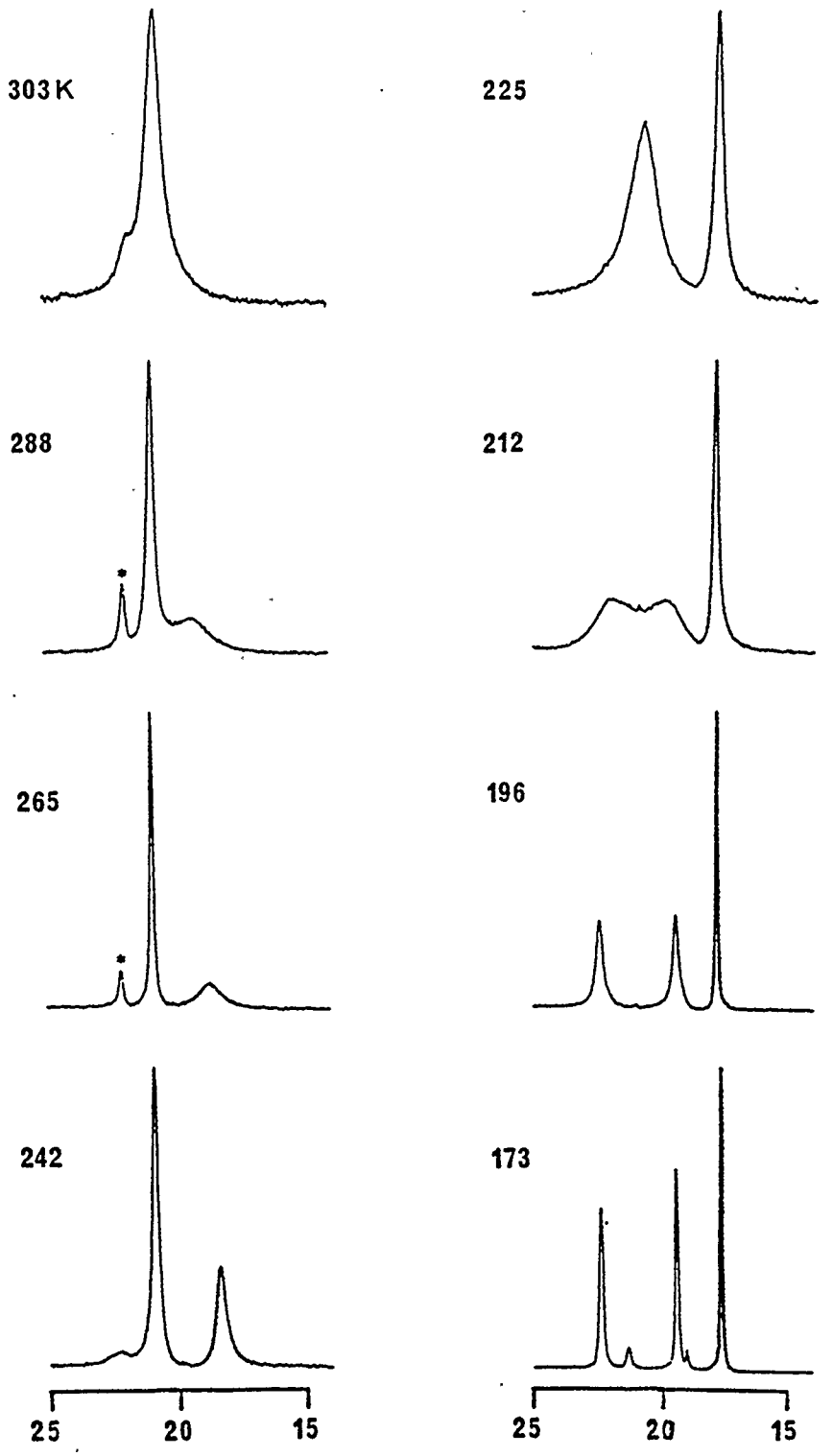

Figure 4.5 - Variable Temperature ^{31}P NMR Spectra of 1,5-$Ph_4P_2N_4S_2Me^-$, **67**.

At 173 K three distinct resonances are observed; two singlets of equal integration at 22.5 ppm and 19.5 ppm, and a third singlet at 17.8 ppm. As the temperature is gradually raised the two low field signals are observed to broaden at the same rate and eventually collapse to give one resonance at 20.5 ppm. The coalescence temperature for this process is 213 ± 2 K. This signal initially sharpens at higher temperatures but as the temperature is raised even further it, as well as the resonance at 17.8 ppm, broadens and the two signals gradually coalesce. Finally at 317 K all that remains is one broad resonance at 20.6 ppm. The reverse of these changes is observed as the solution is cooled again. The activation energy for the lower temperature fluxional process has been determined to be 8.1 kcal mol^{-1} at the coalescence temperature (213 K) [227].

There are two possible mechanisms that can be used to explain this observed fluxional behavior. The first assumes that two structural isomers are present in a solution of the methyl-monoanion, an N-methylated isomer and an S-methylated isomer. The N-methylated isomer would give rise to two signals of equal area in the ^{31}P NMR spectrum (22.5 and 19.5 ppm) while for the S-methylated isomer only one signal (17.8 ppm) would be observed as the two phosphorus atoms are magnetically equivalent. Thus, a total of three resonances would be expected which is consistent with the NMR spectrum acquired at a low temperature (179 K).

A [1,3] methyl shift is then proposed for the N-methylated derivative. At higher temperatures such a shift would cause the two signals for this isomer to broaden and eventually collapse into one signal. For the S-methylated isomer a [1,2] methyl shift from sulfur to nitrogen is proposed and at high temperatures would result in broadening and coalescence of the two remaining signals. These proposed methyl shifts are illustrated in Figure 4.6.

Although there are no reports of [1,3] methyl shifts between nitrogen atoms separated by a sulfur center, the analogous migration of the trimethylsilyl groups of N,N′,N″-tris(trimethylsilyl)-S-methylaminosulfimine has been described (Equation 4.15) [257]. The

bis(trimethylsilyl)aminophosphinimines, $R_2PN_2(SiMe_3)_3$, also exhibit intramolecular $(CH_3)_3Si$ migration, albeit across a phosphorus center (Equation 4.16) [216]. Activation energies ranging from ca. 13.5-18.5 kcal mol^{-1}, determined by VT ^1H NMR for such phosphorus (V) compounds, are comparable to that observed for the proposed [1,3] methyl migration for **67** (7.9 kcal mol^{-1}).

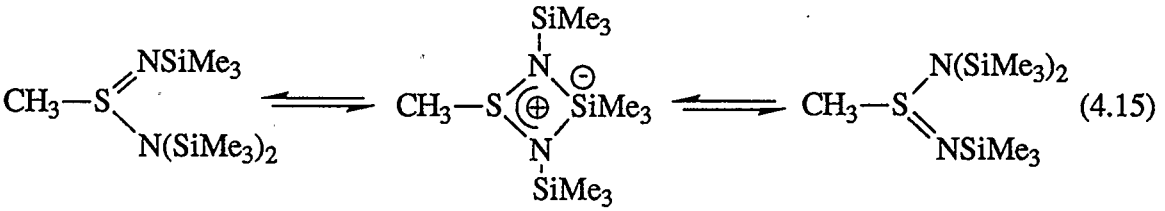

(4.15)

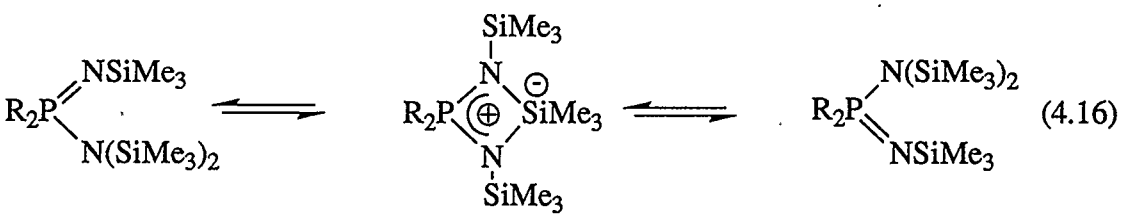

(4.16)

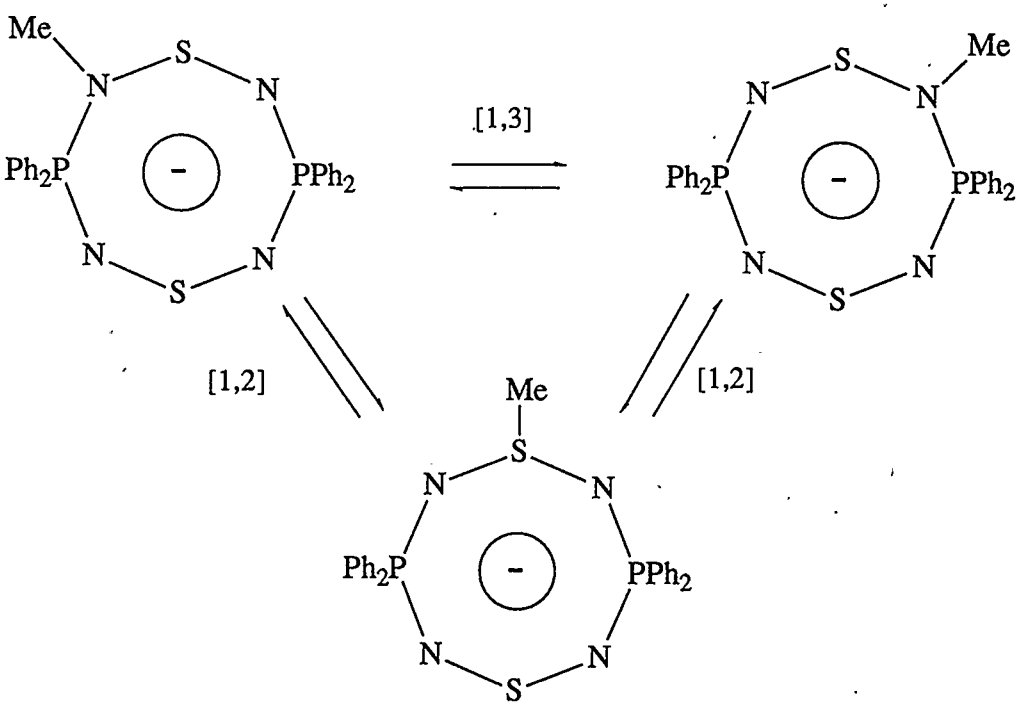

Figure 4.6 - Proposed Methyl Shifts for 1,5-$Ph_4P_2N_4S_2Me^-$, **67**.

If a three site methyl exchange as proposed above is indeed occurring then the chemical shift (weighted average of the low temperature chemical shifts) after complete coalescence is 19.6 ppm while at the highest temperature the observed resonance has a shift of 20.5 ppm.

Although a combination of [1,3] N, N and [1,2] S, N methyl shifts accounts for the observed VT ^{31}P NMR spectra there is no direct evidence for the existence of an N-methylated isomer. In fact, based on the preparation of 1,5-$Ph_4P_2N_4(SMe)_2$, for which each methyl group is bound to sulfur, it appears as though either reactions of the S-methylated isomer are kinetically favoured or the N-methylated isomer does not exist.

The second explanation for the fluxional behavior of **67** does not invoke the existence of an N-methylated isomer but instead assumes that at least two conformational isomers of the S-methylated anion are present (Figure 4.7). The two phosphorus atoms of isomer **67a** are inequivalent as one is closer to the methyl group than the other. If the sulfur atoms undergo rapid inversion, as illustrated in Figure 4.7, the two P atoms could become equivalent on the NMR time scale. This inversion process would account for the coalescence of the two low field signals at 210 K.

The two possible conformations of **67** that could account for the remaining, unassigned resonance in the ^{31}P NMR spectrum are shown in Figure 4.7. For each isomer, **67b** and **67c**, the two heterocyclic P atoms are equivalent. However, if one of the NPN units of **67b** or **67c** folds to the opposite side of the ring then isomer **67a** results. Rapid ring folding of this type, in conjunction with inversion at sulfur, as described previously, would account for the complete coalescence of all three signals. This proposed mechanism is summarized in Figure 4.7.

MNDO molecular orbital calculations have shown that for $RS(NSN)_2SR$ molecules the activation energies for inversion at sulfur fall in the range 27 (R=Cl) to 45 ($R=NH_2$) kcal mol^{-1} [135] while the measured barrier for the related compound 1,2,5-thiadiazole-1-oxide, $C_2H_2N_2SO$, is 33 kcal mol^{-1} [258]. As such values are substantially larger than that experimentally determined for **67**, it appears that inversion at sulfur does not adequately

explain this observed fluxional behavior. Also, this description requires that inversion at sulfur be a more facile process than ring folding and, as inversion at sulfur has a relatively high energy barrier, such a proposition seems unreasonable.

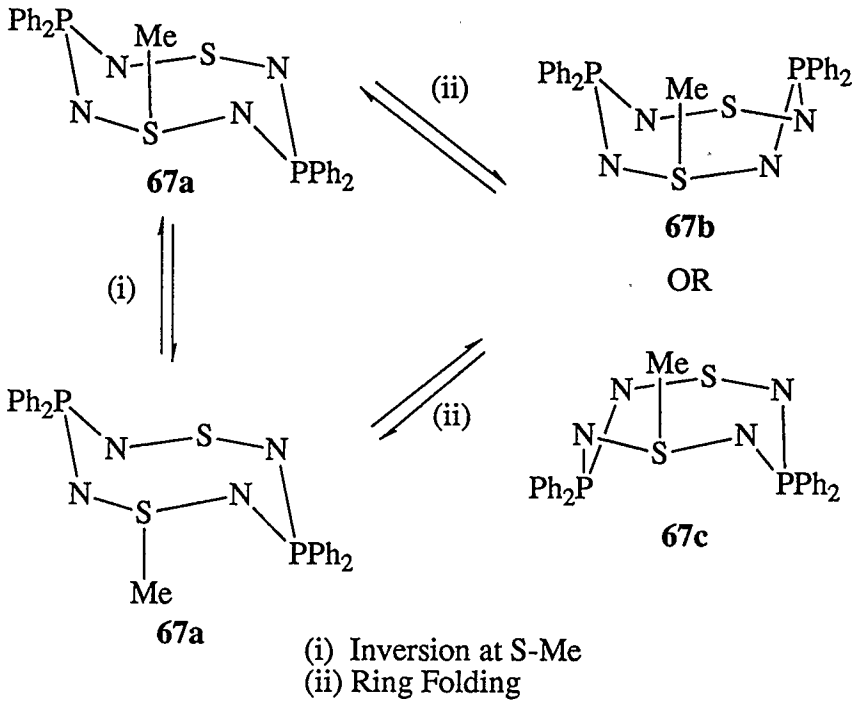

Figure 4.7 - Proposed Conformational Changes for 1,5-$Ph_4P_2N_4S_2Me^-$, **67**.

A VT ^1H NMR study of the methylated anion, **67**, was performed but, due to very broad, unresolved signals no further insight as to the possible mechanism for the observed fluxional behavior was gained. Similarly, the results of a VT ^{13}C NMR study of **67** provided no further information as much of the NMR window of interest was masked by the signals of the solvent (d^8-THF). However, the use of ^{13}C enriched MeLi may provide sufficient information to support the mechanism invoking the involvement of the N-methylated isomer.

4.5.3 VT ^{31}P NMR and Fluxional Behavior of 1,5-$Ph_4P_2N_4S_2(t\text{-}Bu)^-$

In an attempt to slow down the fluxional behavior observed for the methyl-monoanion a

second derivative was prepared using a more sterically bulky alkyl lithium reagent. The addition of one molar equivalent of t-butyl lithium to a THF solution of 1,5-$Ph_4P_2N_4S_2$ at -78°C gives a clear, colorless solution. The species formed is likely analogous to that formed with the use of MeLi, i.e. 1,5-$Ph_4P_2N_4S_2$(t-Bu)$^-$, **69** (Equation 4.17).

$$1,5\text{-}Ph_4P_2N_4S_2 \quad + \quad \text{t-BuLi} \xrightarrow[-78°C]{\text{THF}} \quad 1,5\text{-}Ph_4P_2N_4S_2(\text{t-Bu})^- \quad (4.17)$$

69

The ^{31}P NMR spectrum (Figure 4.8) of such a solution at 305 K shows a very broad resonance at 20.0 ppm. At lower temperatures (179-294 K) the spectra are very similar to those of the methyl-monoanion, **67**, i.e. three signals at 179 K, two of which (21.9 and 20.3 ppm) broaden and collapse at approx. 210 K, leaving two signals, which in turn also broaden and coalesce at 305 K.

The primary difference between the ^{31}P NMR spectra of **67** and **69** is that the two signals which coalesce at the lower temperature differ in chemical shift by only 1.6 ppm for **69** (cf. 3.0 ppm for **67**). However, the activation energies for this fluxional process of 8.1 ± 0.2 kcal mol^{-1} (210 K) for the t-butyl derivative and 7.8 ± 0.2 kcal mol^{-1} (213 K) for the methyl derivative are the same within experimental error [227]. It is likely that the migrating alkyl group (methyl or t-butyl) is too remote from the phenyl groups on phosphorus to have any measurable effect on the activation energies.

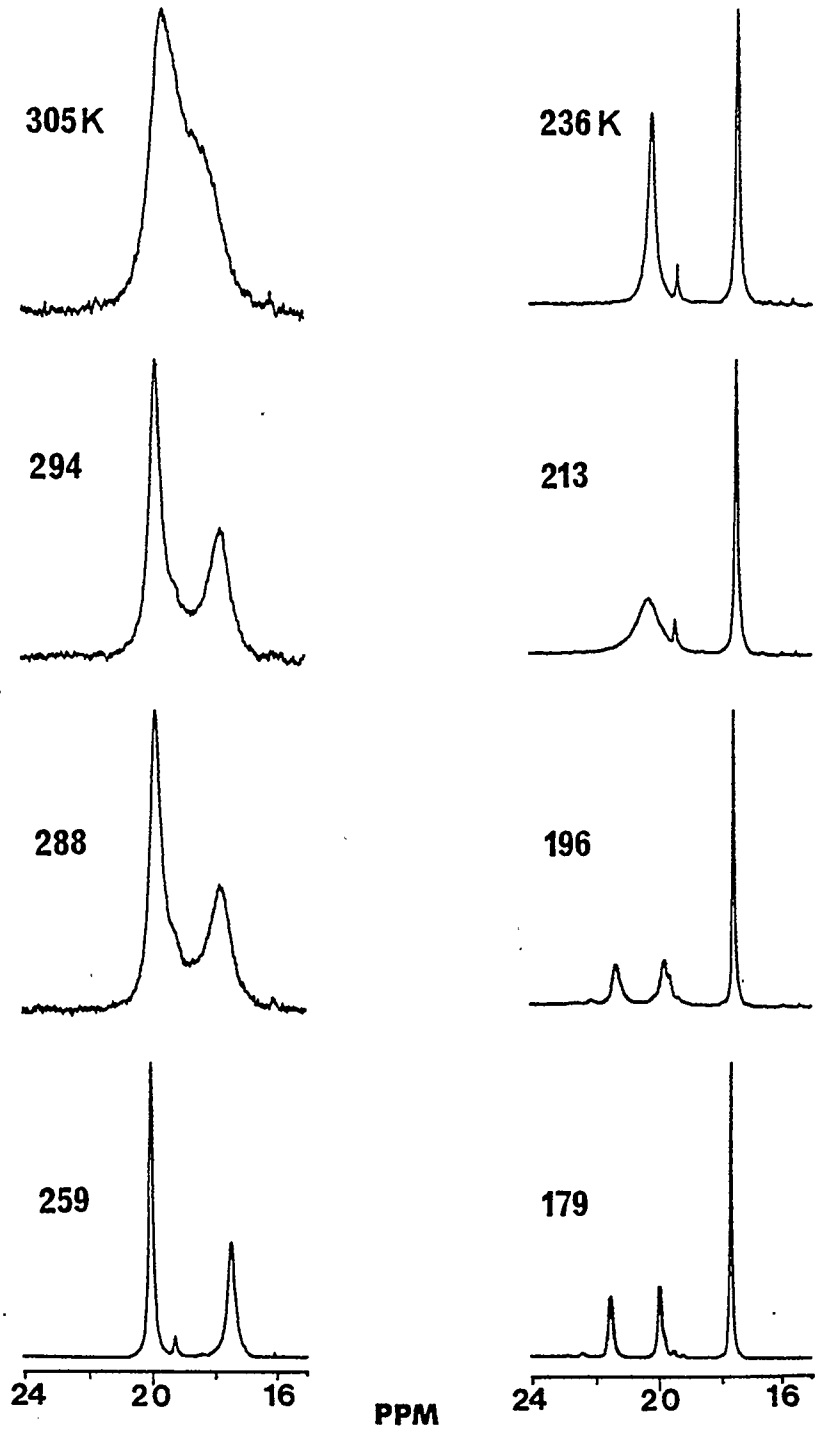

Figure 4.8 - VT ^{31}P NMR Spectra of 1,5-$Ph_4P_2N_4S_2$(t-Butyl)$^-$, **69.**

4.6 Preparation and Reactions of "$Li_2[1,5\text{-}Ph_4P_2N_4S_2]$"

The addition of 2 molar equivalents of a THF solution of super hydride ($LiBEt_3H$) to a solution of $1,5\text{-}Ph_4P_2N_4S_2$ in THF at either -78°C or 0°C, followed by gradual warming to 23°C, results in the formation of a yellow precipitate and the simultaneous evolution of a gas (presumably H_2). This yellow precipitate is formulated to be the dilithium salt of the $1,5\text{-}Ph_4P_2N_4S_2$ dianion, i.e. $Li_2[1,5\text{-}Ph_4P_2N_4S_2]$, **70**, on the basis of its derivative chemistry (Sections 4.6.1 to 4.6.3). It is a highly insoluble material (THF, Et_2O, hexanes, toluene) which can be isolated by means of filtration. The dry yellow powder is stable under an inert atmosphere for several days but decomposes on exposure to air/moisture.

The formation of such a dianion likely involves initial nucleophilic hydride attack at sulfur forming a hydrido monoanion analogous to the anions obtained using alkyl lithium reagents. Subsequent attack by a second hydride, followed by deprotonation and the elimination of hydrogen, would give the dianion **70** (Equation 4.18).

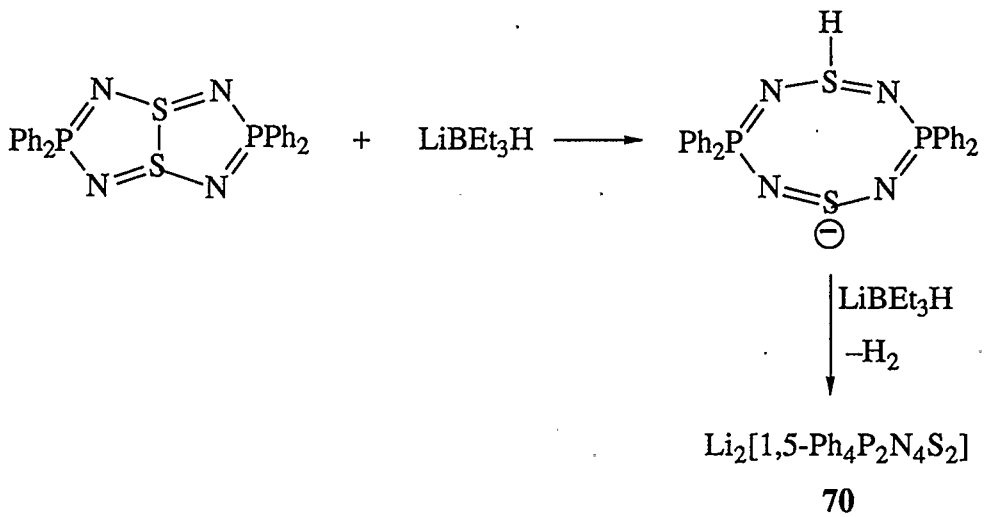

(4.18)

Reaction of the structurally related sulfur diimides with t-butyl lithium produces eight-membered $Li_2N_4S_2$ rings in which the lithium atoms bridge the nitrogen centers (Equation 4.19) [259].

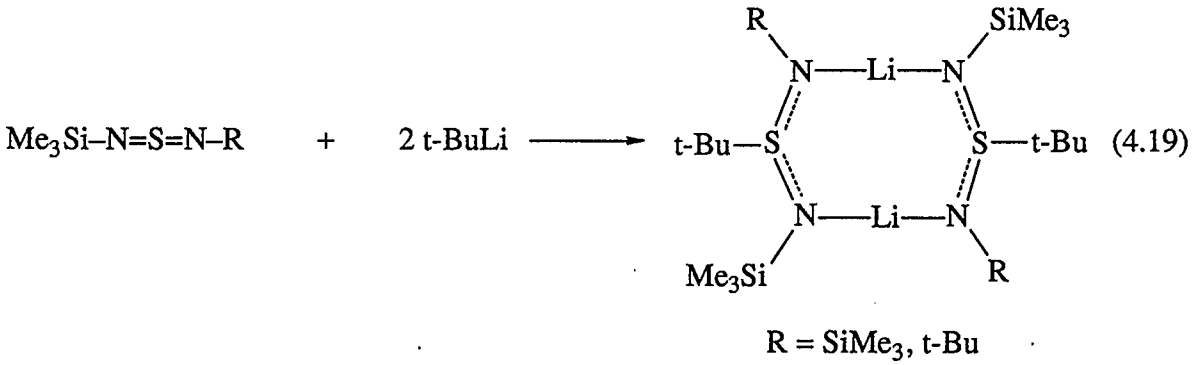

(4.19)

For the 1,5-diphosphadithiatetrazocines, which can be thought of as containing two sulfur diimide (NSN) groups bridged by two phosphorus atoms, a related polymeric structure can be envisaged (Figure 4.9). The use of crown ethers or N,N,N′,N′-tetramethylethylenediamine (TMEDA) may give a lithium salt which is of sufficient solubility to grow crystals for an X-ray structural determination.

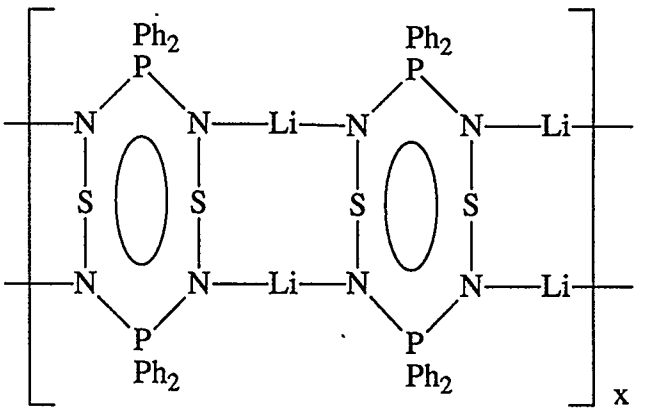

Figure 4.9 - Proposed Polymeric Structure of $Li_2[1,5\text{-}Ph_4P_2N_4S_2]$, **70**

4.6.1 Synthesis of $1,5\text{-}Ph_4P_2N_4(SMe)_2$ from "$Li_2[1,5\text{-}Ph_4P_2N_4S_2]$"

The reaction of an excess of MeI with a slurry of $Li_2[1,5\text{-}Ph_4P_2N_4S_2]$, **70**, in THF gives the S,S′-dimethylated eight-membered ring $1,5\text{-}Ph_4P_2N_4(SMe)_2$, **68**, in 30% yield. This compound was also prepared by treating $1,5\text{-}Ph_4P_2N_4S_2$ with MeLi followed by MeI (Section 4.4.1). The ^1H, ^{13}C, and ^{31}P NMR spectra for the material obtained in this manner

are identical to those obtained for the MeLi/MeI product. The ^{31}P NMR spectrum of **68** shows a singlet at 26 ppm (cf. 21.7 ppm for 1,5-$Ph_4P_2N_4(SeMe)_2$ [260]) indicating that the S-S bond present in the starting material, **16a**, is no longer present. The X-ray structure of the selenium analog of **68**, 1,5-$Ph_4P_2N_4Se_2Me_2$, has been published [260] (Figure 4.10) and based on the ^1H, ^{13}C, and ^{31}P NMR data the two structures are likely very similar, i.e. an eight-membered chair in which the two P atoms and four N atoms are planar, the two chalcogen atoms are displaced on either side of the ring, and the two exocyclic methyl groups occupy axial positions (cf. 1,5-$Ph_4P_2N_4S_2Br_2$, Figure 1.22 [197]).

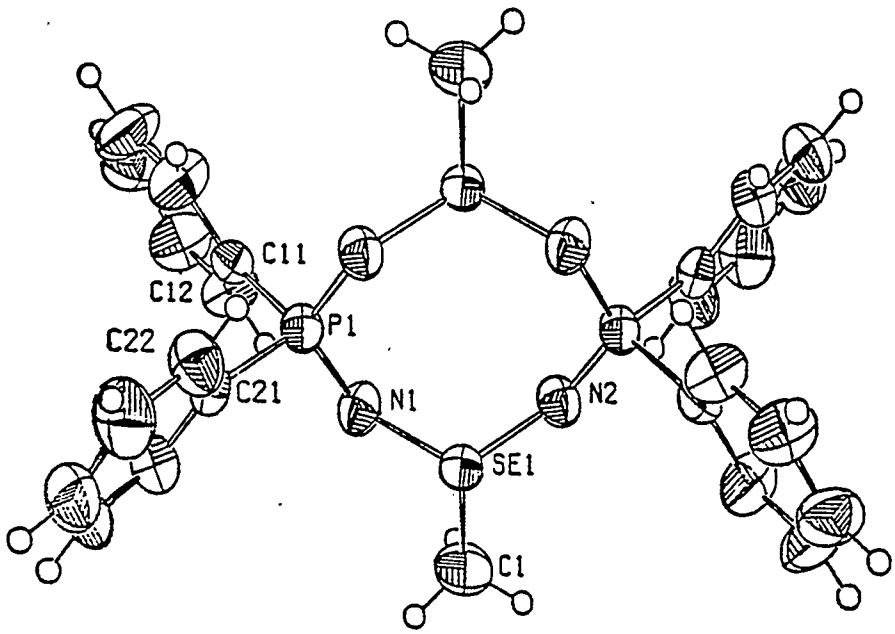

Figure 4.10 - ORTEP Plot of 1,5-$Ph_4P_2N_4(SeMe)_2$. From Ref [260].

4.6.2 Synthesis and X-ray Analysis of $Ph_4P_2N_4S_2CH_2$, **71**

The reaction between a slurry of "Li_2[1,5-$Ph_4P_2N_4S_2$]" and diiodomethane (CH_2I_2) in THF gives $Ph_4P_2N_4S_2CH_2$, **71**, in 23% yield. The solid-state structure of **71** was determined by X-ray crystallography by Prof. M. Cowie (University of Alberta) and Dr. R. Hilts of this department. An ORTEP drawing of **71** with the atomic numbering scheme is shown in Figure 4.11. The crystallographic data and the pertinent bond lengths and angles are summarized in Tables 4.1 and 4.2, respectively. Complete structure analysis details as well as a listing of atomic coordinates and isotropic thermal parameters are given in reference [261].

Table 4.1 : Crystallographic Data for $Ph_4P_2N_4S_2CH_2$, **71**

Chem formula $C_{25}H_{22}N_4P_2S_2$	fw = 504.6
$\underline{a}$ = 10.340(1) Å	space group - P1
$\underline{b}$ = 12.964(2) Å	$\underline{T}$ = 293 K
$\underline{c}$ = 10.175(2) Å	$\underline{\lambda}$ = 0.71069 Å
$\underline{\alpha}$ = 109.96(1)°	$\underline{\rho}_{calcd}$ = 1.40 g cm^{-3}
$\underline{\beta}$ = 108.24(1)°	$\underline{\mu}$ = 1.72 cm^{-1}
$\underline{\gamma}$ = 73.89(1)°	$\underline{R}^a$ = 0.050
$\underline{V}$ = 1195.0(6) $Å^3$	$\underline{R}_w{}^b$ = 0.060
$\underline{Z}$ = 2	

a. $\underline{R} = \Sigma||F_o| - |F_c||/|F_o|$

b. $\underline{R}_w = [\Sigma w\Delta^2/\Sigma F_o^2]^{1/2}$

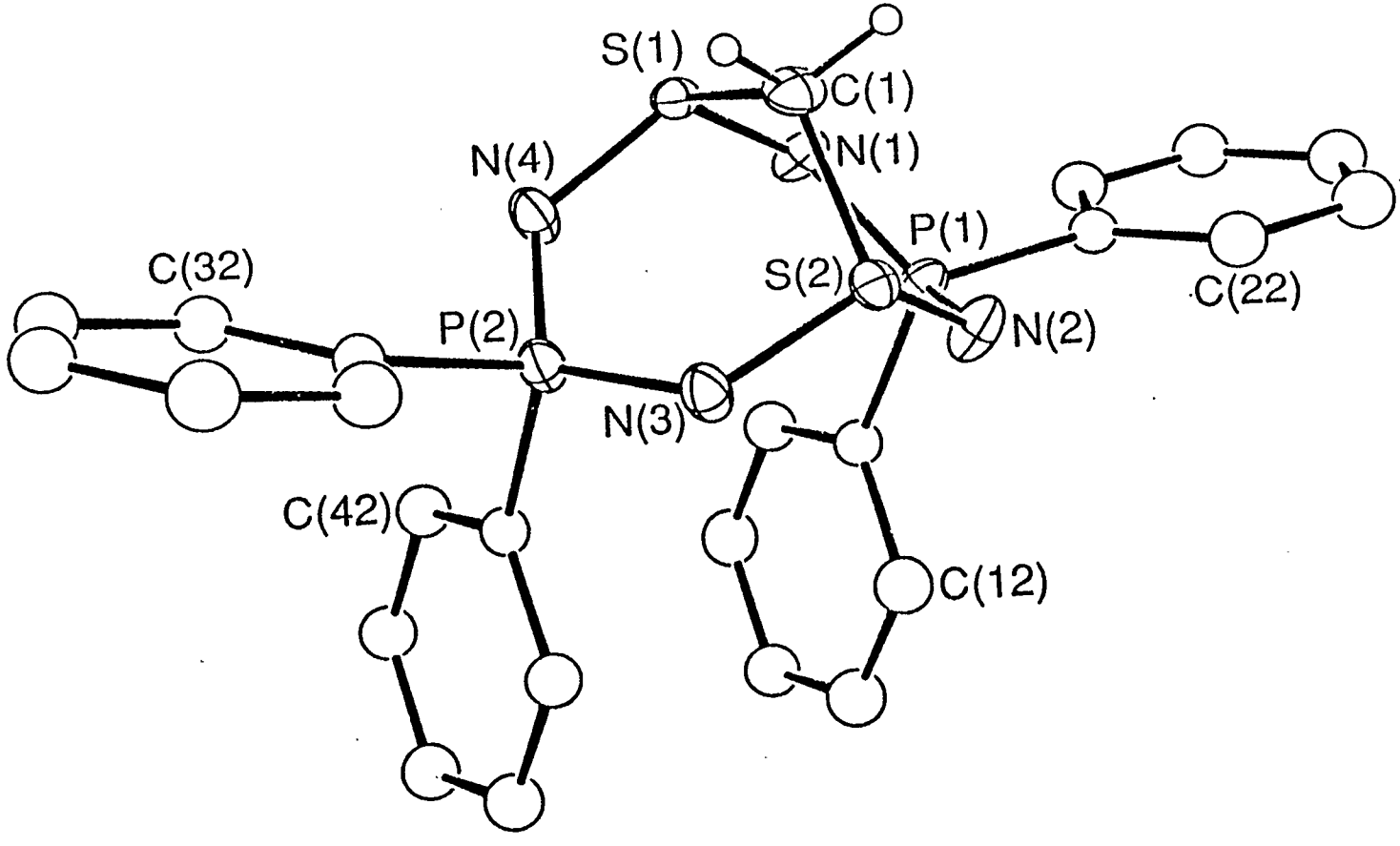

Figure 4.11 - ORTEP Plot of $Ph_4P_2N_4S_2CH_2$, **71**

Table 4.2 : Selected Bond Lengths (Å) and Bond Angles (°) for $Ph_4P_2N_4S_2CH_2$, **71**

Bond lengths (Å)

S(1)-N(1)	1.592(3)	P(1)-N(2)	1.609(3)
S(1)-N(4)	1.595(3)	P(1)-C(11)	1.806(4)
S(1)-C(1)	1.827(4)	P(1)-C(21)	1.798(4)
S(2)-N(2)	1.594(3)	P(2)-N(3)	1.610(3)
S(2)-N(3)	1.597(3)	P(2)-N(4)	1.607(3)
S(2)-C(1)	1.812(4)	P(2)-C(31)	1.808(4)
P(1)-N(1)	1.620(3)	P(2)-C(41)	1.800(4)

Bond angles (°)

S(1)-C(1)-S(2)	113.0(2)	C(11)-P(1)-C(21)	105.0(2)
N(1)-S(1)-N(4)	115.6(2)	N(3)-P(2)-N(4)	119.1(2)
N(1)-S(1)-C(1)	102.5(2)	N(3)-P(2)-C(31)	106.3(2)
N(4)-S(1)-C(1)	102.4(2)	N(3)-P(2)-C(41)	110.3(2)
N(2)-S(2)-N(3)	115.0(2)	N(4)-P(2)-C(31)	107.7(2)
N(2)-S(2)-C(1)	103.4(2)	N(4)-P(2)-C(41)	108.9(2)
N(3)-S(2)-C(1)	103.3(2)	C(31)-P(2)-C(41)	103.5(2)
N(1)-P(1)-N(2)	118.2(2)	S(1)-N(1)-P(1)	123.4(2)
N(1)-P(1)-C(11)	109.5(2)	S(2)-N(2)-P(1)	124.6(2)
N(1)-P(1)-C(21)	106.5(2)	S(2)-N(3)-P(2)	123.8(2)
N(2)-P(1)-C(11)	110.5(2)	S(1)-N(4)-P(2)	126.0(2)
N(2)-P(1)-C(21)	106.3(2)		

The structure of **71** shows a bicyclic molecule in which the methylene group bridges the two sulfur atoms of the heterocyclic ring. As a result there is a substantial opening of S-S bond from 2.551(2) Å in $Ph_4P_2N_4S_2$ to 3.033 Å in **71**, accompanied by a wide S(1)-C(1)-S(2) angle of 113.0(2)° at the methylene carbon. In addition, the methylene bridge enforces larger endocyclic bond angles at phosphorus and nitrogen, resulting in mean N-P-N and S-N-P angles of 118.6(2)° and 124.5(2)° respectively [cf. 110.8(1) and 120.9(2)°, respectively for **16a**]. The mean S-N and P-N bond lengths in **71** are not significantly different from those found for **16a**. Each PN_2S_2 unit is nearly planar and the angle between the two PN_2S_2 planes is 110.31(7)°.

The ^{31}P NMR chemical shift for $Ph_4P_2N_4S_2CH_2$ of -19.4 ppm is very close to that for the related bicyclic compound $Ph_2PN_5S_3$ (-21.4 ppm) [196].

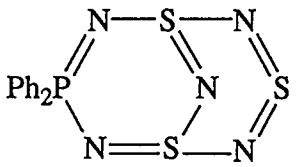

49

As the methylene group of **71** bridges two sulfur atoms it was considered feasible that this bridge could be deprotonated to form a carbanion center. The capacity of sulfur to significantly enhance the acidity of adjacent C-H bonds has been exploited extensively in synthetic organic chemistry [262]. For example, the S-CH_2-S group of 1,3-dithiane, $C_3H_6S_2CH_2$, is readily deprotonated on treatment with n-BuLi [263]. A preliminary experiment, conducted in conjunction with Dr. R. Hilts, provided good evidence that **71** can indeed be deprotonated with n-BuLi. Subsequent treatment of the deprotonated bicyclic with an excess of MeI gives a ^{31}P NMR spectrum that is consistent with the production of $Ph_4P_2N_4S_2CHCH_3$, **72**, i.e. two signals of equal intensity whose chemical shifts are very similar to that of **71** (the two P atoms of **72** are inequivalent) (Equation 4.20). However, insufficient material was available for a complete characterization.

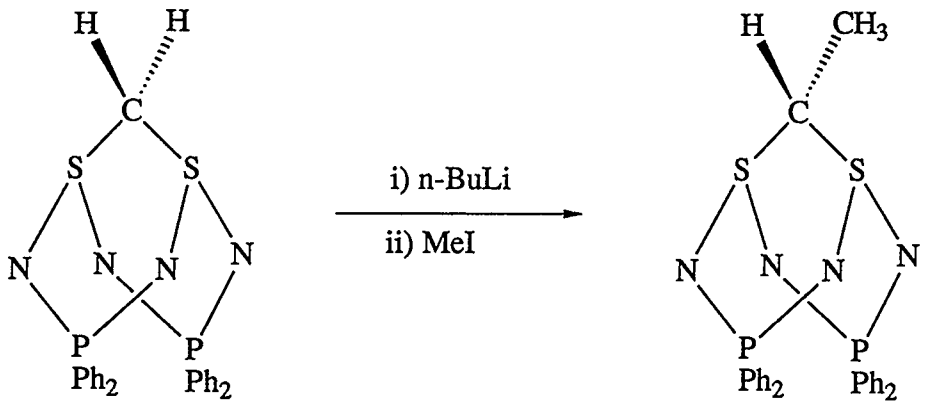

71 **72** (4.20)

4.6.3 Synthesis of Platinum Group Metal Complexes From $Li_2[1,5\text{-}Ph_4P_2N_4S_2]$

The reactions of $Li_2[1,5\text{-}Ph_4P_2N_4S_2]$ with various platinum group metal halides (L_2MCl_2) proceed slowly at room temperature according to Equation 4.21.

$$Li_2[1,5\text{-}Ph_4P_2N_4S_2] + L_2MCl_2 \xrightarrow{-2\ LiCl} ML_2(1,5\text{-}Ph_4P_2N_4S_2) \quad (4.21)$$

60a : M=Pt, L=PPh_3
73 : M=Pt, L=PEt_3
74 : M=Ni, L_2=diphos

The three compounds were only characterized by ^{31}P NMR spectroscopy as several other products were formed making purification difficult. However, the ^{31}P NMR spectrum of each compound was consistent with the formation of a monomeric metal complex analogous to those prepared from the neutral eight-membered rings, $1,5\text{-}R_4P_2N_4S_2$, and the zero-valent platinum ($Pt(PPh_3)_2(C_2H_4)$) and palladium complexes ($Pd(PPh_2R)_4$) as discussed in Chapter 3. The best evidence for the formation of such metal complexes was provided by the ^{31}P NMR spectrum of **60a** which was identical to that of the known compound $Pt(PPh_3)_2(1,5\text{-}Ph_4P_2N_4S_2)$, prepared from $1,5\text{-}Ph_4P_2N_4S_2$ and $Pt(PPh_3)_2(C_2H_4)$. This spectrum consisted of two equally intense triplets [$^4J(^{31}P\text{-}^{31}P)$=4.4 Hz], each with Pt satellites, at 37.9 ppm [$^3J(^{31}P\text{-}^{195}Pt)$=579 Hz] and 17.9 ppm [$^1J(^{31}P\text{-}$

^{195}Pt)=2857 Hz], which can be assigned to the Ph_2P groups and PPh_3 ligands respectively. The ^{31}P NMR spectrum of the second Pt complex, **73** was very similar to that of **60a**, two equally intense triplets $^4J(^{31}P\text{-}^{31}P)$=3.6 Hz, each with Pt satellites, at 35.9 ppm [$^3J(^{31}P\text{-}^{195}Pt)$=536 Hz] and 4.46 ppm [$^1J(^{31}P\text{-}^{195}Pt)$=2733 Hz], indicating that the two structures are very similar, i.e. η^2–S, S′ coordination of the eight-membered heterocyclic ring as illustrated in Figure 4.12.

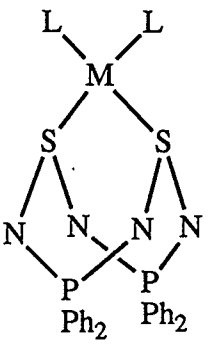

Figure 4.12 - η^2-S,S′ Pt and Ni complexes, **60a**, **73**, and **74**, prepared from $Li_2[1,5\text{-}Ph_4P_2N_4S_2]$.

The ^{31}P NMR spectrum obtained for the reaction between the dianion and $Ni(diphos)Cl_2$ suggested that the product was also a monomeric complex. Again, two resonances of equal area were observed, each a triplet with $^4J(^{31}P\text{-}^{31}P)$ = 9.3 Hz. The values for the same interaction in the monomeric Pt and Pd complexes are 4.4 Hz and 12.5 Hz respectively. Also, the change in chemical shift of the heterocyclic ligand upon coordination for **16a** (Δ = –69 ppm) is similar to the coordination shifts observed for the Pt and Pd complexes reported in Chapter 3 (Δ = –75 and -60 ppm). Thus, compound **74** is proposed to be similar in structure to the monomeric Pt and Pd complexes reported in Chapter 3 (Figure 4.12). It is of particular note that all attempts to prepare a monomeric nickel complex from zero-valent nickel reagents such as $Ni(PPh_3)_4$ or $Ni(diphos)(CO)_2$ and neutral 1,5-diphosphadithiatetrazocines were unsuccessful (Section 3.2.1).

4.6.4 Reactions of $Li_2[1,5\text{-}Ph_4P_2N_4S_2]$ with Other Electrophiles

Attempts to prepare germanium or phosphorus bridged compounds, analogous in structure to $Ph_4P_2N_4S_2CH_2$, by reaction of the dianion with neat $GeCl_4$ or $PhPCl_2$, proved to be unsuccessful (Equation 4.22). Instead the quantitative regeneration of $1,5\text{-}Ph_4P_2N_4S_2$, **16a**, is observed. The occurrence of this redox process may limit the application of the dianion reagent.

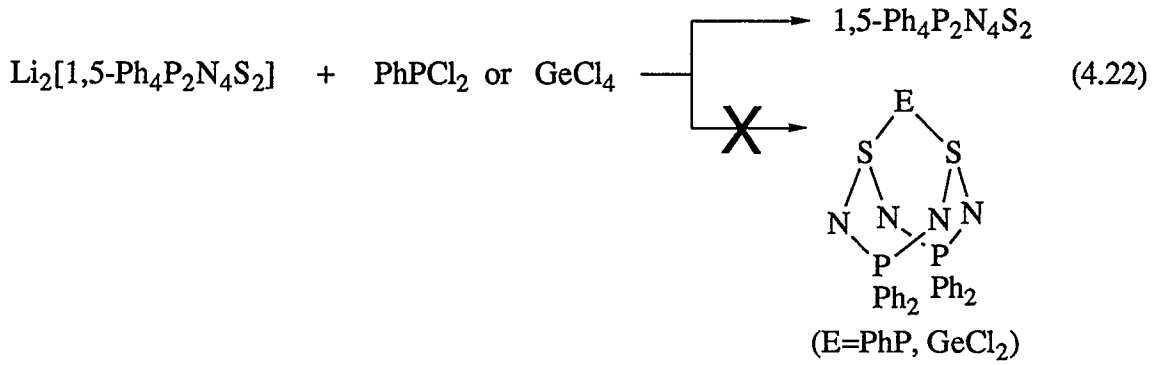

(4.22)

4.7 Conclusions

In contrast to S_4N_4, which undergoes either ring contraction or ring opening in its reaction with nucleophiles, the 1,5-diphosphadithiatetrazocine, $1,5\text{-}Ph_4P_2N_4S_2$, reacts readily with either MeLi or t-BuLi to produce alkylated monoanions in which the eight-membered heterocycle remains intact. Both anions were found to be fluxional by VT ^{31}P NMR spectroscopy. The fluxional process is proposed to involve either a combination of [1,3] N,N and [1,2] N,S methyl shifts for N-methylated and S-methylated structural isomers or conformational changes in an S-methylated isomer alone. The reaction of the methyl-monoanion with MeI gives the known S, S′-dimethylated heterocycle $1,5\text{-}Ph_4P_2N_4(SMe)_2$.

Reduction of $1,5\text{-}Ph_4P_2N_4S_2$ with two molar equivalents of $Li[BEt_3H]$ (super hydride) gives a yellow solid that, although not fully characterized due to its highly insoluble nature and sensitivity to oxygen/moisture, is likely $Li_2^+[1,5\text{-}Ph_4P_2N_4S_2]^{2-}$. This material was found to react readily with MeI to give $1,5\text{-}Ph_4P_2N_4(SMe)_2$ or with CH_2I_2 to give a novel

bicyclic compound, $Ph_4P_2N_4S_2CH_2$, in which the methylene group bridges two sulfur atoms. A preliminary experiment has provided good evidence that this methylene bridge can be deprotonated with n-BuLi and subsequently derivatized.

It has been discovered that the monomeric metal complexes discussed in Chapter 3 can also be prepared by reacting $Li_2[1,5\text{-}Ph_4P_2N_4S_2]$ with phosphine-halide complexes of the platinum group metals (Pt, Pd, and Ni).

For the cyclophosphathiazene $1,5\text{-}Ph_4P_2N_4S_2$ both the alkylated-monoanions and the lithium salt of the dianion have proven to be very interesting and, more importantly, versatile reagents. Reactions of such anions with electrophiles will undoubtedly allow many new heterocyclic compounds to be prepared.

4.8 Experimental Section

4.8.1 Reagents and General Procedures

All solvents were dried and distilled before use : tetrahydrofuran (Na), methylene chloride and hexanes (P_4O_{10}), acetonitrile (CaH_2 and P_4O_{10}) and acetone (molecular sieves). Drying agents employed for other solvents used in this section as well as details concerning the manipulation of oxygen/moisture-sensitive products are outlined in Chapter 2, Section 2.6.1. Commercial products used as received were : $Li[BEt_3H]$ (0.9 M solution in THF), MeLi (1.4 M solution in Et_2O), t-BuLi (2.5 M solution in hexanes), CH_2I_2, and cis-Ni(diphos)Cl_2 (Aldrich). MeI (Fisher) was passed through basic alumina before use.

Literature procedures were used for the preparation of $1,5\text{-}Ph_4P_2N_4S_2$ [209], cis-$Pt(PEt_3)_2Cl_2$ [264], and cis-$Pt(PPh_3)_2Cl_2$ [232]. The ^{31}P NMR chemical shifts for these reagents are given in Table 4.3.

Table 4.3 : ^{31}P NMR Data for Selected Transition Metal Dichlorides and 1,5-$Ph_4P_2N_4S_2$

Compound	δ^a	Solvent
1,5-$Ph_4P_2N_4S_2$, **16a**	+120	CH_2Cl_2
cis-$Pt(PPh_3)_2Cl$	+9.7, $^1J_{P\text{-}Pt}$=3509 Hz	CH_2Cl_2
cis-$Pt(PEt_3)_2Cl_2$	+14.3, $^1J_{P\text{-}Pt}$=3674 Hz	CH_2Cl_2
$Ni(diphos)Cl_2$	+57.8	-

a. In ppm relative to 85% H_3PO_4

4.8.2 Instrumentation

Details concerning the instrumentation and methods employed for obtaining NMR spectra (^1H, ^{13}C, and ^{31}P) are outlined in Chapter 2, Section 2.5.2. Electrochemical reductions were performed in a three electrode "H" cell using a HI-TEK DT2101 potentiostat and a HI-TEK PPRI waveform generator. All reduction potentials are given with reference to a SCE. Mass spectra were recorded on a Kratos MS80RFA operating at 70 eV. Chemical analyses were performed by the Analytical Services of the Department of Chemistry, The University of Calgary.

4.8.3 Preparation of 1,5-$Ph_4P_2N_4S_2Me^-$, **67**

To a stirred THF solution (2 ml) of 1,5-$Ph_4P_2N_4S_2$ (0.107 g, 0.218 mmol) at -78°C was added 0.242 ml of a 1.4 M MeLi/Et_2O solution via syringe. After 5 min the resulting clear, pale yellow solution was allowed to warm to room temperature. The ^{31}P NMR data for 1,5-$Ph_4P_2N_4S_2Me^-$ are given in Section 4.5.2 and in Table 4.4.

4.8.4 Preparation of 1,5-$Ph_4P_2N_4(SMe)_2$, **68**, and 1,5-$Ph_4P_2N_4S(Me)S(Et)$ From 1,5-$Ph_4P_2N_4S_2Me^-$, **67**

To a stirred THF solution (50 ml) of 1,5-$Ph_4P_2N_4S_2$ (0.25 g, 0.60 mmol) at -78°C was added 0.36 ml of a 1.4 M $MeLi/Et_2O$ solution via syringe. The resulting clear, pale yellow solution was stirred for 45 min at -78°C then MeI (0.8 ml) was added and the solution was stirred for a further 1.5 h. After warming to room temperature the ^{31}P NMR spectrum of the reaction solution shows only a singlet at 15.9 ppm attributed to an intermediate of unknown identity. The solvent and excess MeI were removed in vacuo and the resulting off-white solid was washed once with 15 ml of distilled H_2O then dried under vacuum to give 0.23 g (87% yield) of 1,5-$Ph_4P_2N_4(SMe)_2$ as an off-white solid. The compound was characterized by comparison of its ^{31}P, ^1H, and ^{13}C NMR spectra with those of an authentic sample prepared from 1,5-$Ph_4P_2N_4S_2^{2-}$ and MeI (Section 4.8.6).

The reaction of 90 μmol of a THF solution of **67** (prepared in the same manner as above) with a large excess of EtI (0.3 ml), at room temperature, was monitored by ^{31}P NMR for 18 hours. The resulting product was characterized by ^{31}P NMR spectroscopy (Table 4.4).

4.8.5 Preparation of "Li_2[1,5-$Ph_4P_2N_4S_2$]", **70**

To a stirred THF solution (10 ml) of 1,5-$Ph_4P_2N_4S_2$ (0.15 g, 0.31 mmol) at -78°C was added 0.68 ml of a $Li[BEt_3H]$/THF solution. After 5 min at -78°C the solution was allowed to warm to room temperature resulting in the slow formation of a yellow precipitate and the evolution of a colorless gas (presumably H_2). The slurry was stirred for 2.5 h and then filtered by using a filter needle. The precipitate was washed once with THF (10 ml) and then dried under vacuum to yield Li_2[1,5-$Ph_4P_2N_4S_2$] as a yellow solid (0.12 g). Upon exposure to air this material decomposed to give a white solid and, as a result, elemental analysis gave poor results.

4.8.6 Preparation of 1,5-$Ph_4P_2N_4(SMe)_2$, **68**, From "$Li_2[1,5\text{-}Ph_4P_2N_4S_2]$"

To an unstirred THF solution (15 ml, freshly distilled) of 1,5-$Ph_4P_2N_4S_2$ (0.24 g, 0.49 mmol) was added 1.1 ml of a 0.9 M Super hydride/THF solution at -78°C. The resulting yellow solution was kept at -78°C for 5 min then allowed to warm to room temperature over a 30 min period during which a yellow precipitate formed and a gas, presumably H_2, was seen to evolve. The slurry was cooled to -78°C and CH_3I (0.2 ml, 3.2 mmol) was added by syringe. After 5 min the cold bath was removed and the yellow precipitate slowly reacted leaving a clear, pale yellow solution. The ^{31}P NMR spectrum of this bulk solution showed singlets at +15.9 ppm and +114 ppm (1,5-$Ph_4P_2N_4S_2$). After removal of the solvent and excess CH_3I by vacuum the off-white solid was extracted with 10 ml of CH_3CN at 23°C. The filtrate was pumped to dryness and was washed once with distilled water (10 ml, 5 min) and extracted with CH_2Cl_2 (5 ml). The extracted material was recrystallized from CH_3CN (7 ml) at -25°C to give 73 mg of off-white crystals. The ^{31}P NMR chemical shift of **68** is reported in Table 4.4. Other data are as follows :

^1H NMR
δ = 2.80 ppm, triplet, $^4J_{H\text{-}P}$=1.15 Hz, 6 H, CH_3
δ = 7.3-7.5 ppm, multiplet, 12 H, C_6H_5
δ = 7.6-8.0 ppm, multiplet, 8 H, C_6H_5
δ = 2.00 ppm, singlet, 2.25 H, CH_3CN
1,5-$Ph_4P_2N_4S_2$: CH_3CN = 1 : 0.75

^{13}C NMR
δ = 45.7 ppm, triplet, $^3J_{C\text{-}P}$=21 Hz

MS
520 (M^+,6.7%), 505 (M^+-Me, 100%), 490 (M^+-2Me, 39%), 444 (M^+- 2Me-SN, 50%), 245 ($Ph_2PN_2S^+$, 26%), 199 (Ph_2PN, 13%), 122 ($PhPN^+$)

EA
For $C_{26}H_{26}N_4P_2S_2 \cdot 0.75\ CH_3CN$
Calcd. : C, 59.91; H, 5.16; N, 12.07.
Found : C, 59.97; H, 5.13; N, 11.94

m.p. 195°C

For comparison R. Appel and K. Eichenhofer [254] report :

^{1}H NMR δ = 2.86 ppm, triplet, $^4J_{H-P}$=1.4 Hz
δ = 7.3-8.1 ppm, multiplet

MS 520 (M^+), 505 (M^+-Me), 490 (M^+-2Me)

m.p. 220°C (Recrystallized from CH_3CN/C_6H_5Br)

4.8.7 Preparation of $Ph_4P_2N_4S_2CH_2$, **71**

To a stirred solution THF solution (15 ml) of 1,5-$Ph_4P_2N_4S_2$ (30 mg, 0.61mmol) was added 1.36 ml of a 0.9 M Super-hydride/THF solution at -78°C. The resulting clear yellow solution was stirred while allowing it to warm to room temperature resulting in the precipitation of a yellow solid. The slurry was cooled again to -78°C and CH_2I_2 (0.10 ml, 1.2 mmol) was added via syringe. There was no apparent reaction after 10 min. so the cold bath was removed and the vessel slowly warmed to room temperature. After 30 min. the slurry had changed to a clear, light yellow solution which was stirred for a further 72 hrs.. The solvent and excess CH_2I_2 were removed under vacuum and the remaining off-white solid was recrystallized once from CH_3CN (-25°C) and once from CH_2Cl_2/Hexanes (2:1, -25°C) and finally extracted once with CH_2Cl_2 to give 70 mg (23%) of the title compound. The ^{31}P NMR data for **71** is given in Table 4.4. Other pertinent data are as follows :

^{1}H NMR δ = 2.96 ppm, triplet, $^4J_{P-P}$= 0.7 Hz, 2 H, CH_2
δ = 6.9-7.9 ppm, multiplet, 20 H, C_6H_5

^{13}C NMR δ = 33.1 ppm, triplet, $^3J_{C-P}$= 43.1 Hz

EA For $C_{25}H_{22}N_4P_2S_2$
Calc C : 59.51 H : 4.39 N : 11.10

Found C : 59.12 H : 4.27 N : 11.30

MS 504 (M^+, 100%), 458 (M^+- SCH_2 or M^+- SN, 47%), 424 (M^+-SN-H_2S, 35%), 367 (M^+-PhN_2S, 32%), 199 (Ph_2PN^+, 42%),185 (Ph_2P^+, 53%), 183 ($P_2N_4S_2^+$, 68%), 122 ($PhPN^+$, 71%), 77 (Ph^+ or S_2CH^+, 73%), 46 (SN^+ or SCH_2^+, 56%).

4.8.8 Preparation of cis-$Pt(PPh_3)_2$(1,5-$Ph_4P_2N_4S_2$), **60a**, From "Li_2[1,5-$Ph_4P_2N_4S_2$]"

To a THF solution (2 ml) of 1,5-$Ph_4P_2N_4S_2$ (50 mg, 0.1 mmol) at -78°C was added 0.28 ml of a 0.9 M Super-hydride/THF solution. After slowly warming to room temperature a bright yellow precipitate had formed. The ^{31}P NMR spectrum of this slurry shows no signals of any significant intensity, i.e. complete reaction and formation of an insoluble precipitate. To this slurry was added solid cis- $Pt(PPh_3)_2Cl_2$ (85 mg, 0.1 mmol) against a countercurrent of nitrogen. There was no apparent reaction after 18 h so acetone (0.5 ml) was added in order to dissolve the platinum reagent. After 30 min the ^{31}P NMR spectrum showed a significant quantity of the desired product, cis-$Pt(PPh_3)_2$(1,5-$Ph_4P_2N_4S_2$), however this material proved to be difficult to separate from the other products. The ^{31}P NMR data for this compound are given in Table 4.4.

4.8.9 Preparation of cis-$Pt(PEt_3)_2$(1,5-$Ph_4P_2N_4S_2$), **73**, From "Li_2[1,5-$Ph_4P_2N_4S_2$]"

To a stirred THF solution (30 ml) of 1,5-$Ph_4P_2N_4S_2$ (0.302 g, 0.616 mmol) at -78°C was added 1.37 ml of a 0.9 M Super-hydride/THF solution. After stirring at -78°C for 10 min the solution was slowly warmed to room temperature and stirred for 1 h producing a yellow precipitate. The slurry was cooled again to -78°C and solid cis-$Pt(PEt_3)_2Cl_2$ (0.309 g, 0.616 mmol) was added against a countercurrent of nitrogen. After 5 min the solution was gradually warmed to room temperature to give a clear yellow solution of **73**. The ^{31}P NMR data for **73** are given in Table 4.4. Attempts to purify **73** using selective recrystallization were unsuccessful.

4.8.10 Preparation of cis-Ni(diphos)(1,5-$Ph_4P_2N_4S_2$), **74**, From "Li_2[1,5-$Ph_4P_2N_4S_2$]"

To a THF solution (2 ml) of 1,5-$Ph_4P_2N_4S_2$ (31 mg, 0.063 mmol) at -78°C was added 0.16 ml of a 0.8 M Super-hydride/THF solution. After slowly warming to room temperature a bright yellow precipitate had formed. The slurry was cooled again to -78°C and solid cis-Ni(diphos)Cl_2 (34 mg, 0.063 mmol) was added against a countercurrent of nitrogen. To this reaction mixture was added 0.4 ml of acetone to solubilize the Ni reagent. After warming to room temperature the the ^{31}P NMR spectrum of the reaction solution indicated the formation of cis-Ni(diphos)(1,5-$Ph_4P_2N_4S_2$). The results are reported in Table 4.4. After 24 h in solution **74** had fully decomposed.

4.8.11 Preparation of $Ph_4P_2N_4S_2CHCH_3$, **72**, from $Ph_4P_2N_4S_2CH_2$, **71**

To a THF solution (2 ml) of $Ph_4P_2N_4S_2CH_2$ (13 mg, 26 μmol) at -78°C was added 20 μl of a 2.5 M n-BuLi/Hexanes solution via syringe. After 5 min the resulting clear, pale yellow solution was allowed to warm to room temperature afterwhich a large excess of MeI (0.1 ml) was added. The ^{31}P NMR spectrum of the reaction solution was then obtained and the results are reported in Table 4.4. These NMR data are consistent with the formation of $Ph_4P_2N_4S_2CHCH_3$. However, insufficient material was available for complete characterization.

Table 4.4 : ^{31}P NMR Data for Derivatives of 1,5-$Ph_4P_2N_4S_2$ and Related Compounds

Compound	δ^a
1,5-$Ph_4P_2N_4S_2Me_2$, **68**[b]	27.0
1,5-$Ph_4P_2N_4Se_2Me_2$[b]	21.7 [260]
1,5-$Ph_4P_2N_4S(Me)S(Et)$[c]	25.7
1,5-$Ph_4P_2N_4S_2Et_2$[c]	16.5
$Ph_4P_2N_4S_2CH_2$, **71**[b]	– 19.4
$Ph_4P_2N_4S_2CHCH_3$, **72**[c]	– 18.4, – 20.4
$Pt(PPh_3)_2$(1,5-$Ph_4P_2N_4S_2$), **60a**[c]	39.3[d,e], 18.3[d,f]
$Pt(PEt_3)_2$(1,5-$Ph_4P_2N_4S_2$), **73**[c]	35.9[g,h], 4.46[g,i]
Ni(diphos)(1,5-$Ph_4P_2N_4S_2$), **74**[c]	45.5[j], 44.1[j]

a. In ppm relative to 85% H_3PO_4
b. Solvent - CH_2Cl_2
c. Solvent - THF
d. triplet, $^4J(^{31}P\text{-}^{31}P) = 4.4$ Hz
e. $^3J(^{31}P\text{-}^{195}Pt) = 572$ Hz
f. $^1J(^{31}P\text{-}^{195}Pt) = 2861$ Hz
g. triplet, $^4J(^{31}P\text{-}^{31}P) = 3.6$ Hz
h. $^3J(^{31}P\text{-}^{195}Pt) = 536$ Hz
i. $^1J(^{31}P\text{-}^{195}Pt) = 2733$ Hz
j. triplet, $^4J(^{31}P\text{-}^{31}P) = 9.3$ Hz

CHAPTER 5

Solid State ^{31}P NMR Study of Cyclophosphathiazenes

5.1 Introduction

High-resolution ^{31}P NMR solution spectroscopy has proven to be a very important tool in cyclophosphathiazene chemistry. The previous chapters have provided an indication of the diagnostic power of this spectroscopic technique. Spectral parameters for different classes of compounds vary quite substantially. For example, the ^{31}P chemical shifts of the 1,5-diphosphadithiatetrazocines [186,209] are very different than those of related P-N-S rings which do not possess a S-S cross-ring bond. Thus, within a series of related compounds, such as the cyclophosphathiazenes, the approximation that one structural parameter is the major contributor to the ^{31}P NMR chemical shifts may hold true. Many correlations between $\delta(^{31}P)$ and various structural parameters have been developed. The coordination shift $\Delta\delta$ on complexation of phosphines to metal centers [265], the dependence of $\delta(^{31}P)$ in complexes on the cone angle of the ligand [266], and the ring contribution Δ_R for phosphorus atoms involved in chelate rings [267] are several examples of such correlations.

One important and often ignored problem with such correlations is that the $\delta(^{31}P)$ parameters are obtained from solution studies while the structural data are derived from the solid state (X-ray diffraction experiments). Substantial structural changes are not uncommon in going from the solution to the solid state. Since complete structure determinations are impossible in solution, the NMR data should ideally be obtained from the solid state.

Over the past two decades the development of high-power proton decoupling [268] to remove dipolar interactions, magic-angle spinning [269] to reduce the chemical shift anisotropy to its average value, and cross-polarization [270] to enhance the signal-to-noise ratio, has allowed high resolution studies of dilute nuclei (^{13}C, ^{29}Si, ^{31}P) to be performed on solid samples. Solid state NMR therefore allows for the formation of correlations between measurements obtained from the solid state and also provides chemical shift information that is more detailed than solution data.

As a manifestation of the three-dimensional nature of chemical shielding, the spectrum of a stationary powdered sample will show a chemical shift anisotropy (CSA) pattern (Figure 5.1a) [271]. The singularities in this powder pattern correspond to the principal elements of the chemical shift tensor (CST). The CST is a 3x3 matrix which, with the appropriate choice of coordinate system, may be transformed into diagonal form. The principal elements (σ_{11}, σ_{22}, σ_{33}) are the diagonal, non-zero, elements of this matrix and represent the characteristic shielding of the nucleus in three orthogonal directions. In solution, the isotropic tumbling of molecules reduces the matrix to its trace (mean of the three principal elements), which results in the observed isotropic value.

Spinning of a sample at the magic-angle (MAS) at rotation speeds which are below the powder line width (σ_{11}–σ_{33}) causes the CSA patterns to break up into a sharp isotropic line [$\delta_{iso}(solid)=(\sigma_{11}+\sigma_{22}+\sigma_{33})/3$] flanked by spinning sidebands (Figure 5.1b). The intensities of the sidebands are related to the CSA and can be analyzed to recover the principal elements of the CST by either the graphical analysis method of Herzfeld and Berger [272] or by the moment method of Maricq and Waugh [273]. Thus, a complete analysis of a MAS NMR spectrum will provide three shielding parameters ($\sigma_{11\text{-}33}$), one of which may provide a better correlation with structural parameters than the solution isotropic chemical shift alone.

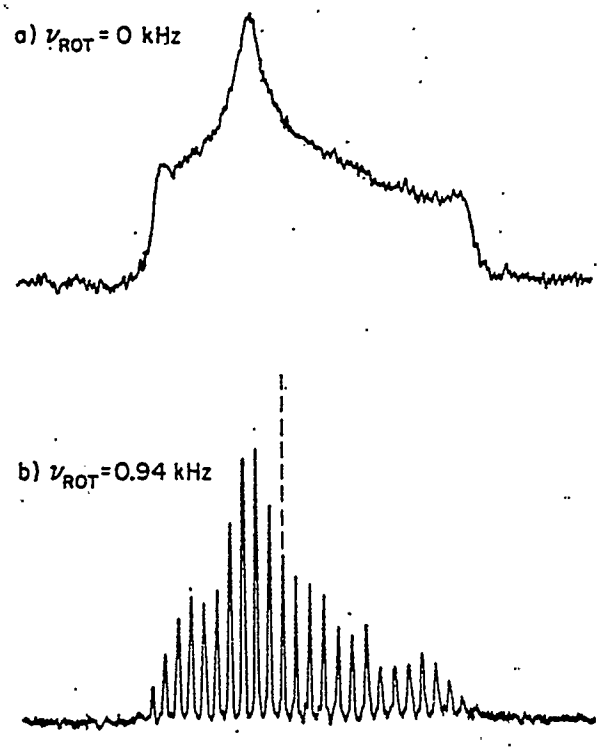

Figure 5.1 - (a) Solid state ^{31}P NMR spectrum of a stationary sample of barium diethyl phosphate (BDEP) with the principal elements of the CST indicated ; (b) Solid state ^{31}P NMR spectrum of a BDEP sample spinning at the magic angle. From Ref. [272].

As mentioned in the previous chapters the 1,5-diphosphadithiatetrazocines all exhibit ^{31}P solution chemical shifts at anomalously low fields compared to related cyclophosphathiazenes. Because of this unusual behavior a CP/MAS solid state ^{31}P NMR study of 1,5-$R_4P_2N_4S_2$ (R=Ph, Me, Et) was undertaken in order to :

1) Gain some insight into the nature of $\delta(^{31}P)$ for the 1,5-diphosphadithiatetrazocines
2) Determine whether there is a correlation between one of the CSA parameters and a structural parameter such as d(S-S) or bond angle at P.
3) Expand on the somewhat limited base of solid state ^{31}P NMR data.

Two related PNS rings, $Ph_2PN_3S_2$, and 1,5-$Ph_4P_2N_4(SPh)_2$ (Figure 5.2), were also

studied for comparison. The results of this study, conducted in conjunction with Prof. C. Fyfe and Dr. L. Randall (University of British Columbia), are presented in this chapter followed by an experimental section.

5.2 CP/MAS ^{31}P NMR Spectra of Cyclophosphathiazenes

5.2.1 Solid State Spectra and Isotropic Chemical Shifts

The CP/MAS ^{31}P NMR spectra of the 1,5-diphosphadithiatetrazocines, **16a-c**, the S, S′–diaryl derivative **75**, and the six-membered ring **15**, have been determined. A typical spectrum is shown in Figure 5.2.

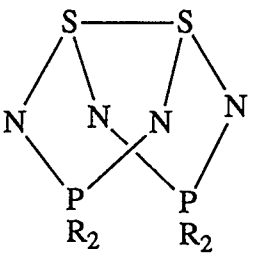

16a : R=Ph
16b : R=Me
16c : R=Et

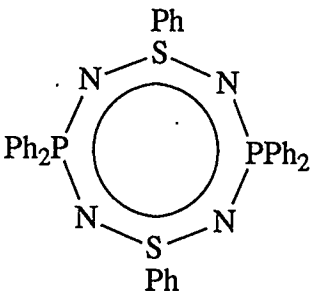

75

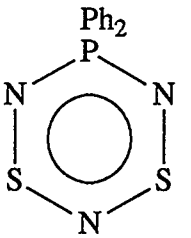

15

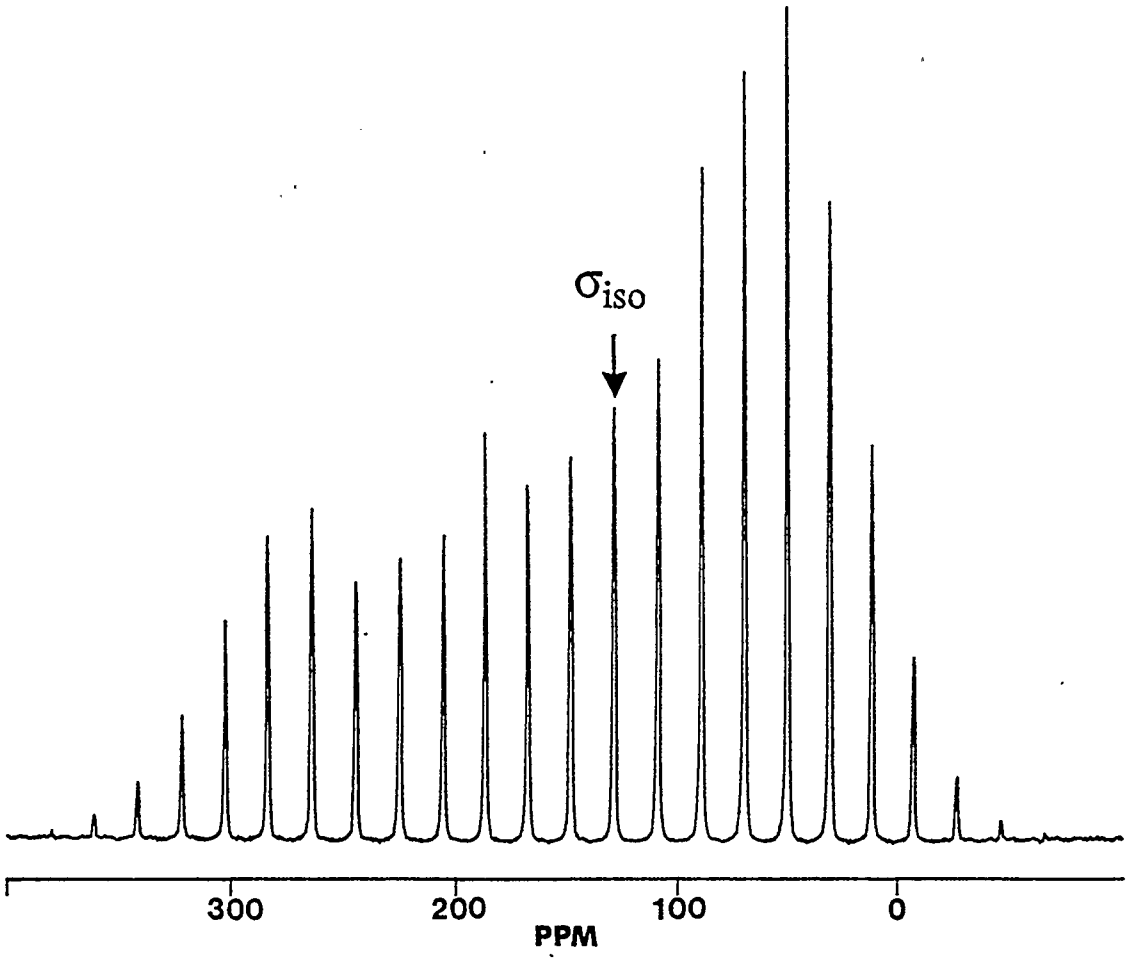

Figure 5.2 - ^{31}P solid state NMR spectrum of 1,5-$Me_4P_2N_4S_2$ obtained at 162.0 MHz by using proton decoupling and $^{1}H \rightarrow ^{31}P$ cross-polarization (rotor frequency=3.173 kHz, NS=64).

The identification of the isotropic chemical shift for each compound was made by acquiring several spectra, each at a different spinning rate. The isotropic shifts remain invariant in position while the position of the spinning sidebands varies directly with spinning speed. The solid state isotropic chemical shifts of **16a-c. 75**, and **15** have been determined in this manner and the results are listed in Table 5.1.

Table 5.1 : Solid state and Solution ^{31}P NMR Isotropic Chemical Shifts for the 1,5-Diphosphadithiatetrazocines and Related Cyclophosphathiazenes.

Compound	σ_{iso}(solid)	σ_{iso}(solution)[a]	σ_{iso}(solid)–σ_{iso}(solution)
1,5-$Ph_4P_2N_4S_2$, **16a**	119.6	113.4	6.2
1,5-$Me_4P_2N_4S_2$, **16b**	127.7	119.7	8.0
1,5-$Et_4P_2N_4S_2$, **16c**	137.2, 141.4	136.1	3.2[b]
1,5-$Ph_4P_2N_4(SPh)_2$, **75**	33.5	29.3	4.2
$Ph_2PN_3S_2$, **15**	-22.4	-21.3	-1.1

a. Solution ^{31}P NMR spectral data were measured in solutions in 10-mm tubes and are relative to external H_3PO_4.

b. Average of the two solid state isotropic chemical shifts used.

Only small differences are found between the solid state and solution isotropic chemical shifts for all of the cyclophosphathiazenes studied, indicating that there are no substantial changes in structure between the two states for any of the compounds. Two isotropic shifts are observed (Figure 5.3) for the inequivalent phosphorus atoms in **16c**; consistent with the X-ray structural data which shows the two P atoms are situated above their respective S_2N_2 planes by 0.064 and 0.238 Å [209].

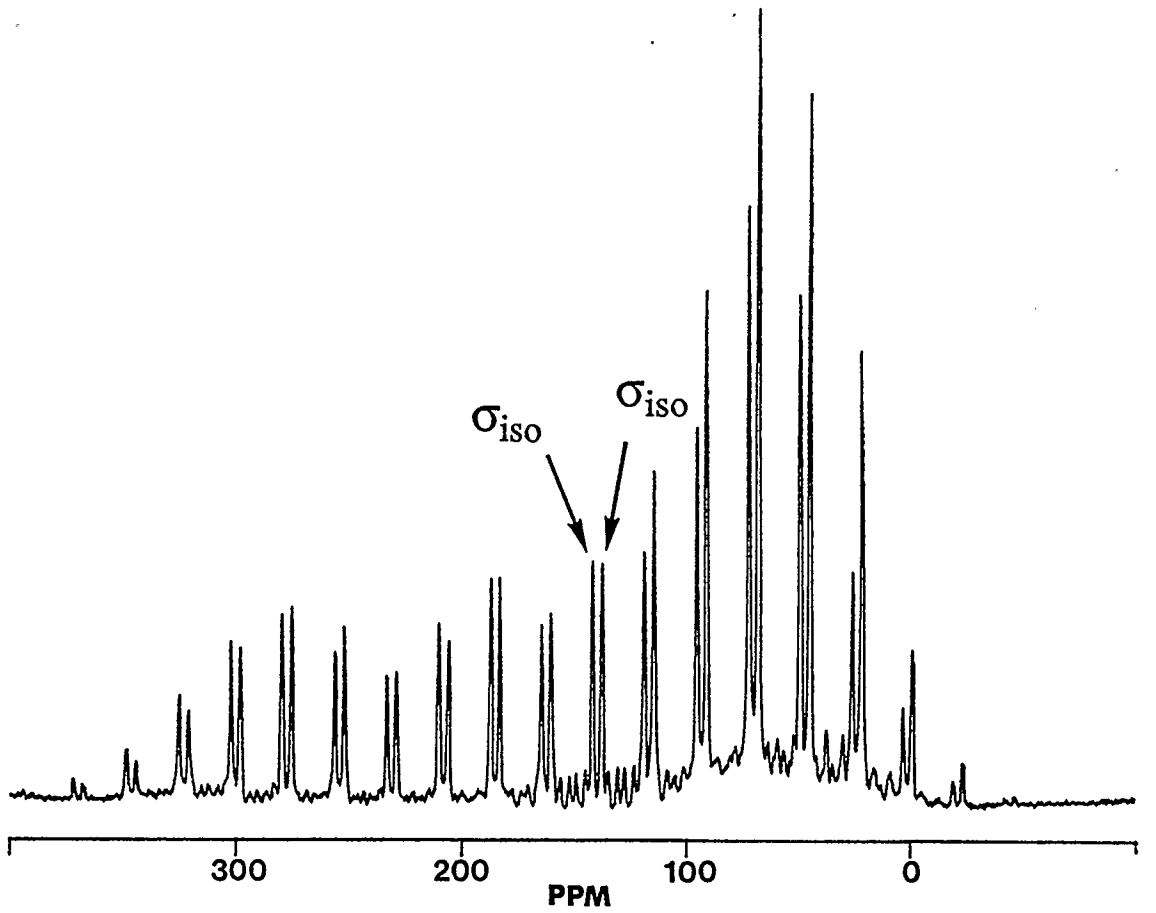

Figure 5.3 - ^{31}P solid state NMR spectrum of 1,5-$Et_4P_2N_4S_2$ obtained at 162.0 MHz by using proton decoupling and $^{1}H \rightarrow ^{31}P$ cross-polarization (rotor frequency=3.71 kHz, NS=32).

For **16a** one isotropic shift is observed for the equivalent P atoms, again consistent with the X-ray data (both P atoms are situated below the S_2N_2 planes by 0.214 Å) [185]. The X-ray structure of **16b** indicates the P atoms lie out of and on opposite sides of the S_2N_2 planes by 0.194 and 0.474 Å [187]. However, the individual isotropic shifts for the inequivalent P atoms in **16b** are not resolved in the solid state. This is due either to the accidental chemical shift equivalence of the P atoms, even though they are

crystallographically inequivalent, or to an undetected disorder in the crystal structure (i.e. the bulk of the crystals contain molecules whose P atoms are equivalent while the structure was determined for a unique crystal with inequivalent P atoms).

In common with the solution NMR data, the solid state isotropic chemical shifts for the 1,5-diphosphadithiatetrazocines, **16a-c**, are substantially different than those of the heterocycles **15** and **75** which do not possess a S-S cross-ring interaction.

5.2.2 Determination of Chemical Shift Anisotropy Parameters

The principal elements of the chemical shift tensor can be obtained directly from a powder (static) pattern as illustrated for 1,5-$Me_4P_2N_4S_2$ in Figure 5.4.

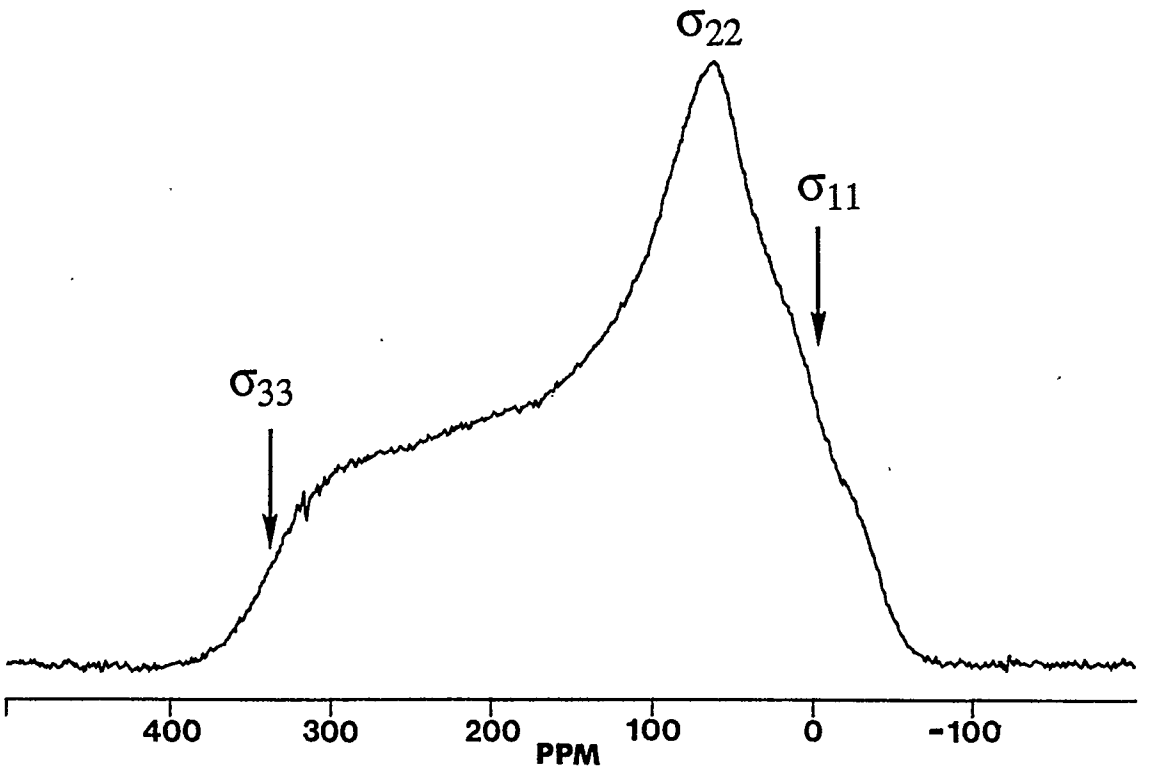

Figure 5.4 - Powder pattern for 1,5-$Me_4P_2N_4S_2$

However, in many cases, there are difficulties in obtaining spectra of good enough *S/N* to accurately determine the singularities. Consequently, the principal elements were

determined by using the graphical analysis method of Herzfeld and Berger [272]. With this technique the chemical shift parameters are derived directly from the intensities of the spinning sidebands. Herzfeld and Berger have developed graphs which show the dependence of the relative intensities of the sidebands and the isotropic peak to the variables μ and ρ (Equations 5.1 and 5.2).

The plots for several sidebands are combined to produce a contour plot whose intersection point gives a value for μ and ρ. From these two parameters, combined with the isotropic chemical shift, the three principal elements of the CST can be calculated using Equations 5.1-5.3.

$$\mu = \frac{(\gamma H_o)(\sigma_{33} - \sigma_{11})}{\omega_r} \qquad (5.1)$$

$$\rho = \frac{(\sigma_{11} + \sigma_{33} - 2\sigma_{22})}{(\sigma_{33} - \sigma_{11})} \qquad (5.2)$$

$$\sigma_{iso} = (\sigma_{11} + \sigma_{22} + \sigma_{33}) / 3 \qquad (5.3)$$

γ = gyromagnetic ratio

H_o = applied magnetic field

ω_r = rotor frequency (positive)

Convention : $\sigma_{33} > \sigma_{22} > \sigma_{11}$

A contour plot for 1,5-$Me_4P_2N_4S_2$ is shown in Figure 5.5. It shows good convergence of 7 of the 8 contour lines at $\mu = 6.9$ and $\rho = +0.45$. The values of the principal elements of the CST have been determined for all compounds using this graphical method and the results are given in Table 5.2.

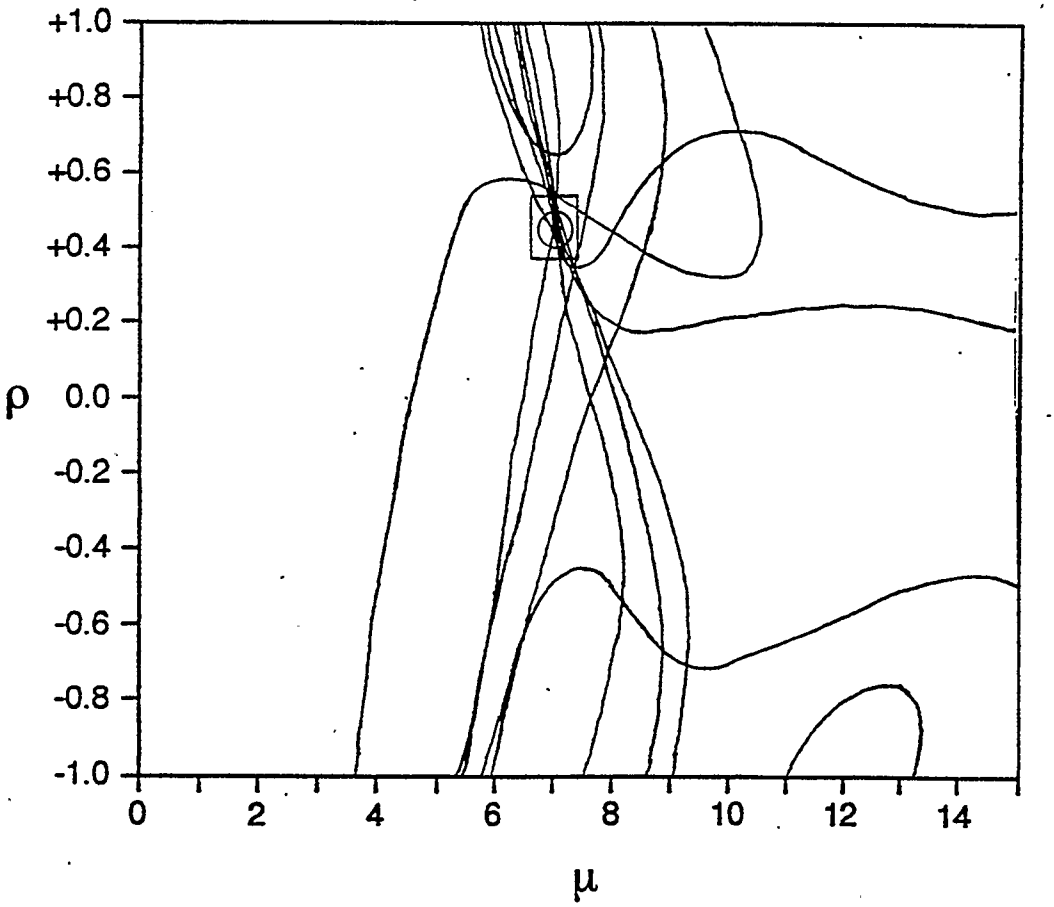

Figure 5.5 - Contour Plot for 1,5-$Me_4P_2N_4S_2$ The estimated values of μ and ρ, and a generous estimate of the uncertainty in those values, are indicated respectively by the circle and rectangle at $\mu \approx 6.9$ and $\rho \approx 4.5$.

Table 5.2 : Calculated Chemical Shift Anisotropy Parameters for the 1,5-Diphosphadithiatetrazocines and Related Cyclophosphathiazenes

Compound	σ_{11}	σ_{22}	σ_{33}	μ	$\Delta\sigma$	η
1,5-$Ph_4P_2N_4S_2$, **16a**	-35	50	341	376	334	0.45
1,5-$Me_4P_2N_4S_2$, **16b**	-9	74	317	326	285	0.51
1,5-$Et_4P_2N_4S_2$, **16c**	-16	91	342	358	305	0.60
1,5-$Ph_4P_2N_4(SPh)_2$, **75**	-12	36	77	89	65	0.92
$Ph_2PN_3S_2$, **15**	-56	-27	16	72	57.5	0.81

a. From graphical analysis of spinning sideband intensities. Estimated errors in σ_{11}, σ_{22}, and σ_{33} are ± 5%. The convention $\sigma_{33}>\sigma_{22}>\sigma_{11}$ has been used.
b. $\mu = \sigma_{33} - \sigma_{11}$.
c. $\Delta\sigma = \sigma_{33} - 1/2(\sigma_{22} + \sigma_{11})$.
d. $\eta = 1 - |\rho|$ where $\rho = (\sigma_{33} - 2\sigma_{22} + \sigma_{11})/(\sigma_{33} - \sigma_{11})$.

A comparison of the chemical shift anisotropy factors for the 1,5-diphospha-dithiatetrazocines, **16a-c**, with those of PNS rings without a transannular S-S interaction, **15** and **75**, shows several differences. The asymmetry factor (η), which relates to the total breadth of the anisotropy pattern, is much smaller for the 1,5-diphosphadithiatetrazocines than for **15** and **75** indicating a large deviation from spherical symmetry, i.e. of the three principal elements for the 1,5-diphosphadithiatetrazocines σ_{33} is skewed to very large downfield values (317-341 ppm), while **15** and **75** are much more spherically symmetric. Perfect spherical symmetry (η=1) arises when all three principal elements are equal, while axial symmetry (η=0) is a result of one unique element.

Secondly, the principal element σ_{33} is primarily responsible for the low field isotropic chemical shifts of **16a-c**, while for **15** and **75** σ_{33} and σ_{11} are equally spaced about σ_{22}, which in turn is very close to the isotropic shift value. However, as the orientation of each

shift tensor with respect to molecular geometry is unknown, the orientation of σ_{33} cannot be defined. This information can be obtained either from a single crystal study using chemical shift versus crystal orientation plots [274] or by dipolar chemical shift solid state NMR spectroscopy [275]. Nevertheless, the similarities of all parameters for **16a-c** suggest that all of the 1,5-diphosphadithiatetrazocines have common shift tensor orientations.

The 1,5-diphosphadithiatetrazocines all have narrow bond angles at phosphorus (107 to 111°) compared to those observed for **75** {119.7(2)° [205]} and **15** {115.8(2)° [184]}, but there is no obvious correlation between these bond angles and individual tensor components or the chemical shift anisotropy ($\Delta\sigma$) or the asymmetry parameter (η) (Table 5.3). Fyfe has stated that, "*In order to best develop quantitative correlations with structural parameters, it is very important that the compounds studied have a common electronic structure with no variation in the number and nature of the atoms in the immediate vicinity of the nucleus of interest that could alter the nature of the bonding.*" [276]. Perhaps then some caution should be taken in trying to develop correlations within the 1,5-diphosphadithiatetrazocine class of PNS rings, as their electronic structure is likely dominated by the exocyclic group on phosphorus (Ph, Et, Me) rather than structural factors alone. Better correlations are likely to arise for a series of compounds in which the phosphorus atom of interest is more distant from any changing functionality.

A comparison of these shift tensors with theoretically calculated ^{31}P chemical shift tensors is difficult as such data is very limited, particularly when phosphorus is involved in multiple bonding. Ab initio coupled Hartree-Fock calculations using large basis sets have provided accurate theoretical results for only simple phosphorus molecules such as P_4, P_2, and PN [277].

Table 5.3 : Structural Parameters for the 1,5-Diphosphadithiatetrazocines **16a**, **16b**, and **16c**.

Compound	**16a**[a]	**16b**[b]	**16c**[c]
d(S-S) (Å)	2.528(1)	2.551(2)	2.495(3)
<(NPN) (deg)	110.8(1)	110.0(2)	110.6(4)
	110.8(1)	107.3(2)	109.0(3)
<(PNS) (deg)[d]	120.9(2)	120.7(2)	121.8(4)
Deviation of P atoms from S_2N_2 planes (Å)	-0.214	+0.194	+0.064
	-0.214	-0.474	+0.238

a. Data taken from ref. [185]. Compound **16a** has a twofold axis that passes through the center of the S-S bond and is perpendicular to it.
b. Data taken from ref. [187].
c. Data taken from ref. [209].
d. Mean values.

5.3 Conclusion

The CP/MAS solid state ^{31}P NMR spectra of the 1,5-diphosphadithiatetrazocines and related cyclophosphathiazenes have been analyzed by using the graphical method of Herzfeld and Berger. The results allow several conclusions to be made.

(i) There are no significant structural changes between the solid state and solution for any of the cyclophosphathiazenes studied.

(ii) Two isotropic shifts are observed for the crystallograpically inequivalent phosphorus atoms of 1,5-$Et_4P_2N_4S_2$, while the individual isotropic shifts of 1,5-$Me_4P_2N_4S_2$ are not resolved as a result of accidental chemical shift equivalence or undetected crystal disorder.

(iii) For the 1,5-diphosphadithiatetrazocines the principal element σ_{33} is primarily

responsible for the observed low field isotropic chemical shifts.

(iv) No obvious correlation exists between the structural parameters of the 1,5-diphosphadithiatetrazocines and individual tensor components.

5.4 Experimental Section

^{31}P CP/MAS NMR spectra were obtained at 40.539 and 161.977 MHz by using Bruker CXP-100 and AM-400 spectrometers, respectively. The magic angle of 54°44′ was set experimentally by optimizing the sideband pattern of the ^{79}Br resonance obtained from a small amount of KBr added to the spinner as described by Frye and Maciel [278]. Literature procedures were used for the preparation of 1,5-$R_4P_2N_4S_2$ (R=Ph [209], R=Me [186], and R=Et [209]), 1,5-$Ph_4P_2N_4(SPh)_2$ [205], and $Ph_2PN_3S_2$ [186].

CHAPTER 6

Conclusions and Directions for Future Research

The objective of this work was to expand the somewhat limited body of chemical data for the 1,5-diphosphadithiatetrazocines. The extension of our understanding of the chemical and physical properties of these unsaturated PNS heterocycles has been realized as illustrated by the results presented in the previous chapters.

Chapter 2 described modifications made to the "building-block" approach used so successfully in the preparation of 1,5-diphosphadithiatetrazocines. The utilization of thionyl chloride rather than sulfur dichloride as the cyclocondensation reagent resulted in not only a slight increase in product yields, but allowed for the preparation of a 1,5-diphosphadithiatetrazocine unavailable from SCl_2, i.e. 1,5-$Et_4P_2N_4S_2$. In addition, the first structural isomers of the 1,5-diphosphadithiatetrazocines were successfully prepared and partially separated, and unusually large four bond ^{31}P-^{31}P coupling constants were observed for the unsymmetrical *exo/endo* isomers. The synthesis of 1,5-$[Cl(CCl_3)P]_2N_4S_2$ provides the first example of a 1,5-diphosphadithiatetrazocine with a potentially reactive P-halogen bond. Nucleophilic substitution reactions, analogous to those used for halocyclophosphazenes (see Sections 1.2.2 and 1.2.3), may provide a means of preparing new derivatives of the $P_2N_4S_2$ ring (Equation 6.1).

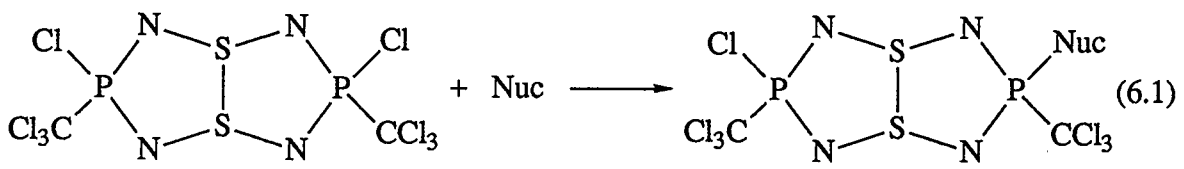

(6.1)

Nuc = R^-, Amine, RO^-, RS^-. . .

Preliminary investigations of the tetrachloro eight-membered ring, 1,5-$Cl_4P_2N_4S_2$, indicate that this compound polymerizes spontaneously in solution to give the first example of a poly(thiaphosphazene), $(Cl_2PNSN)_x$, containing two-coordinate sulfur (Equation 6.2). It is likely that the electronegative chlorine ligands on phosphorus destabilize the ring. It is therefore conceivable that the tetrafluorinated derivative will exhibit similar behavior (Equation 6.2). Consequently, the preparation of 1,5-$F_4P_2N_4S_2$ from $F_2PN_2(SiMe_3)_3$ would be of considerable interest.

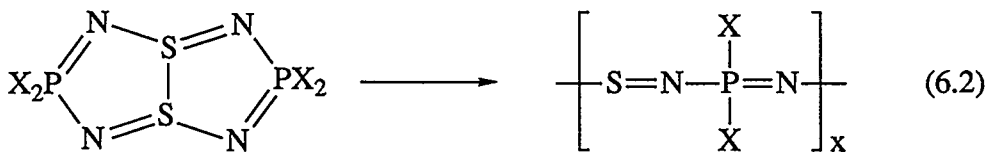

(6.2)

X = Cl, F

The preparation of several mono- and bimetallic platinum and palladium complexes of the 1,5-diphosphadithiatetrazocines, i.e. $M(PPh_2R')_2(1,5\text{-}R_4P_2N_4S_2)$ and $[M(PPh_2R')(1,5\text{-}R_4P_2N_4S_2)]_2$, in which the eight-membered ring remains intact, illustrates that the presence of phosphorus in the heterocyclic framework greatly enhances the stability of the PNS rings relative to the cyclothiazenes. Such complexes may also be structurally similar to proposed intermediates in reactions between transition-metal reagents and cyclothiazenes, especially S_4N_4, i.e. insertion of a metal center into an S-S bond to form η^2-S,S′ complexes.

The synthesis and subsequent study of the reactions of 1,5-$Ph_4P_2N_4S_2Me^-$ and $Li_2^+[1,5\text{-}Ph_4P_2N_4S_2]^{2-}$ are likely the most significant contributions of this work. These compounds are the first examples of anionic cyclophosphathiazenes and hold considerable promise as new reagents. Reaction between these and other related anions and various electrophiles will unquestionably provide many new and interesting compounds. For example, reaction between various alkyl/aryl monoanions and alkyl/aryl halides or triflates may yield both symmetrically and unsymmetrically S,S′ disubstituted eight-membered

rings, while reaction with electrophiles such as metal halides or main group halides, may give rise to numerous other unique unsymmetrical derivatives (Equation 6.3).

By contrast, reactions between the dianion and electrophiles must necessarily give symmetrically substituted products. Reaction with two molar equivalents of alkyl/aryl, metal or main group monohalides, for example, would give symmetrically disubstituted products (Equation 6.4) whereas treatment of the dianion with one molar equivalent of a dihalide would produce bicyclics (Equation 6.5), as was shown by its reaction with platinum and nickel dichloride complexes and CH_2I_2. Finally, the use of tetrahalides may result in the formation of spirocyclic compounds (Equation 6.6).

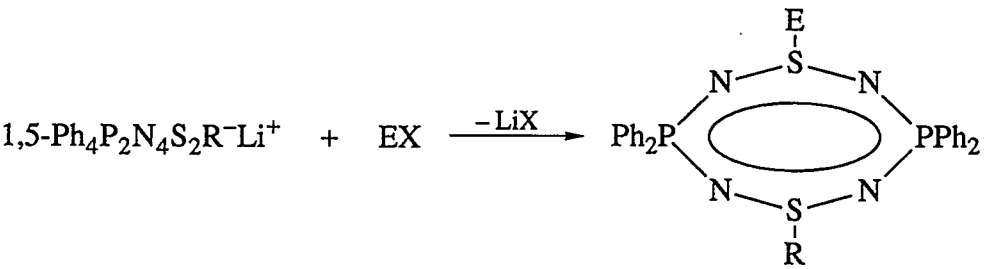

(6.3)

EX = aryl/alkyl halide, transition metal halide, silicon/tin/sulfur halide, etc. . .

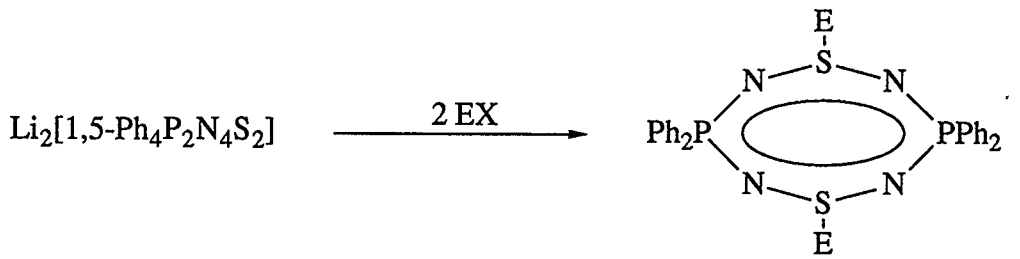

(6.4)

EX = aryl/alkyl halide, transition metal halide, silicon/tin/sulfur halide, etc. . .

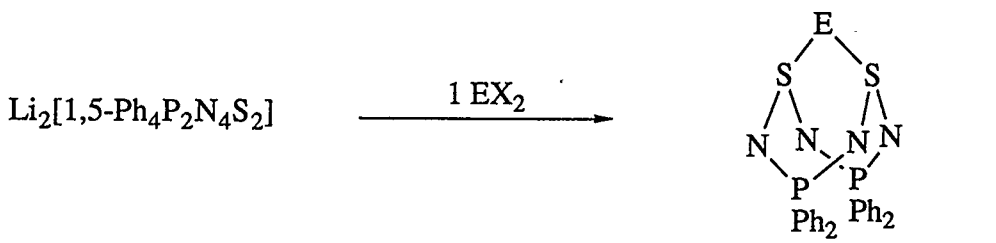

(6.5)

EX_2 = aryl/alkyl dihalide, transition metal dihalide, silicon/tin/sulfur dihalide, etc. . .

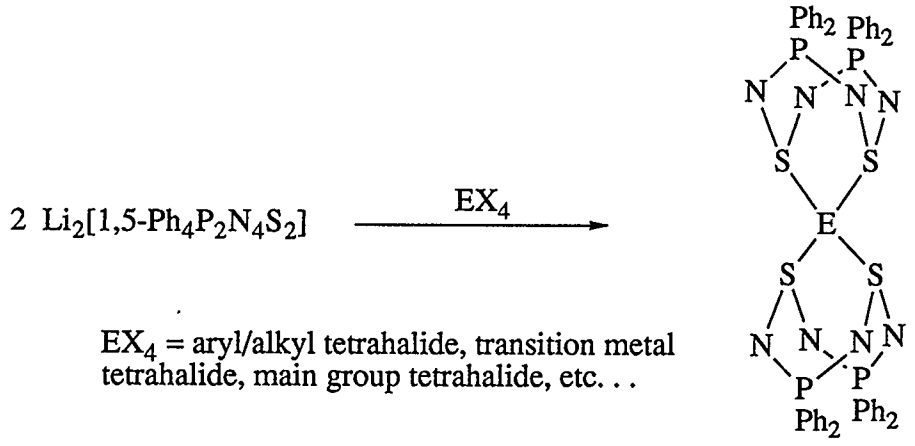

(6.6)

Reaction of the 1,5-diphosphadithiatetrazocines with transition-metals or alkyl lithium reagents, for example, demonstrates that they react readily like cyclothiazenes, but the products are relatively stable, as is usually the case for cyclophosphazene derivatives. As such, the cyclophosphathiazenes can be thought of as incorporating the best aspects of the parent cyclothiazene and cyclophosphazene systems; high reactivity (cyclothiazenes) which enables many derivatives or completely new molecules to be prepared under mild conditions, and relative stability (cyclophosphazenes) which allows for the isolation and characterization of such products.

The solid state ^{31}P NMR study of the 1,5-diphosphadithiatetrazocines and related unsaturated PNS rings revealed that one principal element is primarily responsible for the anomalously low field chemical shift of those rings with a transannular S-S bond. The determination of the absolute orientation of the chemical shift tensor from a single crystal or dipolar chemical shift study may provide further insight into the source of this unusual chemical shift behavior.

REFERENCES

1. J. Liebig and F. Wöhler, Annalen **11**, 139, 1834.
2. W. Gregory, J. Pharm. (Antwerp) **21**, 315, 1835; **22**, 301, 1835.
3. A. Stock and E. Pohland, Chem. Ber. **59**, 2215, 1926.
4. M.M. Labes, P. Love, and L.F. Nichols, Chem. Rev. **79**, 1, 1979.
5. S.S. Krishnamurthy, A.C. Sau, and M. Woods, Adv. Inorg. Chem. Radiochem. **21**, 41, 1978.
6. H.R. Allcock, W.D. Coggio, I. Manners, and M. Parvez, Organometallics **10**, 3090, 1991.
7. C.M. Mikulski, P.J. Russo, M.S. Saran, A.G. MacDiarmid, A.F. Garito, and A.J. Heeger, J. Am. Chem. Soc. **97**, 6358, 1975.
8. Z.Zak, Acta. Crystallogr., Sect. B: Struct. Sci. **37**, 23, 1981.
9. T. Chivers and J. Proctor, J. Chem. Soc., Chem. Commun. 642, 1978.
10. T. Chivers and J. Proctor, Can. J. Chem. **57**, 1286, 1979.
11. J. Bojes, P.M. Boorman, and T. Chivers, Inorg. Nucl. Chem. Lett. **12**, 551, 1976.
12. J. Bojes and T. Chivers, J. Chem. Soc., Chem. Commun. 453, 1977.
13. J. Bojes and T. Chivers, Inorg. Chem. **17**, 318, 1978.
14. T. Chivers, R.T. Oakley, A.W. Cordes, and W.T. Pennington, J. Chem. Soc., Chem. Commun. 1214, 1981.
15. T. Chivers, R.T. Oakley, A.W. Cordes, and W.T. Pennington, Inorg. Chem. **22**, 2429,1983.
16. R. Appel and M. Halstenberg, Angew. Chem. Int. Ed. Engl. **15**, 696, 1976.
17. N. Burford, T. Chivers, P.W. Codding, and R.T. Oakley, Inorg. Chem. **21**, 982, 1982.
18. N. Burford, T. Chivers, and J.F. Richardson, Inorg. Chem. **22**, 1482, 1983.
19. H.N. Stokes, Amer. Chem. J. **19**, 782, 1897.
20. J. Emsley and P.B. Udy, J. Chem. Soc. A 3025, 1970.

21. V.V. Kireev, G.S. Kolesnikov, V.P. Popilin, and S.M. Zhivukhin, Trudy Mosk Khim.-Tekhnol Ist. 157, 1970 (CA **75**, 94201, 1971).

22. V.N. Prons, M.P. Grinblat, and A.L. Kledanski, J. Gen. Chem. USSR **10**, 2108,1970.

23. H.G. Horn, Z. Anorg. Allg. Chem. **406**, 199, 1974.

24. P. Wisian-Neilson, R.H. Neilson, and A.H. Cowley, Inorg. Chem. **16**, 146, 1977.

25. P. Wisian-Neilson and R.H. Neilson, Inorg. Chem. **19**, 1875, 1980.

26. P. Wisian-Neilson and R.H. Neilson, Chem. Rev. **88**, 541, 1988.

27. V.N. Prons, M.P. Grinblat, A.L. Kledanski, and N.B. Zaitsev, J. Gen. Chem. USSR **41**, 2661, 1971.

28. D. Dahmann and H. Rose, Chem. Ztg. **100**, 340,1976.

29. A. Schmidpeter and C. Weingand, Angew. Chem. Int. Ed. Engl. **7**, 210, 1968.

30. A. Schmidpeter, J. Ebeling, H. Stary, and C. Weingand, Z. Anorg. Allg. Chem. **394**, 171, 1972.

31. M. Bermann and J.R. Van Wazer, Inorg. Chem. **11**, 209, 1972.

32. A. Schmidpeter and H. Eiletz, Chem. Ber. **108**, 1454, 1975.

33. R. Appel and G. Saleh, Chem. Ber. **106**, 3455, 1973.

34. C.W. Allen, "Cyclophosphazenes and Heterocyclophosphazenes" in : I. Haiduc and D.B. Sowerby (eds.), The Chemistry of Inorganic Homo- and Heterocycles; Academic Press, London, Vol. 2, p. 501, 1987.

35. I. Haiduc, The Chemistry of Inorganic Ring Systems; Wiley-Interscience, London, 1970, Part 2, Chapt. V, p. 624.

36. H.R. Allcock, Phosphorus-Nitrogen Compounds; Academic Press, New York, 1972.

37. E. Hobbs, D.E.C. Corbridge, and B. Raistrick, Acta Crystallogr. **6**, 621, 1953.

38. K.A.R. Mitchell, Chem. Rev. **69**, 157, 1969.

39. D.P. Craig and N.L. Paddock, Nonbenzenoid Aromatics, **2**, 273, 1971.

40. N.L. Paddock, Quart. Rev., Chem. Soc. **18**, 168, 1964.

41. J.P. Faucher, J.F. Labarre, and R.A. Shaw, Z. Naturforsch. **31b**, 677, 1976.

42. D.P Craig, M.L. Heffernan, R. Mason, and N.L. Paddock, J. Chem. Soc. 1376, 1961.

43. R.C. Haddon, Chem. Phys. Lett. **120**, 372, 1985.

44. D.P. Craig and K.A.R. Mitchell, J. Chem. Soc., London 4682, 1965.

45. R.G. Rice, L.W. Daasch, J.R. Holden, and E.J. Kohn, J. Inorg. Nucl. Chem. **5**, 190, 1958.

46. S.S. Krishnamurthy and M. Woods, Annual Reports on NMR Spectroscopy; G.A. Webb (ed.), Academic Press, London, Vol. 19, p.175, 1987.

47. P. Clare and D.B. Sowerby, J. Inorg. Nucl. Chem. **43**, 467, 1981.

48. C.W. Allen, Chem. Commun. 152, 1970.

49. J.M.E. Goldschmidt, Analytical Chemistry of Phosphorus Compounds; M. Halmann (ed.), Interscience, New York, p. 523, 1972.

50. G. B. Kauffman, B.H. Grump, B.J. Stedjee, and R.A. Houghton, J. Chromatogr. **123**, 448, 1976.

51. B.S. Manhas, S.K. Chu, and T. Moeller, J. Inorg. Nucl. Chem. **30**, 322, 1968.

52. R. Kent and R.A. Shaw, Chem. Ind. (London) 1232, 1964.

53. R. Kent and R.A. Shaw, J. Chem. Soc., London 4067, 1965.

54. B. Grushkin, M.G. Sanchez, M.V. Ernest, J.L. McClanahan, G.E. Ashby, and R.G. Rice, Inorg. Chem. **4**, 1538, 1965.

55. J. Emsley and N.L. Paddock, J. Chem. Soc. A 2590, 1968.

56. R.N. Pas, R.A. Shaw, B.C. Smith, and M. Woods, J. Chem. Soc., Dalton Trans. 709, 1973.

57. R. Hazekamp, T. Migchelsen, and A. Vos, Acta Crystallogr. **15**, 539, 1962.

58. A.J. Wagner and A. Vos, Acta Crystallogr. Sect. B **24**, 707, 1968.

59. H.R. Allcock, Chem. Rev. **72**, 315, 1971.

60. R.W. Jenkins and S. Lanoux, J. Inorg. Nucl Chem. **32**, 2429, 1970.

61. V. Chandrasekhar, S.S. Krishnamurthy, and M. Woods, ACS Symp. Ser. **171**, 481, 1981.

62. J. Trotter and S.S. Whitlow, J. Chem. Soc. A 455, 1970.

63. H.R. Allcock and P.J. Harris, J. Am. Chem. Soc. **101**, 6221, 1979.

64. A. Schmidpeter, K. Blanck, H. Hess, and H. Riffel, Angew. Chem. Int. Ed. Engl. **19**, 650, 1980.

65. R.W. Allen, J.P. O'Brien, and H.R. Allcock, J. Am. Chem. Soc. **99**, 3987, 1977.

66. K.D. Gallicano, N.L. Paddock, S.J. Rettig, and J. Trotter, Can. J. Chem. **59**, 2435, 1981.

67. W.C. Marsh, N.L. Paddock, C.J. Stewart, and J. Trotter, Chem. Commun. 1190, 1970.

68. N.L. Paddock, T.N. Ranganathan, and J.N. Wingfield, J.Chem. Soc., Dalton Trans. 1579, 1972.

69. F.A. Cotton, G.A. Rusholme, and A. Shaver, J. Coord. Chem. **3**, 99, 1973.

70. H.P. Calhoun, N.L. Paddock, J. Trotter, and J.N. Wingfield, Chem. Commun. 875, 1972.

71. H.P. Calhoun, N.L. Paddock, and J. Trotter, J. Chem. Soc., Dalton Trans. 2708, 1973.

72. N.K. Hota and R.O. Harris, Chem. Commun. 407, 1972.

73. I. Haiduc, The Chemistry of Inorganic Ring Systems; Wiley-Interscience, London, 1970.

74. H.G. Heal and A.J. Banister, Phosphorus and Sulfur **5**, 95, 1978.

75. H.W. Roesky, Adv. Inorg. Chem. Radiochem. **22**, 239, 1979.

76. A.J. Banister, Phosphorus and Sulfur **6**, 421, 1979.

77. H.W. Roesky, Angew. Chem. Int. Ed. Engl. **18**, 91, 1979.

78. R. Gleiter, Angew. Chem. Int. Ed. Engl. **20**, 444, 1981.

79. T. Chivers and R.T. Oakley, Top. Curr. Chem. **102**, 119, 1982.

80. T. Chivers, Acc. Chem. Res. **17**, 166, 1984.

81. T. Chivers, Chem. Rev. **85**, 341, 1985.

82. T. Chivers, "Sulfur-Nitrogen Heterocyles" in : I. Haiduc and D.B. Sowerby (eds.), The Chemistry of Inorganic Homo- and Heterocycles, Vol. 2, London, Academic

Press, p. 793, 1987.

83. R.T. Oakley, Progress in Inorganic Chemistry **36**, 299, 1988.

84. W.L. Jolly and K.D. Maguire, Inorg. Synth. **9**, 102, 1967.

85. M. Villeno-Blanco and W.L. Jolly, Inorg. Synth. **9**, 948, 1967.

86. G.G. Alange, A.J. Banister, and B. Bell, J. Chem. Soc., Dalton Trans. 2399, 1972.

87. A.J. Banister, A.J. Fields, R.G. Hey, and N.R.M. Smith, J. Chem. Soc., Dalton Trans. 1457, 1980.

88. M.P. Berthet, H. Vincent, and Y. Monteil, Z. Naturforsch, B : Anorg. Chem., Org. Chem. **35B**, 329, 1980.

89. T. Chivers, R.T. Oakley, O.J. Scherer, and G. Wolmerhäuser, Inorg. Chem. **20**, 914, 1981.

90. R. Adkins and A.G. Turner, J. Chromatogr. **110**, 202, 1975.

91. S.C. Peake and A.J. Downs, J. Chem. Soc., Dalton Trans. 859, 1974.

92. H. Vincent, Y. Monteil, and M.P. Berthet, J. Inorg. Nucl. Chem. **42**, 5, 1980.

93. L. Niinisto and R. Laitinen, Inorg. Nucl. Chem. Lett. **12**, 191, 1976.

94. T. Chivers, P.W. Codding, W.G. Laidlaw, S.W. Liblong, R.T. Oakley, and M. Trsic, J. Am. Chem. Soc. **105**, 1186, 1983.

95. H. Vincent, Y. Monteil, Synth. React. Inorg. Met.-Org. Chem. **8**, 51, 1978.

96. L. Zborilova and P. Gebauer, Z. Anorg. Allg. Chem. **448**, 5, 1979.

97. L. Zborilova and P. Gebauer, Z. Chem. **19**, 32, 1979.

98. R.J. Gillespie, D.R. Slim, and J.D. Tyrer, J. Chem. Soc., Chem. Commun. 253, 1975.

99. R.J. Gillespie, J.P. Kent, J.F. Sawyer, D.R. Slim, and J.D. Tyrer, Inorg. Chem. **20**, 3799, 1981.

100. E.M. Holt and S.L. Holt, Chem. Commun. 1704, 1970.

101. E.M. Holt and S.L. Holt, J. Chem. Soc., Dalton Trans. 1990, 1974.

102. I. Ruppert, V. Bastian, and R. Appel, Chem. Ber. **107**, 3426, 1974.

103. E.M. Holt, S.L. Holt, and K.J. Watson, J. Chem. Soc., Dalton Trans. 514, 1977.

104. T. Chivers, A.W. Cordes, R.T. Oakley, and P.N. Swepston, Can. J. Chem. **59**, 2376, 1981.

105. J. Bojes, T. Chivers, I. Drummond, and G. MacLean, Inorg. Chem. **17**, 3668, 1978.

106. R.J. Gillespie, J.P. Kent, and J.F. Sawyer, Inorg. Chem. **20**, 3784, 1981.

107. R. Steudel, F. Rose, R. Reinhardt, and H. Bradaczek, Z. Naturforsch. **32b**, 488, 1977.

108. H.W. Roesky, W. Schaper, O. Petersen, and T. Muller, Chem. Ber. **110**, 2695, 1978.

109. G. Wolmerhäuser and G.B. Street, Inorg. Chem. **17**, 2685, 1978.

110. R.W. Small, A.J. Banister, and Z.V. Hauptman, J. Chem. Soc., Dalton Trans. 1377, 1984.

111. H.W. Roesky and E. Janssen, Chem. Ztg. **98**, 260, 1974.

112. M. Montenarh and A. Appel, Z. Naturforsch., B : Anorg. Chem., Org. Chem. **31B**, 902, 1976.

113. A.J. Banister and P.J. Dainty, J. Chem. Soc., Dalton Trans. 2658, 1972.

114. A.J. Banister and H.G. Clarke, J. Chem. Soc., Dalton Trans. 2661, 1972.

115. A.J. Banister and H.G. Clarke, Inorg. Synth. **17**, 188, 1977.

116. R. Mews, Angew. Chem. Int. Ed. Engl. **15**, 691, 1976.

117. H.W. Roesky, M.N.S. Rao, T. Nakajima, and W.S. Sheldrick, Chem. Ber. **112**, 3531, 1979.

118. W.S. Sheldrick, M.N.S. Rao, and H.W. Roesky, Inorg. Chem. **19**, 538, 1980

119. T. Chivers and L. Fielding, J. Chem. Soc., Chem. Commun. 212, 1978.

120. T. Chivers, L. Fielding, W.G. Laidlaw, and M. Trsic, Inorg. Chem. **18**, 3379, 1979.

121. A.J. Banister, Nature (London) **237**, 92, 1972.

122. B.M. Gimarc and N. Trinajstic, Pure Appl. Chem. **52**, 1443, 1980.

123. J. Bojes, T. Chivers, W.G. Laidlaw, and M. Trsic, J. Am. Chem. Soc. **101**, 4517, 1979.

124. B.D. Sharma and J. Donohue, Acta Crystallogr. **16**, 891, 1963.

125. M.L. DeLucia and P. Coppens, Inorg. Chem. **17**, 2336, 1978.

126. R. Gleiter, J. Chem. Soc. A 3174, 1970.

127. N. Burford, Ph.D. Thesis, The University of Calgary, 1983.

128. R.H. Findlay, M.H. Palmer, A.J. Downs, R.G. Egdell, and R. Evans, Inorg. Chem. **19**, 1307, 1980.

129. A. Millefiori and S. Millifiori, J. Chem. Res., Synop. 244, 1980.

130. G.N. Dolenko, A.V. Zibarev, and V.Z. Pykhov, Zh. Neorg. Khim. **26**, 1476, 1981.

131. H.W. Roesky, C. Pelz, A. Gieren, and E. Hädicke, Z. Naturforsch. **36b**, 1437, 1981.

132. H.W. Roesky, M.N.S. Rao, C. Graf, A. Gieren, and E. Hädicke, Angew. Chem. Int. Ed. Engl. **20**, 592, 1981.

133. J. Bojes, T. Chivers, G. MacLean, R.T. Oakley, and A.W. Cordes, Can. J. Chem. **57**, 3171, 1979.

134. J. Bojes, T. Chivers, A.W. Cordes, G. MacLean, and R.T. Oakley, Inorg. Chem. **20**, 16, 1981.

135. R.T. Oakley, Can. J. Chem. **62**, 2763, 1984.

136. R. Bartetzko and R. Gleiter, Chem. Ber. **113**, 1138, 1980.

137. I. Ernst, W. Holick, G. Rihs, D. Schomburg, G. Shoham, D. Wenkert, and R.B. Woodward, J. Am. Chem. Soc. **103**, 1540, 1981.

138. R. Gleiter, R. Bartetzko, and D. Cremer, J. Am. Chem. Soc. **106**, 3437, 1984.

139. S. Millefiori and A. Millefiori, Inorg. Chim. Acta **90**, L55, 1984.

140. R.J. Gillespie, P.R. Ireland, and J.E. Vekris, Can. J. Chem. **59**, 3147, 1981.

141. A.J. Banister, H.G. Clarke, I. Rayment, and H.M.M. Shearer, Inorg. Nucl. Chem. Lett. **10**

142. R. Gleiter and R. Bartetzko, Z. Naturforsch. **35B**, 1166, 1980.

143. J. Weiss, Fortschr. Chem. Forsch. **5**, 635, 1966.

144. T. Chivers and F. Edelmann, Polyhedron **5**, 1661, 1986.

145. P.F. Kelly and J.D. Woollins, Polyhedron **5**, 607, 1986.

146. O.C.M. Davis, J. Chem. Soc. **89**, 1575, 1906.

147. H. Wölbling, Z. Anorg. Allg. Chem. **57**, 286, 1908.

148. U. Thewalt and B. Müller, Z. Anorg. Allg. Chem. **462**, 214, 1980.

149. U. Thewalt and M. Burger, Angew. Chem. Int. Ed. Engl. **21**, 634, 1982.

150. U. Thewalt and K. Holl, Z. Naturforsch. **39B**, 145, 1984.

151. H.W. Roesky, J. Anhaus, H.G. Schmidt, G.M. Sheldrick, and M. Noltemeyer, J. Chem. Soc., Dalton Trans. 1207, 1983.

152. H.W. Roesky, J. Anhaus, and W.S. Sheldrick, Inorg. Chem. **23**, 75, 1984.

153. J. Eicher, P. Klingelhöfer, U Müller, and K. Dehnicke, Z. Anorg. Allg. Chem. **514**, 79, 1984.

154. J. Hanich, M. Krestel, U. Müller, and K. Dehnicke, Z. Anorg. Allg. Chem. **522**, 92, 1985.

155. J. Hanich and K. Dehnicke, Z. Naturforsch. **39B**, 1467, 1984.

156. M. Bénard, New J. Chem. **10**, 529, 1986.

157. G.G. Alange and A.J. Banister, J. Inorg. Nucl. Chem. **40**, 203, 1978.

158. U. Thewalt and G. Albrecht, Z. Natforsch. **37B**, 10948, 1982.

159. U. Thewalt, Z. Naturforsch. **35B**, 855, 1980.

160. U. Thewalt, Angew. Chem. Int. Ed. Engl. **15**, 765, 1976.

161. U. Thewalt and B. Müller, Z. Naturforsch. **37B**, 828, 1982.

162. U. Thewalt, Chem. Ber. **462**, 221, 1980.

163. R. Drews, U. Behrens, and F. Edelmann, unpublished results - quoted in Ref. [144].

164. T. Chivers, F. Edelmann, U. Behrens, and R. Drews, Inorg. Chim. Acta **116**, 145, 1986.

165. J. Weiss, Z. Anorg. Allg. Chem. **502**, 165, 1983.

166. C.A. Ghilardi, S. Midollini, S. Moneti, and A. Orlandini, J. Organomet. Chem. **286**, 419, 1985.

167. R. Jones, P.F. Kelly, D.J. Williams, and J.D. Woollins, J. Chem. Soc., Chem. Commun. 1325, 1985.

168. J.M. Jolliffe, P.F. Kelly, and J.D. Woollins, J. Chem. Soc., Dalton Trans. 2179, 1989.

169. C.W. Allen, P.F. Kelly, and J.D. Woollins, J. Chem. Soc., Dalton Trans. 1343, 1991.

170. J. Bojes and T. Chivers, J. Chem. Soc., Chem. Commun. 1023, 1980.

171. J. Bojes, T. Chivers, W.G. Laidlaw, and M. Trsic, J. Am. Chem. Soc. **104**, 4837, 1982.

172. J. Weiss, Angew. Chem. Int. Ed. Engl. **21**, 705, 1982.

173. H. Endres and E. Galantai, Angew. Chem. Int. Ed. Engl. **19**, 653, 1980.

174. F. Edelmann, H.W. Roesky, C.S. Spang, M. Noltemeyer, and G.M. Sheldrick, Angew. Chem. Int. Ed. Engl. **25**, 931, 1986.

175. M.B. Hursthouse, M. Motevalli, P.F. Kelly, and J.D. Woollins, Polyhedron, **8**, 997, 1989.

176. P.F. Kelly and J.D. Woollins, Polyhedron **8**, 2907, 1989.

177. N. Burford, T. Chivers, M.N.S. Rao, and J.F. Richardson, ACS Symp. Ser. **232**, 81, 1983.

178. J.C. van de Grampel, Rev. Inorg. Chem. **3**, 1, 1981.

179. T. Chivers, D.D. Doxsee, M. Edwards, and R.W. Hilts in : R. Steudel (ed.), The Chemistry of Inorganic Ring Systems; Elsevier, Amsterdam, 1992, in press.

180. S. Pohl, O. Petersen, and H.W. Roesky, Chem. Ber. **112**, 1545, 1979.

181. a) J.A. Dodge, I. Manners, H.R. Allcock, G. Renner, and O. Nuyken, J. Am. Chem. Soc. **112**, 1268, 1990.

b) M. Liang and I. Manners, J. Am. Chem. Soc. **113**, 4044, 1991.

182. T. Chivers, M.N.S. Rao, and J.F. Richardson, J. Chem. Soc., Chem. Commun. 982, 1982.

183. N. Burford, T. Chivers, R.T. Oakley, A.W. Cordes, and P.N. Swepston, J. Chem. Soc., Chem. Commun. 1204, 1980.

184. N. Burford, T. Chivers, A.W. Cordes, W.G. Laidlaw, M.C. Noble, R.T. Oakley, and P.N. Swepston, J. Am. Chem. Soc. **104**, 1282, 1982.

185. N. Burford, T. Chivers, and J.F. Richardson, Inorg. Chem. **22**, 1482, 1983.

186. T. Chivers, K.S. Dhathathreyan, S.W. Liblong, and T. Parks, Inorg. Chem. **27**, 1305, 1988.

187. N. Burford, T. Chivers, P.W. Codding, and R.T. Oakley, Inorg. Chem. **21**, 982, 1982.

188. T. Chivers and M.N.S. Rao, Can. J. Chem. **61**, 1957, 1983.

189. J. Weiss, Acta Crystallogr. **B33**, 2272, 1977.

190. M.J. Begley, D.B. Sowerby, and R.J. Tillot, J. Chem. Soc., Dalton Trans. 2527, 1974.

191. M.W. Dougill, J. Chem. Soc. 5471, 1961.

192. A. Berces, T. Chivers, D.D. Doxsee, and T. Ziegler, unpublished results.

193. T. Chivers, M.N.S. Rao, and J.F. Richardson, J. Chem. Soc., Chem. Commun. 186, 1983.

194. T. Chivers, M.N.S. Rao, and J.F. Richardson, Inorg. Chem. **24**, 2237, 1985.

195. N. Burford, T. Chivers, M.N.S. Rao, and J.F. Richardson, Adv. Chem. Ser. **232**, 81, 1983.

196. N. Burford, T. Chivers, R.T. Oakley, and T. Oswald, Can. J. Chem. **62**, 712, 1984.

197. N. Burford, T. Chivers, M.N.S. Rao, and J.F. Richardson, Inorg. Chem. **23**, 1946, 1984.

198. R.T. Boeré, A.W. Cordes, S.L. Craig, R.T. Oakley, and R.W. Reed, J. Am. Chem. Soc. **109**, 868, 1987.

199. A.J. Downs and C.J. Adams, Comprehensive Inorganic Chemistry; Pergamon Press: Oxford, Vol. 2, p. 1536, 1973.

200. T. Chivers, S.W. Liblong, J.F. Richardson, and T. Ziegler, Inorg. Chem. **27**, 4344,1988.

201. S.W. Liblong, Ph.D. Thesis The University of Calgary, 1988.

202. T. Chivers, G.Y. Dénès, S.W. Liblong, and J.F. Richardson, Inorg. Chem. **28**, 3683, 1989.

203. T. Chivers, R.W. Hilts, and M. Parvez, unpublished results.

204. T. Chivers, K.S. Dhathathreyan, and T. Ziegler, J. Chem. Soc., Chem. Commun. 86, 1989.

205. T. Chivers, S.S. Kumaravel, A. Meetsma, J.C. van de Grampel, and A. van der Lee, Inorg. Chem. **29**, 4591, 1990.

206. D.W. Allen and J.C. Tebby, J. Chem. Soc. B 1527, 1970.

207. G.M. Blackburn, J.S. Cohen, and I. Weatherall, Tetrahedron **27**, 2903, 1971.

208. T. Chivers and K.S. Dhathathreyan. Unpublished observations.

209. T. Chivers, M. Edwards and M. Parvez. Inorg. Chem., Accepted for publication.

210. N. Burford, T. Chivers and M. Edwards. Unpublished observations.

211. M. Biddlestone, R. Keat, H.G. Parkes, H. Rose, D.S. Rycroft and R. Shaw. Phosphorus and Sulfur, **25**, 25, 1985.

212. K.S. Dhathathreyan and S.S. Krishnamurthy. J. Chem. Soc. Dalton Trans., 2151, 1982.

213. J.C. Wilburn and R.H. Neilson. Inorg. Chem., **10**, 2519, 1977.

214. J.C. Wilburn, P. Wisian-Neilson, and R.H. Neilson. Inorg. Chem., **18**, 1429, 1979.

215. B. Li, J.S. Engenito Jr., R.H. Neilson, and P. Wisian-Neilson. Inorg. Chem., **22**, 575, 1983.

216. R.H. Neilson and J.S. Engenito Jr.. Organomet., **1**, 1270, 1982.

217. E. Niecke and W. Bitter. Chem. Ber., **109**, 415, 1976.

218. R.H. Neilson and P. Wisian-Neilson. Inorg. Chem., **21**, 3568, 1982.

219. T. Chivers, M. Edwards and M.N.S. Rao, Unpublished observations.

220. A.A. Bhattacharyya, J.A. McLean, Jr. and A.G. Turner. Inorg. Chim. Acta, **34**, L199, 1979.

221. T. Chivers, M. Edwards, P.N. Kapoor, A. Meetsma, J.C. van de Grampel, and A. van der Lee. Inorg. Chem., **29**, 3068, 1990.

222. N. Hadj-Bagheri, L. Manojlovi´c-Muir, A. Stefanovi´c, and R.J. Puddephatt. J. Chem. Soc. Dalton Trans., 535, 1990.

223. R. Colton and T.A. Stephenson. Polyhedron, **3**, 231, 1984.

224. I.P. Parkin, M.J. Pilkington, A.M.Z. Slawin, D.J. Williams, and J.D. Woollins. Polyhedron, **9**, 987, 1990.

225. J. Mason (ed). Multinuclear NMR; Plenum Press: New York, 396, 1987.

226. T. Chivers, M. Edwards, A. Meetsma, J.C. van de Grampel, and A. van der Lee. Inorg. Chem., submitted for publication.

227. J. Sandström. Dynamic NMR Spectroscopy; Academic Press: New York, 1982.

228. S.J. Higgins, R. Taylor, and B.L Shaw. J. Organomet. Chem., **325**, 285, 1987.

229. R. Uson, P. Royo, and J. Gimeno. J. Organomet. Chem., **72**, 299, 1974.

230. D.E. Berry, J. Browning, K.R. Dixon, and R.W. Hilts. Can. J. Chem., **66**, 1272, 1988.

231. R. Ugo, F. Cariata, and G. LaMonica. Inorg. Synth., **11**, 105, 1968.

232. U. Nagel. Chem. Ber., **115**, 1998, 1988.

233. R.A. Shaw, Z. Naturforsch. **31b**, 641, 1976.

234. S.S. Krishnamurthy, A.R. Vasudeva Murthy, R.A. Shaw, and M. Woods, Adv. Inorg. Radiochem. **21**, 41, 1978.

235. J.L. Schmutz and H.R. Allcock, Inorg. Chem. **14**, 2433, 1975.

236. B. Thomas and G. Grossmann, Z. Anorg. Allg. Chem. **448**, 100, 1979.

237. C.W. Allen, Ind. Eng. Chem. Prod. Res. Dev. **20**, 77, 1981

238. H.R. Allcock, P.J. Harris, and M.S. Connolly, Inorg. Chem. **20**, 11, 1981.

239. H.R. Allcock, M.N. Mang, G.H. Riding, and R.R. Whittle, Organometallics **5**, 2244, 1986.

240. H.R. Allcock, M.N. Mang, G.S. McDonnell, and M. Parvez, Macromolecules **20**, 2060, 1986.

241. K. Tanaka, T. Yamabe, A. Tachibana, H. Kato, and K. Fukui, J. Chem. Phys., **82**, 2121, 1978.

242. M. Hojo, Bull. Chem. Soc. Jpn., **53**, 2856, 1980.

243. T. Chivers and M. Hojo, Inorg. Chem. **23**, 1526, 1984.

244. J.W. Tweh and A.G. Turner, Inorg. Chim. Acta **48** 173, 1981.

245. N. Burford, T. Chivers, M. Hojo, W.G. Laidlaw, and J.F. Richardson, Inorg. Chem. **24**, 709, 1985.

246. R. Jones, P.F. Kelly, D.J. Williams, and J.D. Wollins, Polyhedron **7**, 1541, 1987.

247. H.W. Roesky, M. Witt, B. Krebs, G. Henkel, and H.J. Korte, Chem. Ber. **114**, 201, 1981.

248. T. Chivers, A. W. Cordes, R.T. Oakley, and P.N. Swepston, Inorg. Chem. **20**, 2376, 1981.

249. H. Roesky and M. Dietl, Angew. Chem. Int. Ed. Engl. **12**, 424, 1973.

250. H. Roesky and H. Wiezer, Angew. Chem. Int. Ed. Engl. **12**, 674, 1973.

251. H. Roesky, Z. Naturforsch. **31B**, 680, 1975.

252. A.J. Banister and J.R. House, Inorg. Nucl. Chem. **33**, 4057, 1971.

253. S. Mataka, K. Takahashi, H. Yamamoto, and M. Tashiro, J. Chem. Soc., Perkin Trans. 1 2417, 1980.

254. R. Appel and K.W. Eichenhofer, Chem. Ber. **104**, 3859, 1971.

255. R.W. Hilts, Unpublished observations.

256. T. Chivers, R.W. Hilts, A. Meetsma, and J.C. van de Grampel, unpublished observations.

257. O.J. Scherer and R. Schmidt, J. Organomet. Chem. **16**, 11, 1969.

258. J.S. Amato, S. Karady, R.A. Reamer, H.B. Schlegel, J.P. Springer, and L.M. Weinstock, J. Am. Chem. Soc. **104**, 1375, 1982.

259. F. Pauer and D. Stalke, J. Organomet. Chem. **418**, 127, 1991.

260. T. Chivers, D.D. Doxsee, and J.F. Fait, J. Chem. Soc., Chem. Commun. 1704, 1989.

261. T. Chivers, M. Cowie, M. Edwards, and R.W. Hilts, Inorg. Chem. Submitted for publication.

262. E. Block, Reactions of Organosulfur Compounds; Academic Press, New York, Chapter 2, 1978.

263. E.J. Corey and D. Seebach, Angew. Chem. Int. Ed. Engl. **4**, 1075, 1077, 1965.

264. G.W. Parshall, Inorg. Synth. **12**, 27, 1970.

265. B.E. Mann, C. Masters, B.L. Shaw, R.M. Slade, and R.E. Stainbank, Inorg. Nucl. Chem. Lett., **7**, 881, 1971.

266. C.A. Tolman, Chem.Rev. **77**, 313, 1977.

267. P.E. Garrou, Chem. Rev. **81**, 229, 1981.

268. J. Schaefer and E.O. Stejskal, J. Chem. Phys. **98**, 1031, 1976.

269. E.R. Andrew, Prog. Nucl. Magn. Reson. Spectrosc. **8**, 1, 1971.

270. A. Pines, M. G. Gibby, and J.S. Waugh, J. Chem. Phys. **56**, 1776, 1972.

271. C.A. Fyfe, Solid State NMR for Chemists; C.F.C Press: Guelph, Ontario, Canada, 1983.

272. J. Herzfeld and A.E. Berger, J. Chem. Phys. **73**, 6021, 1980.

273. M.M. Maricq and J.S. Waugh, J. Chem. Phys. **70**, 3300, 1979.

274. H. Hauser, C. Radloff, R.R. Ernst, S. Sundells, and I. Pascher, J. Am. Chem. Soc. **110**, 1054, 1988.

275. R.D. Curtis, M.J. Schriver, and R.E. Wasylishen, J. Am. Chem. Soc. **113**, 1493, 1991.

276. A.J. Carty, C.A. Fyfe, M. Lettinga, S. Johnson, and L.H. Randall, Inorg. Chem. **28**, 4120, 1989.

277. P. Lazzeretti and J.A. Tossell, J. Phys. Chem. **91**, 800, 1987.

278. J.S. Frye and G.E. Maciel, J. Magn. Reson. **48**, 125, 1982.